INTERIM REPORT ORNL/NUREG/TM-337

Bundle B-2 Test Data
Multirod Burst Test Program

R. H. Chapman
D. O. Hobson
J. L. Crowley
A. W. Longest

Prepared for the U.S. Nuclear Regulatory Commission
Office of Nuclear Regulatory Research
Under Interagency Agreements DOE 40-551-75 and 40-552-75

OAK RIDGE NATIONAL LABORATORY
OPERATED BY UNION CARBIDE CORPORATION · FOR THE DEPARTMENT OF ENERGY

Printed in the United States of America. Available from
National Technical Information Service
U.S. Department of Commerce
5285 Port Royal Road, Springfield, Virginia 22161

INTERIM REPORT

Accession No. _____

ORNL/NUREG/TM-337

Contract Program or Project Title: MULTIROD BURST TESTS

Subject of this Document: BUNDLE B-2 TEST DATA

Type of Document: DATA REPORT

Authors: R. H. Chapman, D. O. Hobson, J. L. Crowley, A. W. Longest

Date of Document: August 1, 1979

Date Published: August 1979

Responsible NRC Individual and NRC Office or Division: M. L. Picklesimer, Fuel Behavior Branch, Division of Reactor Safety Research, Office of Nuclear Regulatory Research

Prepared for the
U.S. Nuclear Regulatory Commission
Office of Nuclear Regulatory Research
Under Interagency Agreements DOE 40-551-75 and 40-552-75

NRC FIN No. B0120

Prepared by the
OAK RIDGE NATIONAL LABORATORY
Oak Ridge, Tennessee 37830
operated by
UNION CARBIDE CORPORATION
for the
DEPARTMENT OF ENERGY

Contract No. W-7405-eng-26

INTERIM REPORT

CONTENTS

LIST OF TABLES

LIST OF TABLES (continued)

LIST OF TABLES (continued)

LIST OF FIGURES

LIST OF FIGURES (continued)

LIST OF FIGURES (continued)

LIST OF FIGURES (continued)

LIST OF FIGURES (continued)

LIST OF FIGURES (continued)

FOREWORD

Examination, analysis, and interpretation of a bundle test take place over a long period of time, and it is our practice to report progress and results as they become available. Dissemination of the information in this manner results in its being disjointed and scattered throughout several publications. This presents some problems to the users in that one is never sure if the information at hand is the most recent. It is our intention to alleviate some of these problems by (1) publication (with limited distribution) of a data report on each bundle test and (2) publication of interpretative reports when sufficient information has been developed to warrant such action.

Consistent with this intention, the objective of this report is to provide a reference source of information and results obtained during the B-2 test and from pretest and posttest examination of the test array. We believe the data presented herein, consisting of plots, tabulations, and photographs, are both necessary and sufficient for interpretation of the test. In deciding what (and how much) information should be included, we had to anticipate to a certain extent the potential uses of the data. As a result, certain data have been excluded, but these contain information that can be characterized as analysis and "second generation" data, such as comparative temperature vs time plots and computer-drawn cross sections.

Also, it was decided that the data should be presented in this reference source with a minimum of interpretation. We will continue to publish interpretations in our progress reports, and, finally, we plan to publish an interpretative report on all the bundle tests. This final report will be based on data reported in the individual test data reports, such as this one, and information reported in the progress reports.

This report is derived from research performed by the Multirod Burst Test (MRBT) Program at Oak Ridge National Laboratory (ORNL). This research is sponsored by the Division of Reactor Safety Research of the Nuclear Regulatory Commission, and the results are published routinely in a series of progress reports, topical reports, quick-look reports, and data reports. This particular report is in the last category.

Progress reports published by the MRBT Program include:

NUREG Report No.	ORNL Report No.	Period covered
	ORNL/TM-4729	July–September 1974
	ORNL/TM-4805	October–December 1974
	ORNL/TM-4914	January–March 1975
	ORNL/TM-5021	April–June 1975
	ORNL/TM-5154	July–September 1975
	ORNL/NUREG/TM-10	October–December 1975
	ORNL/NUREG/TM-36	January–March 1976
	ORNL/NUREG/TM-74	April–June 1976
	ORNL/NUREG/TM-77	July–September 1976
	ORNL/NUREG/TM-95	October–December 1976
	ORNL/NUREG/TM-108	January–March 1977
	ORNL/NUREG/TM-135	April–June 1977
NUREG/CR-0103	ORNL/NUREG/TM-200	July–December 1977
NUREG/CR-0225	ORNL/NUREG/TM-217	January–March 1978
NUREG/CR-0398	ORNL/NUREG/TM-243	April–June 1978
NUREG/CR-0655	ORNL/NUREG/TM-297	July–December 1978
NUREG/CR-0817	ORNL/NUREG/TM-323	January–March 1979

Topical reports pertaining to research and development carried out by this program are:

1. R. H. Chapman (comp.), *Characterization of Zircaloy-4 Tubing Procured for Fuel Cladding Research Programs*, ORNL/NUREG/TM-29 (July 1976).
2. W. E. Baucum and R. E. Dial, *An Apparatus for Spot Welding Sheathed Thermocouples to the Inside of Small-Diameter Tubes at Precise Locations*, ORNL/NUREG/TM-33 (August 1976).
3. W. A. Simpson, Jr., et al., *Infrared Inspection and Characterization of Fuel-Pin Simulators*, ORNL/NUREG/TM-55 (November 1976).
4. R. H. Chapman et al., *Effect of Creep Time and Heating Rate on Deformation of Zircaloy-4 Tubes Tested in Steam with Internal Heaters*, NUREG/CR-0343 (ORNL/NUREG/TM-245) (October 1978).

The following limited-distribution quick-look and data reports have been issued by this program:

1. R. H. Chapman (comp.), *Quick-look Report on MRBT No. 1 4 × 4 Bundle Burst Test*, Internal Report ORNL/MRBT-2 (September 1977).
2. R. H. Chapman (comp.), *Quick-look Report on MRBT No. 2 4 × 4 Bundle Burst Test*, Internal Report ORNL/MRBT-3 (November 1977).
3. R. H. Chapman, *Quick-look Report on MRBT No. 3 4 × 4 Bundle Burst Test*, Internal Report ORNL/MRBT-4 (August 1978).
4. R. H. Chapman et al., *Bundle B-1 Test Data*, ORNL/NUREG/TM-322 (June 1979).

ABSTRACT

A compilation of B-2 test data is presented. These data were obtained during the test and from pretest and posttest examination of the test array. They are presented in considerable detail with minimum interpretation, which will be the subject of a future report.

The B-2 test is the second of a series of 4 × 4 bundle tests performed by the Multirod Burst Test (MRBT) Program at Oak Ridge National Laboratory (ORNL). This research is sponsored by the Nuclear Regulatory Commission (NRC).

A brief description of the experiment and a summary of bundle performance are also included with the results of the B-2 test. Both graphical and tabular formats are used to show temperature, pressure, and tube rupture data as functions of test time; strain data for the cladding in each of the fuel rod simulators; and flow test results obtained after the bundle test. Photographic documentation is provided for both the overall bundle, before and after testing, and the 53 cross sections cut from the tested bundle for strain measurements.

The purpose of this report is to provide a background document for interpretative reports published previously and to be published in the future.

1. INTRODUCTION

This report presents, in detail, the experimental data for the second 4 × 4 multirod burst test (B-2), conducted within the framework of the Multirod Burst Test (MRBT) Program at Oak Ridge National Laboratory (ORNL). This work is sponsored by the Division of Reactor Safety Research of the Nuclear Regulatory Commission (NRC). The report is intended primarily as a source document for B-2 test results, with a minimum amount of interpretation of the data. Because of this, it should be read in conjunction with the published[1-5] results and interpretations.

No inferences should be drawn from the tabular data in this report concerning their precision. In most instances, the tabulations were generated by computer routines from data tapes, and the values are given to more significant figures than the data warrant. The appropriately referenced reports should be consulted for insight into both the precision and the accuracy of the data contained herein.

The primary objective of the B-2 test, which was performed successfully on October 3, 1977, was to determine if a relatively large temperature difference between the electrically heated bundle and its surrounding shroud would have a significant effect on bundle deformation. A secondary objective was to clarify some questions raised in the B-1 test relative to the performance of the shroud and its associated instrumentation. These objectives could be satisfied best by conducting the B-2 test under nominally the same conditions as the B-1 test except for omitting electrical heating of the B-2 shroud. This exception is, therefore, the major difference in the two tests.

Following the format of the previous report[6] in this series, a brief description of the test design and procedure will be given, followed by the test results.

2. TEST DESCRIPTION

Figure 1 is a simplified drawing of the test assembly as used for the first bundle (i.e., the B-1) test; internal modifications, consistent with test objectives, were made to the assembly for the B-2 test. These modifications (not shown in the figure) included (1) a means for bypassing the electrical current around the shroud, (2) addition of 6 shroud thermocouples (12 total), and (3) replacement of the "Fiberfrax" insulation board around the shroud with a static steam gap and reflective-type insulation to minimize shroud heat losses and possible heat sinks. The gap between the shroud and the reflective insulation was maintained by 13-mm-OD by 7.6-mm-ID spacers of glass-bonded-mica material as shown in Fig. 2.

Table 1 and Fig. 3 give pertinent details of the fuel pin simulators. The fuel simulators (internal heaters) used in the test assemblies were the best available from the last lot supplied by SEMCO. In general, the fuel simulators were of equivalent quality (based on axial temperature distribution as determined from the pretest infrared characterization scans) to those used in the first bundle test.

The Zircaloy-4 tubes (10.92 mm OD × 0.635 mm wall thickness) used to fabricate the test assemblies came from the master lot of tubing purchased[7] for use in all the NRC-sponsored cladding research programs. Serial numbers of the tubes are given in Table 1.

Each fuel pin simulator was instrumented with a fast response, strain-gage-type pressure transducer and four Inconel-sheathed (0.71 mm OD), type K thermocouples with ungrounded juctions. The thermocouples were spot-welded (using a device[8] developed specifically for this purpose) to the inside of the Zircaloy-4 tubes at axial and azimuthal positions (nominally the same as used in the B-1 test) selected to provide an overall indication of the temperature distribution within the test array. All the simulator thermocouples were operative during the test. Twelve thermocouples (0.71 mm OD, stainless steel sheathed, type K, with ungrounded "duckbill" junctions) were spot-welded to the outside of the 0.25-mm-thick shroud surrounding the rod array. One face of the shroud had six thermocouples to provide information on the axial temperature

distribution, while two thermocouples were located on each of the other three faces. Figures 4 and 5 give the thermocouple identifications (for use in subsequent tables and figures) and nominal as-built locations as used in the test.

Millivolt signals from the pressure transducers, thermocouples, and electrical power measuring instruments were recorded on magnetic tape by a computer controlled data acquisition system (CCDAS) for subsequent analysis.

Preparations for the test began early on October 3, 1977, with heatup of the test vessel and checkout of the instrumentation. Thermal equilibrium of the assembly was achieved in about 6 hr; leak rates of the fuel pin simulators were acceptably low (<35 kPa pressure loss per minute). A short powered run (4-sec transient) was then conducted to ascertain that the CCDAS and all the instrumentation were functioning properly and that the performance of the test assembly was as expected. Examination of the quick-look data from this short transient showed that the indicated performance was as expected, except that one fuel pin simulator (No. 9) had developed a moderate leak (about 200 kPa pressure loss per minute). Although this leak was not nearly as severe as that experienced by one of the simulators in the B-1 test, on-the-spot checks were insufficient to identify (and correct) the source. It was decided to proceed with the test as soon as thermal equilibrium was reestablished.

Following stabilization of the bundle temperature at about 335°C after the short powered run, all the fuel pin simulators were pressurized simultaneously with helium to approximately 8800 kPa and isolated from the pressure supply system. Superheated steam (inlet conditions of 332°C and 200 kPa) flowed downward through the bundle (flow rate, ~5 kg/hr; Re = 290 based on inlet conditions and undeformed bundle dimensions) during the transient. The steam flow was increased to ~30 kg/hr when power was terminated to facilitate cooldown; the test vessel was vented to atmospheric pressure simultaneously with the increased steam flow.

The test could be terminated by any of four actions: (1) CCDAS action resulting from a signal that all 16 simulators had burst, (2) CCDAS action that 10 thermocouples had exceeded the upper temperature limit (100°C above the expected burst temperature) for 3 successive scans, (3) a

timer that limited the transient to a predetermined length of time, and (4) operator override. Even though the simulator 9 burst was delayed slightly (due to a small loss in pressure), the test was terminated by the first criterion — all 16 simulators burst before the high-temperature limit was reached.

Following the burst test, the bundle was removed and examined visually; characteristic dimensions were made for comparison with pretest measurements, and extensive photography was performed to document the physical appearance. The fuel simulators were then removed and the bundle was flow tested in a water test loop to characterize the flow resistance caused by the deformation. Similar flow tests were performed on an undeformed reference bundle for comparison. Both the B-2 and the reference bundle were flow tested in each of two flow shrouds identified in pertinent MRBT reports as shrouds 1 and 2.

After completion of the flow tests, the B-2 bundle was cast into an epoxy matrix and sectioned at approximately 53 axial positions, and the deformation was determined on each tube in each section by analyzing photographs (5×) of each section.

3. SUMMARY OF BUNDLE PERFORMANCE

Table 2 summarizes pertinent data from the test; these data have been revised slightly from those included in the B-2 quick-look report.[1] Initial pressure conditions for the test were essentially the same as those used in the B-1 test;[6] however, the initial temperature in this test was about 20°C lower. As indicated in the table, the initial temperature distribution throughout the bundle was very uniform. All 12 thermocouples on the shroud indicated initial temperatures in the same range (333 to 335°C); the inlet steam conditions remained constant (5 kg/hr downflow at 332°C and 200 kPa) throughout the transient.

The table also lists the temperature indicated by each of the thermocouples at the time of burst for the respective simulators. The spread in temperatures in a given simulator is not unusual, considering the location of the thermocouples (see Fig. 5) and the power distribution of the fuel simulators as determined from the pretest infrared characterization scans. The last column in the table gives the burst temperature predicted from the correlation[9] derived from our single-rod tests, using the measured burst pressure as input. Comparison of the measured burst temperatures (underlined values in the table) with the predicted values shows reasonable agreement.

The performance of the simulators was about the same with the exception of No. 9, which reflected the loss in pressure discussed earlier. The first two bursts (simulators 8 and 11) occurred simultaneously (i.e., within the 0.05-sec resolution time of the CCDAS clock) 17.80 sec after start of the transient; the 12th through 15th bursts (simulators 1, 3, 4, and 14) occurred simultaneously after 18.30 sec of heating, and the last burst (No. 9) took place 1.75 sec later. Power to the bundle was terminated 0.30 sec after the last burst by a signal generated by the CCDAS that all 16 simulators had burst.

Table 3 lists some of the volume-related data for the B-2 tubes. It can be seen that the initial gas volumes were quite uniform among the tubes — ranging from 48.5 to 51.0 cm^3 — but bore little relation to either the fractional pressure decreases or the fractional volume increases. Although the simulator gas volume is reasonably typical, the

distribution of the volume is not typical of a full-length fuel rod. Of the total initial volume (at room temperature), about 13% is in the heated portion of the annulus between the fuel simulator and the inside diameter of the Zircaloy tube, 10% is in the unheated portion of the annulus, 33% is in the pressure transducer and connecting tube, and 44% is distributed in the end regions (mostly at the upper end) of the fuel pin simulator. At any given time during the test all these volumes have different temperatures (the major volumes remain at or near room temperature), ranging from room temperature to cladding temperature, and one cannot calculate the fractional volume increase from the pressure decrease in a straightforward manner. Instead, we calculated the volume increase from the tube deformation profiles (assuming circular cross sections).

Table 4 is a computer printout of the conditions existing at the time of maximum pressure (corresponding approximately to the beginning of plastic deformation) of each simulator. It should be noted in this and other computer printouts of data that simulator 9 developed a leak prior to the transient and its behavior was abnormal. Tables giving pressure and temperature conditions throughout the bundle at the time of each burst are presented later in the report.

Table 5 gives the time distribution of the bursts; a histogram is given in Fig. 6. As is evident, most of the bursts (15) occurred in a 0.5-sec interval, the same as observed in the B-1 test. Also, the bursts in B-2 occurred about 0.8 sec later into the transient than was the case for the B-1 test. The delay is accounted for almost entirely by the approximately 20°C lower initial temperature condition for the B-2 test and slightly different heating rates. The average heating rate for the B-2 test over the time interval 3 to 15 sec was 29.9°C/sec, and for the B-1 test it was 30.1°C; this time interval represents the more or less linear portion of the average temperature versus time curve.

The burst temperature-burst pressure data for the B-2 test (excluding the No. 9 simulator) are compared in Fig. 7 to the B-1 data, to our single-rod correlation,[9] and to the two single-rod tests (SR-28 and SR-29) that were conducted[9] for comparison with the bundle simulators. We have assumed the burst temperature (underlined value in Table 2) for the individual simulators to be the highest measured at the time of failure; this is

consistent with the definition used for the B-1 test and for the single-rod tests. At first glance it appears that the bundle data indicate higher burst temperatures than would be predicted from the single-rod correlation; however, it should be noted that the correlation is based on external bare-wire thermocouple measurements, whereas the bundle temperature measurements were obtained from internal sheathed thermocouples, which indicate, in general, slightly higher temperatures. The range of burst pressures was about the same as observed in the B-1 test. In general, the B-2 tubes burst at slightly higher pressures and lower temperatures, as shown in Fig. 7. Also, the B-2 data are in slightly better agreement with the single-rod correlation.

4. BUNDLE TEST RESULTS

This section presents, in a number of subsections, the detailed results of the B-2 test. The purpose of this presentation is to provide a fairly complete reference source of uninterpreted data.

Part of the following presentation will be in the form of data plots to provide an overall picture of the progress of the test. Much of this graphical information is backed up by exhaustive computer-acquired data listings which are stored on magnetic data tapes. For example, the temperature-time and pressure-time curves are plotted from readings taken at 0.05-sec intervals during the temperature transient. Tabular data are presented where detail is deemed important, for example, the conditions of the bundle at the time of each tube rupture.

4.1 Transient Results

4.1.1 Bundle average behavior

The information contained in this section was obtained during the course of the B-2 test transient. The data were recorded by the data acquisition system in the continuous scan mode (i.e., 10,000 samples/sec; ~100 sensors) over a period of about 10 min. Each rod was instrumented with four thermocouples attached to the interior surface at various elevations (see Fig. 5) above the bottom of the heated zone. In addition, the heated shroud was monitored by 12 thermocouples attached to its outer surface. These locations are shown in Fig. 4. Average bundle and shroud temperatures and heating rates were obtained by averaging the thermocouple measurements in various combinations.

Figure 8 shows the average bundle and shroud temperatures and the bundle-shroud temperature difference as a function of heating time, until the first tube burst. Figure 9 shows the average bundle and shroud heating rates as a function of heating time over the same period. The pressure of rod 8 (the first to burst) is shown in the figure for reference. Figure 10 shows the average temperature of the bundle over a much longer portion of the test.

The radial distribution was obtained by averaging certain thermocouple measurements, as shown in Fig. 11. The axial distribution was obtained by averaging thermocouple measurements at various elevations in the bundle. The axial and radial distributions are shown in Figs. 12 and 13, respectively, for times up until the first tube burst. The number of measurements averaged to obtain the plotted data points are indicated in each of the figures.

The axial distribution of the tube bursts is noted on the right side of Fig. 12; however, burst times and temperatures are not depicted in this figure. Figure 14 shows (until the end of the continuous data scan) the axial temperature distribution during the posttest cooldown. The dashed lines indicate the distribution at the time of the first tube burst (17.80 sec) and the time power was terminated (20.35 sec).

4.1.2 Pressure and temperature plots as a function of time

Individual pressure and temperature curves for the simulators are shown in Figs. 15 through 30. These curves were computer-plotted at 0.05-sec intervals from the magnetic data storage tapes. Each of the figures is comprised of four temperature plots (corresponding to the four thermocouples attached to the individual simulator) and one pressure curve. Thermocouple identification in the figures follows the numbering scheme shown in Figs. 4 and 5.

In general, the burst time for each simulator can be detected by the sudden drop in the pressure curve. This is also reflected in the temperature curves as sudden changes in their slopes. The time of maximum pressure (see Table 4) is also the time at which the major expansion of the rod began. Subsequent plastic deformation caused a continuing decrease in pressure until rupture occurred. The behavior of simulator 9 was different (e.g., compare Figs. 23 and 24) due to a leak that developed prior to the transient.

4.1.3 Bundle conditions at the time of rupture

The preceding section showed graphically the progress of the B-2 bundle through the test transient. Qualitative information on burst-time, temperature, etc., can be obtained from the various figures, but more

quantitative information on the bundle conditions at the individual burst times is given in Tables 6 through 21. These tables (computer printouts from the data tape) list the times from power-on and power-off for which the tabulation was made, the simulator differential pressure, simulator temperatures (with minimum, maximum, and average values), and times from the other tube bursts (relative to that for which the table pertains). Pertinent miscellaneous data are also printed out. These include shroud temperatures (TE 17-1 through TE 19-4), steam inlet (TE-304) and exit (TE-305) temperatures, vessel pressure (PE-301), bundle current (EIE-10), and bundle voltage (EEE-10). The thermocouples for measuring steam temperature (TE-304 and TE-305) were positioned (the same as in the B-1 test) such that they did not provide true values. In comparing the various simulators, it should be noted that the No. 9 simulator behaved abnormally due to partial depressurization.

4.2 Pretest and Posttest Results

The information contained in this section was obtained from the pretest and posttest examinations of the B-2 test array. Some information, such as the simulator infrared scans,[10] resulted from quality assurance efforts made to characterize the test components. Other information, such as bundle cross-section photographs, were obtained as a step in the posttest examination of the bundle. The results are presented in considerable detail, since we believe these data are extremely important to the interpretation of the test in terms of deformation behavior and distribution.

4.2.1 Pretest bundle photographs

Although not directly applicable to the interpretation of the B-2 test, selected photographs of the bundle assembly are included in this section for general interest. Various details of the grid spacers, pressure lines, and monitoring instrumentation may be seen.

The shroud assembly for B-1 was modified for the B-2 test. These modifications, which are consistent with test objectives, included (1) bypassing the shroud with the current from the bundle and (2) replacing the laminated alumina-silica insulation board around the shroud with a combination gas-gap and reflective-type insulation, as shown previously in

Fig. 2. The shroud thermocouples were also revised in type and number. Since the shroud was not electrically heated, it was unnecessary to provide isolation of the thermocouples attached to it. Twelve 0.71-mm-OD, stainless-steel-sheathed, type K (with ungrounded duckbill junction) thermocouples were spot-welded to the outside surface of the unheated shroud surrounding the rod array at the locations given in Fig. 4.

Figure 31 shows the B-2 test array just prior to installation of the unheated shroud. One face of the shroud box with the gas-gap reflective insulation is shown beneath the array. Portions of the original laminated alumina-silica board remain at the upper and lower ends to prevent bypassing of steam flow around the bundle. The spacers on the shroud box are standoffs (see Fig. 2) machined from glass-bonded mica. These provide for spacing of the shroud and shroud box while presenting a minimum of contact area to the shroud. The white areas on the grid spacers are also laminated alumina-silica insulators.

Figure 32 shows the B-2 array completely assembled and ready to install in the burst test facility. The bundle current return conductors (nickel rods) are shown exiting through the upper flange instead of returning through the shroud as was done in the B-1 test.

4.2.2 Posttest bundle photographs

After the test was completed, B-2 was removed from the test vessel for examination. Figure 33 is an overall view of the bundle (above) and the shroud (below) after partial disassembly. The four grid spacers can be seen, as well as the heated length which appears as the shiny black region of the bundle.

The following photographs show all four faces of B-2 immediately after removal from the test vessel. A meter scale is provided to indicate distance along the bundle relative to the bottom of the original heated length. The faces are identified as N, E, S, and W, a nomenclature that was retained throughout all subsequent analysis of the test. Figures 34-A, 34-B, and 34-C show the north (N) face of B-2 and of the shroud. Several test effects are noticeable: (1) bursts and relatively large expansions occurred in two localized regions of the bundle, (2) the shroud was not particularly deformed by the bursts, (3) the heated zone

produced a shiny black surface, and (4) the rods in the bundle changed lengths by different amounts. The latter effect can be seen both in the surface discoloration at the lower end and in the different positions of the lower end fittings. (These were aligned prior to the test.) Figures 35, 36, and 37 show similar views of the east, south, and west faces, respectively, of the bundle and shroud. Comments about Fig. 34 apply equally to these photographs.

Figure 38 is a close-up of the lower end of the bundle and illustrates the different length changes (see Table 22) among the rods. All rods were originally of equal length. This phenomenon is caused by the preferred orientation or texture of the Zircaloy combined with burst temperatures in the α-phase, and it is discussed in Ref. 11.

Following preliminary examination, photography, and flow testing (to be described later), the bundle was encapsulated in epoxy for sectioning. Figure 39 shows a marked bundle (test B-2) and a sectioned bundle (test B-1). The scribed lines across the face of the bundle indicate the positions at which the sections were subsequently cut. The longitudinal line and the angled longitudinal line aided in positioning the cut sections relative to the heated length. Four typical cut sections are shown at the bottom of the photograph.

4.2.3 Bundle cross section photographs

The encapsulated bundle was sectioned at 53 axial positions, and each of the sections was photographed for strain determinations. Figures 40 through 92 present photographs (~1×) of all the cross sections. The series starts at a section 6.9 cm below the start of the heated length (i.e., in the undeformed region) and continues to a section 91.5 cm above the start of that length, or approximately at the top of the heated length. The photographs were made (looking down on the surface at the given elevation) with the sections in the same relative position, i.e., with the No. 1 simulator in the upper left corner. Thus the photographs are oriented the same as the layout given in Fig. 4, which can be used to identify the individual tubes.

Starting with Fig. 42, all the figures have white arrow points in the upper left corner. The distance along the edge of the epoxy matrix

between the arrow points is proportional to the elevation of the section and can be used to calculate the height (above the bottom of the heated zone) at which the actual cut was made.

Figure 40, taken 6.9 cm below the bottom of the heated zone, is representative of the undeformed bundle. All the tubes had moderate strain peaks (a minimum of 8.3% on No. 16 and a maximum of 18.8% on No. 6) about halfway between the start of the heated zone and the lower grid (see Fig. 44). A section through the lower grid (at elevation 11.5 cm) is shown in Fig. 47; the restraining influence of the grid (due to lateral grid forces and/or local cooling of the tubes by the grid) is clearly evident by the range of strains (2.9 to 5.6%) observed in this section. Figure 51 shows localized wall thinning and distortion just below the burst in the No. 14 simulator, which is shown in Fig. 52.

Figure 58 shows a section representative of those in a broad minimum in the coolant channel flow area restriction that will be discussed later. The maximum burst strain (57.8%) occurred in the No. 6 simulator and is shown in Fig. 62. Localized wall thinning toward the interior of the bundle is evident on several of the simulators, particularly the corner ones, in this and a number of other sections. There is little evidence on the four interior rods of wall thinning toward the center of the bundle. Bursts in the outer ring of simulators tend to be directed toward adjacent rods or the bundle interior. These observations are consistent with the bundle radial temperature profile shown in Fig. 13.

4.2.4 Strain data and tube strain profiles

Strain measurements were obtained from enlarged (~5x) photographs of the sections, using the methodology reported for the B-1 test.[6] Table 23 tabulates the strains determined thusly for each tube in each section. The maximum observed strain was 57.8%; this occurred at the burst in the No. 6 simulator (Fig. 62). The minimum burst strain, 29.2%, was experienced by the No. 9 simulator (Fig. 83), which underwent partial depressurization (see Table 4) due to a leak during the test. The cross section with the maximum total deformation (sum of all tubes) is shown in Fig. 84.

The strain data were used to plot axial profiles of the individual tubes; these are presented in Figs. 93 through 108. The pretest infrared

characterization scans of the fuel simulators (internal heaters) and the axial positions of the thermocouples are also shown for reference purposes.

In general, the strain increases sharply at each end of the heated length, reflecting the strength associated with the sharp axial temperature gradients in these regions. The upper ends reflect the short thermal entrance region required to heat the incoming steam (~332°C) to near the tube surface temperature. The Reynolds number of the steam, based on inlet conditions and original tube dimensions, was 290; this is compared to a range of 600 to 800 used in our single-rod tests. The higher steam flow in the single-rod tests produced a longer thermal entrance region and suppressed deformation and bursts in the upper 20 cm of the heated zone of those tests. On the other hand, the short thermal entrance zone in the B-1 and B-2 tests caused higher temperatures in this region, resulting in deformation and bursts. This was demonstrated[3] by single-rod tests performed later with the fuel simulator (internal heater) from the No. 4 rod in the B-2 test.

All the profiles show about 5% strain in the grid positions (i.e., centered at the 10- and 66-cm elevations), reflecting grid restraint on the tubes and/or higher cladding strength at the lower temperature (see Fig. 12) in these regions. It should be noted that these effects influence the strain significantly for about 5 cm on either side of the grid. The strain profiles show good correlation with the pretest characterization scans. Considering the facts that (1) the grids had a strong restraining effect, (2) circumferential temperature gradients are known to exist in the fuel simulators, and (3) the characterization scans are for a single angular orientation, there is generally good agreement between the scans and the burst positions. Figure 95 for tube 3 would appear to be a notable exception; however, the scan for an adjacent quadrant (not included in this report) clearly shows a peak at the burst position.

Excessive ballooning over an extended length is of concern in LOCA analyses. For the tubes and spacing (10.92 mm OD on a 14.43-mm-square pitch; 1.32 pitch-to-diameter ratio) used in our tests, adjacent tubes will touch with 32% uniform expansion. Figure 109 plots those portions of each tube over which the strain exceeds 32%; maximum deformation in

tube 9, which leaked prior to the transient, was less than this value, as indicated in Fig. 101. In tube 6, greater than 32% expansion occurred over a length equal to about 15 tube (original) diameters; all the rest were relatively short (i.e., less than 7 tube diameters in length).

The volume increase over the heated length is perhaps a more meaningful characterization of the deformation with respect to coolant flow restriction. This parameter is related to (about a factor of 2 greater than) the average deformation and was obtained by integrating the individual deformation profiles, assuming circular cross sections. The data are summarized in Table 3.

The locations of the individual tube bursts are tabulated in Table 24; axial and angular distributions are depicted graphically in Figs. 110 and 111, respectively. A composite layout of the bursts, in which the tube-to-tube pitch is greatly exaggerated for clarity, is shown in Fig. 112. The angular orientations were difficult to determine from the burst cross sections; however, a study of the positions of maximum wall thinning in adjacent cross sections provided additional information to aid in defining the orientations. Thus, the data given in Table 24 are our best estimates of the burst locations.

Figures 111 and 112 show that the burst orientations of the inner ring of tubes were generally directed outward, while those in the outer ring of tubes were generally directed inward or toward adjacent tubes; none of the bursts were directed toward the shroud. This suggests that the relatively cold shroud had an effect on localizing wall thinning toward the interior of the bundle. No evidence was found to indicate the presence of burst propagation.

4.2.5 Coolant channel flow area restriction

As evident from the deformation profiles for the individual tubes, significant deformation was observed at a number of points. However, the total expansion for all the tubes at any cross section is much more important, since it determines the coolant channel flow area restriction.

One method for calculating the restriction is to consider unit cells centered about the open space between fuel rods; an alternative method considers unit cells centered about the fuel rods. Obviously, both

methods give the same results for infinite arrays, but, for small test arrays, different results will be obtained. The percentage of coolant channel flow area restriction was calculated with the rod-centered unit cell method, using the equation

$$B = 100 \times \frac{\sum_{n=16} (A_{d,n} - A_o)}{16\ (p^2 - A_o)} ,$$

where

B = percentage of restriction in coolant channel flow area,

$A_{d,n}$ = outside area of deformed tube (mm^2),

A_o = outside area of original tube (mm^2),

p = tube-to-tube pitch in square array (mm).

With this definition, B is zero for no deformation and 100 if all the tubes deform into a square whose sides are of length p (completely filling the open area). For the case of uniform ballooning such that the tubes just come into contact (i.e., 32% strain for the dimensions appropriate to this test), B is 61%.

In summing the deformed tube areas in the above equation for those sections that contain bursts, one must decide how to treat the burst tube flare-out. We used two definitions that appear to be reasonable upper and lower limits of the coolant channel flow area restriction. The first definition, which we believe is representative of the upper limit, consists of drawing straight lines between the ends of the tube flare-outs to establish a burst tube area, as illustrated in Fig. 113. Special consideration was given to those flare-outs that enclosed adjacent tubes to exclude overlapping areas, as noted by tube 4 in the figure. The second definition, which we believe is representative of the lower limit, considered the burst tube cross section as a circle (see tube 7 in the figure) with a perimeter equal to that of the tube. The latter definition is considered a reasonable approximation of the tube just before burst.

The deformed tube areas were obtained by the data analysis techniques reported[6] for the B-1 test. Table 25 gives the deformed tube areas,

$A_{d,n}$, for each tube at each section based on the first definition for the burst tube area, and Table 26 gives similar information based on the second definition. The last column (on the right side) gives the summation of the individual $A_{d,n}$. The summed areas were used in the above equation to calculate the coolant channel flow area restriction at each section; the results are given in Table 27 and plotted in Fig. 114 as a function of heated length. The flow channel restriction differs only in the sections where tube bursts occurred. The cross-sectional area occupied by the grids (~47 mm^2) was not included in the calculation; including this area would slightly increase the restriction at the grid locations (centered about elevations 10 and 66 cm). The maximum restriction (at elevation 76.2 cm) was 64 or 53%, depending on which method for handling the tube flare-out was used.

4.2.6 Flow test results

Flow tests were conducted with the B-2 test array in each of two flow shrouds. The first shroud, designated as shroud 1, was used previously for the B-1 flow tests. Prior to its use in the B-1 flow tests, it was modified somewhat from its original design in order to accommodate the B-1 tube burst flare-outs. One modification consisted of the substitution of a 0.80-cm-diam gasket for the original 0.32-cm-diam gasket used to seal the removable shroud coverplate to the shroud walls. While this modification provided additional clearance in one direction, relief grooves had to be cut into the shroud walls at three locations to obtain clearance for the B-1 tube bursts in the other direction. The effect of these modifications was not significant.[5] The tube 3 burst flare-out in the B-2 bundle (see Figs. 33, 34-A, and 37-A) was such that the bundle would not fit within shroud 1. Rather than machining another groove in the shroud (which would have interfered with the gasket seating surface), the flare-out was bent slightly, as shown in Fig. 115, to provide the necessary clearance.

To avoid the need for such modifications in the future a second (larger) shroud (designated as shroud 2) was constructed. Based on previous experience, its larger flow channel should accommodate burst tube flare-outs and yet be sufficiently close fitting to ensure easily

recognizable (but less pronounced) pressure losses induced by bundle deformation. Provisions were made to recess the sealing gasket so that the flow channel would more closely approximate a square cross section rather than a rectangle. To ensure the accurate centering of bundles in shroud 2, set screws were installed to position the lower bundle grid in place. The screws penetrate the shroud from the channel faces not housing the pressure taps to minimize adverse effects on the pressure loss measurements. Figures 116 and 117 show the orientation of the B-2 bundle in flow shrouds 1 and 2, respectively.

A reference (or dummy) bundle geometrically identical with respect to spacer-grid placement (after the burst tests) and tube OD (before the burst tests) was constructed and flow tested to provide a reference base for all 4 x 4 pressure loss measurements. The reference bundle was constructed from centerless-ground stainless steel rods and flow tested in shroud 1, as modified to accommodate the tube flare-outs of B-1, and in shroud 2.

The pressure taps for the flow tests were positioned as shown in Table 28 for shroud 1 and in Table 29 for shroud 2. The spacings are given relative to the average position of the lower end of the heated zone of B-2.

Flow test data are presented in the form of graphs and tables. The interpretative report[5] of the flow tests should be consulted for a detailed description of the test procedures and, more importantly, a discussion of the accuracy and precision of the test data. It should be noted that these data are for particular flow configurations, and extrapolation to other flow configurations should be made with care.

A total of ten flow tests were performed with shroud 1 — six on the reference bundle and four on the B-2 bundle. Figures 118 through 121 show comparisons of the average differential pressure loss profiles for the B-2 and reference bundles at four different nominal flow rates. Figures 122 and 123 show the results of two additional flow tests of the reference bundle. The pressure loss over the instrumented length of the bundle is plotted as a function of Reynolds number in Fig. 124 for the B-2 and the reference bundle in shroud 1. Least-squares fitted equations of the data are also given in the figure.

Tabulated data for the ten shroud 1 flow tests are given in Tables 30 through 39 relative to the bottom taps on each side of the flow shroud. These data were averaged, for each flow test, to produce the graphs in Figs. 118 through 121 and were used directly in Figs. 122 and 123.

Twelve flow tests were performed with shroud 2 — seven on the reference bundle and five on the B-2 bundle. Figures 125 through 129 show comparisons of the average differential pressure loss profiles for the B-2 and reference bundles at five different nominal flow rates. Figures 130 and 131 show the results of two additional flow tests of the reference bundle. The pressure loss over the instrumented length of the bundle is plotted as a function of Reynolds number in Fig. 132 for the B-2 and reference bundle in shroud 2. Least-squares fitted equations of the data are also given in the figure.

Tabulated data for the 12 shroud 2 flow tests are given in Tables 40 through 51 relative to the bottom taps on each side of the flow shroud. These data were averaged, for each flow test, to produce the graphs in Figs. 125 through 129 and were used directly in Figs. 130 and 131.

While the general shapes of the pressure loss profiles for B-2 in shroud 2 are very similar to those in shroud 1, the magnitudes of the pressure losses were much less in shroud 2 (compare Figs. 124 and 132). This resulted primarily from the larger (about 19%) water flow area in the nondeformed regions.

5. ACKNOWLEDGMENTS

Data presented in this report reflect the combined effort of a number of people over an extended period of time, spanning fabrication, testing, and pretest and posttest examination of the test array.

We wish to acknowledge the contribution of K. R. Carr for his careful attention to all the instrumentation and control aspects of the test; E. L. Biddle, J. N. Money, and C. Cross for assembly of the test array and for the many other necessary support tasks; F. R. Gibson for programming and operation of the computer-controlled data acquisition system; J. F. Mincey for conducting the flow tests; N. M. Atchley for sectioning and photographing the bundle cross sections; E. G. Sewell for programming and processing the strain data; the Fuel Pin Simulator Development Group, under the leadership of R. W. McCulloch, for development and procurement of the fuel simulators; and the many other groups and individuals who had a part in the successful fulfillment of the test objectives.

6. REFERENCES

1. R. H. Chapman, compiler, *Quick-look Report on MRBT No. 2 4 × 4 Bundle Burst Test,* Internal Report ORNL/MRBT-3 (November 1977).
2. R. H. Chapman, *Multirod Burst Test Program Progress Report for July–December 1977,* NUREG/CR-0103 (ORNL/NUREG/TM-200).
3. R. H. Chapman, *Multirod Burst Test Program Progress Report for January–March 1978,* NUREG/CR-0225 (ORNL/NUREG/TM-217).
4. R. H. Chapman, *Multirod Burst Test Program Progress Report for July–December 1978,* NUREG/CR-0655 (ORNL/NUREG/TM-297).
5. J. F. Mincey, *Steady-State Axial Pressure Losses Along the Exterior of Deformed Multirod Burst Test (MRBT) Bundles B-1 and B-2,* ORNL/NUREG/TM report (in preparation).
6. R. H. Chapman et al., *Bundle B-1 Test Data,* ORNL/NUREG/TM-322 (June 1979).
7. R. H. Chapman, compiler, *Characterization of Zircaloy-4 Tubing Procured for Fuel Cladding Research Programs,* ORNL/NUREG/TM-29 (July 1976).
8. W. E. Baucum and R. E. Dial, *An Apparatus for Spot Welding Sheathed Thermocouples to the Inside of Small-Diameter Tubes at Precise Locations,* ORNL/NUREG/TM-33 (August 1976).
9. R. H. Chapman, *Multirod Burst Test Program Progress Report for April–June 1977,* ORNL/NUREG/TM-135.
10. W. A. Simpson, Jr., et al., *Infrared Inspection and Characterization of Fuel-Pin Simulators,* ORNL/NUREG/TM-55 (November 1976).
11. R. H. Chapman, *Multirod Burst Test Program Quarterly Progress Report for January–March 1977,* ORNL/NUREG/TM-108.

Table 1. As-built data for fuel pin simulators used in B-2 test

Bundle position No.	Zircaloy tube serial No.	Internal heater[a]		Fuel pin simulator gas volume[b] (cm^3)
		Serial No.	Element resistance (Ω)	
1	0688	2828072	4.08	48.5
2	0003	2828082	4.07	49.7
3	0689	2828067	4.10	48.8
4	0004	2828079	4.05	49.4
5	0047	2828080	4.04	49.5
6	0690	2828071	4.04	48.9
7	0049	2828081	4.09	51.0
8	0695	2828083	4.04	49.5
9	0700	2828068	4.07	48.9
10	0002	2828069	4.15	49.8
11	0697	2828078	4.15	48.8
12	0048	2828073	4.12	50.1
13	0045	2828084	4.04	48.6
14	0698	2828064A	4.05	49.1
15	0046	2828086	4.18	49.6
16	0699	2828085	4.10	48.5

[a] All 16 internal heaters were fabricatd by SEMCO.

[b] The fuel pin simulator volume, measured at room temperature before assembly of the bundle, includes a pressure transducer and connecting tube identical to the test facility hookup for each simulator.

Table 2. Summary of burst test results

Rod No.	Initial conditions					Approximate maximum pressure differential (kPa)	Approximate burst conditions					Time (sec)	Burst temperature predicted from burst pressure[b] (°C)
	Differential pressure (kPa)	Temperature (°C)					Differential pressure (kPa)	Temperature[a] (°C)					
		TE-1	TE-2	TE-3	TE-4			TE-1	TE-2	TE-3	TE-4		
1	8810	334	335	334	335	9240	7700	790	803	825	870	18.30	846
2	8805	335	335	336	339	9220	7685	818	841	846	844	18.00	847
3	8795	333	334	332	336	9245	7560	852	853	845	826	18.30	849
4	8775	336	336	333	337	9205	7585	861	872	807	854	18.30	848
5	8775	333	334	336	336	9205	7770	854	866	835	852	17.85	845
6	8785	335	335	334	335	9220	6925	857	827	843	834	17.95	858
7	8740	334	333	333	333	9160	7360	824	861	838	850	17.85	852
8	8750	335	334	333	334	9200	7565	856	840	813	792	17.80	849
9[c]	7715[c]	335	334	332	335	7715[c]	6110[c]	928	846	864	871	20.05[c]	872
10	8730	334	334	332	334	9175	9345	827	862	827	856	18.10	852
11	8735	333	334	332	333	9165	7670	832	819	832	853	17.80	847
12	8760	336	334	334	333	9200	7545	851	832	829	827	18.15	849
13	8755	338	333	334	332	8175	7820	856	805	883	867	18.15	845
14	8755	333	334	334	335	9140	7230	828	858	832	855	18.30	854
15	8790	336	334	334	337	9205	7945	824	807	799	836	18.05	843
16	8790	333	334	333	334	9220	7700	848	839	795	814	18.15	846

[a] Underlined value is burst temperature based on premise that maximum measured value is minimum possible burst temperature.

[b] Based on burst temperature—burst pressure correlation from single-rod burst tests (external bare-wire thermocouples).

[c] Rod 9 developed a moderate leak prior to the test and its behavior is abnormal.

Table 3. Summary of B-2 test results related to volume changes

Rod No.	Initial gas volume[a] (cm^3)	Approximate burst condition			Fractional[b] pressure decrease	Fractional[c] volume increase	Volume increase[d] of tube over heated length (%)	Average strain[e] (%)
		Pressure (kPa)	Temperature (°C)	Strain (%)				
1	48.5	7700	870	35	1.14	1.56	31.8	15
2	49.7	7685	846	39	1.15	1.57	33.2	15
3	48.8	7560	853	40	1.16	1.74	42.0	19
4	49.4	7585	872	42	1.16	1.62	35.8	17
5	49.5	7770	866	35	1.13	1.56	32.6	15
6	48.9	6925	857	58	1.27	1.91	51.8	23
7	51.0	7360	861	56	1.19	1.69	41.2	19
8	49.5	7565	856	38	1.16	1.62	36.0	17
9[f]	48.9	6110[f]	928[f]	29[f]	1.26[f]	1.50[f]	28.7[f]	13[f]
10	49.8	7345	862	43	1.19	1.70	40.9	19
11	48.8	7670	853	40	1.14	1.59	33.4	15
12	50.1	7545	851	40	1.16	1.63	36.9	17
13	48.6	7820	867	41	1.12	1.52	29.4	14
14	49.1	7230	858	42	1.21	1.71	40.9	19
15	49.6	7945	836	35	1.11	1.49	28.5	13
16	48.5	7700	848	42	1.14	1.56	31.7	15

[a]Measured at room temperature; includes fuel pin simulator (FPS), pressure transducer, and connecting tube.

[b]Ratio of initial pressure to burst pressure.

[c]Ratio of final to initial gas volume; includes FPS, pressure transducer, and connecting tube.

[d]Obtained from deformation profiles assuming circular cross sections.

[e]Assumes volume increase is uniformly distributed over heated length.

[f]Tube developed moderate leak prior to transient; deformation behavior is abnormal.

Table 4. Summary of maximum pressures

ROD NO.	INITIAL CONDITIONS					CONDITIONS AT TIME OF MAXIMUM PRESSURES					
	DIFFERENTIAL PRESSURE (KPA)	TEMPERATURES (DEG C)				DIFFERENTIAL PRESSURE (KPA)	TEMPERATURES (DEG C)				TIME (SEC)
		TE-1	TE-2	TE-3	TE-4		TE-1	TE-2	TE-3	TE-4	
1	8810.9	334.1	335.0	334.1	335.0	9238.1	653.3	665.3	668.1	670.9	11.15
2	8807.5	335.0	335.0	336.0	338.8	9218.9	682.1	691.4	686.7	670.9	11.80
3	8793.1	333.2	334.1	332.3	336.0	9244.0	682.1	676.5	675.5	674.6	11.50
4	8774.1	336.0	336.0	333.2	336.9	9202.6	705.3	705.3	699.7	707.2	12.45
5	8776.3	333.2	334.1	336.0	336.0	9205.2	682.1	682.1	679.3	673.7	11.65
6	8783.6	335.0	335.0	334.1	335.0	9218.5	682.1	683.0	693.2	689.5	11.70
7	8739.3	334.1	333.2	333.2	333.2	9160.3	658.9	671.8	662.6	668.1	11.35
8	8747.8	335.0	334.1	333.2	334.1	9201.8	686.7	679.3	674.6	666.3	11.20
9	7744.0	335.0	334.1	332.3	335.0	7716.6	367.5	353.6	352.7	361.0	1.20
10	8728.4	334.1	334.1	332.3	334.1	9174.5	674.6	683.9	674.6	680.2	11.80
11	8735.7	333.2	334.1	332.3	333.2	9164.3	680.2	667.2	677.4	668.1	11.60
12	8759.5	336.0	334.1	334.1	333.2	9198.8	689.5	686.7	668.1	667.2	11.75
13	8754.4	337.8	333.2	334.1	332.3	9176.6	702.5	689.5	707.2	698.8	12.45
14	8752.6	333.2	334.1	333.2	335.0	9139.0	649.6	674.6	672.8	663.5	11.15
15	8790.8	336.0	334.1	334.1	336.9	9206.9	670.0	689.5	671.8	691.4	11.95
16	8791.6	333.2	334.1	333.2	334.1	9220.9	682.1	672.8	673.7	659.8	11.55

Table 5. Distribution of bursts with time in B-2 test[a]

Time (sec)	Number of bursts	Simulator No.
17.80	2	8, 11
17.85	2	5, 7
17.90	0	
17.95	1	6
18.00	1	2
18.05	1	15
18.10	1	10
18.15	3	12, 13, 16
18.20	0	
18.25	0	
18.30	4	1, 3, 4, 14
20.05	1	9

[a]Power was terminated at 20.35 sec.

Table 6. Test conditions summary at rod 1 burst time

TIME FROM POWER-ON 18.30 SEC. TIME FROM POWER-OFF -2.05 SEC.

ROD NO.	DIFFERENTIAL PRESSURE (KPA)	TEMPERATURES (DEG C)							TIME FROM BURST (SEC)
		TE-1	TE-2	TE-3	TE-4	MINIMUM	MAXIMUM	AVERAGE	
1	7698.9	790.2	802.6	824.6	870.1	790.2	870.1	821.9	0.00
2	704.0	813.1	841.0	851.6	843.9	813.1	851.6	837.4	0.30
3	7259.6	851.6	852.6	844.9	825.6	825.6	852.6	843.7	0.00
4	7587.1	861.3	872.0	807.4	853.6	807.4	872.0	848.6	0.00
5	403.7	858.4	854.6	842.0	827.5	827.5	858.4	845.6	0.45
6	459.5	864.3	832.3	842.9	836.2	832.3	864.3	843.9	0.35
7	333.0	829.5	862.3	841.0	841.0	829.5	862.3	843.4	0.45
8	144.7	850.7	841.0	820.8	805.5	805.5	850.7	829.5	0.50
9	6772.8	883.7	819.8	839.1	842.9	819.8	883.7	846.4	-1.75
10	2045.9	832.3	851.6	827.5	861.3	827.5	861.3	843.2	0.20
11	385.5	835.2	824.6	840.1	863.3	824.6	863.3	840.8	0.50
12	3254.9	839.1	824.6	807.4	804.5	804.5	839.1	818.9	0.15
13	2511.8	831.4	797.8	870.1	864.3	797.8	870.1	840.9	0.15
14	7231.8	828.5	858.4	832.3	855.5	828.5	858.4	843.7	0.00
15	1582.6	823.7	807.4	794.0	823.7	794.0	823.7	812.2	0.25
16	2262.1	844.9	813.1	798.8	818.9	798.8	844.9	818.9	0.15

MISCELLANEOUS INSTRUMENTS

58	TE-305	323.8 DEG C	124	TE-17-1	506.1 DEG C	125	TE-17-2	501.5 DEG C
126	TE-17-3	516.1 DEG C	127	TE-17-4	503.3 DEG C	136	TE-18-1	486.8 DEG C
137	TE-18-2	464.8 DEG C	138	TE-18-3	506.1 DEG C	139	TE-18-4	499.7 DEG C
140	TE-19-1	488.7 DEG C	141	TE-19-2	486.8 DEG C	142	TE-19-3	515.2 DEG C
143	TE-19-4	454.7 DEG C	457	PE-301	255.2 KPA	472	EIE-10	737.5 AMPS
473	EEE-10	199.0 VOLTS	478	TE-304	331.9 DEG C			

Table 7. Test conditions summary at rod 2 burst time

TIME FROM POWER-ON 18.00 SEC. TIME FROM POWER-OFF -2.35 SEC.

ROD NO.	DIFFERENTIAL PRESSURE (KPA)	TEMPERATURES (DEG C)							TIME FROM BURST (SEC)
		TE-1	TE-2	TE-3	TE-4	MINIMUM	MAXIMUM	AVERAGE	
1	8014.9	795.0	804.5	821.8	865.2	795.0	865.2	821.6	-0.30
2	7682.6	817.9	841.0	845.8	843.9	817.9	845.8	837.2	0.00
3	7703.9	856.5	848.7	844.9	839.1	839.1	856.5	847.3	-0.30
4	7986.2	853.6	864.3	805.5	852.6	805.5	864.3	844.0	-0.30
5	3502.6	853.6	846.8	831.4	834.3	831.4	853.6	841.5	0.15
6	5527.2	854.6	826.6	838.1	832.3	826.6	854.6	837.9	0.05
7	3162.9	818.9	853.6	833.3	840.1	818.9	853.6	836.5	0.15
8	1694.4	849.7	833.3	813.1	801.7	801.7	849.7	824.5	0.20
9	6886.1	874.9	820.8	834.3	838.1	820.8	874.9	842.0	-2.05
10	7503.7	822.7	864.3	823.7	854.6	822.7	864.3	841.3	-0.10
11	2715.6	823.7	817.0	829.5	852.6	817.0	852.6	830.7	0.20
12	7756.4	847.8	831.4	831.4	842.9	831.4	847.8	838.4	-0.15
13	7986.7	852.6	804.5	879.8	862.3	804.5	879.8	849.8	-0.15
14	7632.6	823.7	866.2	826.6	853.6	823.7	866.2	842.5	-0.30
15	8006.3	822.7	806.4	798.8	834.3	798.8	834.3	815.6	-0.05
16	7907.6	849.7	850.7	794.0	822.7	794.0	850.7	829.3	-0.15

MISCELLANEOUS INSTRUMENTS

58	TE-305	323.3 DEG C	124	TE-17-1	492.3 DEG C	125	TE-17-2	493.2 DEG C
126	TE-17-3	507.0 DEG C	127	TE-17-4	494.2 DEG C	136	TE-18-1	478.6 DEG C
137	TE-18-2	459.3 DEG C	138	TE-18-3	496.9 DEG C	139	TE-18-4	490.5 DEG C
140	TE-19-1	482.2 DEG C	141	TE-19-2	479.5 DEG C	142	TE-19-3	500.6 DEG C
143	TE-19-4	445.4 DEG C	457	PE-301	226.5 KPA	472	EIE-10	736.9 AMPS
473	EEE-10	199.0 VOLTS	478	TE-304	331.6 DEG C			

Table 8. Test conditions summary at rod 3 burst time

TIME FROM POWER-ON 18.30 SEC. TIME FROM POWER-OFF -2.05 SEC.

ROD NO.	DIFFERENTIAL PRESSURE (KPA)	TEMPERATURES (DEG C) TE-1	TE-2	TE-3	TE-4	MINIMUM	MAXIMUM	AVERAGE	TIME FROM BURST (SEC)
1	7698.9	790.2	802.6	824.6	870.1	790.2	870.1	821.9	0.00
2	704.0	813.1	841.0	851.6	843.9	813.1	851.6	837.4	0.30
3	7259.6	851.6	852.6	844.9	825.6	825.6	852.6	843.7	0.00
4	7587.1	861.3	872.0	807.4	853.6	807.4	872.0	848.6	0.00
5	403.7	858.4	854.6	842.0	827.5	827.5	858.4	845.6	0.45
6	459.5	864.3	832.3	842.9	836.2	832.3	864.3	843.9	0.35
7	333.0	829.5	862.3	841.0	841.0	829.5	862.3	843.4	0.45
8	144.7	850.7	841.0	820.8	805.5	805.5	850.7	829.5	0.50
9	6772.8	883.7	819.8	839.1	842.9	819.8	883.7	846.4	-1.75
10	2045.9	832.3	851.6	827.5	861.3	827.5	861.3	843.2	0.20
11	385.5	835.2	824.6	840.1	863.3	824.6	863.3	840.8	0.50
12	3254.9	839.1	824.6	807.4	804.5	804.5	839.1	818.9	0.15
13	2511.8	831.4	797.8	870.1	864.3	797.8	870.1	840.9	0.15
14	7231.8	828.5	858.4	832.3	855.5	828.5	858.4	843.7	0.00
15	1582.6	823.7	807.4	794.0	823.7	794.0	823.7	812.2	0.25
16	2262.1	844.9	813.1	798.8	818.9	798.8	844.9	818.9	0.15

MISCELLANEOUS INSTRUMENTS

58	TE-305	323.8 DEG C	124	TE-17-1	506.1 DEG C	125	TE-17-2	501.5 DEG C
126	TE-17-3	516.1 DEG C	127	TE-17-4	503.3 DEG C	136	TE-18-1	486.8 DEG C
137	TE-18-2	464.8 DEG C	138	TE-18-3	506.1 DEG C	139	TE-18-4	499.7 DEG C
140	TE-19-1	488.7 DEG C	141	TE-19-2	486.8 DEG C	142	TE-19-3	515.2 DEG C
143	TE-19-4	454.7 DEG C	457	PE-301	255.2 KPA	472	EIE-10	737.5 AMPS
473	EEE-10	199.0 VOLTS	478	TE-304	331.9 DEG C			

Table 9. Test conditions summary at rod 4 burst time

TIME FROM POWER-ON 18.30 SEC. TIME FROM POWER-OFF -2.05 SEC.

ROD NO.	DIFFERENTIAL PRESSURE (KPA)	TEMPERATURES (DEG C)							TIME FROM BURST (SEC)
		TE-1	TE-2	TE-3	TE-4	MINIMUM	MAXIMUM	AVERAGE	
1	7698.9	790.2	802.6	824.6	870.1	790.2	870.1	821.9	0.00
2	704.0	813.1	841.0	851.6	843.9	813.1	851.6	837.4	0.30
3	7259.6	851.6	852.6	844.9	825.6	825.6	852.6	843.7	0.00
4	7587.1	861.3	872.0	807.4	853.6	807.4	872.0	848.6	0.00
5	403.7	858.4	854.6	842.0	827.5	827.5	858.4	845.6	0.45
6	459.5	864.3	832.3	842.9	836.2	832.3	864.3	843.9	0.35
7	333.0	829.5	862.3	841.0	841.0	829.5	862.3	843.4	0.45
8	144.7	850.7	841.0	820.8	805.5	805.5	850.7	829.5	0.50
9	6772.8	883.7	819.8	839.1	842.9	819.8	883.7	846.4	-1.75
10	2045.9	832.3	851.6	827.5	861.3	827.5	861.3	843.2	0.20
11	385.5	835.2	824.6	840.1	863.3	824.6	863.3	840.8	0.50
12	3254.9	839.1	824.6	807.4	804.5	804.5	839.1	818.9	0.15
13	2511.8	831.4	797.8	870.1	864.3	797.8	870.1	840.9	0.15
14	7231.8	828.5	858.4	832.3	855.5	828.5	858.4	843.7	0.00
15	1582.6	823.7	807.4	794.0	823.7	794.0	823.7	812.2	0.25
16	2262.1	844.9	813.1	798.8	818.9	798.8	844.9	818.9	0.15

****

MISCELLANEOUS INSTRUMENTS

58	TE-305	323.8 DEG C	124	TE-17-1	506.1 DEG C	125	TE-17-2	501.5 DEG C
126	TE-17-3	516.1 DEG C	127	TE-17-4	503.3 DEG C	136	TE-18-1	486.8 DEG C
137	TE-18-2	464.8 DEG C	138	TE-18-3	506.1 DEG C	139	TE-18-4	499.7 DEG C
140	TE-19-1	488.7 DEG C	141	TE-19-2	486.8 DEG C	142	TE-19-3	515.2 DEG C
143	TE-19-4	454.7 DEG C	457	PE-301	255.2 KPA	472	EIE-10	737.5 AMPS
473	EEE-10	199.0 VOLTS	478	TE-304	331.9 DEG C			

Table 10. Test conditions summary at rod 5 burst time

TIME FROM POWER-ON 17.85 SEC. TIME FROM POWER-OFF -2.50 SEC.

ROD NO.	DIFFERENTIAL PRESSURE (KPA)	TEMPERATURES (DEG C)							TIME FROM BURST (SEC)
		TE-1	TE-2	TE-3	TE-4	MINIMUM	MAXIMUM	AVERAGE	
1	8159.6	795.9	804.5	819.8	861.3	795.9	861.3	820.4	-0.45
2	7906.9	817.0	838.1	842.0	841.0	817.0	842.0	834.5	-0.15
3	7898.6	855.5	844.9	841.0	834.3	834.3	855.5	843.9	-0.45
4	8142.7	849.7	858.4	803.6	849.7	803.6	858.4	840.4	-0.45
5	7771.0	853.6	866.2	835.2	851.6	835.2	866.2	851.7	0.00
6	7143.6	856.5	825.6	842.9	835.2	825.6	856.5	840.1	-0.10
7	7360.2	823.7	861.3	838.1	849.7	823.7	861.3	843.2	0.00
8	6110.1	852.6	832.3	806.4	787.4	787.4	852.6	819.7	0.05
9	6939.9	874.9	817.9	831.4	834.3	817.9	874.9	839.6	-2.20
10	7727.0	817.9	860.4	821.8	851.6	817.9	860.4	837.9	-0.25
11	7443.1	828.5	817.9	832.3	850.7	817.9	850.7	832.4	0.05
12	7945.0	844.9	829.5	834.3	857.5	829.5	857.5	841.5	-0.30
13	8143.5	848.7	802.6	874.9	857.5	802.6	874.9	845.9	-0.30
14	7808.5	817.9	868.1	820.8	851.6	817.9	868.1	839.6	-0.45
15	8185.4	820.8	805.5	797.8	836.2	797.8	836.2	815.1	-0.20
16	8084.3	848.7	847.8	791.2	820.8	791.2	848.7	827.1	-0.30

****

MISCELLANEOUS INSTRUMENTS

58	TE-305	323.3 DEG C	124	TE-17-1	485.9 DEG C	125	TE-17-2	490.5 DEG C
126	TE-17-3	500.6 DEG C	127	TE-17-4	491.4 DEG C	136	TE-18-1	475.8 DEG C
137	TE-18-2	456.5 DEG C	138	TE-18-3	495.1 DEG C	139	TE-18-4	487.8 DEG C
140	TE-19-1	480.4 DEG C	141	TE-19-2	475.8 DEG C	142	TE-19-3	496.9 DEG C
143	TE-19-4	443.6 DEG C	457	PE-301	208.0 KPA	472	EIE-10	736.9 AMPS
473	EEE-10	199.0 VOLTS	478	TE-304	331.6 DEG C			

Table 11. Test conditions summary at rod 6 burst time

TIME FROM POWER-ON 17.95 SEC. TIME FROM POWER-OFF -2.40 SEC.

ROD NO.	DIFFERENTIAL PRESSURE (KPA)	TEMPERATURES (DEG C)							TIME FROM BURST (SEC)
		TE-1	TE-2	TE-3	TE-4	MINIMUM	MAXIMUM	AVERAGE	
1	8070.7	795.0	804.5	820.8	864.3	795.0	864.3	821.1	-0.35
2	7760.3	817.9	841.0	844.9	842.9	817.9	844.9	836.7	-0.05
3	7767.0	857.5	847.8	846.8	837.2	837.2	857.5	847.3	-0.35
4	8043.8	852.6	862.3	805.5	851.6	805.5	862.3	843.0	-0.35
5	5158.5	851.6	842.9	830.4	837.2	830.4	851.6	840.5	0.10
6	6925.0	857.5	826.6	842.9	834.3	826.6	857.5	840.3	0.00
7	4769.1	817.9	852.6	833.3	841.0	817.9	852.6	836.2	0.10
8	2537.4	849.7	831.4	811.2	798.8	798.8	849.7	822.8	0.15
9	6907.0	874.0	819.8	833.3	837.2	819.8	874.0	841.1	-2.10
10	7583.6	820.8	864.3	822.7	853.6	820.8	864.3	840.3	-0.15
11	3794.3	821.8	815.0	827.5	849.7	815.0	849.7	828.5	0.15
12	7819.9	846.8	831.4	833.3	848.7	831.4	848.7	840.1	-0.20
13	8029.8	851.6	803.6	878.8	860.4	803.6	878.8	848.6	-0.20
14	7689.4	821.8	869.1	824.6	852.6	821.8	869.1	842.0	-0.35
15	8071.4	822.7	806.4	798.8	836.2	798.8	836.2	816.0	-0.10
16	7974.6	849.7	849.7	792.1	821.8	792.1	849.7	828.3	-0.20

****

MISCELLANEOUS INSTRUMENTS

58	TE-305	323.8 DEG C	124	TE-17-1	489.6 DEG C	125	TE-17-2	492.3 DEG C
126	TE-17-3	505.1 DEG C	127	TE-17-4	494.2 DEG C	136	TE-18-1	477.7 DEG C
137	TE-18-2	457.4 DEG C	138	TE-18-3	496.0 DEG C	139	TE-18-4	489.6 DEG C
140	TE-19-1	482.2 DEG C	141	TE-19-2	478.6 DEG C	142	TE-19-3	499.7 DEG C
143	TE-19-4	445.4 DEG C	457	PE-301	219.8 KPA	472	EIE-10	737.5 AMPS
473	EEE-10	199.0 VOLTS	478	TE-304	331.6 DEG C			

Table 12. Test conditions summary at rod 7 burst time

TIME FROM POWER-ON 17.85 SEC. TIME FROM POWER-OFF -2.50 SEC.

ROD NO.	DIFFERENTIAL PRESSURE (KPA)	TEMPERATURES (DEG C)							TIME FROM BURST (SEC)
		TE-1	TE-2	TE-3	TE-4	MINIMUM	MAXIMUM	AVERAGE	
1	8159.6	795.9	804.5	819.8	861.3	795.9	861.3	820.4	-0.45
2	7906.9	817.0	838.1	842.0	841.0	817.0	842.0	834.5	-0.15
3	7898.6	855.5	844.9	841.0	834.3	834.3	855.5	843.9	-0.45
4	8142.7	849.7	858.4	803.6	849.7	803.6	858.4	840.4	-0.45
5	7771.0	853.6	866.2	835.2	851.6	835.2	866.2	851.7	0.00
6	7143.6	856.5	825.6	842.9	835.2	825.6	856.5	840.1	-0.10
7	7360.2	823.7	861.3	838.1	849.7	823.7	861.3	843.2	0.00
8	6110.1	852.6	832.3	806.4	787.4	787.4	852.6	819.7	0.05
9	6939.9	874.9	817.9	831.4	834.3	817.9	874.9	839.6	-2.20
10	7727.0	817.9	860.4	821.8	851.6	817.9	860.4	837.9	-0.25
11	7443.1	828.5	817.9	832.3	850.7	817.9	850.7	832.4	0.05
12	7945.0	844.9	829.5	834.3	857.5	829.5	857.5	841.5	-0.30
13	8143.5	848.7	802.6	874.9	857.5	802.6	874.9	845.9	-0.30
14	7808.5	817.9	868.1	820.8	851.6	817.9	868.1	839.6	-0.45
15	8185.4	820.8	805.5	797.8	836.2	797.8	836.2	815.1	-0.20
16	8084.3	848.7	847.8	791.2	820.8	791.2	848.7	827.1	-0.30

MISCELLANEOUS INSTRUMENTS

58	TE-305	323.3 DEG C	124	TE-17-1	485.9 DEG C	125	TE-17-2	490.5 DEG C
126	TE-17-3	500.6 DEG C	127	TE-17-4	491.4 DEG C	136	TE-18-1	475.8 DEG C
137	TE-18-2	456.5 DEG C	138	TE-18-3	495.1 DEG C	139	TE-18-4	487.8 DEG C
140	TE-19-1	480.4 DEG C	141	TE-19-2	475.8 DEG C	142	TE-19-3	496.9 DEG C
143	TE-19-4	443.6 DEG C	457	PE-301	208.0 KPA	472	EIE-10	736.9 AMPS
473	EEE-10	199.0 VOLTS	478	TE-304	331.6 DEG C			

Table 13. Test conditions summary at rod 8 burst time

TIME FROM POWER-ON 17.80 SEC. TIME FROM POWER-OFF -2.55 SEC.

ROD NO.	DIFFERENTIAL PRESSURE (KPA)	TEMPERATURES (DEG C)							TIME FROM BURST (SEC)
		TE-1	TE-2	TE-3	TE-4	MINIMUM	MAXIMUM	AVERAGE	
1	8214.9	795.9	804.5	819.8	860.4	795.9	860.4	820.2	-0.50
2	7969.9	816.0	837.2	840.1	839.1	816.0	840.1	833.1	-0.20
3	7961.3	854.6	843.9	836.2	833.3	833.3	854.6	842.0	-0.50
4	8207.1	847.8	857.5	802.6	848.7	802.6	857.5	839.1	-0.50
5	7840.6	851.6	864.3	834.3	852.6	834.3	864.3	850.7	-0.05
6	7228.4	855.5	824.6	842.9	835.2	824.6	855.5	839.6	-0.15
7	7453.7	822.7	859.4	837.2	848.7	822.7	859.4	842.0	-0.05
8	7565.2	856.5	840.1	813.1	792.1	792.1	856.5	825.4	0.00
9	6960.3	874.0	817.0	830.4	833.3	817.0	874.0	838.7	-2.25
10	7799.2	817.0	859.4	819.8	851.6	817.0	859.4	837.0	-0.30
11	7670.8	832.3	818.9	832.3	852.6	818.9	852.6	834.0	0.00
12	8008.0	843.9	828.5	835.2	857.5	828.5	857.5	841.3	-0.35
13	8186.2	847.8	803.6	874.0	854.6	803.6	874.0	845.0	-0.35
14	7864.9	816.0	865.2	819.8	848.7	816.0	865.2	837.5	-0.50
15	8235.5	819.8	805.5	797.8	835.2	797.8	835.2	814.6	-0.25
16	8135.8	847.8	846.8	791.2	820.8	791.2	847.8	826.6	-0.35

****

MISCELLANEOUS INSTRUMENTS

58	TE-305	323.8 DEG C	124	TE-17-1	485.0 DEG C	125	TE-17-2	489.6 DEG C
126	TE-17-3	499.7 DEG C	127	TE-17-4	491.4 DEG C	136	TE-18-1	474.9 DEG C
137	TE-18-2	455.6 DEG C	138	TE-18-3	495.1 DEG C	139	TE-18-4	487.8 DEG C
140	TE-19-1	479.5 DEG C	141	TE-19-2	475.8 DEG C	142	TE-19-3	496.9 DEG C
143	TE-19-4	442.7 DEG C	457	PE-301	201.7 KPA	472	EIE-10	737.5 AMPS
473	EEE-10	199.0 VOLTS	478	TE-304	331.9 DEG C			

Table 14. Test conditions summary at rod 9 burst time

TIME FROM POWER-ON 20.05 SEC. TIME FROM POWER-OFF -0.30 SEC.

ROD NO.	DIFFERENTIAL PRESSURE (KPA)	TEMPERATURES (DEG C)							TIME FROM BURST (SEC)
		TE-1	TE-2	TE-3	TE-4	MINIMUM	MAXIMUM	AVERAGE	
1	24.2	831.4	832.3	865.2	850.7	831.4	865.2	844.9	1.75
2	15.9	844.9	879.8	887.6	851.6	844.9	887.6	866.0	2.05
3	21.9	862.3	890.6	883.7	832.3	832.3	890.6	867.2	1.75
4	10.1	891.5	885.7	832.3	875.9	832.3	891.5	871.4	1.75
5	24.3	884.7	884.7	885.7	851.6	851.6	885.7	876.7	2.20
6	24.8	903.3	866.2	877.9	866.2	866.2	903.3	878.4	2.10
7	28.0	869.1	898.4	874.9	872.0	869.1	898.4	878.6	2.20
8	22.9	875.9	879.8	847.8	826.6	826.6	879.8	857.5	2.25
9	6110.5	927.9	845.8	864.3	871.1	845.8	927.9	877.3	0.00
10	26.1	869.1	870.1	865.2	910.2	865.2	910.2	878.6	1.95
11	21.9	874.9	861.3	882.7	905.3	861.3	905.3	881.1	2.25
12	14.6	866.2	860.4	851.6	820.8	820.8	866.2	849.8	1.90
13	21.5	892.5	838.1	920.0	911.2	838.1	920.0	890.4	1.90
14	22.6	839.1	862.3	859.4	856.5	839.1	862.3	854.3	1.75
15	24.9	865.2	831.4	818.9	869.1	818.9	869.1	846.1	2.00
16	21.1	874.9	862.3	849.7	854.6	849.7	874.9	860.4	1.90

****

MISCELLANEOUS INSTRUMENTS

58	TE-305	326.6 DEG C	124	TE-17-1	551.0 DEG C	125	TE-17-2	536.3 DEG C
126	TE-17-3	560.2 DEG C	127	TE-17-4	544.6 DEG C	136	TE-18-1	530.8 DEG C
137	TE-18-2	493.2 DEG C	138	TE-18-3	561.1 DEG C	139	TE-18-4	539.1 DEG C
140	TE-19-1	533.5 DEG C	141	TE-19-2	530.8 DEG C	142	TE-19-3	574.9 DEG C
143	TE-19-4	497.8 DEG C	457	PE-301	247.2 KPA	472	EIE-10	736.2 AMPS
473	EEE-10	199.0 VOLTS	478	TE-304	331.6 DEG C			

Table 15. Test conditions summary at rod 10 burst time

TIME FROM POWER-ON 18.10 SEC. TIME FROM POWER-OFF -2.25 SEC.

ROD NO.	DIFFERENTIAL PRESSURE (KPA)	TEMPERATURES (DEG C)							TIME FROM BURST (SEC)
		TE-1	TE-2	TE-3	TE-4	MINIMUM	MAXIMUM	AVERAGE	
1	7923.7	793.1	803.6	821.8	867.2	793.1	867.2	821.4	-0.20
2	3530.6	808.3	835.2	842.0	840.1	808.3	842.0	831.4	0.10
3	7577.0	855.5	850.7	844.9	835.2	835.2	855.5	846.6	-0.20
4	7870.1	856.5	868.1	806.4	852.6	806.4	868.1	845.9	-0.20
5	1714.1	857.5	851.6	835.2	831.4	831.4	857.5	843.9	0.25
6	2265.9	854.6	827.5	837.2	834.3	827.5	854.6	838.4	0.15
7	1504.4	822.7	858.4	836.2	841.0	822.7	858.4	839.6	0.25
8	793.4	849.7	835.2	816.0	802.6	802.6	849.7	825.9	0.30
9	6850.7	874.0	819.8	836.2	838.1	819.8	874.0	842.0	-1.95
10	7343.0	826.6	862.3	826.6	856.5	826.6	862.3	843.0	0.00
11	1436.3	828.5	819.8	833.3	857.5	819.8	857.5	834.8	0.30
12	7621.7	849.7	833.3	829.5	832.3	829.5	849.7	836.2	-0.05
13	7870.4	854.6	805.5	881.8	865.2	805.5	881.8	851.8	-0.05
14	7510.9	824.6	854.6	829.5	855.5	824.6	855.5	841.0	-0.20
15	7261.5	821.8	801.7	795.0	827.5	795.0	827.5	811.5	0.05
16	7779.9	847.8	848.7	795.0	822.7	795.0	848.7	828.6	-0.05

MISCELLANEOUS INSTRUMENTS

58	TE-305	323.8 DEG C	124	TE-17-1	497.8 DEG C	125	TE-17-2	496.0 DEG C
126	TE-17-3	510.6 DEG C	127	TE-17-4	496.9 DEG C	136	TE-18-1	481.3 DEG C
137	TE-18-2	461.1 DEG C	138	TE-18-3	499.7 DEG C	139	TE-18-4	494.2 DEG C
140	TE-19-1	483.2 DEG C	141	TE-19-2	482.2 DEG C	142	TE-19-3	502.4 DEG C
143	TE-19-4	448.2 DEG C	457	PE-301	233.7 KPA	472	EIE-10	737.5 AMPS
473	EEE-10	199.0 VOLTS	478	TE-304	331.9 DEG C			

Table 16. Test conditions summary at rod 11 burst time

TIME FROM POWER-ON 17.80 SEC. TIME FROM POWER-OFF -2.55 SEC.

ROD NO.	DIFFERENTIAL PRESSURE (KPA)	TEMPERATURES (DEG C)							TIME FROM BURST (SEC)
		TE-1	TE-2	TE-3	TE-4	MINIMUM	MAXIMUM	AVERAGE	
1	8214.9	795.9	804.5	819.8	860.4	795.9	860.4	820.2	-0.50
2	7969.9	816.0	837.2	840.1	839.1	816.0	840.1	833.1	-0.20
3	7961.3	854.6	843.9	836.2	833.3	833.3	854.6	842.0	-0.50
4	8207.1	847.8	857.5	802.6	848.7	802.6	857.5	839.1	-0.50
5	7840.6	851.6	864.3	834.3	852.6	834.3	864.3	850.7	-0.05
6	7228.4	855.5	824.6	842.9	835.2	824.6	855.5	839.6	-0.15
7	7453.7	822.7	859.4	837.2	848.7	822.7	859.4	842.0	-0.05
8	7565.2	856.5	840.1	813.1	792.1	792.1	856.5	825.4	0.00
9	6960.3	874.0	817.0	830.4	833.3	817.0	874.0	838.7	-2.25
10	7799.2	817.0	859.4	819.8	851.6	817.0	859.4	837.0	-0.30
11	7670.8	832.3	818.9	832.3	852.6	818.9	852.6	834.0	0.00
12	8008.0	843.9	828.5	835.2	857.5	828.5	857.5	841.3	-0.35
13	8186.2	847.8	803.6	874.0	854.6	803.6	874.0	845.0	-0.35
14	7864.9	816.0	865.2	819.8	848.7	816.0	865.2	837.5	-0.50
15	8235.5	819.8	805.5	797.8	835.2	797.8	835.2	814.6	-0.25
16	8135.8	847.8	846.8	791.2	820.8	791.2	847.8	826.6	-0.35

MISCELLANEOUS INSTRUMENTS

58	TE-305	323.8 DEG C	124	TE-17-1	485.0 DEG C	125	TE-17-2	489.6 DEG C
126	TE-17-3	499.7 DEG C	127	TE-17-4	491.4 DEG C	136	TE-18-1	474.9 DEG C
137	TE-18-2	455.6 DEG C	138	TE-18-3	495.1 DEG C	139	TE-18-4	487.8 DEG C
140	TE-19-1	479.5 DEG C	141	TE-19-2	475.8 DEG C	142	TE-19-3	496.9 DEG C
143	TE-19-4	442.7 DEG C	457	PE-301	201.7 KPA	472	EIE-10	737.5 AMPS
473	EEE-10	199.0 VOLTS	478	TE-304	331.9 DEG C			

Table 17. Test conditions summary at rod 12 burst time

TIME FROM POWER-ON 18.15 SEC. TIME FROM POWER-OFF -2.20 SEC.

ROD NO.	DIFFERENTIAL PRESSURE (KPA)	TEMPERATURES (DEG C)							TIME FROM BURST (SEC)
		TE-1	TE-2	TE-3	TE-4	MINIMUM	MAXIMUM	AVERAGE	
1	7868.3	794.0	802.6	823.7	867.2	794.0	867.2	821.9	-0.15
2	2317.2	810.3	835.2	844.9	840.1	810.3	844.9	832.6	0.15
3	7493.2	853.6	850.7	843.9	832.3	832.3	853.6	845.1	-0.15
4	7798.4	857.5	870.1	806.4	853.6	806.4	870.1	846.9	-0.15
5	1214.8	857.5	852.6	837.2	830.4	830.4	857.5	844.4	0.30
6	1510.0	856.5	828.5	837.2	835.2	828.5	856.5	839.3	0.20
7	1046.9	823.7	860.4	837.2	841.0	823.7	860.4	840.6	0.30
8	527.5	849.7	837.2	817.0	804.5	804.5	849.7	827.1	0.35
9	6830.3	874.0	820.8	837.2	840.1	820.8	874.0	843.0	-1.90
10	6012.6	825.6	857.5	824.6	852.6	824.6	857.5	840.1	0.05
11	1058.3	830.4	820.8	835.2	859.4	820.8	859.4	836.5	0.35
12	7544.5	850.7	832.3	829.5	826.6	826.6	850.7	834.8	0.00
13	7820.4	856.5	805.5	882.7	867.2	805.5	882.7	853.0	0.00
14	7447.3	826.6	855.5	829.5	856.5	826.6	856.5	842.0	-0.15
15	4946.6	819.8	803.6	791.2	819.8	791.2	819.8	808.6	0.10
16	7698.2	847.8	839.1	795.0	814.1	795.0	847.8	824.0	0.00

****

MISCELLANEOUS INSTRUMENTS

58	TE-305	323.8 DEG C	124	TE-17-1	498.7 DEG C	125	TE-17-2	496.9 DEG C
126	TE-17-3	510.6 DEG C	127	TE-17-4	498.7 DEG C	136	TE-18-1	483.2 DEG C
137	TE-18-2	461.1 DEG C	138	TE-18-3	499.7 DEG C	139	TE-18-4	494.2 DEG C
140	TE-19-1	484.1 DEG C	141	TE-19-2	483.2 DEG C	142	TE-19-3	503.3 DEG C
143	TE-19-4	450.0 DEG C	457	PE-301	240.0 KPA	472	EIE-10	737.5 AMPS
473	EEE-10	199.0 VOLTS	478	TE-304	332.2 DEG C			

Table 18. Test conditions summary at rod 13 burst time

TIME FROM POWER-ON 18.15 SEC. TIME FROM POWER-OFF -2.20 SEC.

ROD NO.	DIFFERENTIAL PRESSURE (KPA)	TEMPERATURES (DEG C)							TIME FROM BURST (SEC)
		TE-1	TE-2	TE-3	TE-4	MINIMUM	MAXIMUM	AVERAGE	
1	7868.3	794.0	802.6	823.7	867.2	794.0	867.2	821.9	-0.15
2	2317.2	810.3	835.2	844.9	840.1	810.3	844.9	832.6	0.15
3	7493.2	853.6	850.7	843.9	832.3	832.3	853.6	845.1	-0.15
4	7798.4	857.5	870.1	806.4	853.6	806.4	870.1	846.9	-0.15
5	1214.8	857.5	852.6	837.2	830.4	830.4	857.5	844.4	0.30
6	1510.0	856.5	828.5	837.2	835.2	828.5	856.5	839.3	0.20
7	1046.9	823.7	860.4	837.2	841.0	823.7	860.4	840.6	0.30
8	527.5	849.7	837.2	817.0	804.5	804.5	849.7	827.1	0.35
9	6830.3	874.0	820.8	837.2	840.1	820.8	874.0	843.0	-1.90
10	6012.6	825.6	857.5	824.6	852.6	824.6	857.5	840.1	0.05
11	1058.3	830.4	820.8	835.2	859.4	820.8	859.4	836.5	0.35
12	7544.5	850.7	832.3	829.5	826.6	826.6	850.7	834.8	0.00
13	7820.4	856.5	805.5	882.7	867.2	805.5	882.7	853.0	0.00
14	7447.3	826.6	855.5	829.5	856.5	826.6	856.5	842.0	-0.15
15	4946.6	819.8	803.6	791.2	819.8	791.2	819.8	808.6	0.10
16	7698.2	847.8	839.1	795.0	814.1	795.0	847.8	824.0	0.00

****

MISCELLANEOUS INSTRUMENTS

58	TE-305	323.8 DEG C	124	TE-17-1	498.7 DEG C	125	TE-17-2	496.9 DEG C
126	TE-17-3	510.6 DEG C	127	TE-17-4	498.7 DEG C	136	TE-18-1	483.2 DEG C
137	TE-18-2	461.1 DEG C	138	TE-18-3	499.7 DEG C	139	TE-18-4	494.2 DEG C
140	TE-19-1	484.1 DEG C	141	TE-19-2	483.2 DEG C	142	TE-19-3	503.3 DEG C
143	TE-19-4	450.0 DEG C	457	PE-301	240.0 KPA	472	EIE-10	737.5 AMPS
473	EEE-10	199.0 VOLTS	478	TE-304	332.2 DEG C			

Table 19. Test conditions summary at rod 14 burst time

TIME FROM POWER-ON 18.30 SEC. TIME FROM POWER-OFF -2.05 SEC.

ROD NO.	DIFFERENTIAL PRESSURE (KPA)	TEMPERATURES (DEG C)							TIME FROM BURST (SEC)
		TE-1	TE-2	TE-3	TE-4	MINIMUM	MAXIMUM	AVERAGE	
1	7698.9	790.2	802.6	824.6	870.1	790.2	870.1	821.9	0.00
2	704.0	813.1	841.0	851.6	843.9	813.1	851.6	837.4	0.30
3	7259.6	851.6	852.6	844.9	825.6	825.6	852.6	843.7	0.00
4	7587.1	861.3	872.0	807.4	853.6	807.4	872.0	848.6	0.00
5	403.7	858.4	854.6	842.0	827.5	827.5	858.4	845.6	0.45
6	459.5	864.3	832.3	842.9	836.2	832.3	864.3	843.9	0.35
7	333.0	829.5	862.3	841.0	841.0	829.5	862.3	843.4	0.45
8	144.7	850.7	841.0	820.8	805.5	805.5	850.7	829.5	0.50
9	6772.8	883.7	819.8	839.1	842.9	819.8	883.7	846.4	-1.75
10	2045.9	832.3	851.6	827.5	861.3	827.5	861.3	843.2	0.20
11	385.5	835.2	824.6	840.1	863.3	824.6	863.3	840.8	0.50
12	3254.9	839.1	824.6	807.4	804.5	804.5	839.1	818.9	0.15
13	2511.8	831.4	797.8	870.1	864.3	797.8	870.1	840.9	0.15
14	7231.8	828.5	858.4	832.3	855.5	828.5	858.4	843.7	0.00
15	1582.6	823.7	807.4	794.0	823.7	794.0	823.7	812.2	0.25
16	2262.1	844.9	813.1	798.8	818.9	798.8	844.9	818.9	0.15

****

MISCELLANEOUS INSTRUMENTS

58	TE-305	323.8 DEG C	124	TE-17-1	506.1 DEG C	125	TE-17-2	501.5 DEG C
126	TE-17-3	516.1 DEG C	127	TE-17-4	503.3 DEG C	136	TE-18-1	486.8 DEG C
137	TE-18-2	464.8 DEG C	138	TE-18-3	506.1 DEG C	139	TE-18-4	499.7 DEG C
140	TE-19-1	488.7 DEG C	141	TE-19-2	486.8 DEG C	142	TE-19-3	515.2 DEG C
143	TE-19-4	454.7 DEG C	457	PE-301	255.2 KPA	472	EIE-10	737.5 AMPS
473	EEE-10	199.0 VOLTS	478	TE-304	331.9 DEG C			

Table 20. Test conditions summary at rod 15 burst time

TIME FROM POWER-ON 18.05 SEC. TIME FROM POWER-OFF -2.30 SEC.

ROD NO.	DIFFERENTIAL PRESSURE (KPA)	TEMPERATURES (DEG C) TE-1	TE-2	TE-3	TE-4	MINIMUM	MAXIMUM	AVERAGE	TIME FROM BURST (SEC)
1	7976.5	795.0	803.6	821.8	866.2	795.0	866.2	821.6	-0.25
2	5507.8	810.3	835.2	842.0	841.0	810.3	842.0	832.1	0.05
3	7637.2	856.5	849.7	844.9	837.2	837.2	856.5	847.1	-0.25
4	7924.8	855.5	866.2	806.4	852.6	806.4	866.2	845.2	-0.25
5	2429.1	855.5	849.7	833.3	832.3	832.3	855.5	842.7	0.20
6	3490.2	853.6	825.6	836.2	832.3	825.6	853.6	836.9	0.10
7	2155.7	819.8	856.5	835.2	842.0	819.8	856.5	838.4	0.20
8	1150.4	849.7	835.2	815.0	803.6	803.6	849.7	825.9	0.25
9	6868.7	874.0	820.8	835.2	838.1	820.8	874.0	842.0	-2.00
10	7427.2	824.6	864.3	824.6	856.5	824.6	864.3	842.5	-0.05
11	1961.8	825.6	817.9	831.4	854.6	817.9	854.6	832.4	0.25
12	7689.3	849.7	832.3	831.4	836.2	831.4	849.7	837.4	-0.10
13	7925.1	853.6	804.5	880.8	863.3	804.5	880.8	850.5	-0.10
14	7571.9	823.7	858.4	827.5	854.6	823.7	858.4	841.0	-0.25
15	7944.5	823.7	807.4	798.8	836.2	798.8	836.2	816.5	0.00
16	7851.5	848.7	850.7	794.0	822.7	794.0	850.7	829.0	-0.10

****

MISCELLANEOUS INSTRUMENTS

58	TE-305	323.8 DEG C	124	TE-17-1	494.2 DEG C	125	TE-17-2	494.2 DEG C
126	TE-17-3	508.8 DEG C	127	TE-17-4	496.9 DEG C	136	TE-18-1	480.4 DEG C
137	TE-18-2	459.3 DEG C	138	TE-18-3	498.7 DEG C	139	TE-18-4	491.4 DEG C
140	TE-19-1	483.2 DEG C	141	TE-19-2	480.4 DEG C	142	TE-19-3	501.5 DEG C
143	TE-19-4	447.3 DEG C	457	PE-301	229.9 KPA	472	EIE-10	737.5 AMPS
473	EEE-10	199.0 VOLTS	478	TE-304	331.9 DEG C			

Table 21. Test conditions summary at rod 16 burst time

TIME FROM POWER-ON 18.15 SEC. TIME FROM POWER-OFF -2.20 SEC.

ROD NO.	DIFFERENTIAL PRESSURE (KPA)	TEMPERATURES (DEG C)							TIME FROM BURST (SEC)
		TE-1	TE-2	TE-3	TE-4	MINIMUM	MAXIMUM	AVERAGE	
1	7868.3	794.0	802.6	823.7	867.2	794.0	867.2	821.9	-0.15
2	2317.2	810.3	835.2	844.9	840.1	810.3	844.9	832.6	0.15
3	7493.2	853.6	850.7	843.9	832.3	832.3	853.6	845.1	-0.15
4	7798.4	857.5	870.1	806.4	853.6	806.4	870.1	846.9	-0.15
5	1214.8	857.5	852.6	837.2	830.4	830.4	857.5	844.4	0.30
6	1510.0	856.5	828.5	837.2	835.2	828.5	856.5	839.3	0.20
7	1046.9	823.7	860.4	837.2	841.0	823.7	860.4	840.6	0.30
8	527.5	849.7	837.2	817.0	804.5	804.5	849.7	827.1	0.35
9	6830.3	874.0	820.8	837.2	840.1	820.8	874.0	843.0	-1.90
10	6012.6	825.6	857.5	824.6	852.6	824.6	857.5	840.1	0.05
11	1058.3	830.4	820.8	835.2	859.4	820.8	859.4	836.5	0.35
12	7544.5	850.7	832.3	829.5	826.6	826.6	850.7	834.8	0.00
13	7820.4	856.5	805.5	882.7	867.2	805.5	882.7	853.0	0.00
14	7447.3	826.6	855.5	829.5	856.5	826.6	856.5	842.0	-0.15
15	4946.6	819.8	803.6	791.2	819.8	791.2	819.8	808.6	0.10
16	7698.2	847.8	839.1	795.0	814.1	795.0	847.8	824.0	0.00

MISCELLANEOUS INSTRUMENTS

58	TE-305	323.8 DEG C	124	TE-17-1	498.7 DEG C	125	TE-17-2	496.9 DEG C
126	TE-17-3	510.6 DEG C	127	TE-17-4	498.7 DEG C	136	TE-18-1	483.2 DEG C
137	TE-18-2	461.1 DEG C	138	TE-18-3	499.7 DEG C	139	TE-18-4	494.2 DEG C
140	TE-19-1	484.1 DEG C	141	TE-19-2	483.2 DEG C	142	TE-19-3	503.3 DEG C
143	TE-19-4	450.0 DEG C	457	PE-301	240.0 KPA	472	EIE-10	737.5 AMPS
473	EEE-10	199.0 VOLTS	478	TE-304	332.2 DEG C			

Table 22. Axial shrinkage of tubes in B-2 test

Simulator No.	Burst temperature (°C)	Heated length change (%)
1	870	1.4
2	846	1.3
3	853	1.4
4	872	1.3
5	866	1.2
6	857	1.4
7	861	1.3
8	856	1.2
9[a]	928[a]	1.0
10	862	1.2
11	853	1.2
12	851	1.3
13	867	1.2
14	858	1.4
15	836	1.3
16	848	1.3

[a]Tube developed leak prior to test; deformation behavior was abnormal.

Table 23. Percent circumferential strain in the tubes of the B-2 test

Elevation (cm)	Tube No.															
	1	2	3	4	5	6	7	8	9	10	11	12	13	14	15	16
0.0	-0.2	-0.2	-0.3	0.3	0.0	-0.4	-0.1	0.3	-0.8	-0.6	-0.4	0.1	-0.9	-0.5	-0.4	0.0
1.8	4.4	5.7	6.0	5.8	4.1	7.1	7.4	6.9	4.6	5.1	5.1	7.2	4.1	6.3	4.8	4.8
3.4	10.5	11.3	12.3	10.6	10.5	18.8	14.1	11.6	8.2	10.6	10.9	13.0	8.9	15.0	9.6	7.7
5.0	10.4	11.5	11.0	11.5	9.9	17.1	12.8	11.1	8.5	10.7	11.0	11.2	9.3	13.2	10.4	8.3
6.5	8.5	9.7	8.0	7.8	7.6	13.5	10.4	7.5	7.0	9.0	9.0	8.5	7.4	9.8	7.5	6.6
8.8	4.6	4.9	3.9	4.1	3.9	5.0	4.4	4.2	3.1	3.1	3.9	3.9	3.5	3.7	3.1	3.1
11.5	3.7	3.9	3.9	4.4	3.7	5.6	4.3	4.5	3.4	3.7	4.8	4.6	3.5	4.2	2.9	4.3
13.3	8.6	7.7	9.2	7.9	6.7	14.7	12.1	9.8	9.3	9.4	13.2	10.5	8.2	10.3	5.1	6.5
15.1	13.3	11.4	11.5	9.5	8.5	20.9	15.1	13.2	10.7	12.4	16.8	15.6	11.6	17.3	6.8	7.1
16.8	15.3	16.3	14.6	11.6	11.7	22.9	15.7	16.2	10.9	16.2	18.3	17.5	14.4	28.4	11.2	10.5
18.1	15.8	18.2	17.6	13.0	14.3	23.2	15.6	18.7	11.0	16.5	16.9	17.9	15.7	37.8	12.3	11.7
19.5	19.2	19.5	19.7	13.7	18.7	22.4	17.9	21.1	14.7	21.5	16.6	20.7	20.9	41.8	12.6	12.9
21.4	19.8	17.5	19.9	10.8	18.0	21.6	17.9	22.8	13.8	22.6	15.2	24.7	19.5	32.4	11.1	11.8
23.2	19.5	16.1	21.4	9.7	18.3	24.7	18.4	27.0	14.9	23.3	15.1	21.8	18.5	25.8	13.1	13.3
25.0	16.2	13.8	24.4	11.0	17.4	23.4	21.0	27.4	15.4	21.0	13.5	18.5	16.0	22.3	15.5	14.7
26.5	15.4	11.5	25.9	13.5	14.6	19.8	23.4	20.7	14.5	21.1	13.5	18.7	14.9	15.7	17.3	11.8
28.5	16.5	12.7	29.8	16.7	15.1	21.0	24.5	17.4	14.8	23.8	14.3	19.5	14.8	15.5	18.4	10.7
30.0	14.7	12.4	32.5	18.6	14.9	21.5	23.3	16.1	13.2	23.3	15.1	18.8	12.4	15.8	17.5	11.7
32.0	12.6	15.3	28.0	19.8	14.7	20.8	21.8	16.2	13.3	21.0	14.4	20.2	12.8	17.3	13.7	13.5
34.0	11.6	15.4	22.0	17.7	14.8	23.8	19.4	15.1	13.8	18.6	14.8	20.7	16.1	17.7	12.7	13.2
35.5	12.9	18.0	21.6	14.0	15.3	44.3	17.4	16.1	13.5	20.1	16.7	18.1	16.5	22.7	13.9	11.7
37.7	13.5	18.7	24.0	13.5	17.9	57.8	15.7	20.7	15.0	25.0	16.2	15.5	14.6	30.1	16.2	12.7
39.5	12.2	15.0	20.1	13.8	15.6	39.6	18.4	23.4	13.5	32.6	14.4	14.2	12.3	28.9	16.0	13.3
41.2	18.8	15.7	23.7	15.6	16.4	35.3	23.1	29.6	16.2	42.8	16.9	18.9	17.5	26.8	17.3	16.9
43.3	22.2	15.8	29.5	17.0	15.6	44.3	19.7	37.6	14.2	33.0	16.8	21.0	17.1	21.3	15.3	18.3
44.7	23.4	15.0	37.7	18.3	14.9	40.7	17.3	33.0	14.4	27.3	16.0	18.4	15.9	18.9	12.9	21.6
46.2	27.8	17.0	38.4	19.7	16.0	36.4	17.2	23.3	17.0	23.2	16.1	18.1	14.7	17.9	11.8	29.0
47.7	34.5	18.9	30.8	19.8	19.0	37.3	20.1	18.2	21.1	24.5	17.7	18.8	16.0	18.3	13.5	30.8
49.7	28.5	19.6	21.5	18.9	20.7	34.9	20.6	17.4	19.0	22.2	19.9	20.4	14.3	19.2	16.5	22.2
51.6	21.0	20.0	16.0	23.4	27.1	28.9	17.3	18.4	17.7	20.5	18.5	22.1	14.5	20.8	17.4	19.6
53.5	18.1	19.7	19.3	29.4	35.0	25.9	20.1	17.5	19.5	21.8	18.3	25.7	22.0	23.5	20.6	28.2
54.9	19.1	21.9	19.2	27.2	29.0	26.0	22.6	17.6	18.1	22.6	17.6	27.1	29.9	24.2	20.5	37.1
56.2	20.7	25.3	21.3	27.2	25.2	25.6	23.6	22.2	17.6	24.8	17.7	28.1	41.4	27.7	23.2	41.7
57.6	17.1	22.3	21.4	28.1	21.5	21.3	19.3	24.1	14.7	21.6	13.6	23.4	34.6	25.2	20.4	32.4
59.8	13.4	14.7	18.7	23.7	15.0	17.7	16.9	16.8	12.9	17.3	10.9	17.4	16.1	18.2	14.1	17.0
61.8	11.0	10.3	12.4	12.7	10.5	13.6	14.8	11.8	11.2	13.6	10.5	14.0	13.1	12.1	10.5	10.8
63.8	5.1	5.3	4.9	6.1	5.1	5.5	5.7	6.0	3.7	5.4	5.3	5.8	6.4	5.7	5.0	6.4
66.5	4.8	4.9	5.2	6.5	4.7	5.8	6.3	5.9	4.1	5.1	5.5	5.2	5.5	5.0	4.0	5.1
68.4	10.2	10.8	13.6	10.8	11.0	17.7	18.1	11.6	12.4	13.7	15.0	11.0	10.9	10.8	8.2	9.3
70.1	14.6	18.3	19.7	15.9	16.0	27.0	23.1	16.7	17.0	17.8	20.7	16.8	9.7	19.1	12.6	12.6
71.6	15.0	22.2	21.3	21.5	20.6	27.0	21.8	17.8	19.4	18.1	20.2	16.6	9.7	25.8	12.7	14.3
73.1	16.1	25.1	24.8	30.5	22.0	25.6	23.1	19.3	23.0	18.7	20.9	17.7	10.8	26.7	13.5	17.6
74.6	21.7	33.0	37.4	37.8	23.3	30.6	27.7	22.1	29.2	22.2	26.4	19.7	16.5	24.8	17.0	20.1
76.2	23.2	38.5	40.3	42.0	22.0	35.4	31.9	22.3	23.9	25.3	34.4	23.2	17.3	22.7	22.2	22.5
78.0	24.3	29.0	33.6	33.2	23.6	28.8	34.2	21.9	20.2	27.6	39.8	26.3	17.3	23.1	31.4	23.1
79.5	22.9	20.7	22.4	27.1	23.9	22.5	39.7	21.6	19.6	28.0	35.2	29.4	16.7	22.2	35.1	22.0
81.6	17.3	17.9	16.8	26.5	19.0	23.8	55.6	16.3	19.1	28.3	25.9	39.7	14.3	18.7	25.2	16.2
83.8	11.4	15.9	15.6	18.9	14.1	24.0	32.7	12.8	16.1	21.1	20.1	21.8	10.6	16.1	14.4	11.6
86.0	8.0	13.8	12.7	12.9	15.4	14.8	20.7	11.5	13.9	23.0	14.6	11.8	7.5	14.3	9.8	10.8
88.1	6.5	8.1	6.3	7.5	10.3	9.2	12.2	8.4	7.8	12.1	7.8	7.1	5.2	9.7	6.8	8.4
89.5	1.2	1.6	1.7	3.0	1.9	1.9	2.4	1.2	1.5	3.5	0.7	3.3	-0.1	2.4	0.3	1.1
91.5	0.4	0.4	0.8	1.2	1.1	0.1	1.0	-0.1	0.5	1.7	0.5	0.9	0.1	1.5	0.4	0.5

Table 24. Summary of B-2 burst data

Rod No.	Burst characteristics		Approximate position	
	Temperature (°C)	Strain (%)	Elevation[a] (cm)	Angle[b] (deg)
1	870	35	47.7	135
2	846	39	76.2	115
3	853	40	76.2	85
4	872	42	76.2	180
5	866	35	53.5	165
6	857	58	37.7	220
7	861	56	81.6	350
8	856	38	43.3	280
9[c]	928[c]	29[c]	74.6	45
10	862	43	41.2	190
11	853	40	78.0	20
12	851	40	81.6	295
13	867	41	56.2	100
14	858	42	19.5	65
15	836	35	79.5	15
16	848	42	56.2	255

[a]Elevation above bottom of heated zone.

[b]Looking down on bundle and measured clockwise from bundle north.

[c]Tube developed leak prior to transient; deformation behavior is abnormal.

Table 25. Upper limit of B-2 deformed tube areas (mm^2)

Elevation (cm)	Tube No. 1	2	3	4	5	6	7	8	9	10	11	12	13	14	15	16	TOTAL
0.0	93	93	93	94	93	92	93	94	92	92	92	93	91	92	92	93	1490
1.8	102	104	105	104	101	107	107	106	102	103	103	107	101	105	102	102	1670
3.4	114	115	117	114	114	132	121	116	109	114	115	119	111	123	112	108	1862
5.0	114	116	115	116	113	128	119	115	110	114	115	115	111	119	114	109	1850
6.9	110	112	109	108	108	120	114	108	107	111	111	110	107	112	108	106	1767
8.8	102	103	101	101	100	103	101	101	99	99	101	100	100	100	99	99	1616
11.5	100	101	101	102	100	104	101	102	100	100	102	102	100	101	99	101	1622
13.3	110	108	111	108	106	123	117	112	111	112	119	114	109	113	103	106	1791
15.1	120	116	116	112	110	136	124	119	114	118	127	125	116	128	106	107	1902
16.8	124	126	122	116	116	141	125	126	115	126	131	129	122	154	115	114	2009
18.1	125	130	129	119	122	142	125	131	115	127	128	130	125	177	118	116	2065
19.5	133	133	134	121	131	140	130	137	123	138	127	136	136	233	118	119	2195
21.4	134	129	134	114	130	138	130	141	121	140	124	145	133	164	115	117	2115
23.2	133	126	138	112	131	145	131	151	123	142	123	139	131	148	119	120	2118
25.0	126	121	144	115	129	142	137	152	124	137	120	131	126	140	124	123	2096
26.9	124	116	148	120	122	134	142	136	122	137	120	132	123	125	128	117	2054
28.5	127	118	157	127	123	137	145	129	123	143	122	133	123	124	131	114	2083
30.0	123	118	164	131	123	138	142	126	120	142	124	132	118	125	129	116	2076
32.0	118	124	153	134	123	136	138	126	120	137	122	135	119	128	121	120	2060
34.0	116	124	139	129	123	143	133	123	121	131	123	136	126	129	119	119	2042
35.9	119	130	138	121	124	194	129	126	120	134	127	130	127	140	121	116	2105
37.7	120	131	143	120	130	248	125	136	123	146	126	124	122	158	126	118	2205
39.5	117	123	135	121	125	182	131	142	120	164	122	122	118	155	125	120	2128
41.2	132	125	143	125	126	171	141	157	126	256	127	132	129	150	128	127	2302
43.3	139	125	156	128	125	194	133	259	122	165	127	137	128	137	124	131	2338
44.7	142	123	177	131	123	185	128	165	122	151	126	131	125	132	119	138	2225
46.2	152	128	179	134	126	174	128	142	128	142	126	130	123	130	117	155	2218
47.7	204	132	160	134	132	176	135	130	137	145	129	132	125	131	120	160	2288
49.7	155	133	138	132	136	170	136	129	132	135	134	135	122	133	127	139	2196
51.6	136	134	126	142	151	155	128	131	129	136	131	139	122	136	129	133	2166
53.5	130	134	133	156	261	148	134	129	133	138	130	147	139	142	136	153	2352
54.9	132	139	133	151	155	148	140	129	130	140	129	151	158	144	135	175	2296
56.2	136	146	137	151	146	147	143	139	129	145	129	153	253	152	142	271	2527
57.6	128	140	138	153	138	137	133	144	123	138	120	142	169	146	135	164	2254
59.8	120	123	131	143	123	129	127	127	119	128	115	129	126	130	121	128	2027
61.8	115	113	118	118	114	120	123	117	115	120	114	121	119	117	114	114	1881
63.8	103	103	103	105	103	104	104	105	100	103	103	104	105	104	103	105	1665
66.5	102	102	103	106	102	104	105	104	101	103	104	103	104	103	101	103	1658
68.4	113	115	120	114	115	129	130	116	118	121	123	115	115	114	109	111	1886
70.1	123	130	134	125	126	151	141	127	128	129	136	127	112	132	118	118	2065
71.6	123	139	137	138	136	151	138	129	133	130	135	127	112	148	119	122	2124
73.1	126	146	145	159	139	147	141	133	141	131	136	129	114	150	120	129	2195
74.6	138	165	174	177	142	159	152	139	184	139	149	134	127	145	128	135	2394
76.2	142	203	264	288	139	171	162	139	143	146	168	141	128	140	139	140	2663
78.0	144	155	166	166	143	155	168	139	135	152	228	149	128	141	161	141	2478
79.5	141	136	140	151	143	140	182	138	134	153	170	156	127	139	189	139	2384
81.6	128	130	127	149	132	143	295	126	132	154	148	228	122	131	146	126	2425
83.8	116	125	125	132	121	143	164	119	126	137	135	138	114	126	122	116	2066
86.0	109	121	118	119	124	123	136	116	121	141	122	117	108	122	112	114	1930
88.1	106	109	105	108	113	111	117	109	108	117	108	107	103	112	106	109	1758
89.9	95	96	96	99	97	97	98	95	96	100	94	99	93	98	94	95	1550
91.5	94	94	95	95	95	93	95	93	94	96	94	95	93	96	94	94	1518

Table 26. Lower limit of B-2 deformed tube areas (mm^2)

Elevation (cm)	Tube No.																
	1	2	3	4	5	6	7	8	9	10	11	12	13	14	15	16	TOTAL
0.0	93	93	93	94	93	92	93	94	92	92	92	93	91	92	92	93	1490
1.8	102	104	105	104	101	107	107	106	102	103	103	107	101	105	102	102	1670
3.4	114	115	117	114	114	132	121	116	109	114	115	119	111	123	112	108	1862
5.0	114	116	115	116	113	128	119	115	110	114	115	115	111	119	114	109	1850
6.5	110	112	109	108	108	120	114	108	107	111	111	110	107	112	108	106	1767
8.8	102	103	101	101	100	103	101	101	99	99	101	100	100	100	99	99	1616
11.5	100	101	101	102	100	104	101	102	100	100	102	102	100	101	99	101	1622
13.3	110	108	111	108	106	123	117	112	111	112	119	114	109	113	103	106	1791
15.1	120	116	116	112	110	136	124	119	114	118	127	125	116	128	106	107	1902
16.8	124	126	122	116	116	141	125	126	115	126	131	129	122	154	115	114	2009
18.1	125	130	129	119	122	142	125	131	115	127	128	130	125	177	118	116	2065
19.5	133	133	134	121	131	140	130	137	123	138	127	136	136	188	118	119	2150
21.4	134	129	134	114	130	138	130	141	121	140	124	145	133	164	115	117	2115
23.2	133	126	138	112	131	145	131	151	123	142	123	139	131	148	119	120	2118
25.0	126	121	144	115	129	142	137	152	124	137	120	131	126	140	124	123	2096
26.5	124	116	148	120	122	134	142	136	122	137	120	132	123	125	128	117	2054
28.5	127	118	157	127	123	137	145	129	123	143	122	133	123	124	131	114	2083
30.0	123	118	164	131	123	138	142	126	120	142	124	132	118	125	129	116	2076
32.0	118	124	153	134	123	136	138	126	120	137	122	135	119	128	121	120	2060
34.0	116	124	139	129	123	143	133	123	121	131	123	136	126	129	119	119	2042
35.5	119	130	138	121	124	194	129	126	120	134	127	130	127	140	121	116	2105
37.7	120	131	143	120	130	233	125	136	123	146	126	124	122	158	126	118	2190
39.5	117	123	135	121	125	182	131	142	120	164	122	122	118	155	125	120	2128
41.2	132	125	143	125	126	171	141	157	126	191	127	132	129	150	128	127	2237
43.3	139	125	156	128	125	194	133	177	122	165	127	137	128	137	124	131	2256
44.7	142	123	177	131	123	185	128	165	122	151	126	131	125	132	119	138	2225
46.2	152	128	179	134	126	174	128	142	128	142	126	130	123	130	117	155	2218
47.7	169	132	160	134	132	176	135	130	137	145	129	132	125	131	120	160	2253
49.7	155	133	138	132	136	170	136	129	132	135	134	135	122	133	127	139	2196
51.6	136	134	126	142	151	155	128	131	129	136	131	139	122	136	129	133	2166
53.5	130	134	133	156	170	148	134	129	133	138	130	147	139	142	136	153	2261
54.5	132	139	133	151	155	148	140	129	130	140	129	151	158	144	135	175	2296
56.2	136	146	137	151	146	147	143	139	129	145	129	153	187	152	142	188	2378
57.6	128	140	138	153	138	137	133	144	123	138	120	142	169	146	135	164	2254
59.8	120	123	131	143	123	129	127	127	119	128	115	129	126	130	121	128	2027
61.8	115	113	118	118	114	120	123	117	115	120	114	121	119	117	114	114	1881
63.8	103	103	103	105	103	104	104	105	100	103	103	104	105	104	103	105	1665
66.5	102	102	103	106	102	104	105	104	101	103	104	103	104	103	101	103	1658
68.4	113	115	120	114	115	129	130	116	118	121	123	115	115	114	109	111	1886
70.1	123	130	134	125	126	151	141	127	128	129	136	127	112	132	118	118	2065
71.6	123	139	137	138	136	151	138	129	133	130	135	127	112	148	119	122	2124
73.1	126	146	145	159	139	147	141	133	141	131	136	129	114	150	120	129	2195
74.6	138	165	174	177	142	159	152	139	156	135	149	134	127	145	128	135	2366
76.2	142	179	184	188	139	171	162	139	143	146	168	141	128	140	139	140	2459
78.0	144	155	166	166	143	155	168	139	135	152	183	149	128	141	161	141	2432
79.5	141	136	140	151	143	140	182	138	134	153	170	156	127	139	170	139	2366
81.6	128	130	127	149	132	143	226	126	132	154	148	182	122	131	146	126	2311
83.8	116	125	125	132	121	143	164	119	126	137	135	138	114	126	122	116	2066
86.0	109	121	118	119	124	123	136	116	121	141	122	117	108	122	112	114	1930
88.1	106	109	105	108	113	111	117	109	108	117	108	107	103	112	106	109	1758
89.5	95	96	96	99	97	97	98	95	96	100	94	99	93	98	94	95	1550
91.5	94	94	95	95	95	93	95	93	94	96	94	95	93	96	94	94	1518

Table 27. B-2 coolant channel restriction

Elevation (cm)	Upper limit (%)	Lower limit (%)
0.0	-0.5	-0.5
1.8	9.4	9.4
3.4	19.9	19.9
5.0	19.2	19.2
6.9	14.7	14.7
8.8	6.4	6.4
11.5	6.7	6.7
13.3	16.0	16.0
15.1	22.0	22.0
16.8	27.9	27.9
18.1	30.9	30.9
19.5	38.0	35.6
21.4	33.6	33.6
23.2	33.8	33.8
25.0	32.7	32.7
26.9	30.3	30.3
28.5	31.9	31.9
30.0	31.5	31.5
32.0	30.7	30.7
34.0	29.7	29.7
35.9	33.1	33.1
37.7	38.6	37.7
39.5	34.4	34.4
41.2	43.9	40.3
43.3	45.8	41.3
44.7	39.7	39.7
46.2	39.3	39.3
47.7	43.1	41.2
49.7	38.1	38.1
51.6	36.5	36.5
53.5	46.6	41.7
54.9	43.6	43.6
56.2	56.2	48.0
57.6	41.2	41.2
59.8	28.9	28.9
61.8	20.9	20.9
63.8	9.1	9.1
66.5	8.7	8.7
68.4	21.2	21.2
70.1	31.0	31.0
71.6	34.2	34.2
73.1	38.0	38.0
74.6	48.9	47.4
76.2	63.6	52.5
78.0	53.5	51.0
79.5	48.4	47.4
81.6	50.6	44.4
83.8	31.0	31.0
86.0	23.6	23.6
88.1	14.2	14.2
89.9	2.8	2.8
91.5	1.1	1.1

Table 28. Pressure tap positions of shroud 1 relative to the bottom of the heated zone of bundle B-2

Tap No.	Distance above bottom of heated zone (cm)	Tap No.	Distance above bottom of heated zone (cm)
1-2	96.16	41-42	37.74
3-4	91.08	43-44	35.20
5-6	86.00	45-46	32.66
7-8	83.46	47-48	30.12
9-10	80.92	49-50	27.58
11-12	78.38	51-52	25.04
13-14	75.84	53-54	22.50
15-16	73.30	55-56	19.96
17-18	70.76	57-58	17.42
19-20	68.22	59-60	14.88
21-22	63.14	61-62	12.34
23-24	60.60	63-64	7.26
25-26	58.06	65-66	5.72
27-28	55.52	67-68	2.18
29-30	52.98	69-70	-2.90
31-32	50.44	71-72	-7.98
33-34	47.90	73-74	-13.06
35-36	45.36	75-76	-18.14
37-38	42.82	77-78	-37.35
39-40	40.28	79-80	-47.51

Table 29. Pressure tap positions of shroud 2 relative to the bottom of the heated zone of bundle B-2

Tap No.	Distance above bottom of heated zone (cm)	Tap No.	Distance above bottom of heated zone (cm)
1-2	95.95	41-42	37.53
3-4	90.24	43-44	34.99
5-6	85.79	45-46	32.45
7-8	83.25	47-48	29.91
9-10	80.71	49-50	27.37
11-12	78.17	51-52	24.83
13-14	75.63	53-54	22.29
15-16	23.09	55-56	19.75
17-18	70.55	57-58	17.21
19-20	68.01	59-60	14.67
21-22	62.93	61-62	12.13
23-24	60.39	63-64	7.05
25-26	57.85	65-66	4.51
27-28	55.31	67-68	1.97
29-30	52.77	69-70	-1.20
31-32	50.23	71-72	-8.82
33-34	47.69	73-74	-15.81
35-36	45.15	75-76	-20.89
37-38	42.61	77-78	-37.55
39-40	40.07	79-80	-47.71

Table 30. Differential pressure drops for bundle B-2 at a flow rate of 0.0095 m^3/sec in shroud 1

Tap No.	Pressure (kPa)	Tap No.	Pressure (kPa)
1	39.78	2	38.77
3	39.60	4	39.50
5	41.22	6	41.86
7	43.02	8	42.18
9	42.38	10	43.48
11	41.51	12	44.48
13	44.66	14	39.01
15	34.62	16	36.09
17	32.31	18	33.86
19	30.93	20	31.56
21	28.35	22	27.63
23	28.07	24	27.73
25	28.98	26	29.62
27	28.97	28	30.12
29	27.20	30	26.07
31	26.57	32	25.58
33	26.40	34	24.71
35	25.71	36	24.69
37	23.40	38	24.27
39	22.10	40	23.36
41	21.92	42	21.93
43	20.90	44	20.64
45	20.01	46	19.79
47	19.88	48	19.56
49	19.12	50	19.11
51	18.69	52	18.71
53	17.98	54	18.49
55	17.08	56	19.07
57	16.29	58	16.86
59	14.98	60	14.72
61	14.56	62	14.21
63	10.04	64	9.55
65	9.86	66	9.44
67	8.86	68	9.06
69	7.27	70	7.30
71	6.80	72	6.81
73	6.21	74	6.43
75	6.72	76	6.07
77	1.50	78	1.83
79	0.0	80	0.0

Table 31. Differential pressure drops for bundle B-2 at a flow rate of 0.0126 m^3/sec in shroud 1

Tap No.	Pressure (kPa)	Tap No.	Pressure (kPa)
1	64.27	2	62.36
3	63.65	4	63.82
5	65.87	6	66.96
7	68.22	8	66.75
9	68.02	10	70.00
11	66.68	12	70.57
13	72.39	14	63.06
15	55.41	16	57.22
17	52.51	18	53.83
19	50.59	20	50.36
21	45.91	22	44.59
23	45.54	24	44.30
25	47.27	26	47.08
27	46.44	28	47.96
29	43.99	30	40.99
31	42.96	32	40.88
33	41.75	34	39.90
35	41.66	36	39.23
37	37.93	38	39.05
39	35.88	40	37.72
41	35.28	42	35.55
43	33.81	44	32.80
45	32.65	46	31.76
47	32.05	48	30.96
49	30.96	50	30.13
51	30.16	52	29.94
53	29.59	54	29.21
55	28.07	56	30.35
57	26.50	58	26.94
59	24.23	60	23.92
61	23.84	62	22.75
63	15.96	64	15.38
65	15.72	66	15.47
67	14.15	68	14.46
69	11.68	70	11.42
71	10.79	72	10.81
73	9.98	74	10.21
75	10.80	76	9.59
77	2.56	78	3.04
79	0.0	80	0.0

Table 32. Differential pressure drops for bundle B-2 at a flow rate of 0.019 m^3/sec in shroud 1

Tap No.	Pressure (kPa)	Tap No.	Pressure (kPa)
1	139.15	2	131.09
3	137.19	4	136.73
5	143.11	6	146.34
7	149.47	8	149.30
9	148.30	10	148.88
11	145.89	12	155.90
13	164.04	14	137.77
15	119.89	16	125.74
17	114.22	18	117.89
19	108.91	20	109.31
21	97.38	22	98.00
23	98.37	24	97.05
25	102.62	26	104.05
27	99.94	28	106.41
29	96.07	30	90.42
31	92.50	32	89.71
33	91.09	34	86.25
35	89.60	36	85.49
37	81.55	38	85.22
39	76.41	40	82.74
41	76.38	42	78.32
43	71.11	44	72.18
45	70.30	46	69.49
47	68.82	48	67.60
49	66.46	50	66.41
51	64.94	52	64.76
53	63.19	54	64.36
55	60.49	56	66.50
57	57.22	58	59.30
59	51.98	60	52.13
61	51.03	62	50.71
63	34.37	64	33.63
65	34.04	66	33.68
67	30.56	68	32.13
69	25.39	70	24.94
71	22.96	72	24.17
73	21.82	74	23.31
75	24.49	76	21.78
77	6.87	78	7.36
79	0.0	80	0.0

Table 33. Differential pressure drops for bundle B-2 at a flow rate of 0.022 m^3/sec in shroud 1

Tap No.	Pressure (kPa)	Tap No.	Pressure (kPa)
1	180.42	2	170.69
3	180.21	4	176.08
5	187.09	6	189.44
7	194.62	8	192.47
9	191.74	10	200.59
11	190.22	12	203.72
13	214.55	14	179.18
15	159.11	16	162.43
17	149.32	18	153.48
19	142.83	20	142.39
21	128.21	22	126.95
23	127.93	24	127.25
25	134.84	26	135.21
27	132.70	28	137.84
29	125.71	30	118.03
31	121.59	32	117.54
33	120.27	34	112.72
35	119.97	36	112.32
37	107.61	38	110.75
39	100.61	40	107.25
41	99.40	42	101.84
43	94.32	44	93.67
45	90.98	46	90.58
47	91.23	48	88.06
49	87.18	50	86.24
51	85.04	52	85.74
53	83.14	54	82.44
55	78.82	56	87.22
57	74.47	58	77.34
59	68.35	60	67.86
61	65.46	62	65.53
63	43.86	64	43.44
65	43.72	66	42.64
67	39.13	68	41.08
69	32.00	70	31.75
71	30.07	72	30.43
73	27.79	74	29.40
75	31.41	76	28.36
77	8.20	78	9.83
79	0.0	80	0.0

Table 34. Differential pressure drops for the reference bundle at a flow rate of 0.0092 m^3/sec in shroud 1

Tap No.	Pressure (kPa)	Tap No.	Pressure (kPa)
1	21.51	2	21.85
3	20.67	4	20.60
5	20.34	6	20.35
7	20.32	8	20.01
9	19.65	10	19.84
11	19.43	12	19.70
13	19.23	14	19.32
15	19.13	16	19.10
17	18.85	18	18.96
19	18.92	20	18.87
21	15.84	22	16.50
23	15.48	24	15.32
25	15.32	26	15.25
27	15.00	28	14.83
29	14.87	30	14.77
31	14.65	32	14.61
33	14.24	34	14.20
35	14.15	36	13.98
37	13.81	38	13.80
39	13.45	40	13.59
41	13.46	42	13.57
43	13.40	44	13.24
45	13.04	46	13.12
47	12.79	48	12.84
49	12.54	50	12.62
51	12.51	52	12.47
53	12.14	54	12.13
55	11.81	56	11.89
57	11.81	58	11.94
59	11.46	60	11.56
61	11.78	62	11.62
63	8.30	64	7.79
65	7.79	66	7.67
67	7.44	68	7.54
69	7.00	70	7.20
71	6.49	72	6.71
73	6.10	74	6.36
75	6.75	76	5.41
77	1.63	78	2.27
79	0.0	80	0.0

Table 35. Differential pressure drops for the reference bundle at a flow rate of 0.0125 m^3/sec in shroud 1

Tap No.	Pressure (kPa)	Tap No.	Pressure (kPa)
1	36.18	2	37.10
3	35.13	4	36.40
5	34.60	6	35.32
7	34.51	8	34.75
9	33.91	10	34.41
11	32.98	12	34.06
13	32.84	14	33.45
15	32.66	16	33.23
17	32.46	18	32.93
19	32.48	20	32.33
21	26.60	22	28.38
23	26.24	24	26.38
25	25.73	26	25.74
27	25.49	28	25.41
29	25.05	30	25.51
31	24.64	32	25.15
33	24.35	34	24.50
35	23.68	36	23.99
37	23.36	38	23.65
39	23.10	40	23.08
41	22.82	42	23.13
43	22.40	44	22.78
45	22.01	46	22.75
47	21.87	48	22.43
49	21.33	50	21.72
51	21.08	52	21.51
53	20.77	54	21.11
55	20.06	56	20.64
57	19.89	58	20.48
59	19.72	60	20.00
61	19.92	62	20.14
63	13.80	64	13.35
65	13.14	66	13.19
67	12.58	68	13.26
69	11.84	70	12.24
71	11.04	72	11.56
73	10.20	74	10.97
75	11.53	76	9.67
77	2.71	78	4.13
79	0.0	80	0.0

Table 36. Differential pressure drops for the reference bundle at a flow rate of 0.019 m^3/sec in shroud 1

Tap No.	Pressure (kPa)	Tap No.	Pressure (kPa)
1	77.90	2	80.53
3	76.29	4	77.24
5	75.09	6	75.84
7	74.33	8	74.72
9	72.47	10	73.63
11	71.18	12	72.23
13	70.47	14	71.45
15	70.28	16	71.29
17	69.00	18	70.55
19	69.87	20	70.11
21	56.79	22	62.21
23	55.96	24	56.42
25	55.06	26	55.79
27	53.93	28	55.27
29	53.84	30	54.30
31	53.17	32	54.08
33	51.90	34	52.66
35	50.80	36	52.15
37	50.57	38	51.37
39	49.70	40	50.66
41	48.42	42	50.56
43	48.46	44	49.17
45	47.52	46	48.18
47	47.09	48	48.11
49	46.35	50	46.69
51	44.84	52	45.92
53	44.56	54	44.98
55	43.74	56	43.85
57	42.72	58	43.86
59	42.38	60	42.94
61	43.15	62	43.21
63	29.34	64	28.91
65	28.08	66	23.26
67	26.99	68	27.99
69	25.34	70	25.76
71	23.63	72	24.52
73	21.65	74	23.57
75	25.56	76	21.71
77	5.91	78	8.77
79	0.0	80	0.0

Table 37. Differential pressure drops for the reference bundle at a flow rate of 0.022 m^3/sec in shroud 1

Tap No.	Pressure (kPa)	Tap No.	Pressure (kPa)
1	103.19	2	104.22
3	101.97	4	101.05
5	97.97	6	99.07
7	96.95	8	97.45
9	95.23	10	95.84
11	93.83	12	94.04
13	92.02	14	93.19
15	92.31	16	90.68
17	90.99	18	91.69
19	91.17	20	91.05
21	73.93	22	80.28
23	72.48	24	73.26
25	71.58	26	72.23
27	70.45	28	71.18
29	69.89	30	69.76
31	68.89	32	69.09
33	67.49	34	68.12
35	66.75	36	67.48
37	65.93	38	66.06
39	64.21	40	65.23
41	63.22	42	65.22
43	62.64	44	63.77
45	61.51	46	62.03
47	61.04	48	61.77
49	59.74	50	60.09
51	58.87	52	58.80
53	58.11	54	57.65
55	56.66	56	56.38
57	55.43	58	56.67
59	54.78	60	54.76
61	55.75	62	55.92
63	37.72	64	37.64
65	35.98	66	35.82
67	34.59	68	36.63
69	32.74	70	33.11
71	30.25	72	31.64
73	27.90	74	30.73
75	33.65	76	29.67
77	7.71	78	10.45
79	0.0	80	0.0

Table 38. Differential pressure drops for the reference bundle at a flow rate of 0.0068 m^3/sec in shroud 1

Tap No.	Pressure (kPa)	Tap No.	Pressure (kPa)
1	11.92	2	11.79
3	11.78	4	11.55
5	10.94	6	11.34
7	10.90	8	11.35
9	10.58	10	10.97
11	10.62	12	10.96
13	10.27	14	11.01
15	10.40	16	10.65
17	10.25	18	10.69
19	10.23	20	10.57
21	8.70	22	8.84
23	8.32	24	8.45
25	8.10	26	8.80
27	8.21	28	8.41
29	8.07	30	8.39
31	7.80	32	8.25
33	7.71	34	8.03
35	7.67	36	7.98
37	7.46	38	7.86
39	7.49	40	8.01
41	7.38	42	7.22
43	7.25	44	7.26
45	6.85	46	6.84
47	7.02	48	7.46
49	6.34	50	7.25
51	6.71	52	7.24
53	6.66	54	6.90
55	6.29	56	6.88
57	6.26	58	6.79
59	6.30	60	6.70
61	6.77	62	6.91
63	4.24	64	4.66
65	4.22	66	5.05
67	3.76	68	4.24
69	3.69	70	4.28
71	3.70	72	4.02
73	3.18	74	3.88
75	3.41	76	3.31
77	0.64	78	1.26
79	0.0	80	0.0

Table 39. Differential pressure drops for the reference bundle at a flow rate of 0.024 m^3/sec in shroud 1

Tap No.	Pressure (kPa)	Tap No.	Pressure (kPa)
1	116.43	2	118.57
3	112.33	4	114.43
5	110.37	6	112.36
7	109.86	8	110.08
9	107.26	10	107.81
11	105.06	12	106.95
13	104.77	14	106.17
15	104.28	16	104.66
17	102.63	18	104.01
19	102.80	20	103.26
21	83.82	22	90.79
23	81.67	24	83.20
25	80.82	26	81.61
27	79.10	28	81.04
29	78.71	30	78.50
31	77.71	32	79.25
33	75.63	34	76.51
35	74.22	36	76.09
37	73.46	38	74.58
39	72.29	40	72.91
41	71.23	42	73.54
43	70.73	44	71.59
45	69.05	46	70.71
47	67.96	48	70.12
49	67.25	50	68.23
51	65.94	52	66.98
53	64.84	54	65.52
55	63.34	56	63.35
57	62.21	58	63.40
59	61.67	60	62.41
61	62.81	62	63.91
63	42.30	64	42.53
65	40.46	66	40.55
67	39.08	68	41.25
69	36.86	70	37.45
71	34.07	72	36.01
73	31.61	74	34.83
75	38.12	76	33.57
77	8.70	78	11.77
79	0.0	80	0.0

Table 40. Differential pressure drops for bundle B-2 at a flow rate of 0.0095 m^3/sec in shroud 2

Tap No.	Pressure (kPa)	Tap No.	Pressure (kPa)
1	20.43	2	19.82
3	20.93	4	20.27
5	21.59	6	21.08
7	21.93	8	21.60
9	22.05	10	21.98
11	21.82	12	22.54
13	23.43	14	20.73
15	18.51	16	18.96
17	17.29	18	17.76
19	16.36	20	16.90
21	15.20	22	15.05
23	15.13	24	14.94
25	15.69	26	15.78
27	15.53	28	16.06
29	14.95	30	14.08
31	14.64	32	13.84
33	14.48	34	13.61
35	14.03	36	13.33
37	13.18	38	13.27
39	12.29	40	13.03
41	12.38	42	12.09
43	11.76	44	11.54
45	11.37	46	11.07
47	11.17	48	10.84
49	10.77	50	10.54
51	10.51	52	10.44
53	10.32	54	10.32
55	9.88	56	11.01
57	9.44	58	9.26
59	8.65	60	8.31
61	8.45	62	7.98
63	5.94	64	5.22
65	5.74	66	5.42
67	5.22	68	5.01
69	4.46	70	4.24
71	3.99	72	3.84
73	3.90	74	3.43
75	2.31	76	1.45
77	0.61	78	0.39
79	0.0	80	0.0

Table 41. Differential pressure drops for bundle B-2 at a flow rate of 0.0125 m^3/sec in shroud 2

Tap No.	Pressure (kPa)	Tap No.	Pressure (kPa)
1	32.83	2	32.65
3	33.51	4	33.60
5	35.16	6	34.98
7	36.07	8	35.71
9	36.61	10	36.79
11	37.55	12	36.86
13	39.23	14	33.92
15	30.33	16	31.17
17	28.21	18	29.47
19	26.77	20	27.58
21	24.77	22	24.59
23	24.19	24	24.26
25	25.70	26	25.83
27	25.13	28	26.02
29	24.40	30	23.03
31	23.69	32	22.87
33	23.85	34	22.73
35	22.84	36	22.05
37	21.26	38	21.81
39	20.35	40	21.43
41	20.11	42	20.01
43	19.30	44	18.92
45	18.37	46	18.08
47	18.17	48	17.80
49	17.44	50	17.52
51	17.10	52	17.38
53	16.68	54	16.88
55	16.04	56	18.36
57	15.37	58	15.67
59	14.03	60	13.89
61	13.61	62	13.44
63	9.41	64	8.77
65	9.09	66	8.96
67	8.22	68	8.26
69	6.99	70	7.08
71	6.28	72	6.46
73	6.31	74	5.89
75	3.69	76	2.61
77	0.96	78	0.97
79	0.0	80	0.0

Table 42. Differential pressure drops for bundle B-2 at a flow rate of 0.016 m^3/sec in shroud 2

Tap No.	Pressure (kPa)	Tap No.	Pressure (kPa)
1	51.13	2	50.33
3	51.99	4	51.91
5	53.50	6	53.48
7	55.45	8	55.51
9	55.70	10	56.75
11	58.11	12	57.09
13	57.99	14	53.23
15	45.78	16	48.46
17	42.13	18	45.45
19	39.84	20	42.74
21	37.26	22	39.13
23	36.62	24	38.27
25	38.39	26	40.55
27	38.04	28	40.59
29	36.91	30	36.30
31	35.50	32	36.08
33	35.72	34	34.59
35	34.26	36	34.39
37	32.13	38	34.29
39	30.54	40	33.21
41	30.40	42	31.37
43	28.60	44	29.74
45	27.94	46	28.54
47	27.39	48	28.10
49	26.84	50	27.23
51	25.82	52	27.77
53	25.56	54	27.11
55	24.29	56	28.94
57	23.15	58	24.54
59	21.26	60	21.80
61	20.57	62	20.77
63	14.37	64	13.82
65	13.98	66	14.29
67	12.65	68	12.93
69	10.61	70	10.93
71	9.53	72	9.94
73	9.55	74	9.05
75	5.78	76	3.90
77	1.44	78	1.35
79	0.0	80	0.0

Table 43. Differential pressure drops for bundle B-2 at a flow rate of 0.019 m^3/sec in shroud 2

Tap No.	Pressure (kPa)	Tap No.	Pressure (kPa)
1	69.36	2	69.05
3	70.11	4	69.98
5	73.96	6	73.43
7	76.32	8	74.57
9	76.97	10	78.01
11	78.53	12	78.64
13	82.75	14	72.28
15	64.98	16	66.87
17	59.38	18	61.65
19	56.52	20	58.60
21	52.16	22	52.44
23	50.97	24	51.26
25	54.19	26	55.04
27	53.83	28	55.11
29	51.77	30	49.14
31	49.89	32	48.54
33	50.37	34	47.69
35	49.07	36	46.55
37	45.61	38	46.64
39	43.17	40	45.04
41	42.99	42	42.54
43	41.62	44	40.12
45	38.99	46	38.58
47	38.76	48	38.26
49	37.25	50	36.76
51	36.54	52	37.04
53	35.67	54	36.10
55	34.02	56	39.29
57	32.77	58	32.87
59	29.95	60	28.92
61	29.20	62	27.86
63	20.40	64	18.62
65	19.87	66	19.13
67	17.98	68	17.63
69	15.18	70	14.89
71	13.55	72	13.63
73	13.35	74	12.30
75	8.01	76	5.43
77	2.06	78	1.93
79	0.0	80	0.0

Table 44. Differential pressure drops for bundle B-2 at a flow rate of 0.022 m^3/sec in shroud 2

Tap No.	Pressure (kPa)	Tap No.	Pressure (kPa)
1	93.43	2	92.23
3	93.96	4	92.81
5	99.15	6	97.66
7	102.34	8	100.70
9	103.81	10	103.94
11	106.23	12	106.41
13	112.21	14	97.10
15	86.73	16	89.21
17	79.74	18	82.79
19	75.14	20	78.15
21	69.47	22	69.54
23	67.62	24	67.78
25	72.88	26	72.21
27	71.45	28	74.07
29	68.99	30	64.74
31	67.17	32	64.29
33	66.87	34	63.51
35	65.84	36	61.97
37	60.35	38	62.38
39	57.21	40	60.74
41	56.92	42	56.83
43	53.61	44	53.28
45	51.84	46	51.23
47	50.84	48	49.90
49	49.61	50	49.01
51	48.01	52	48.94
53	47.27	54	47.64
55	45.22	56	51.82
57	43.16	58	43.67
59	39.38	60	38.40
61	38.39	62	36.89
63	26.96	64	24.78
65	26.43	66	25.53
67	23.73	68	23.78
69	20.37	70	20.03
71	18.32	72	18.25
73	17.76	74	16.48
75	11.13	76	7.48
77	2.87	78	2.79
79	0.0	80	0.0

Table 45. Differential pressure drops for the reference bundle at a flow rate of 0.0095 m^3/sec in shroud 2

Tap No.	Pressure (kPa)	Tap No.	Pressure (kPa)
1	12.96	2	13.05
3	12.66	4	12.79
5	12.54	6	12.52
7	12.33	8	12.39
9	12.14	10	12.28
11	12.10	12	12.14
13	11.91	14	12.04
15	11.94	16	11.95
17	11.87	18	11.84
19	11.93	20	11.78
21	10.58	22	9.89
23	9.70	24	9.58
25	9.57	26	9.44
27	9.41	28	9.36
29	9.29	30	9.22
31	9.13	32	9.08
33	8.99	34	8.97
35	8.90	36	8.78
37	8.71	38	8.68
39	8.50	40	8.55
41	8.42	42	8.44
43	8.26	44	8.30
45	8.13	46	8.11
47	8.01	48	8.03
49	7.87	50	7.83
51	7.76	52	7.77
53	7.57	54	7.56
55	7.43	56	7.50
57	7.41	58	7.29
59	7.18	60	7.10
61	7.33	62	7.06
63	5.13	64	4.93
65	4.80	66	4.72
67	4.66	68	4.65
69	4.47	70	4.47
71	4.11	72	4.05
73	4.12	74	3.70
75	2.65	76	2.24
77	0.59	78	0.58
79	0.0	80	0.0

Table 46. Differential pressure drops for the reference bundle at a flow rate of 0.013 m^3/sec in shroud 2

Tap No.	Pressure (kPa)	Tap No.	Pressure (kPa)
1	22.46	2	22.80
3	21.92	4	22.10
5	21.83	6	21.43
7	21.82	8	21.17
9	21.19	10	21.02
11	20.90	12	20.95
13	20.94	14	20.59
15	21.31	16	20.55
17	20.53	18	20.14
19	20.82	20	20.08
21	18.56	22	17.01
23	17.04	24	16.38
25	16.82	26	16.10
27	16.52	28	16.07
29	16.51	30	15.78
31	16.10	32	15.66
33	15.83	34	15.32
35	15.72	36	15.07
37	15.51	38	14.84
39	15.28	40	14.69
41	15.15	42	14.50
43	14.82	44	14.16
45	14.60	46	13.94
47	14.32	48	13.61
49	14.11	50	13.35
51	13.76	52	13.13
53	13.59	54	12.88
55	13.29	56	12.54
57	13.29	58	12.32
59	12.85	60	11.97
61	12.99	62	11.93
63	9.11	64	8.28
65	8.59	66	7.95
67	8.28	68	7.73
69	7.97	70	7.53
71	7.16	72	6.76
73	6.88	74	6.18
75	4.64	76	3.70
77	1.35	78	0.94
79	0.0	80	0.0

Table 47. Differential pressure drops for the reference bundle at a flow rate of 0.016 m^3/sec in shroud 2

Tap No.	Pressure (kPa)	Tap No.	Pressure (kPa)
1	32.20	2	32.90
3	31.55	4	31.78
5	31.19	6	31.12
7	30.78	8	30.87
9	30.52	10	30.64
11	30.27	12	30.28
13	30.14	14	30.48
15	30.11	16	29.71
17	29.67	18	29.49
19	29.67	20	29.01
21	26.26	22	24.63
23	24.02	24	23.62
25	23.69	26	23.52
27	23.16	28	23.26
29	22.96	30	23.17
31	22.63	32	22.85
33	22.18	34	22.51
35	21.93	36	22.09
37	21.62	38	21.78
39	21.30	40	21.49
41	21.02	42	21.30
43	20.66	44	20.74
45	20.26	46	20.46
47	19.86	48	20.09
49	19.64	50	19.67
51	19.16	52	19.25
53	18.87	54	19.03
55	18.55	56	18.81
57	18.21	58	18.30
59	17.78	60	17.86
61	18.08	62	17.81
63	12.67	64	12.48
65	11.87	66	11.90
67	11.49	68	11.73
69	11.01	70	11.27
71	10.08	72	10.26
73	9.67	74	9.43
75	6.40	76	5.76
77	1.50	78	1.78
79	0.0	80	0.0

Table 48. Differential pressure drops for the reference bundle at a flow rate of 0.019 m^3/sec in shroud 2

Tap No.	Pressure (kPa)	Tap No.	Pressure (kPa)
1	44.58	2	45.26
3	43.61	4	44.08
5	43.56	6	42.81
7	42.37	8	42.65
9	42.21	10	42.36
11	42.02	12	41.77
13	41.66	14	41.36
15	42.05	16	40.89
17	40.98	18	40.81
19	41.25	20	40.19
21	36.89	22	33.80
23	33.29	24	32.52
25	32.85	26	32.53
27	32.35	28	31.91
29	32.03	30	31.82
31	31.55	32	31.31
33	31.02	34	30.69
35	30.67	36	30.18
37	30.02	38	29.84
39	29.87	40	29.46
41	29.35	42	29.18
43	29.17	44	28.56
45	28.82	46	28.25
47	27.95	48	27.59
49	27.50	50	27.17
51	26.81	52	26.55
53	26.25	54	25.94
55	25.80	56	25.56
57	25.67	58	25.12
59	25.09	60	24.35
61	25.41	62	24.30
63	17.59	64	16.85
65	16.46	66	16.19
67	15.92	68	15.82
69	15.45	70	15.28
71	13.93	72	14.02
73	13.64	74	12.61
75	8.94	76	7.44
77	2.11	78	2.00
79	0.0	80	0.0

Table 49. Differential pressure drops for the reference bundle at a flow rate of 0.022 m^3/sec in shroud 2

Tap No.	Pressure (kPa)	Tap No.	Pressure (kPa)
1	59.69	2	60.19
3	58.86	4	58.66
5	58.15	6	57.59
7	57.29	8	56.88
9	57.12	10	55.83
11	56.40	12	55.52
13	55.81	14	54.81
15	56.39	16	54.45
17	54.96	18	54.15
19	55.46	20	53.84
21	49.28	22	45.06
23	44.93	24	43.36
25	44.40	26	42.86
27	43.51	28	42.63
29	43.13	30	42.18
31	42.26	32	41.84
33	41.77	34	41.09
35	41.16	36	40.21
37	40.63	38	39.58
39	39.97	40	39.21
41	39.31	42	38.54
43	38.64	44	38.12
45	37.95	46	37.30
47	37.31	48	36.81
49	37.03	50	35.94
51	36.37	52	35.49
53	35.52	54	34.75
55	34.61	56	33.85
57	34.46	58	33.24
59	33.52	60	32.46
61	34.03	62	32.33
63	23.46	64	22.18
65	22.28	66	21.57
67	21.52	68	20.90
69	20.90	70	20.05
71	18.84	72	18.38
73	18.28	74	16.42
75	12.18	76	9.55
77	3.08	78	2.37
79	0.0	80	0.0

Table 50. Differential pressure drops for the reference bundle at a flow rate of 0.0063 m^3/sec in shroud 2

Tap No.	Pressure (kPa)	Tap No.	Pressure (kPa)
1	6.58	2	6.60
3	6.40	4	6.45
5	6.31	6	6.35
7	6.21	8	6.28
9	6.21	10	6.17
11	6.09	12	6.15
13	6.11	14	6.05
15	6.06	16	6.03
17	5.99	18	5.96
19	6.01	20	5.91
21	5.30	22	4.99
23	4.89	24	4.81
25	4.83	26	4.78
27	4.75	28	4.73
29	4.70	30	4.66
31	4.63	32	4.60
33	4.53	34	4.52
35	4.49	36	4.47
37	4.39	38	4.42
39	4.32	40	4.37
41	4.29	42	4.28
43	4.24	44	4.22
45	4.14	46	4.13
47	4.08	48	4.01
49	3.98	50	3.99
51	3.93	52	3.91
53	3.86	54	3.85
55	3.81	56	3.74
57	3.79	58	3.69
59	3.71	60	3.65
61	3.78	62	3.64
63	2.65	64	2.50
65	2.49	66	2.44
67	2.41	68	2.36
69	2.33	70	2.29
71	2.13	72	2.08
73	2.03	74	1.86
75	1.33	76	1.16
77	0.36	78	0.30
79	0.0	80	0.0

Table 51. Differential pressure drops for the reference bundle at a flow rate of 0.025 m^3/sec in shroud 2

Tap No.	Pressure (kPa)	Tap No.	Pressure (kPa)
1	74.84	2	75.84
3	73.35	4	74.02
5	72.31	6	71.92
7	71.25	8	71.38
9	70.37	10	70.97
11	69.46	12	70.37
13	69.23	14	69.63
15	70.52	16	68.69
17	68.92	18	68.15
19	68.83	20	67.56
21	61.26	22	56.23
23	55.76	24	55.09
25	55.22	26	54.30
27	54.39	28	52.72
29	53.76	30	52.12
31	52.83	32	51.83
33	52.21	34	51.21
35	51.15	36	50.78
37	51.16	38	49.82
39	49.90	40	49.43
41	49.27	42	48.65
43	48.35	44	48.15
45	47.70	46	47.18
47	46.82	48	46.64
49	46.04	50	45.58
51	45.44	52	44.68
53	44.46	54	43.31
55	43.37	56	42.24
57	43.27	58	41.16
59	41.95	60	41.02
61	42.86	62	40.80
63	29.11	64	27.84
65	27.77	66	26.73
67	26.83	68	26.32
69	25.79	70	25.07
71	23.47	72	22.98
73	22.85	74	20.70
75	15.13	76	11.84
77	3.59	78	3.02
79	0.0	80	0.0

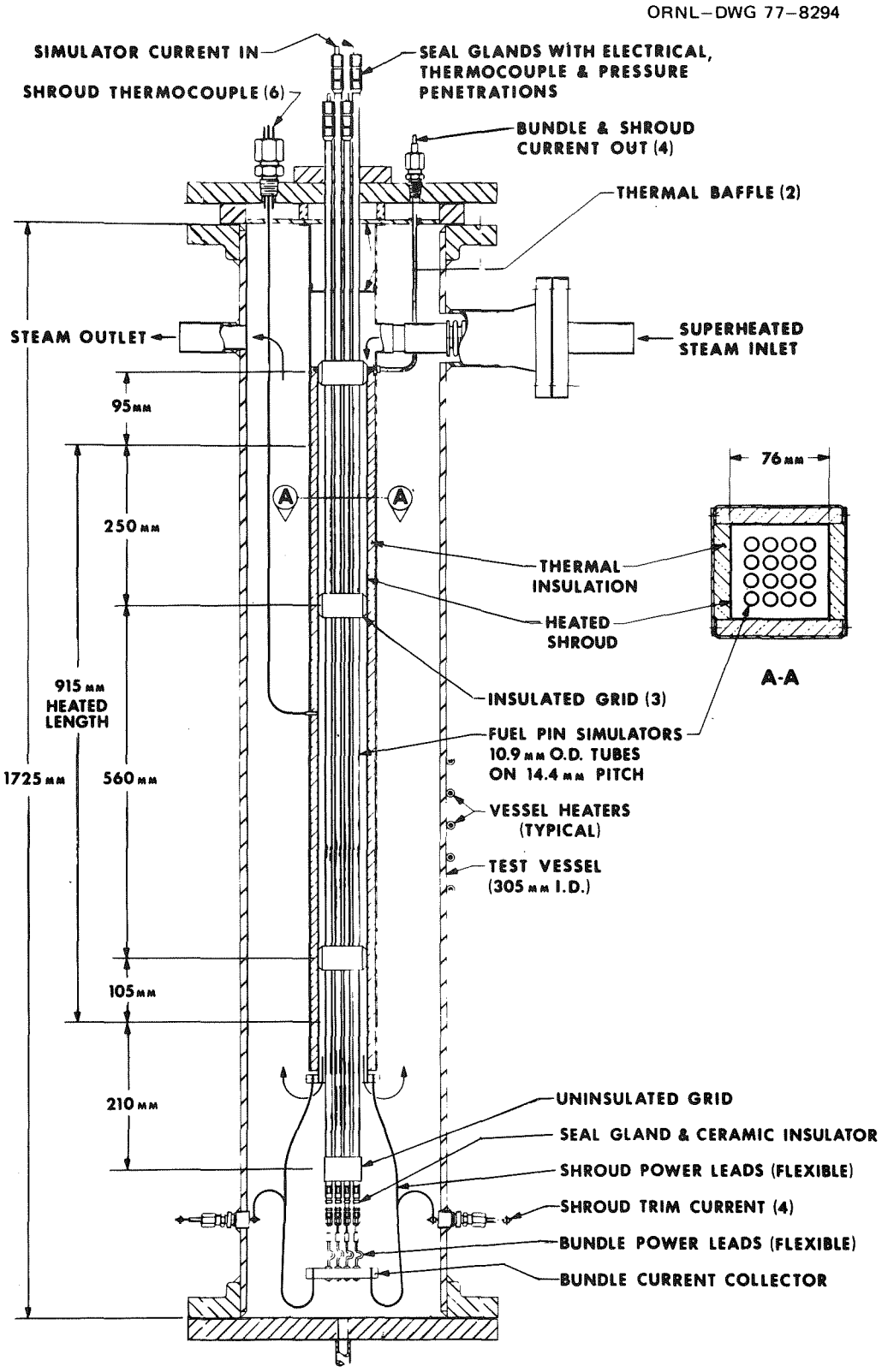

Fig. 1. Schematic of 4 × 4 test assembly. (See text for modifications made for B-2 test.)

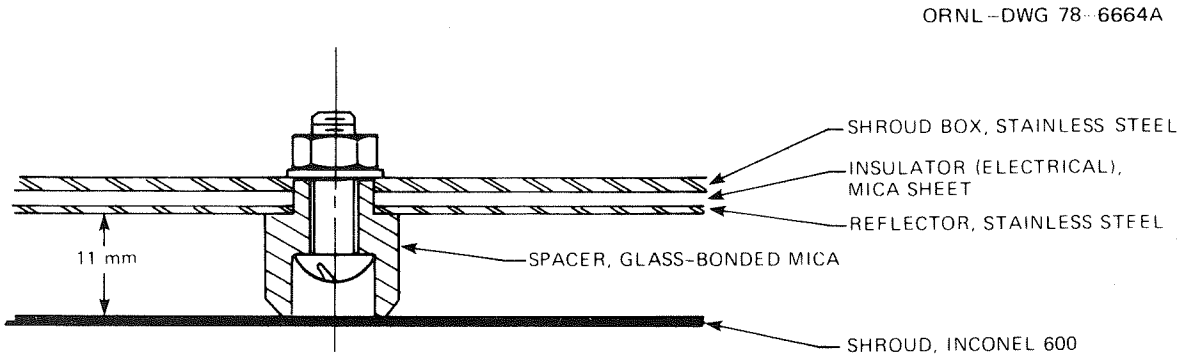

Fig. 2. Revised shroud insulation concept used in the B-2 test.

ORNL–DWG 77–8293

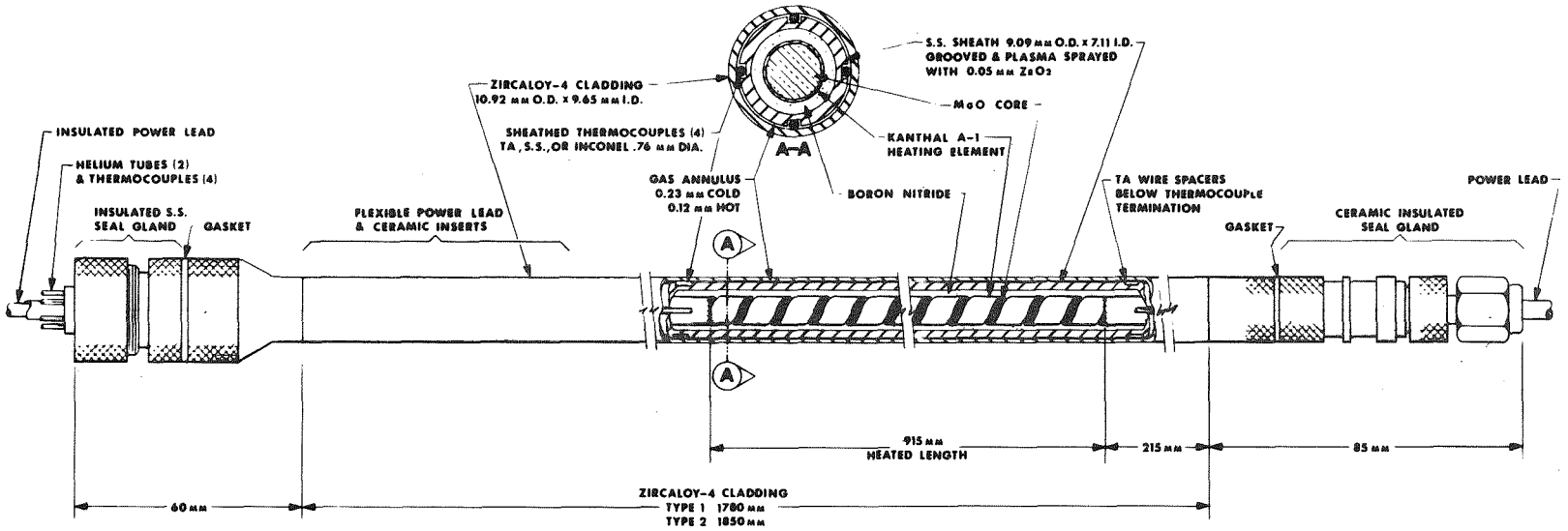

Fig. 3. Typical fuel pin simulator.

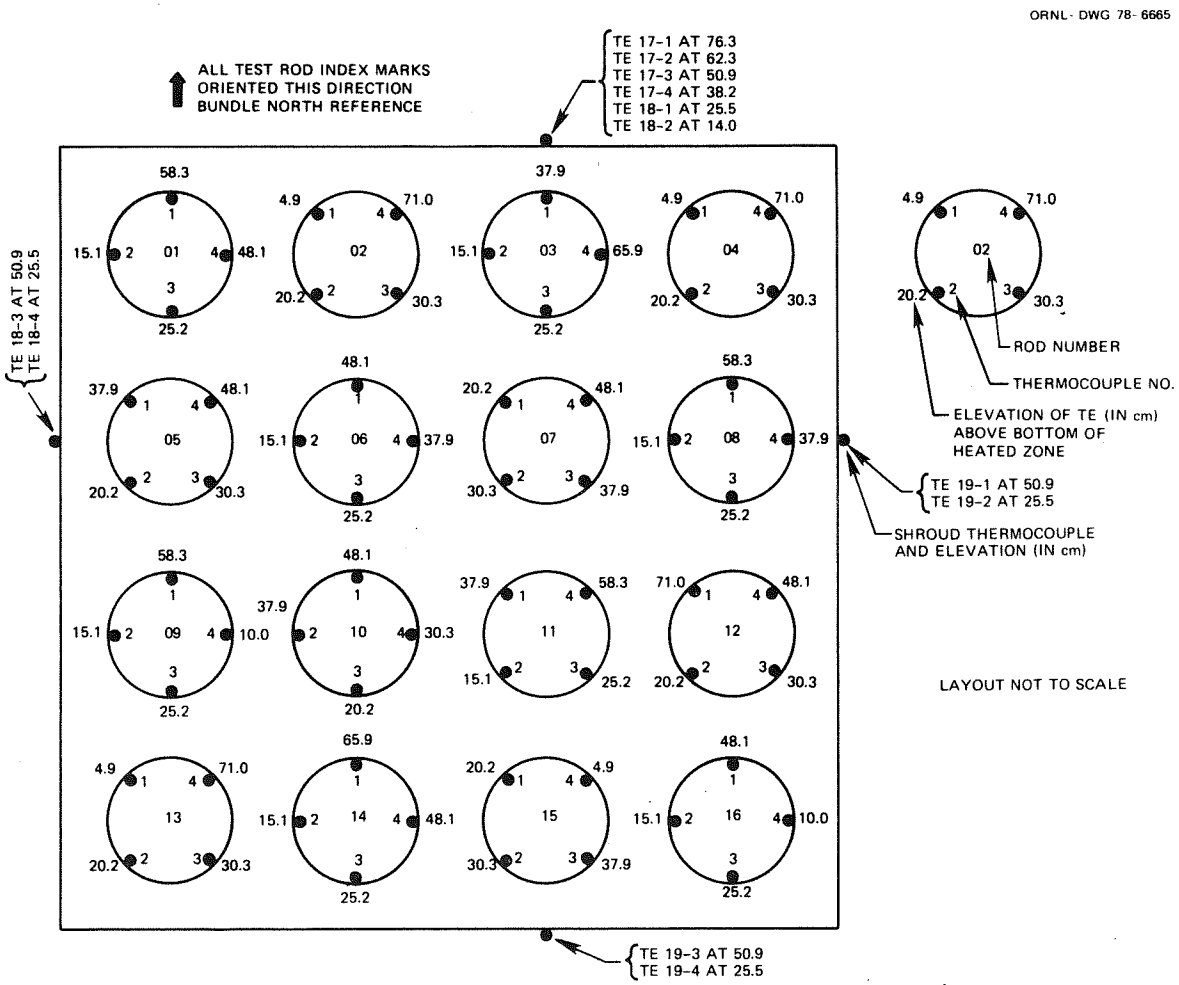

Fig. 4. As-built thermocouple locations and identifications in B-2 test (plan view).

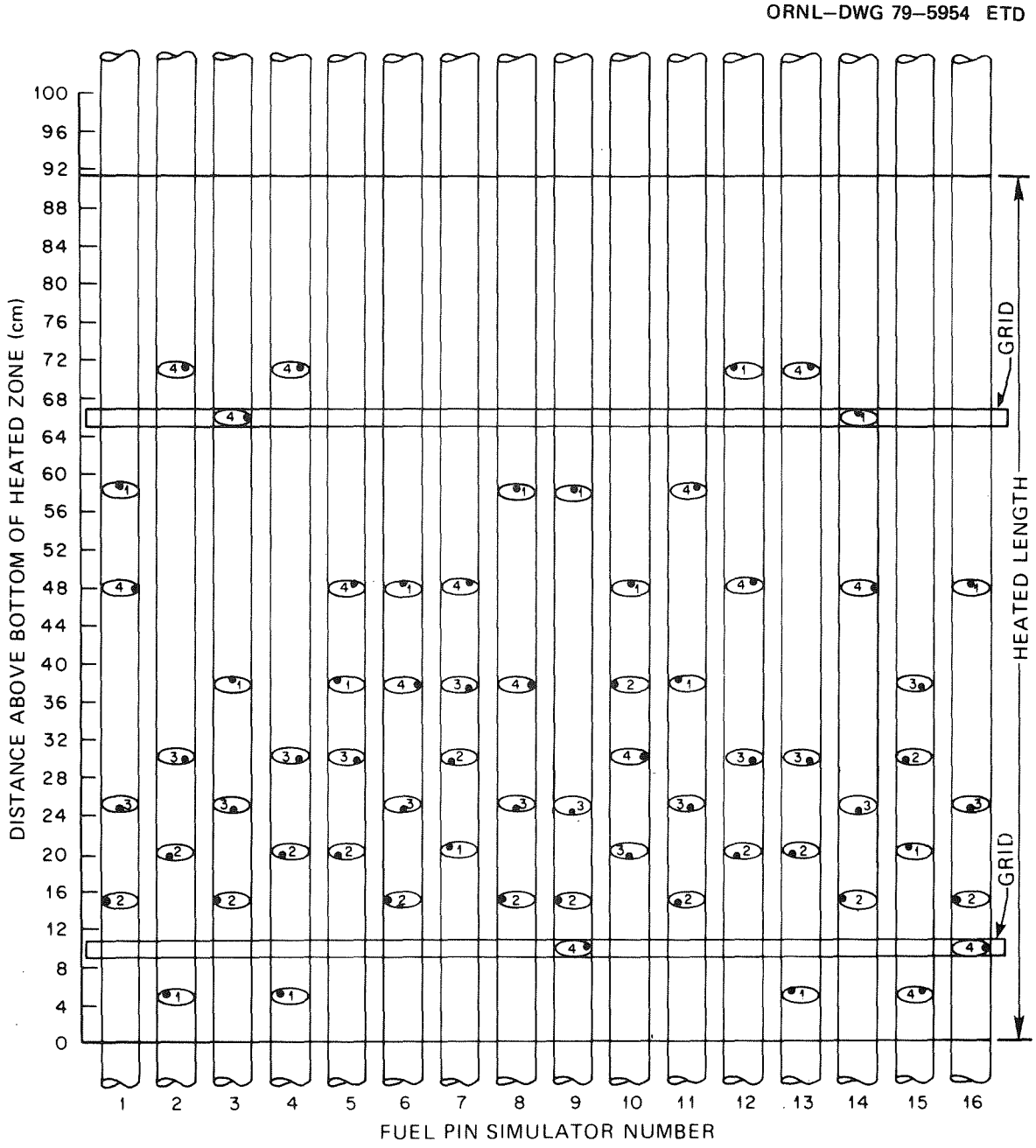

Fig. 5. As-built thermocouple locations in B-2 test (elevation).

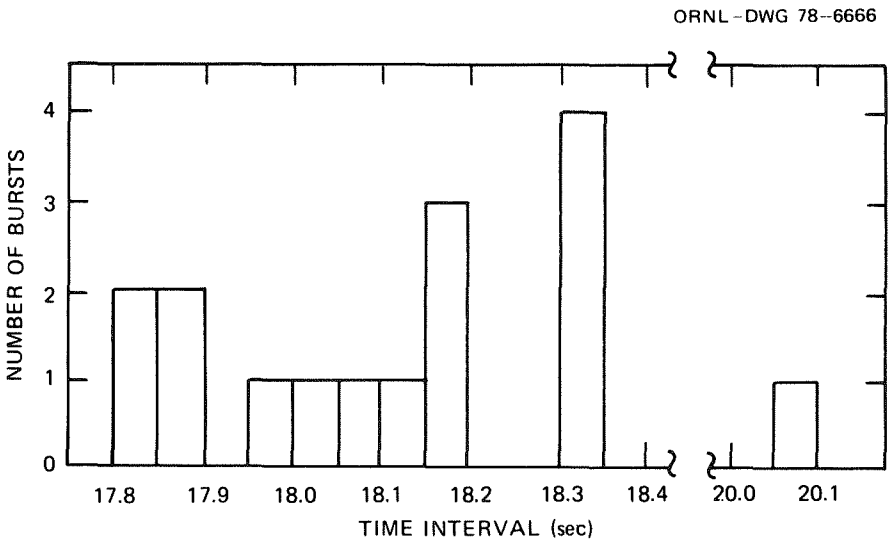

Fig. 6. Burst frequency distribution in B-2 test.

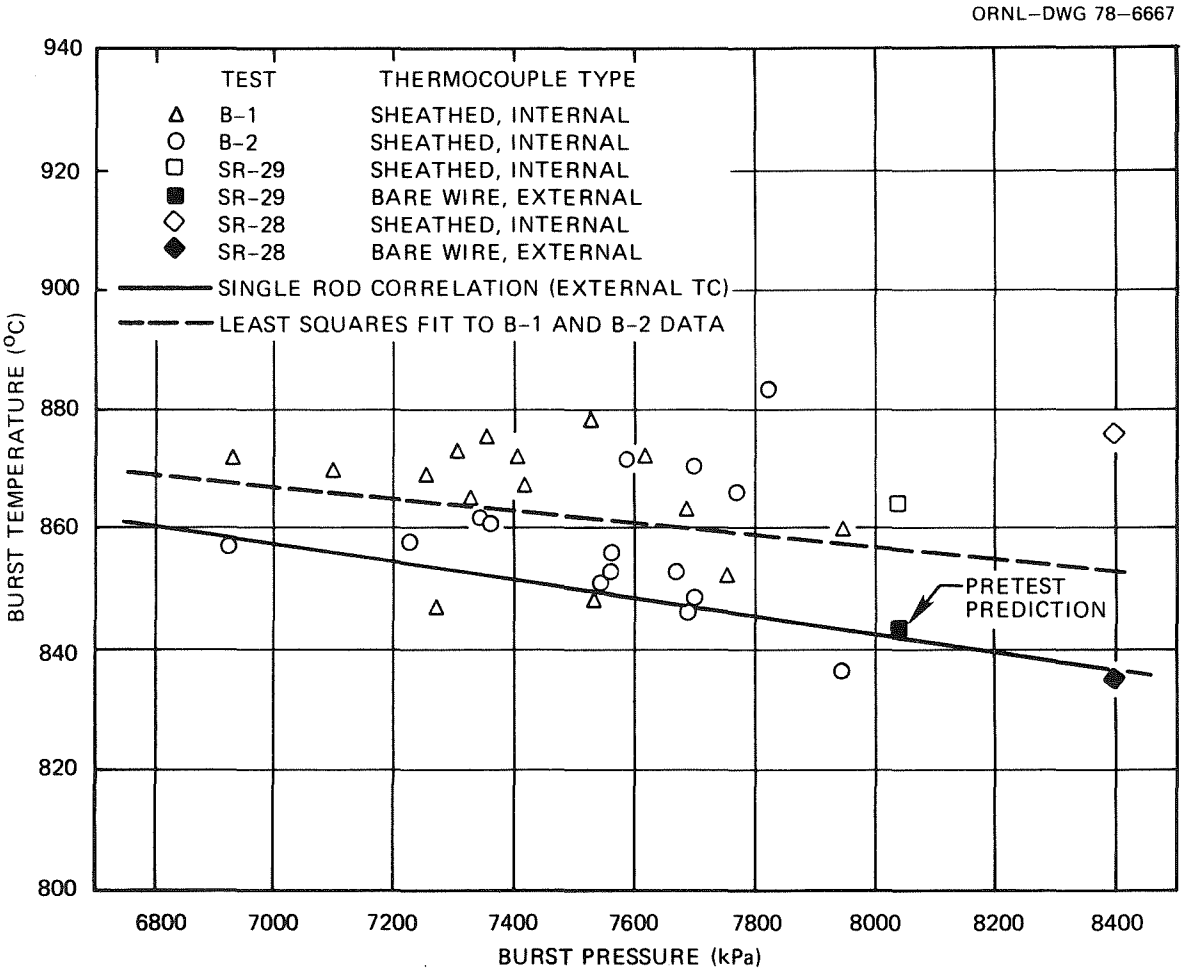

Fig. 7. B-2 burst temperatures compared with B-1 and single-rod test data.

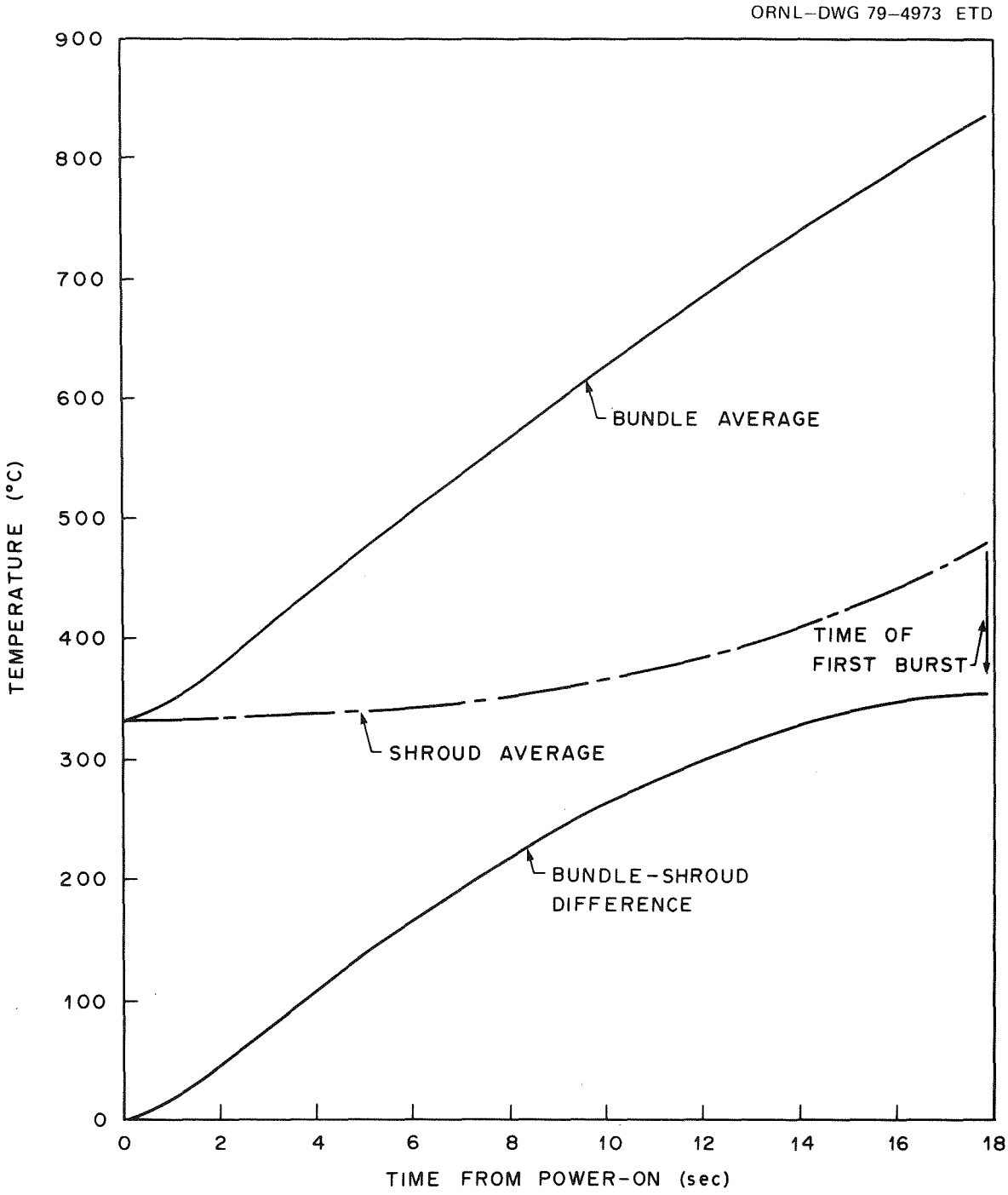

Fig. 8. Average temperatures in B-2 test.

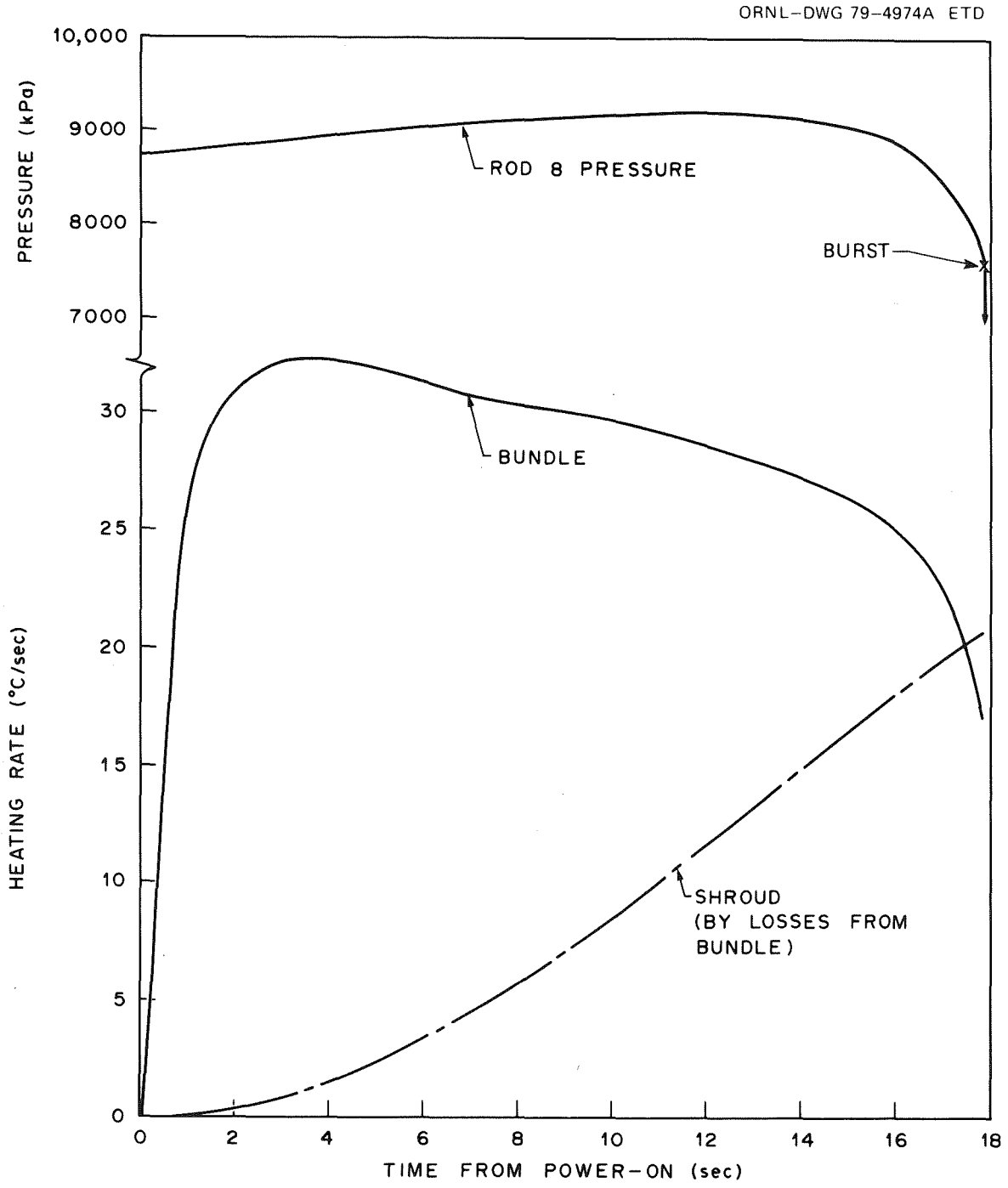

Fig. 9. Bundle and shroud heating rates in B-2 test.

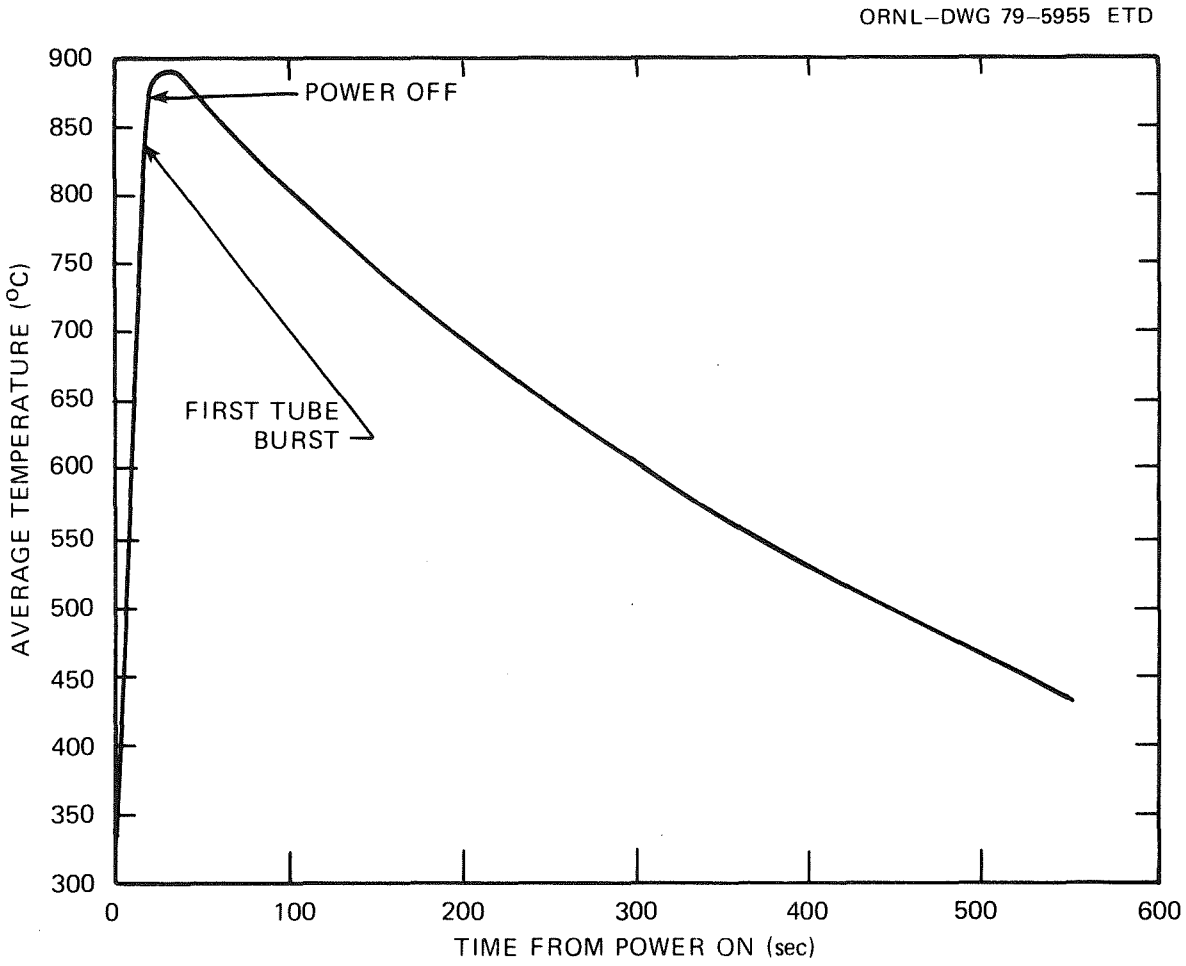

Fig. 10. B-2 average temperature during posttest cooldown.

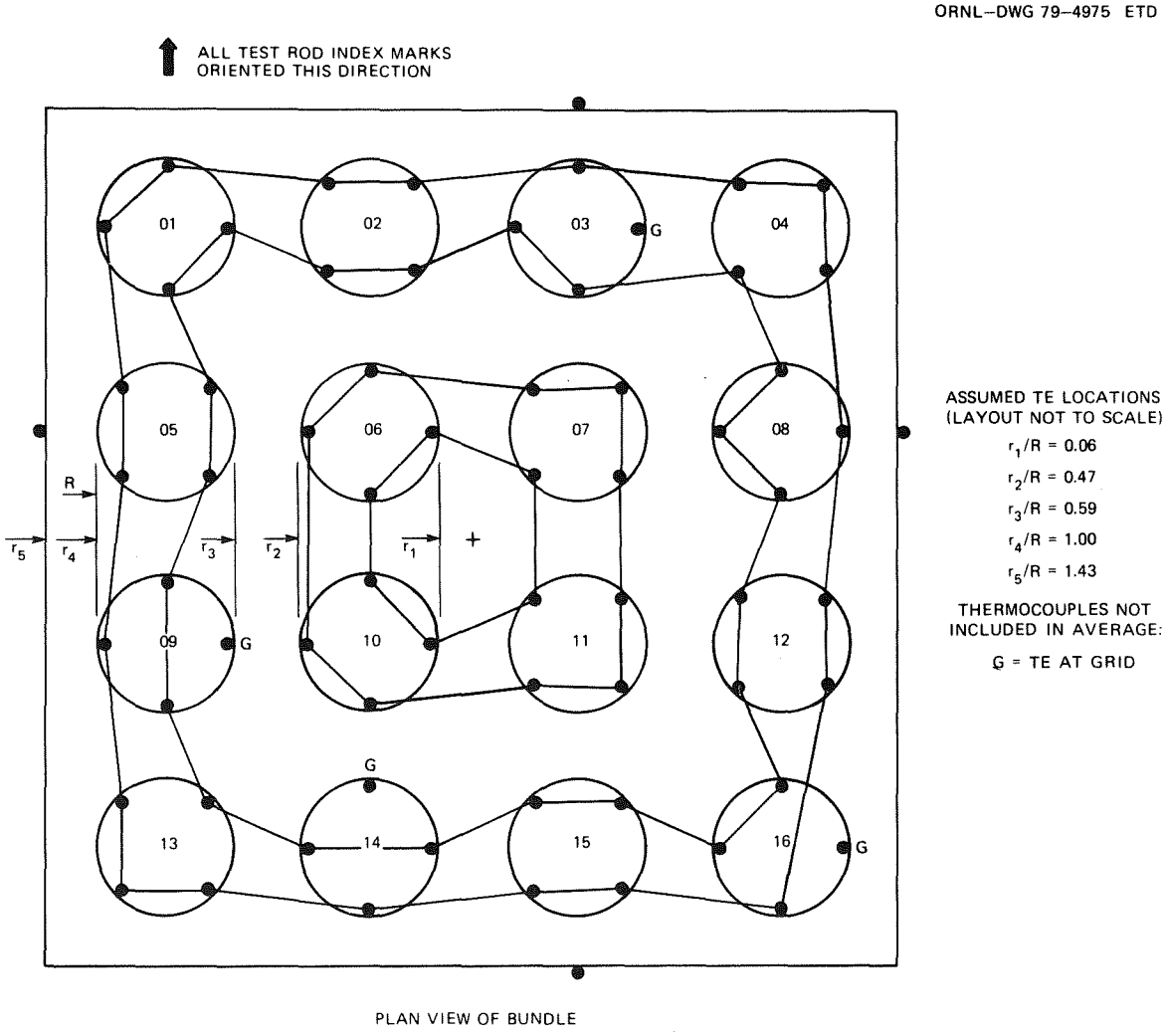

Fig. 11. Thermocouple assignments for calculation of radial temperature profile in B-2 test.

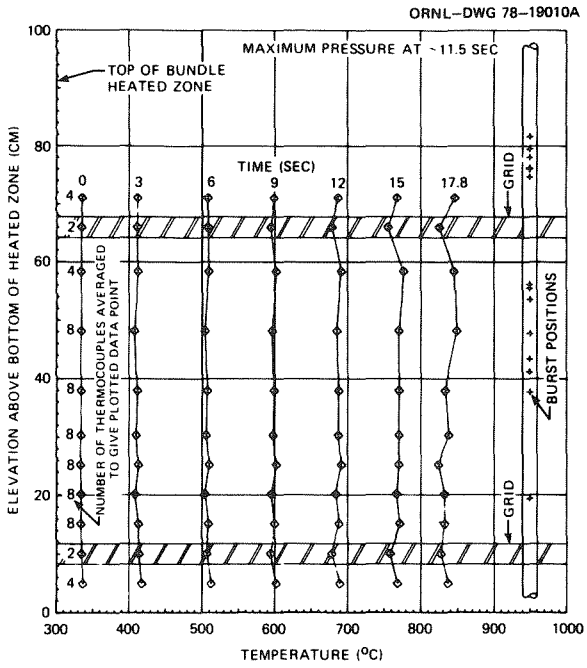

Fig. 12. Axial temperature distribution in the B-2 bundle as a function of time.

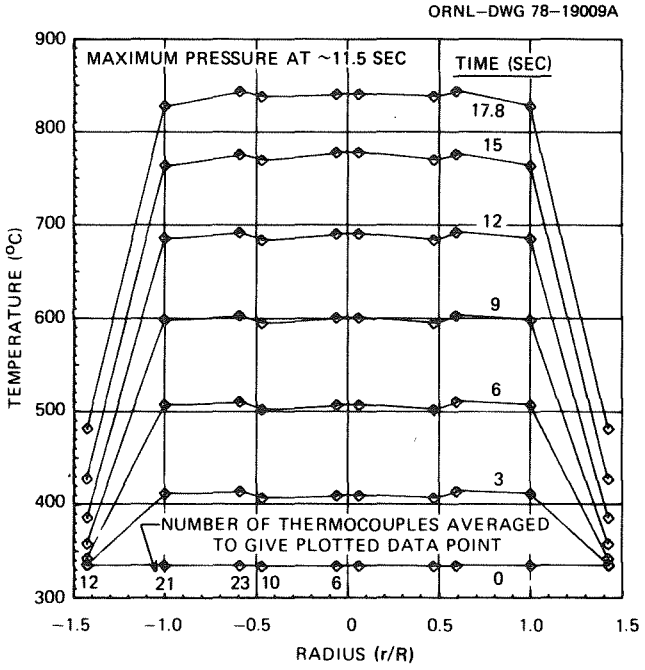

Fig. 13. Radial temperature distribution in the B-2 bundle as a function of time.

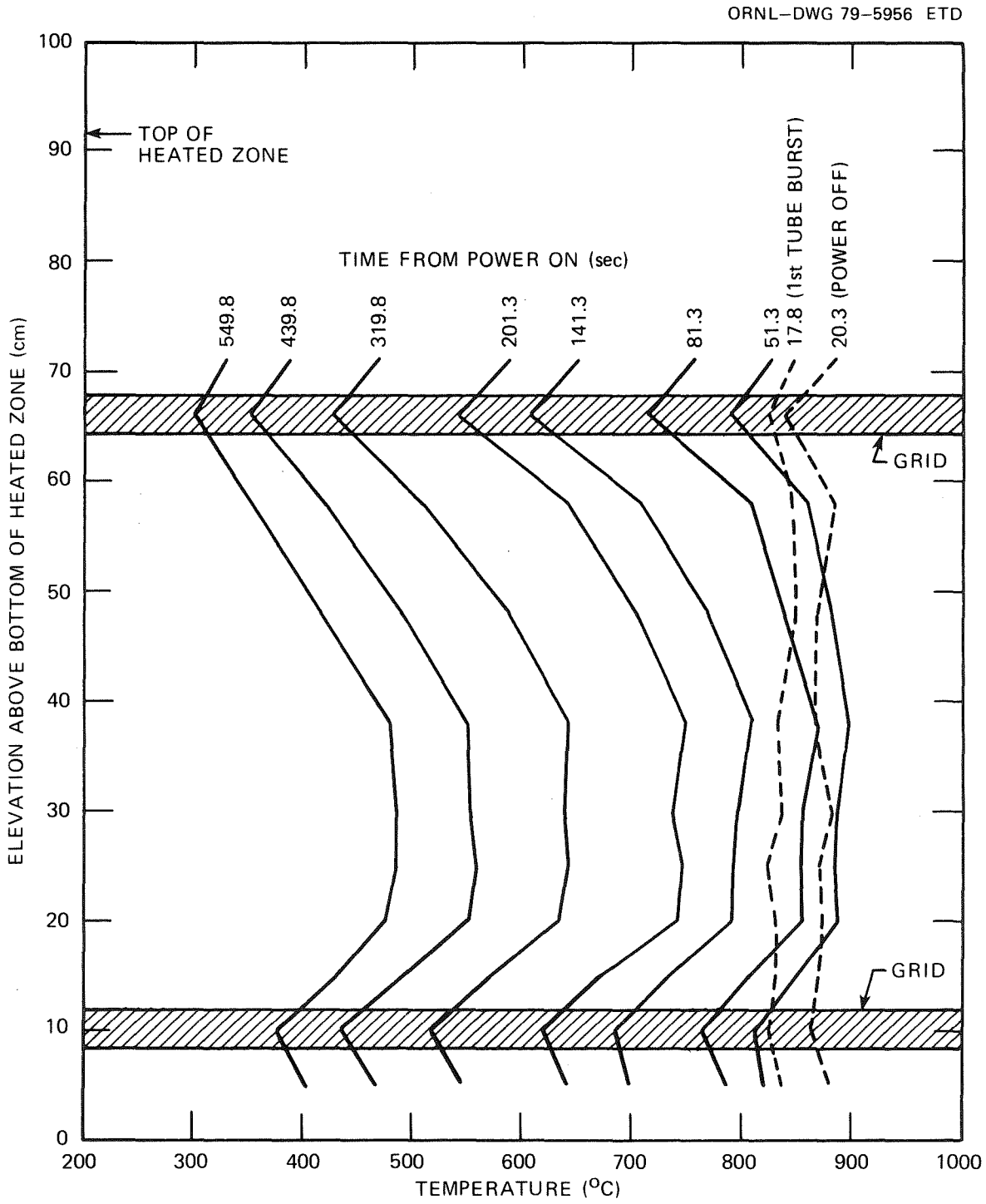

Fig. 14. Axial temperature distribution in B-2 during posttest cooldown.

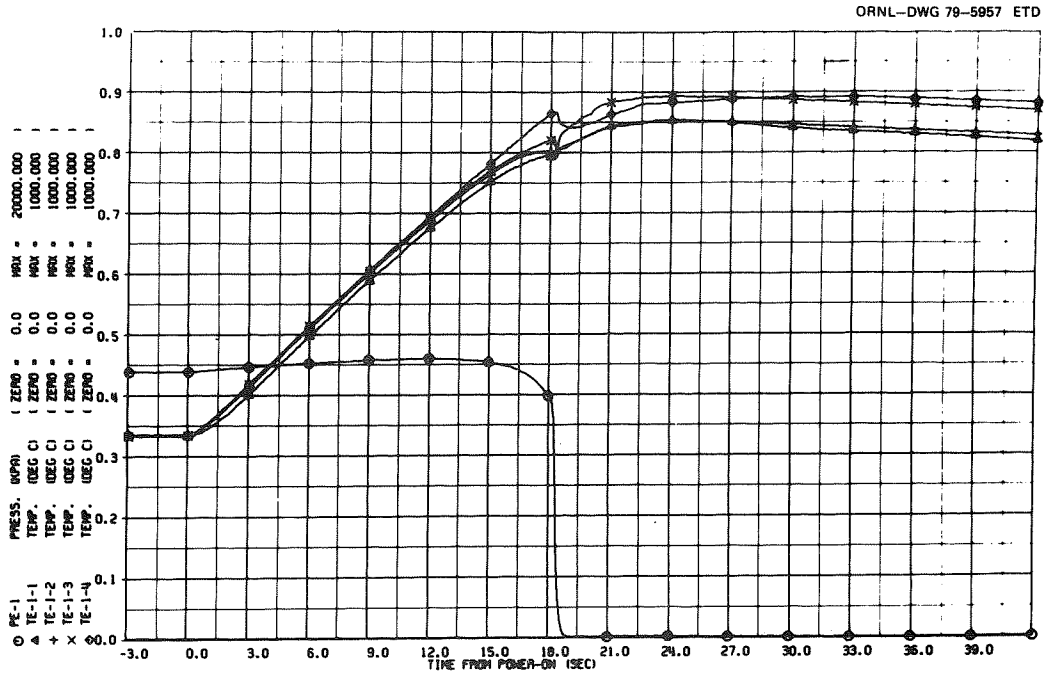

Fig. 15. Temperature and pressure transients for rod No. 1.

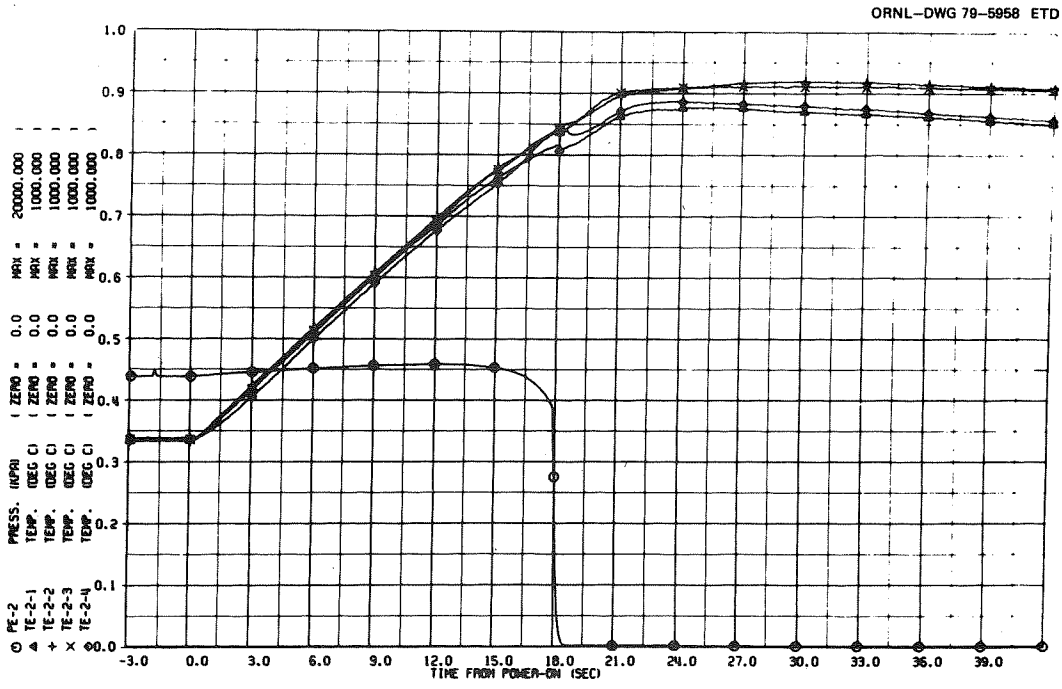

Fig. 16. Temperature and pressure transients for rod No. 2.

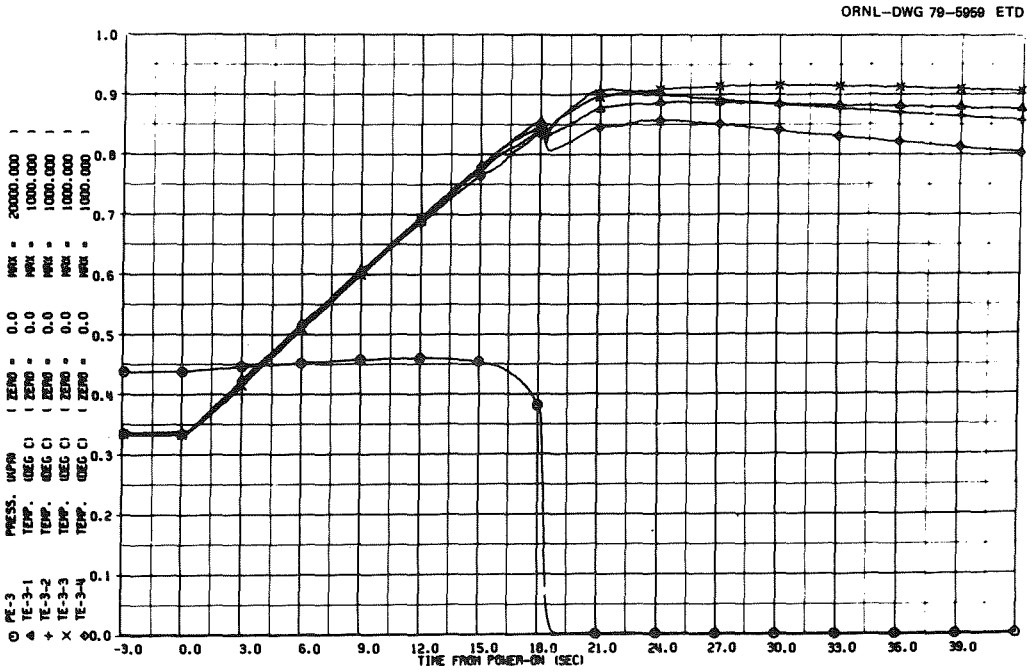

Fig. 17. Temperature and pressure transients for rod No. 3.

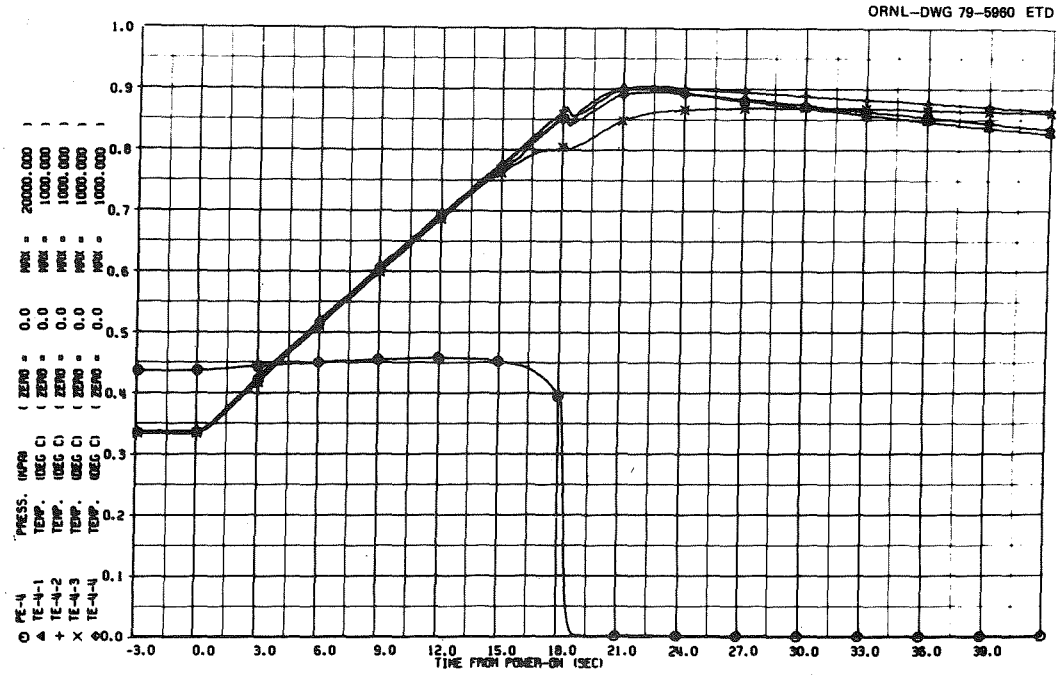

Fig. 18. Temperature and pressure transients for rod No. 4.

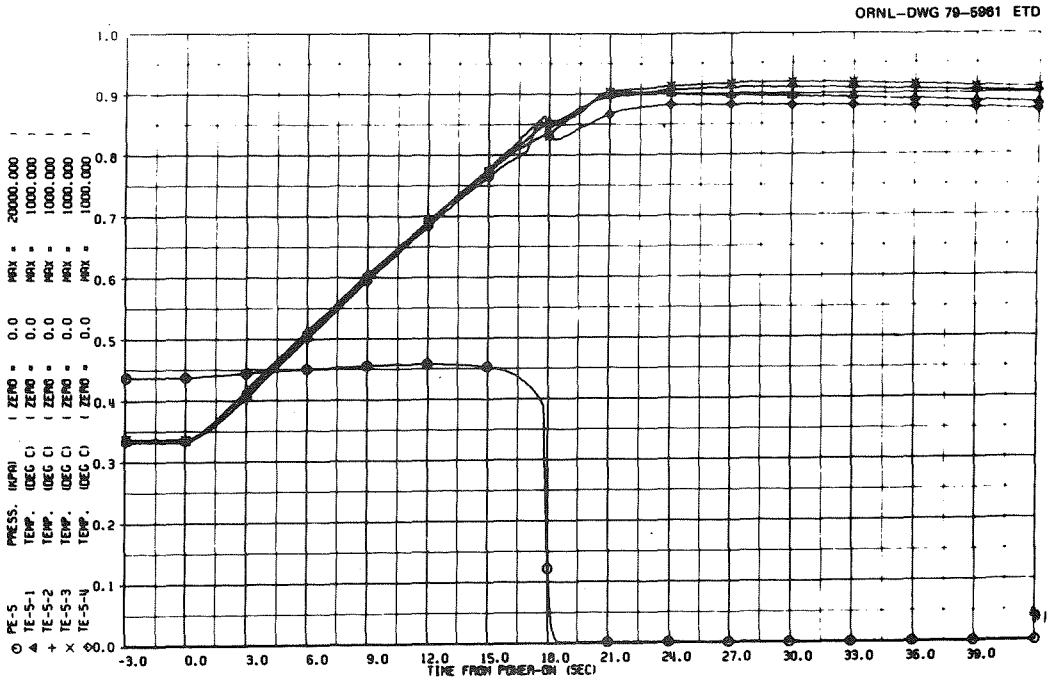

Fig. 19. Temperature and pressure transients for rod No. 5.

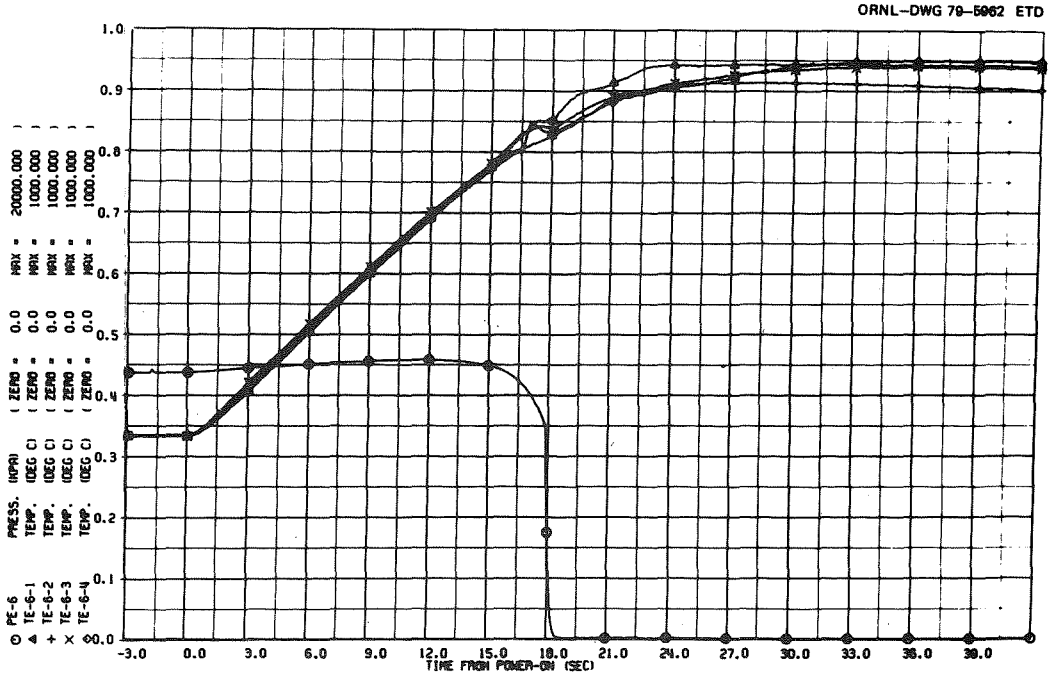

Fig. 20. Temperature and pressure transients for rod No. 6.

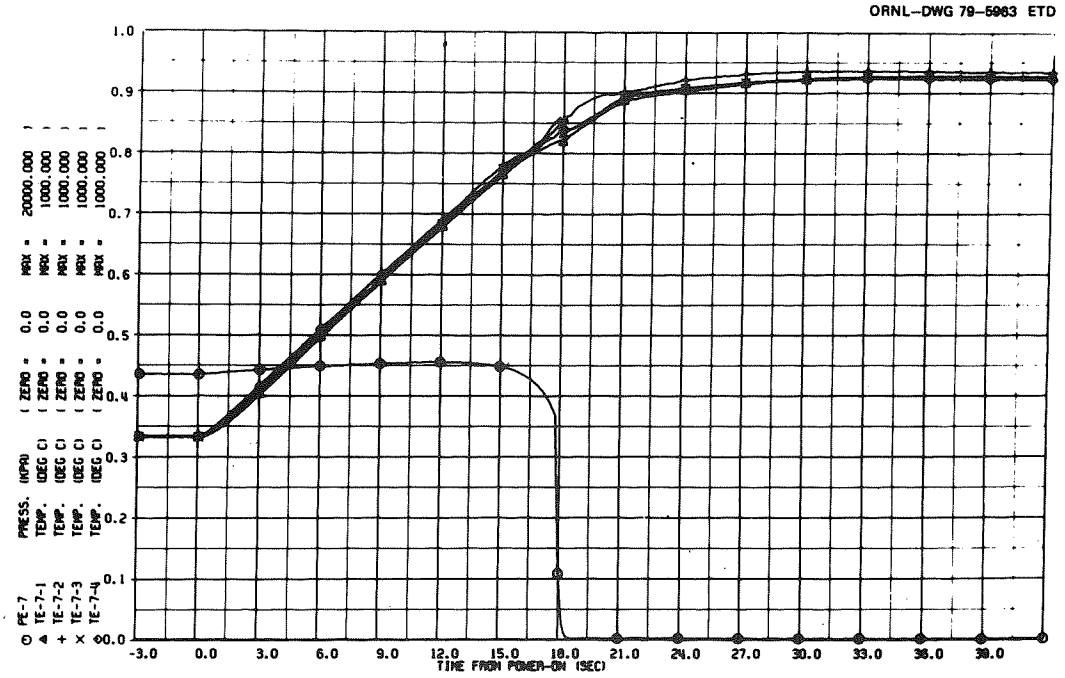

Fig. 21. Temperature and pressure transients for rod No. 7.

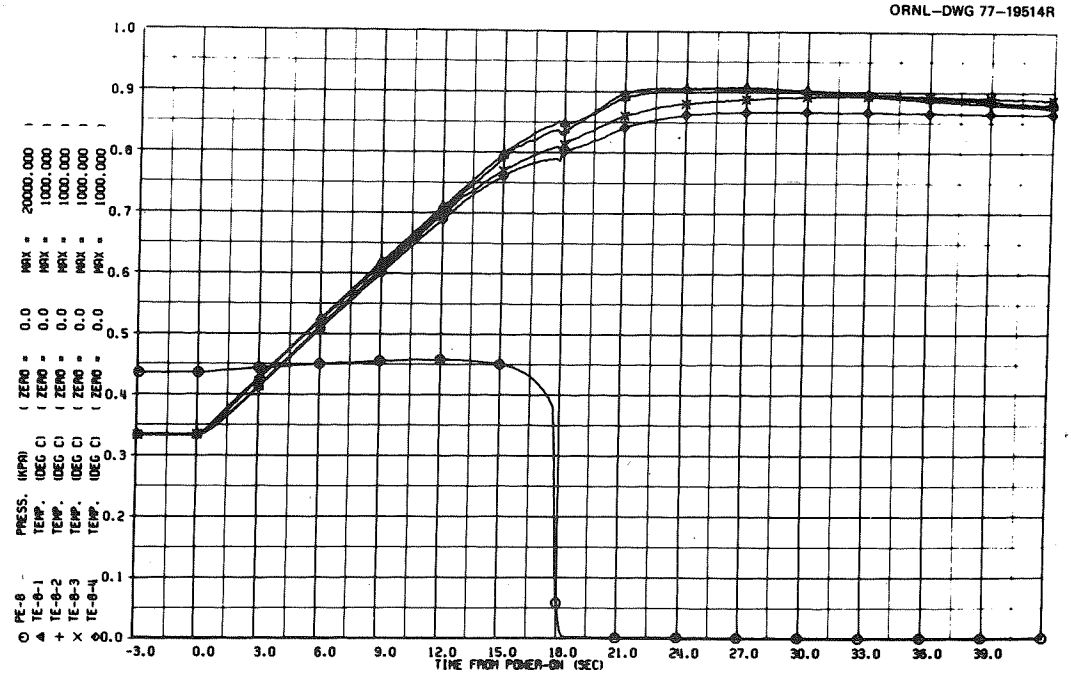

Fig. 22. Temperature and pressure transients for rod No. 8.

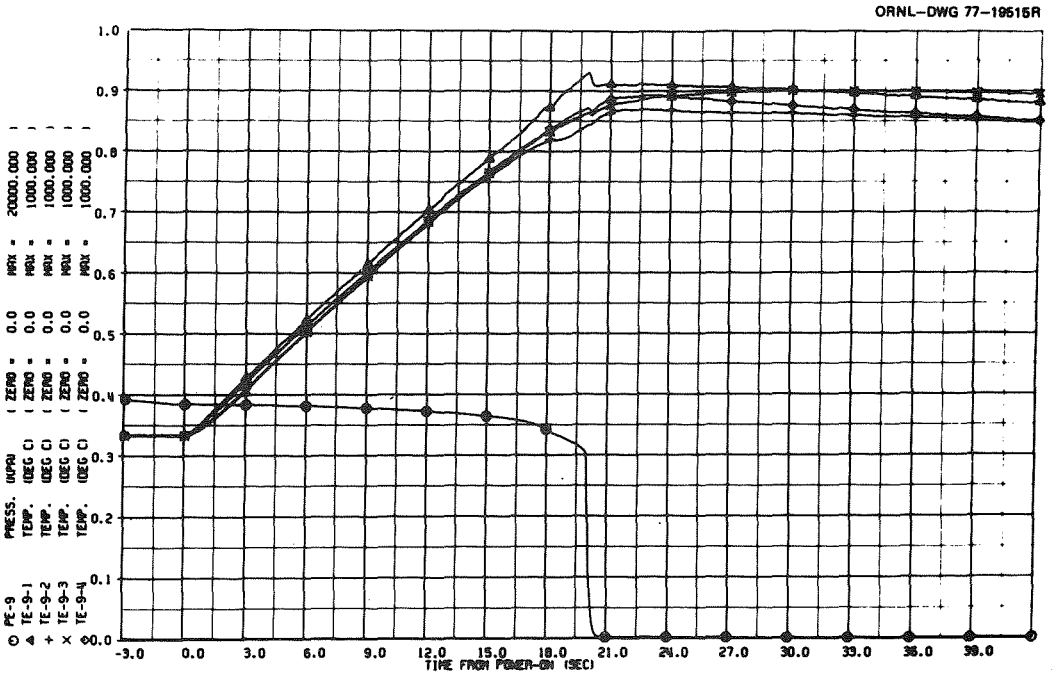

Fig. 23. Temperature and pressure transients for rod No. 9.

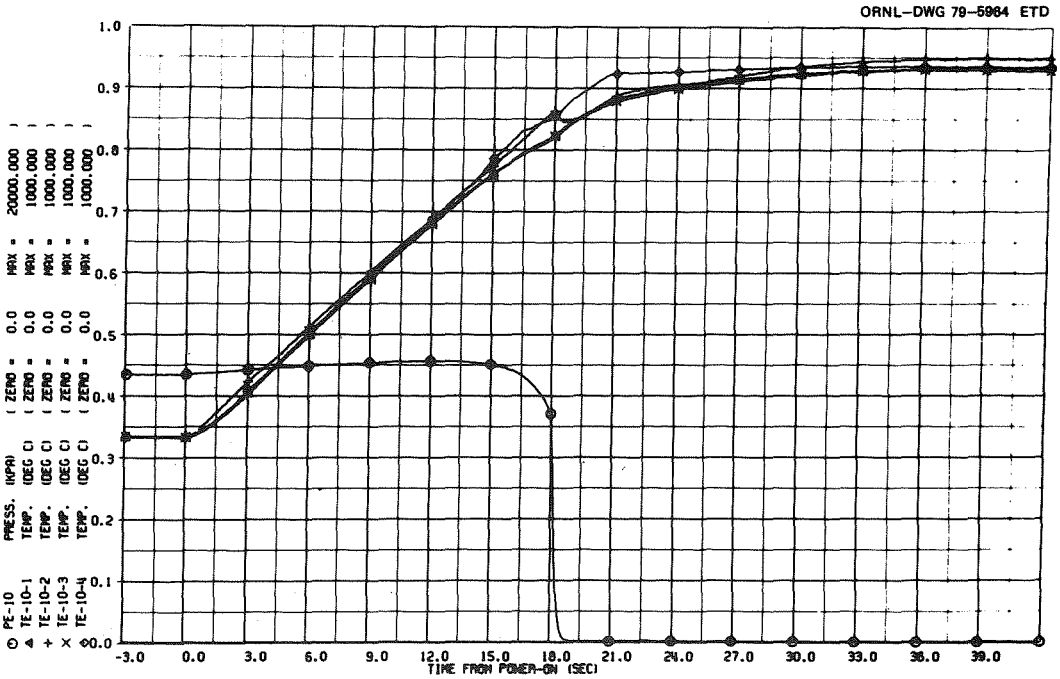

Fig. 24. Temperature and pressure transients for rod No. 10.

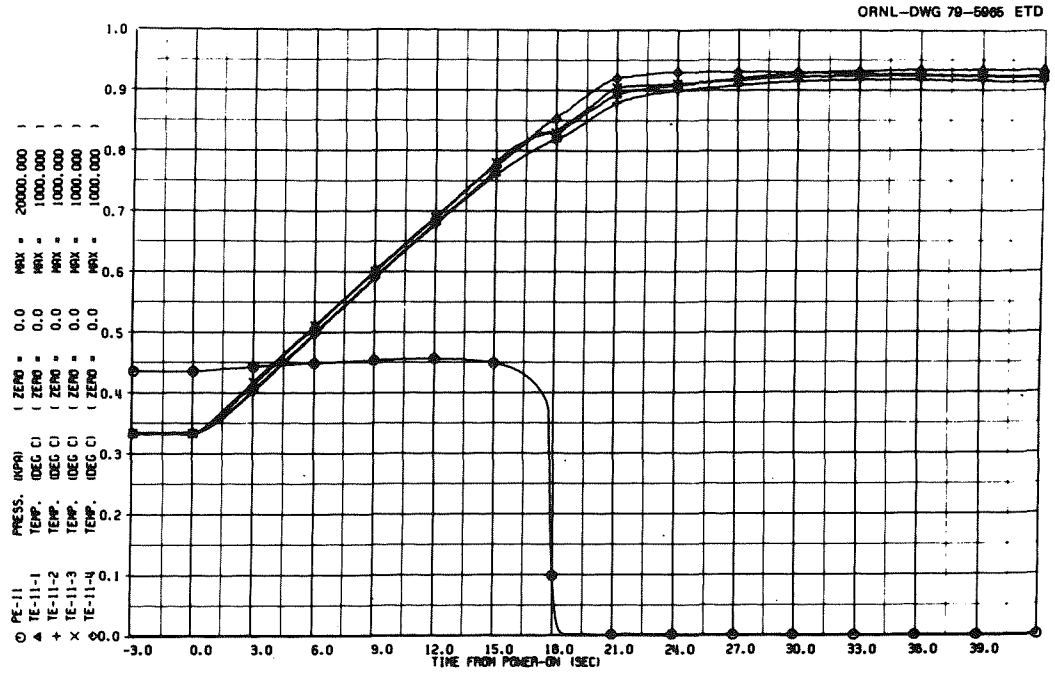

Fig. 25. Temperature and pressure transients for rod No. 11.

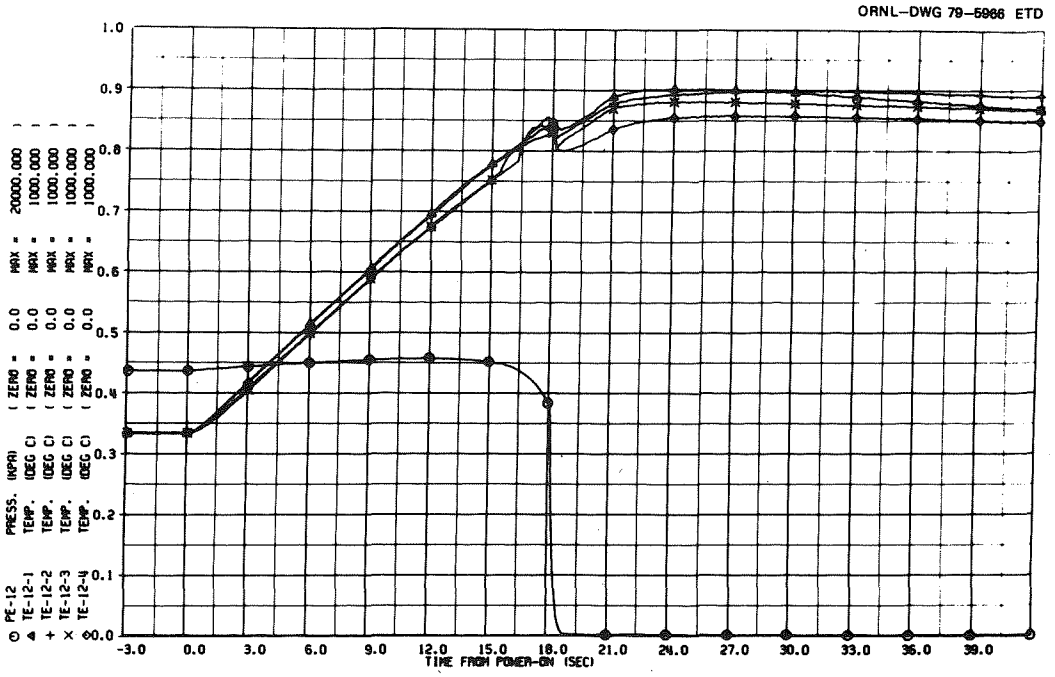

Fig. 26. Temperature and pressure transients for rod No. 12.

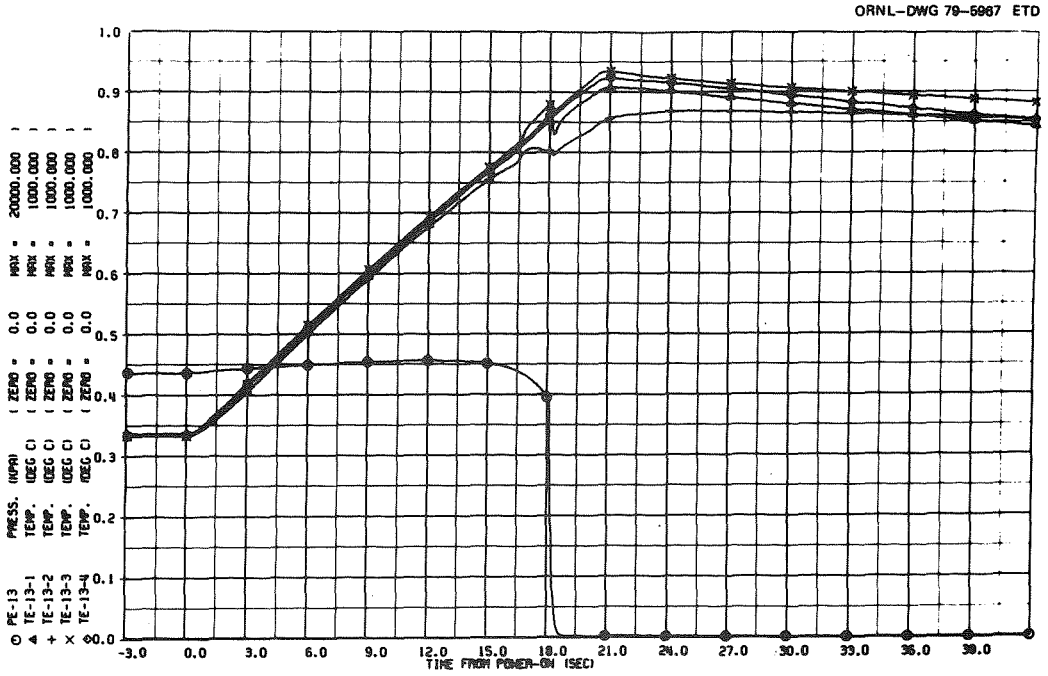

Fig. 27. Temperature and pressure transients for rod No. 13.

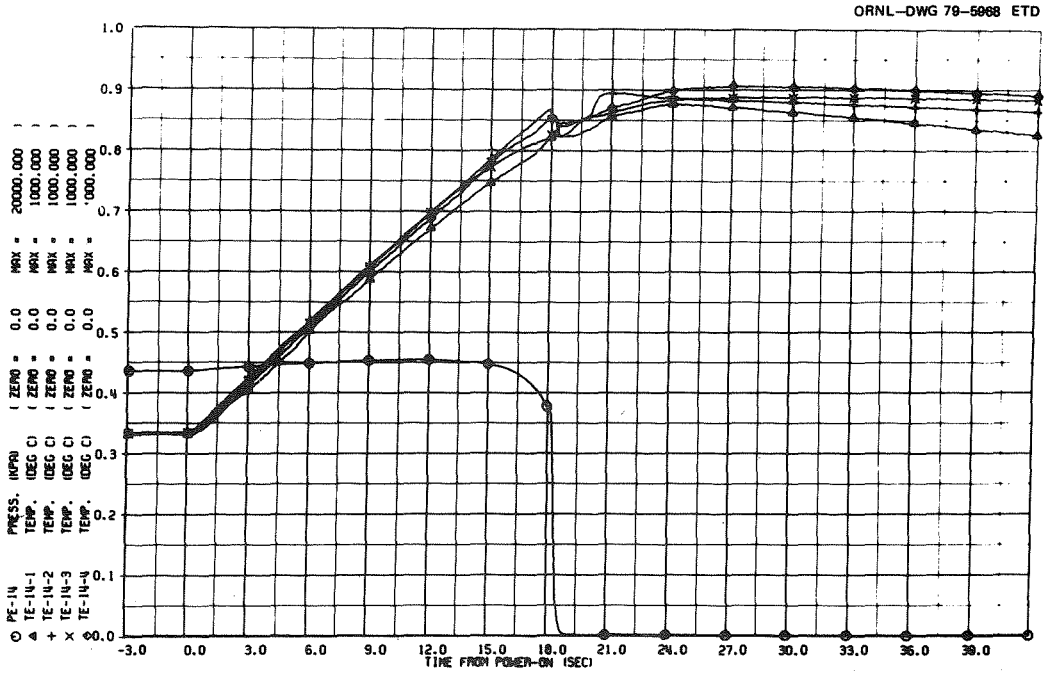

Fig. 28. Temperature and pressure transients for rod No. 14.

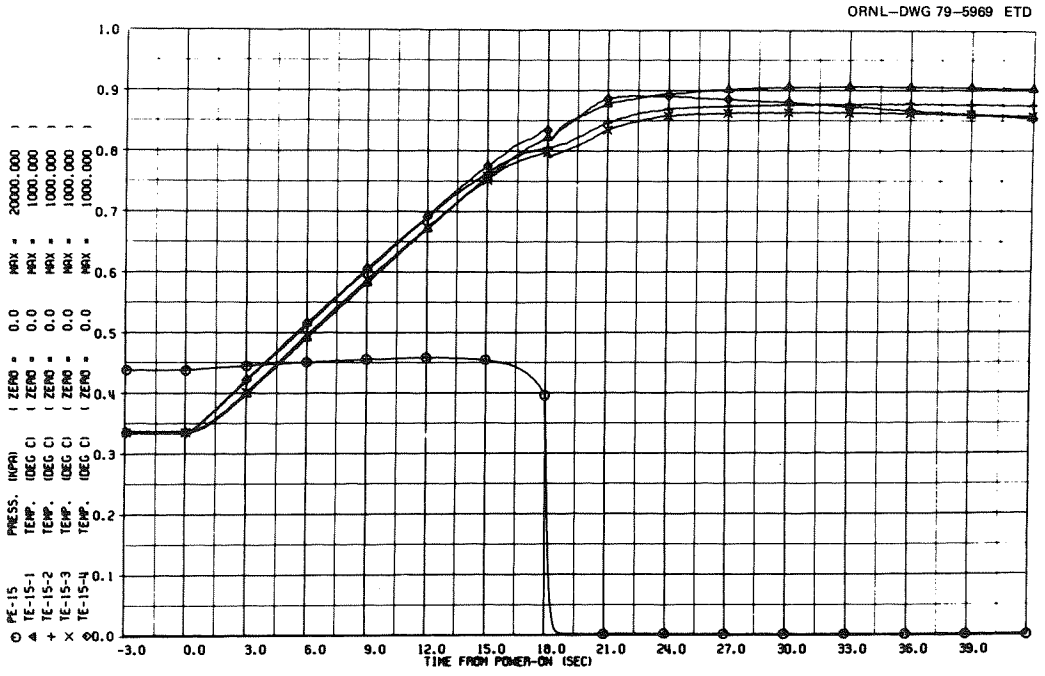

Fig. 29. Temperature and pressure transients for rod No. 15.

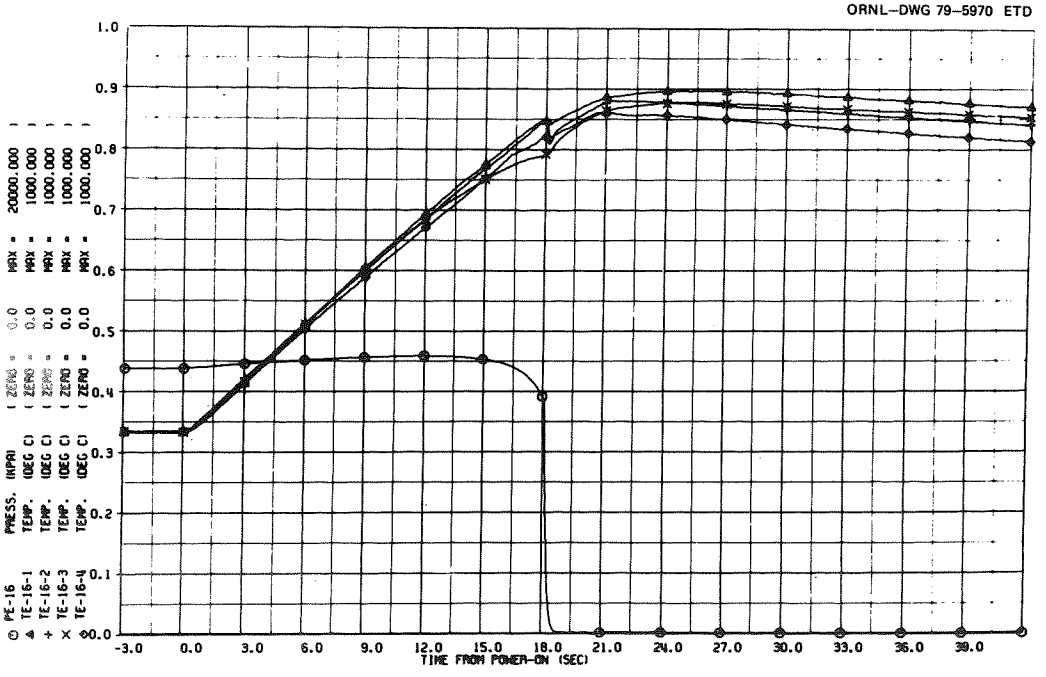

Fig. 30. Temperature and pressure transients for rod No. 16.

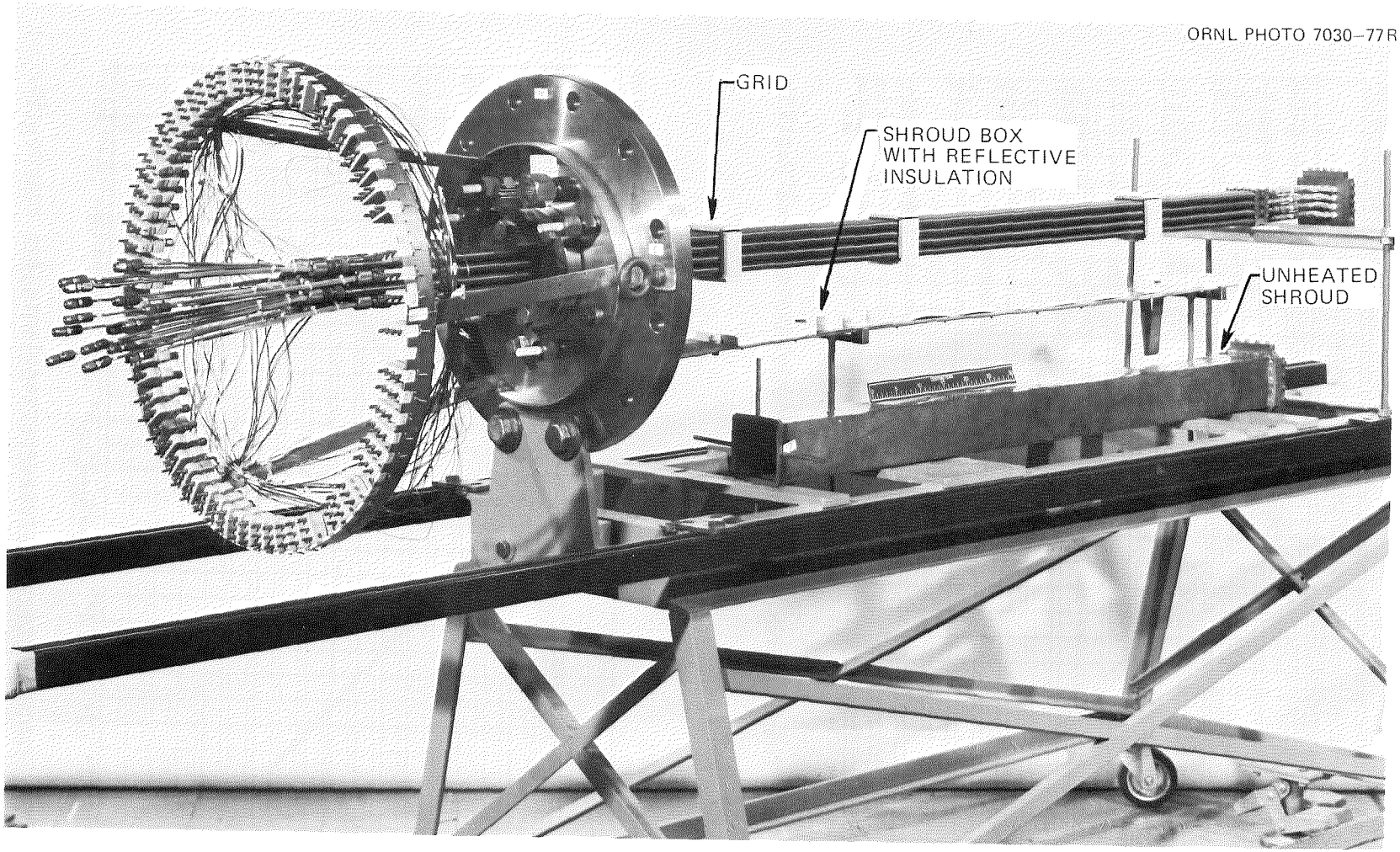

Fig. 31. Bundle B-2 prior to installation of unheated shroud and shroud box.

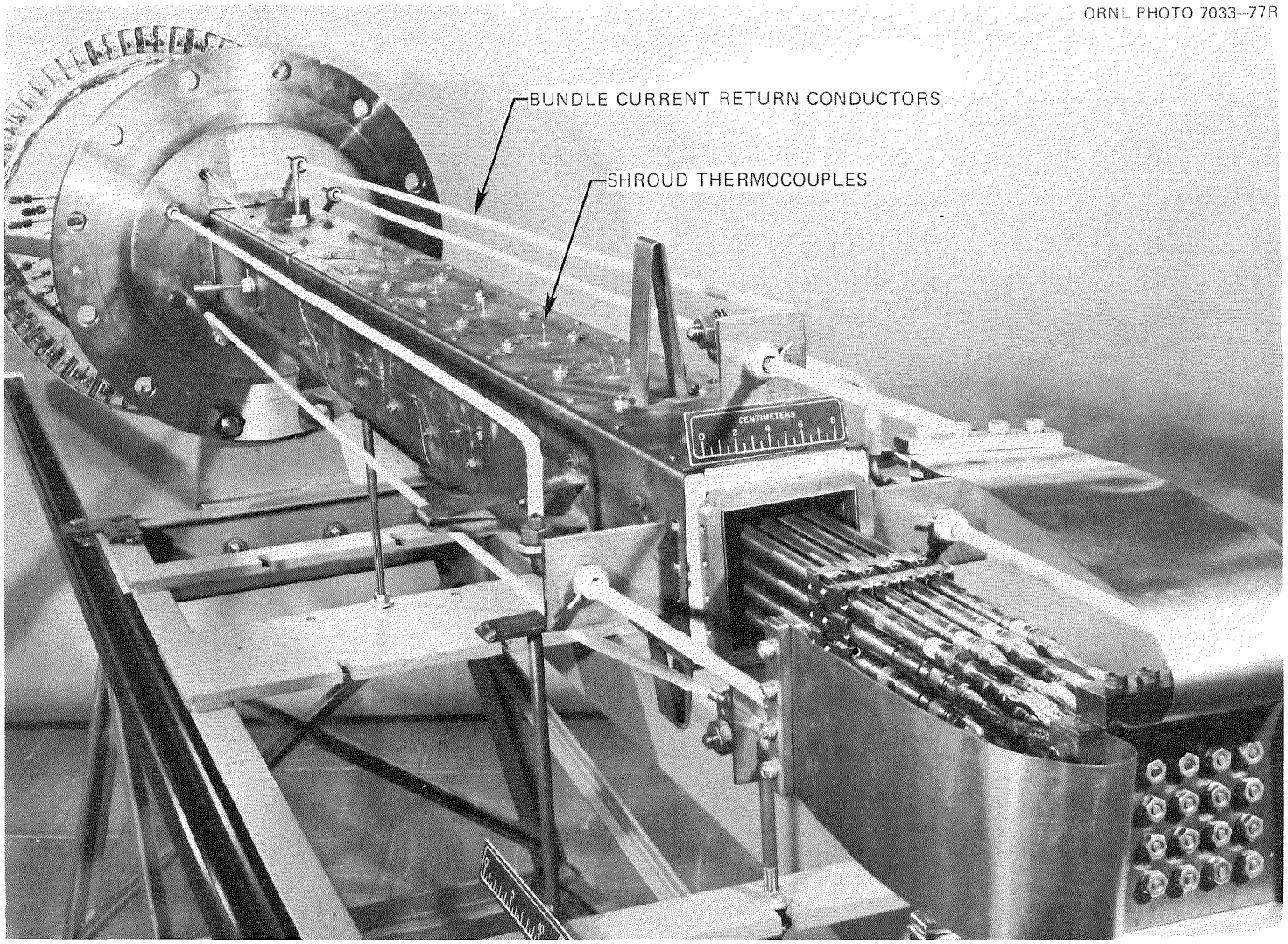

Fig. 32. Completely assembled B-2 test array.

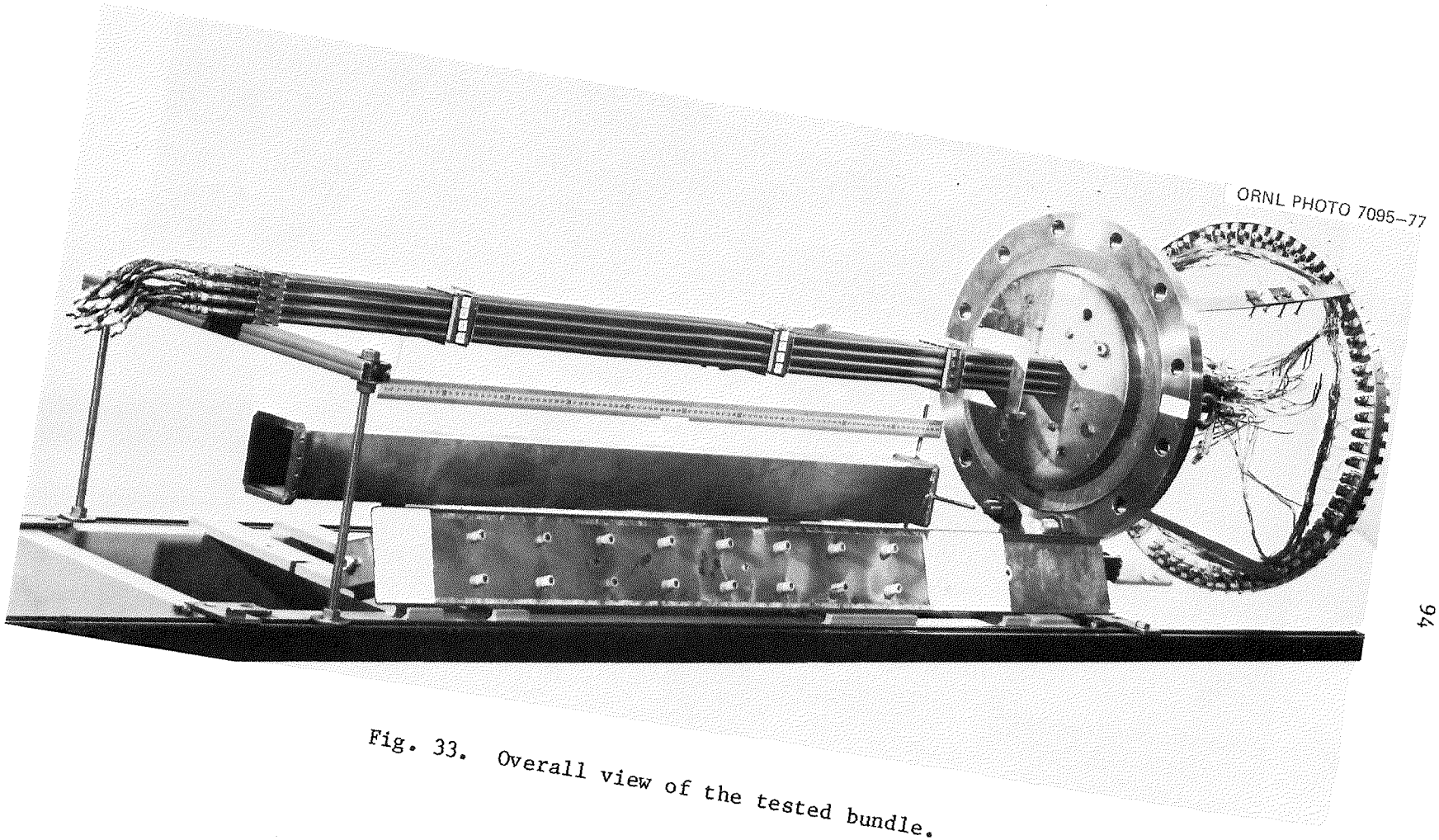

Fig. 33. Overall view of the tested bundle.

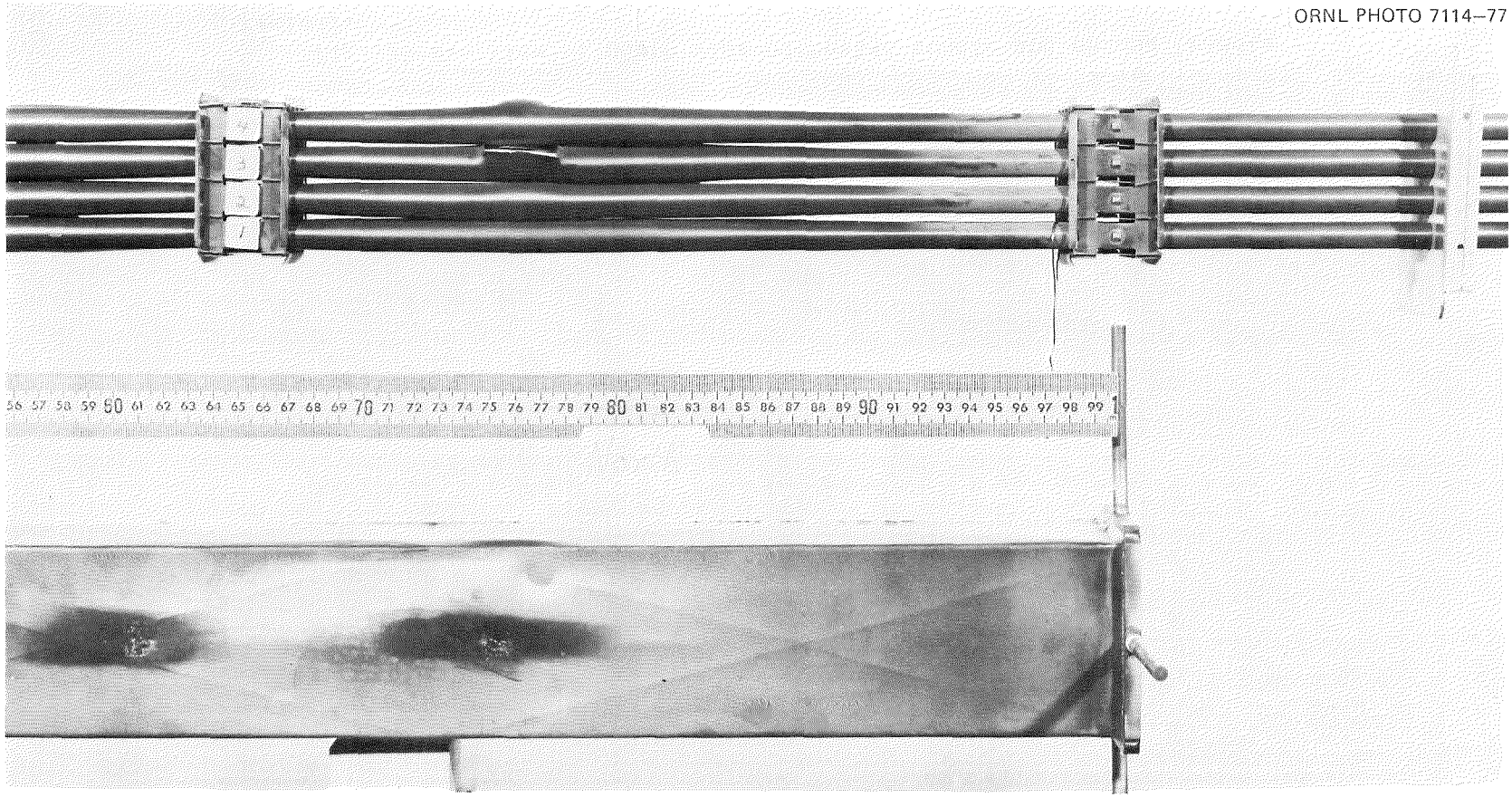

Fig. 34-A. View of north side of tested bundle and shroud (upper end).

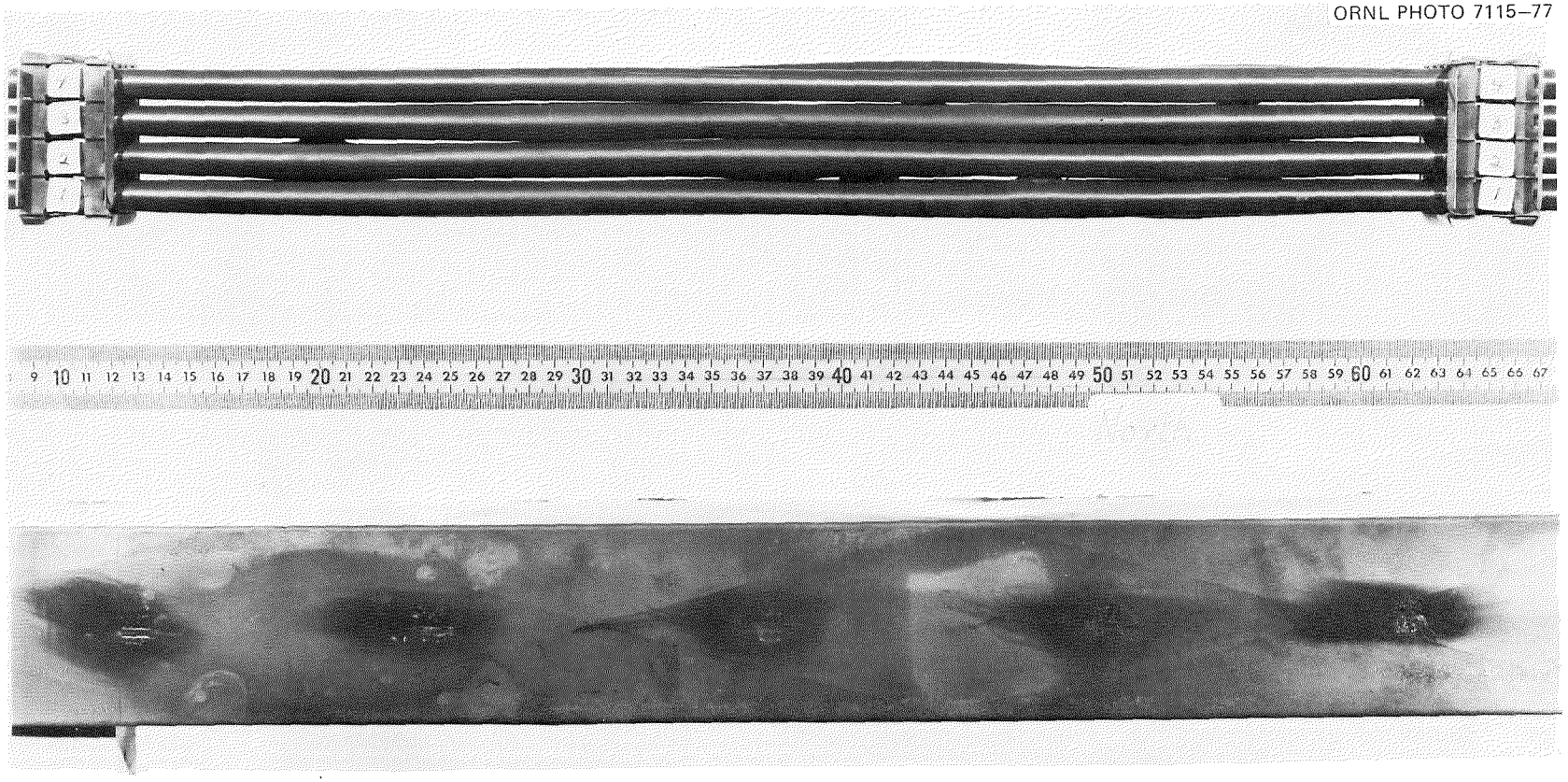

Fig. 34-B. View of north side of tested bundle and shroud (middle region).

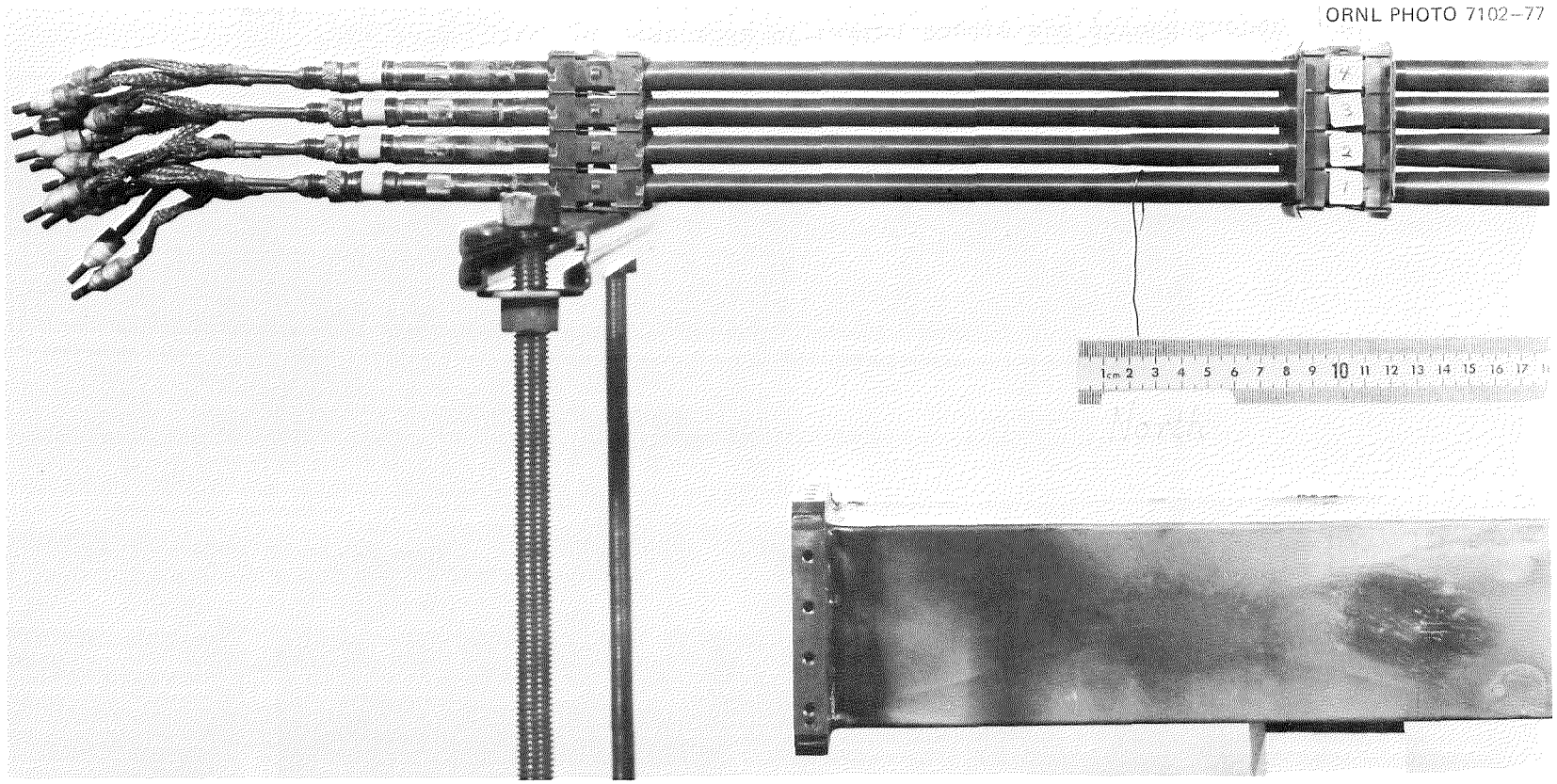

Fig. 34-C. View of north side of tested bundle and shroud (bottom end).

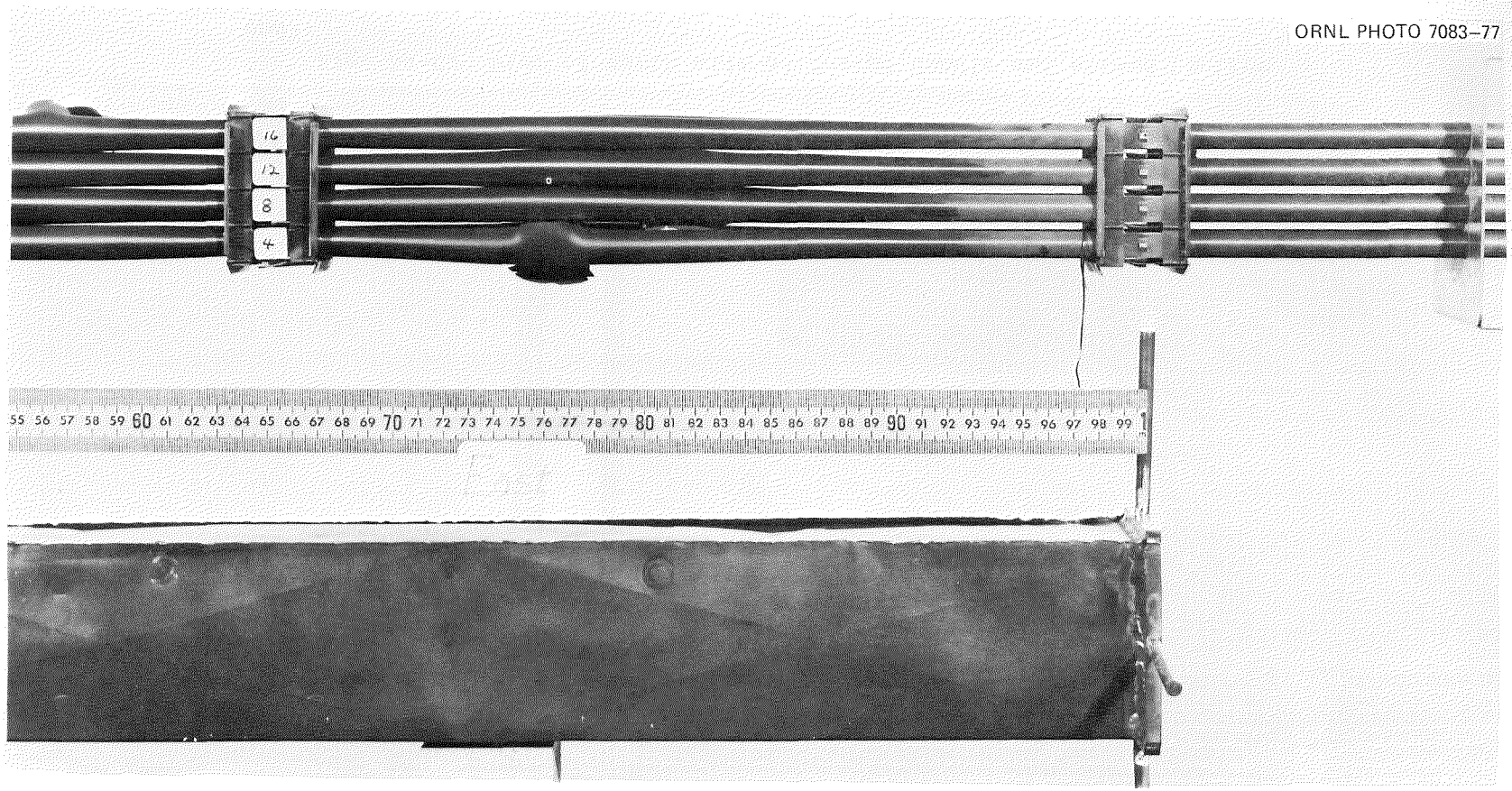

Fig. 35-A. View of east side of tested bundle and shroud (upper end).

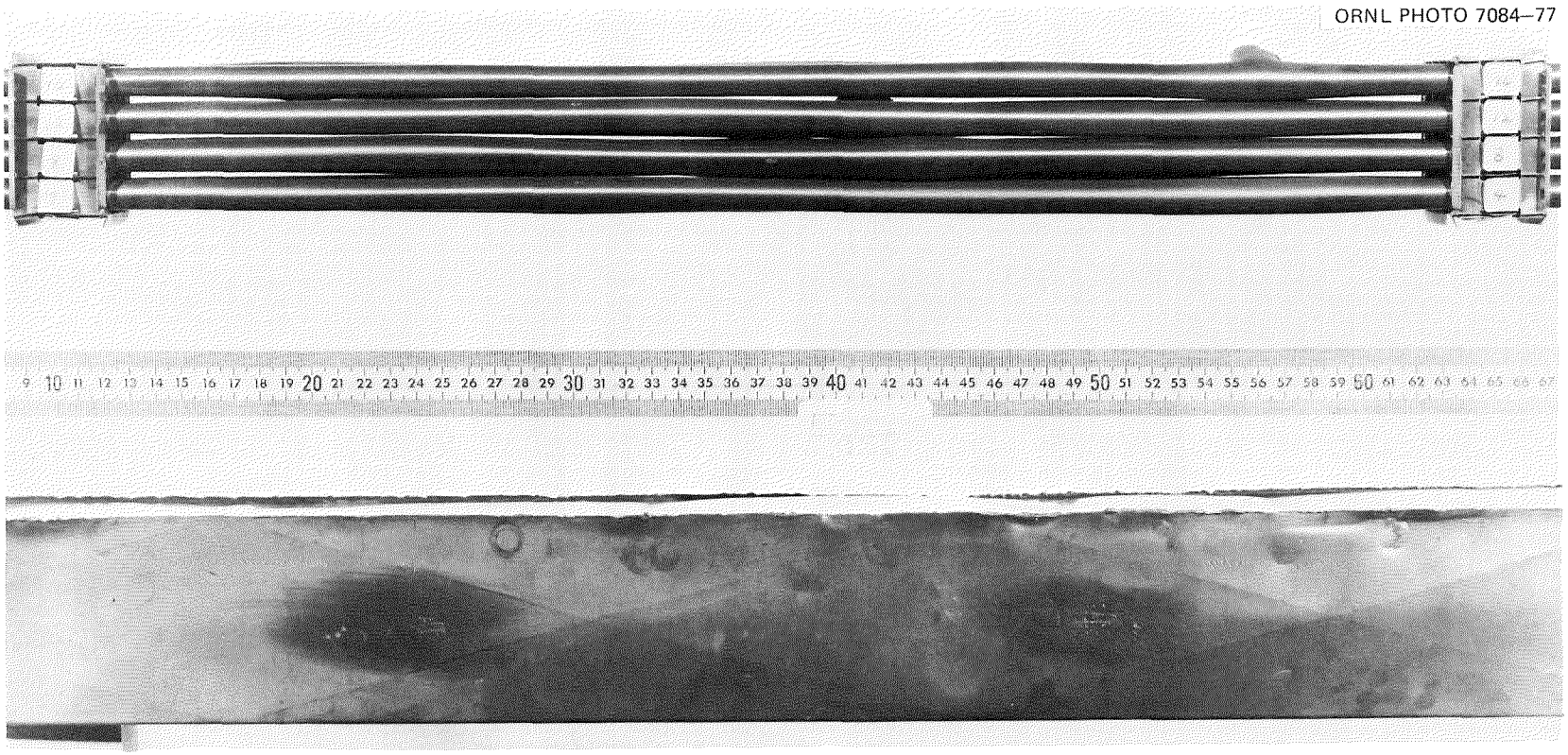

Fig. 35-B. View of east side of tested bundle and shroud (middle region).

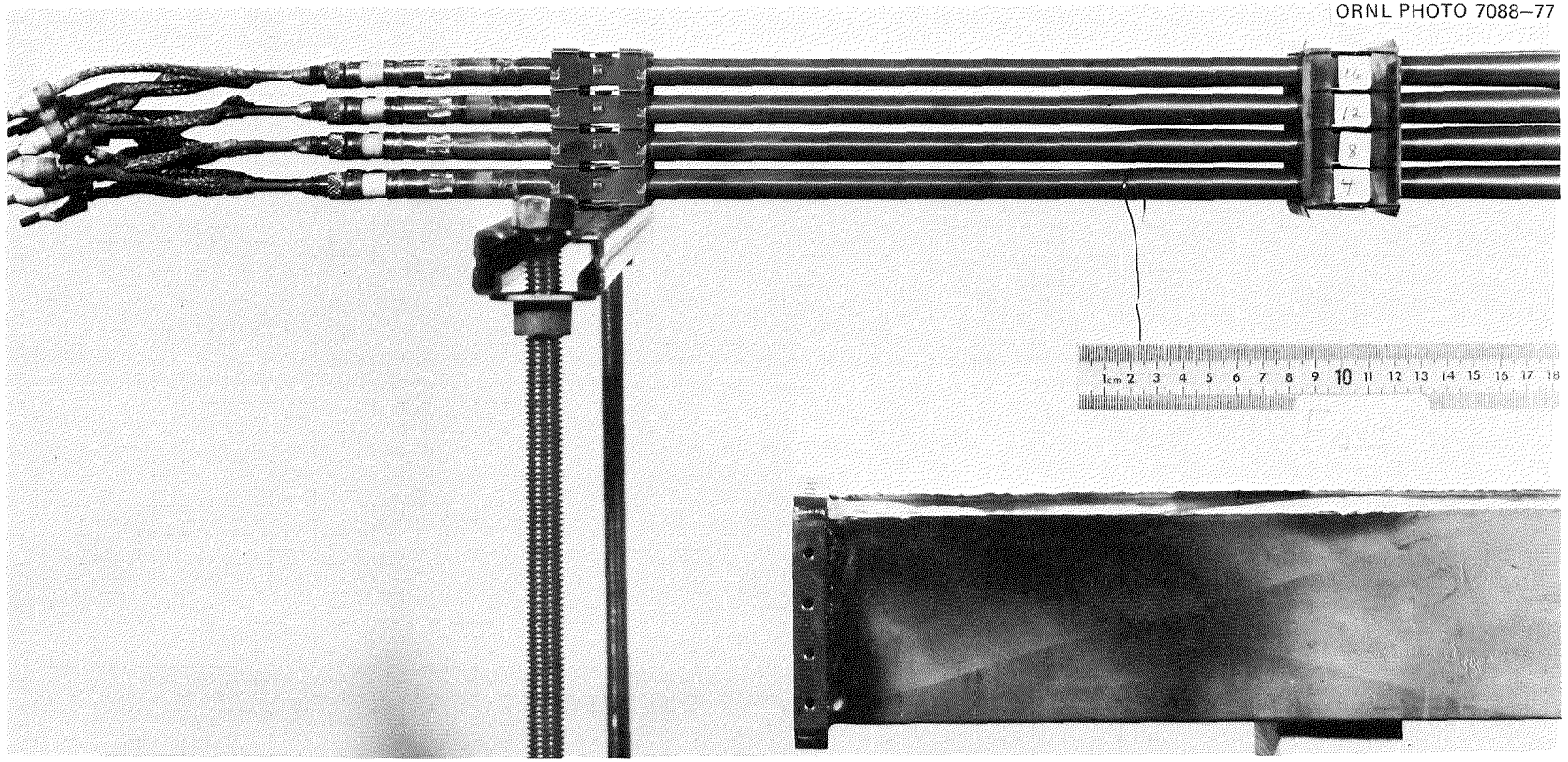

Fig. 35-C. View of east side of tested bundle and shroud (bottom end).

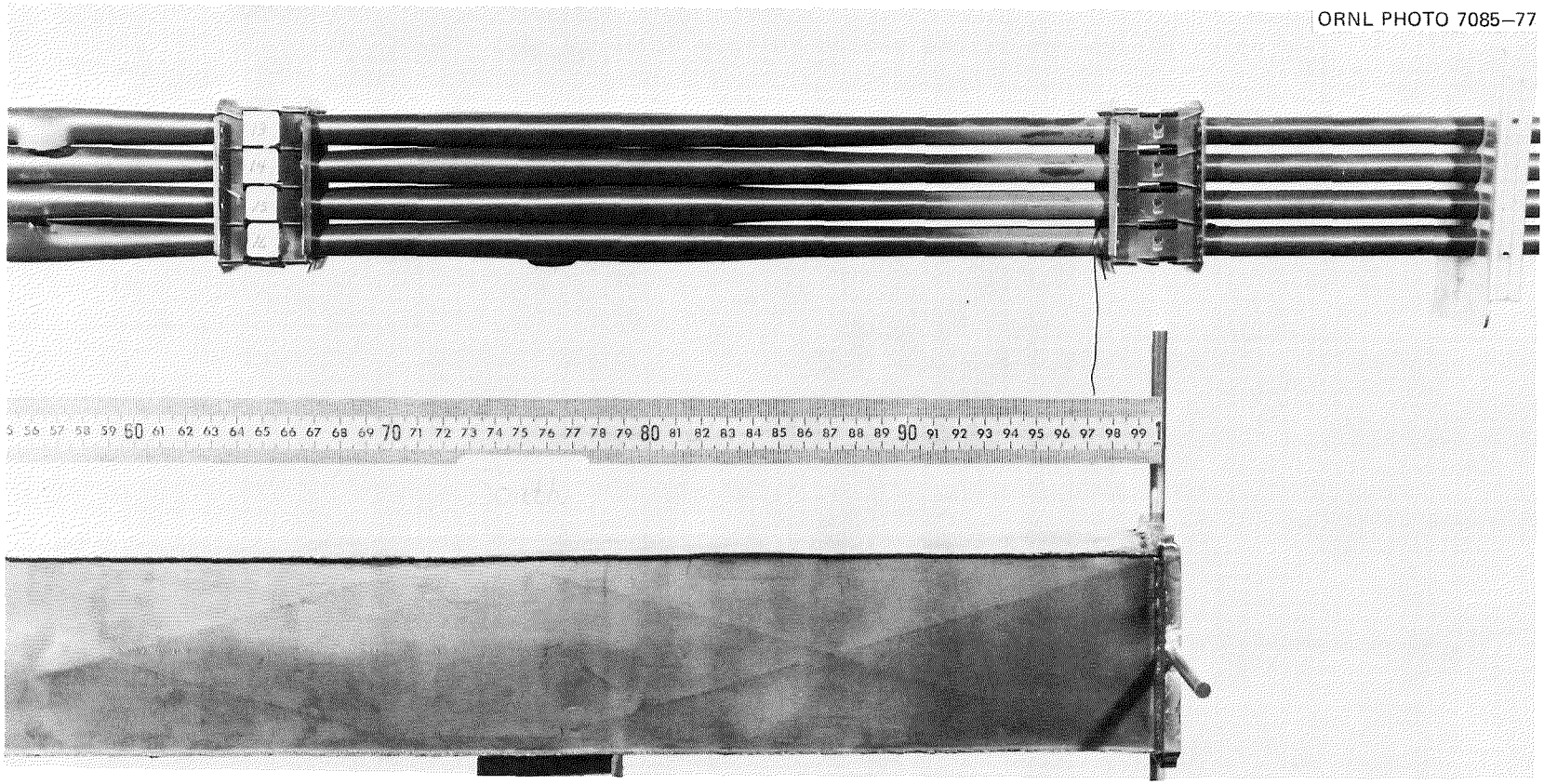

Fig. 36-A. View of south side of tested bundle and shroud (upper end).

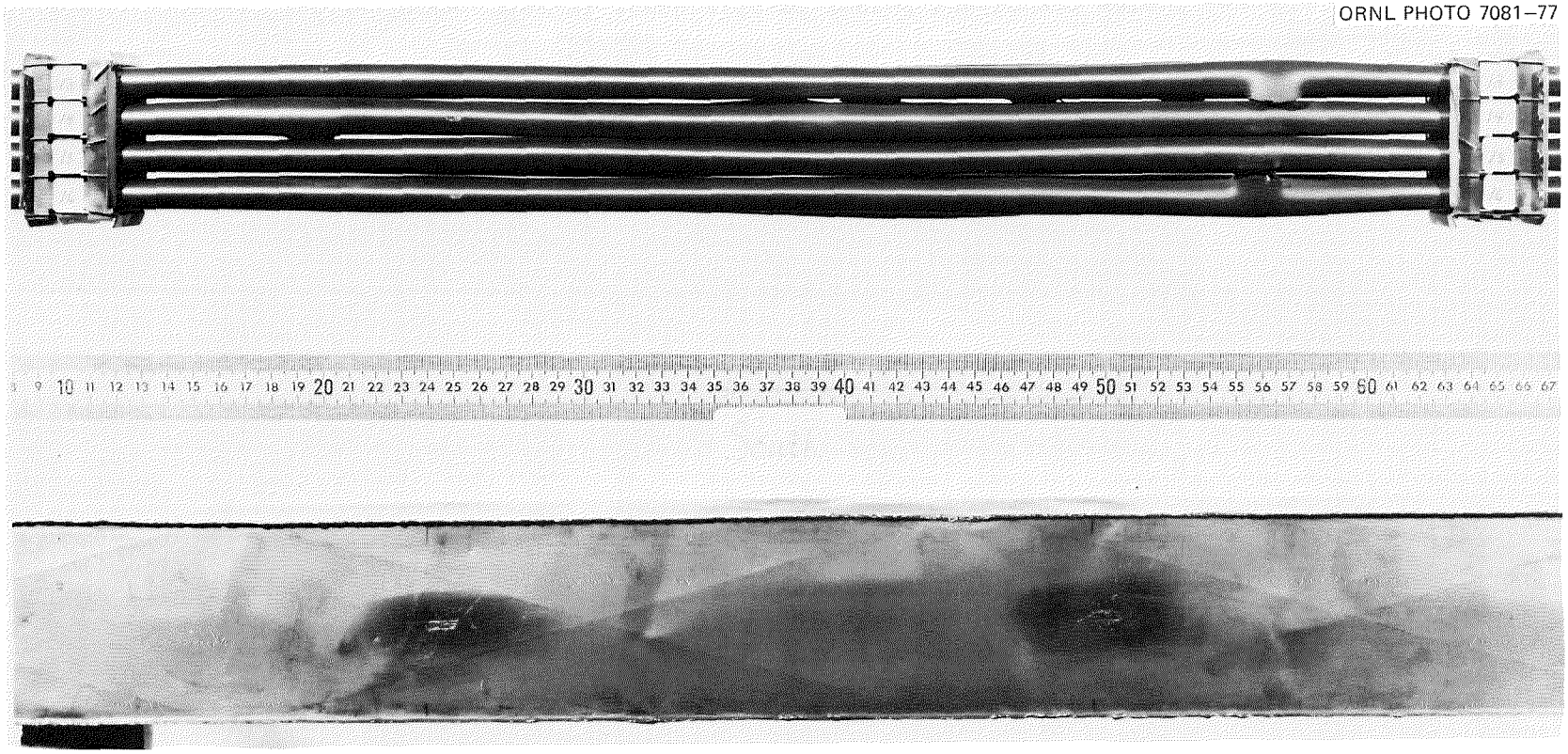

Fig. 36-B. View of south side of tested bundle and shroud (middle region).

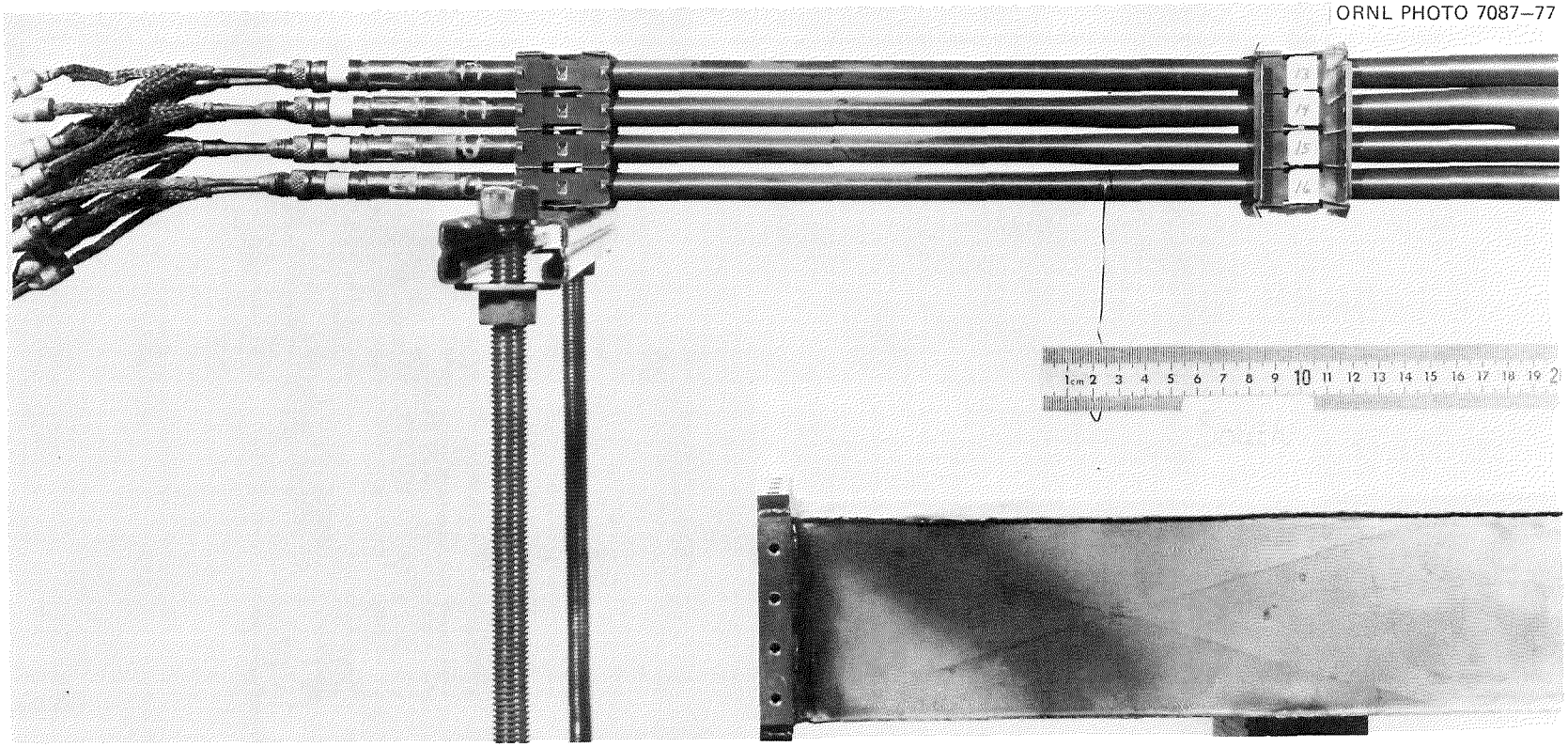

Fig. 36-C. View of south side of tested bundle and shroud (bottom end).

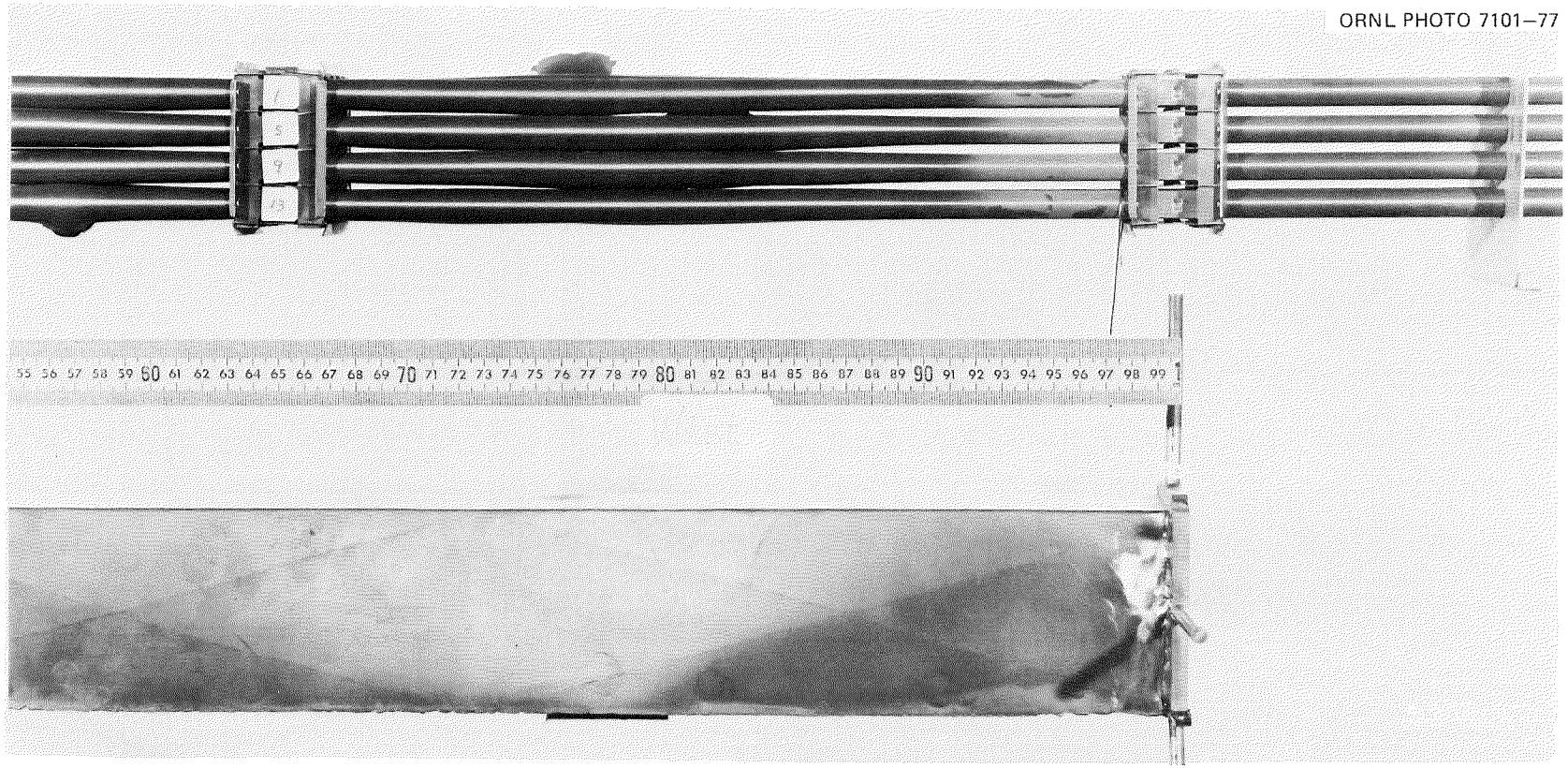

Fig. 37-A. View of west side of tested bundle and shroud (upper end).

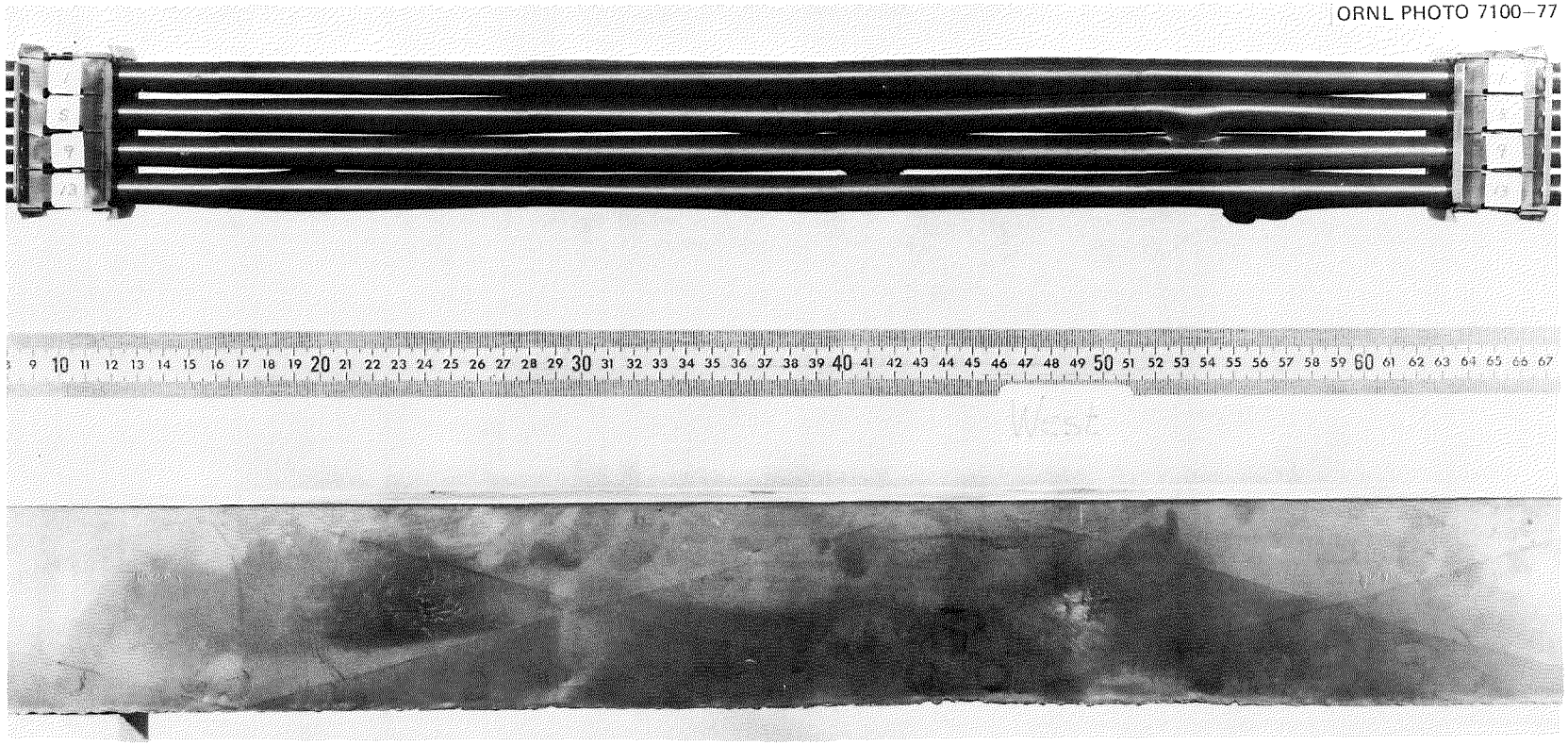

Fig. 37-B. View of west side of tested bundle and shroud (middle region).

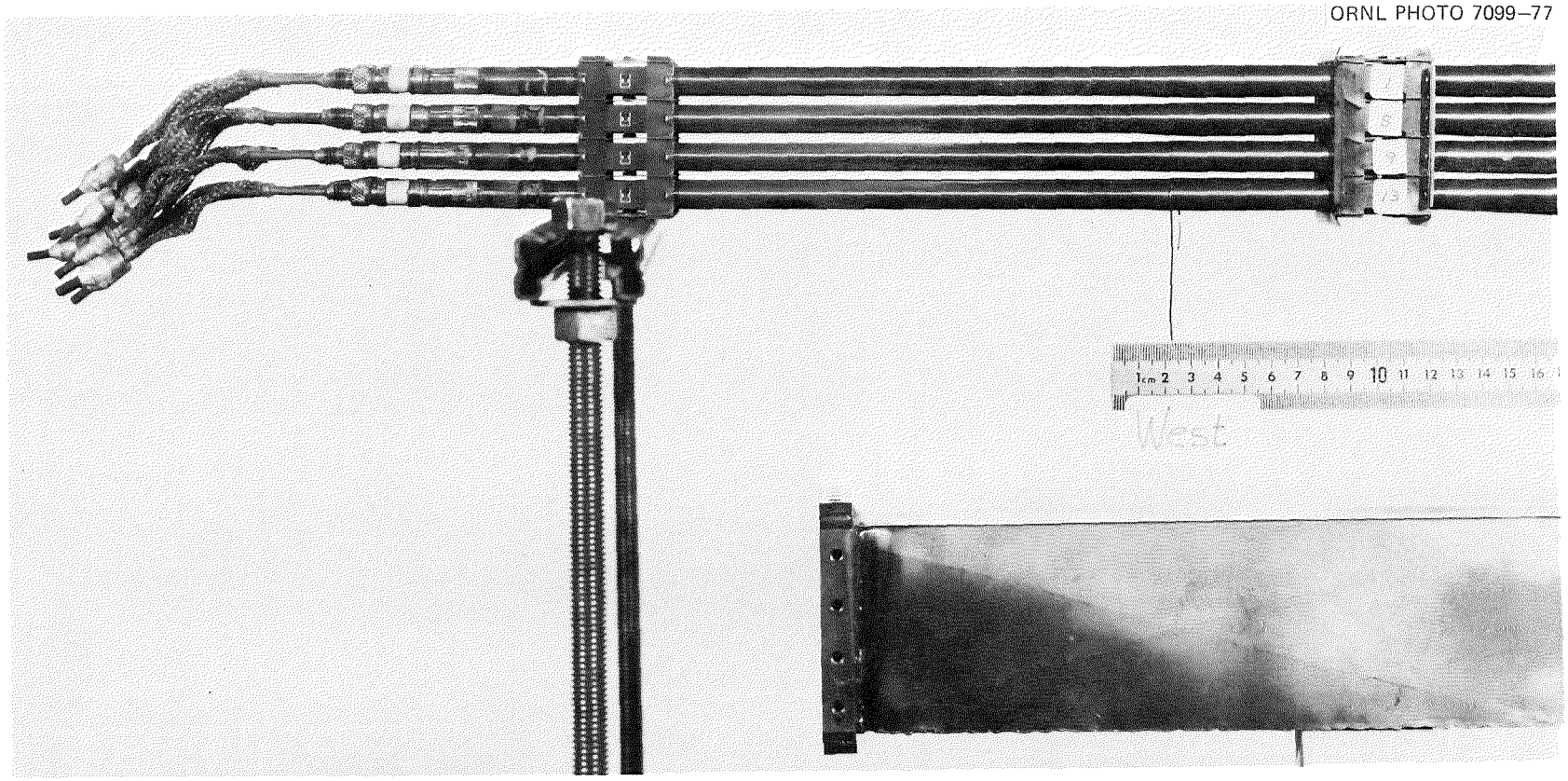

Fig. 37-C. View of west side of tested bundle and shroud (bottom end).

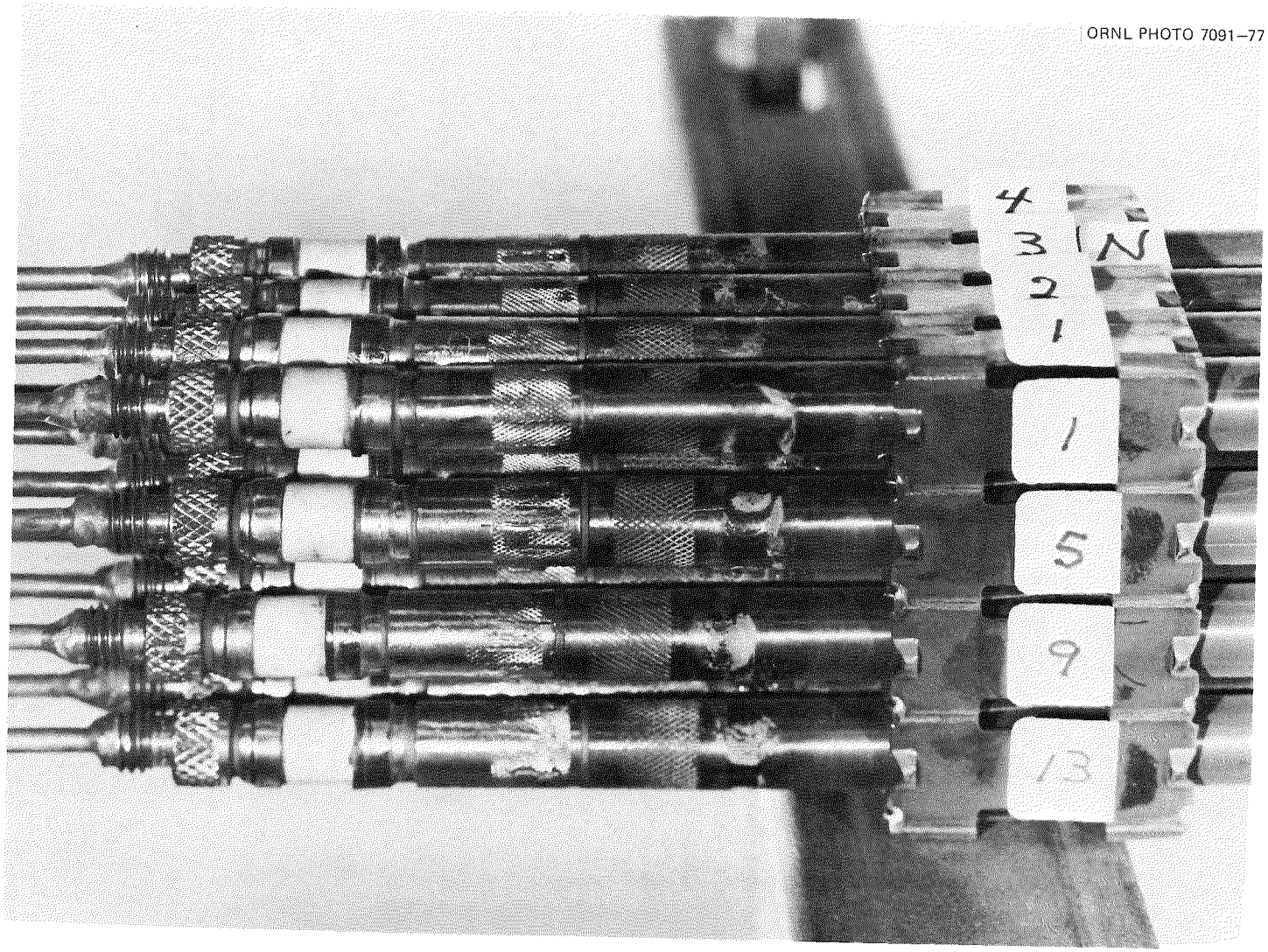

Fig. 38. Close-up of lower end of bundle showing rod length changes.

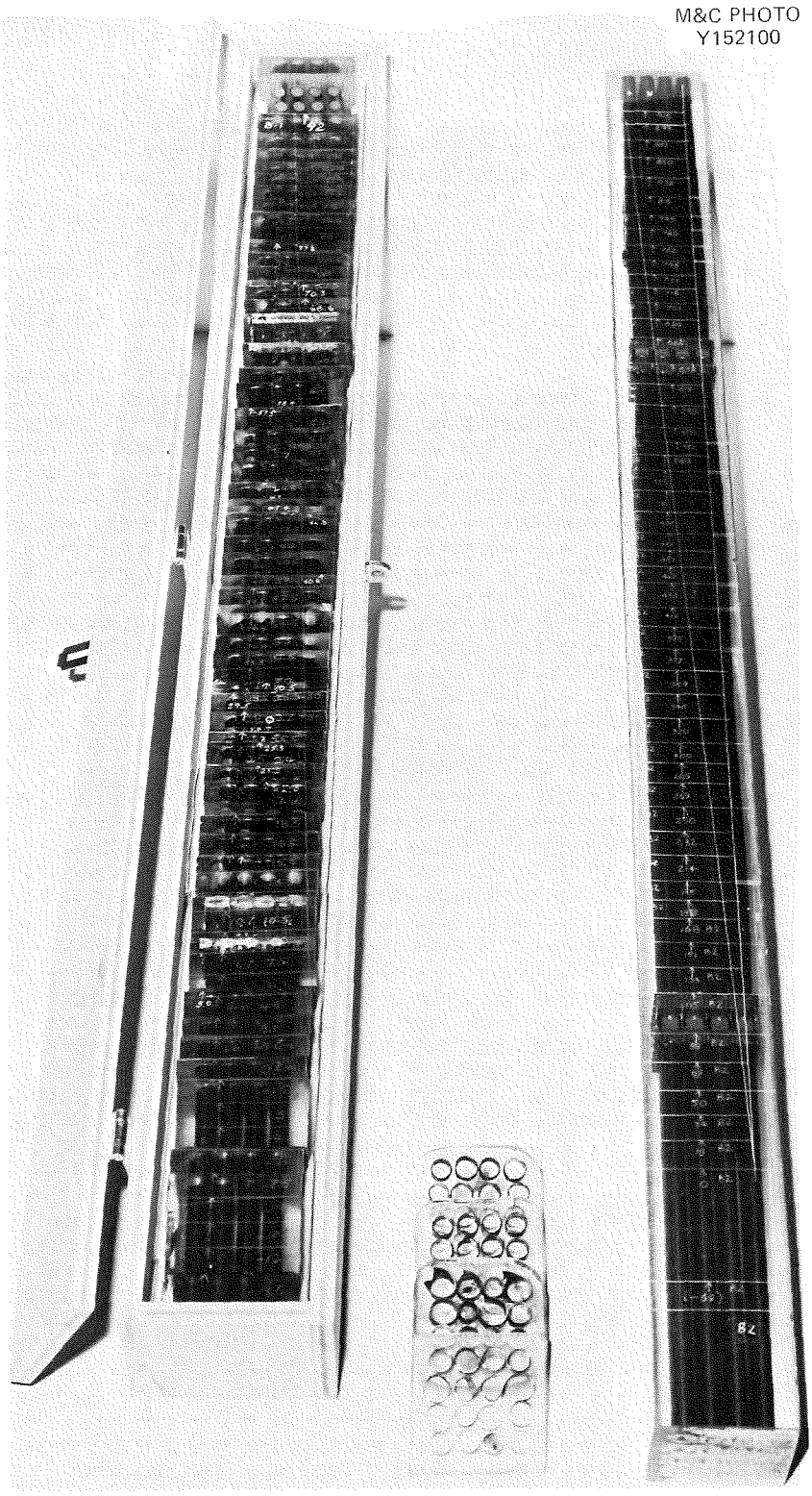

Fig. 39. Two encapsulated test bundles (B-1 and B-2). Bundle B-2 (on right) has been marked for sectioning. Bundle B-1 (on left) has been sectioned. Representative cross sections of B-1 are shown in the center.

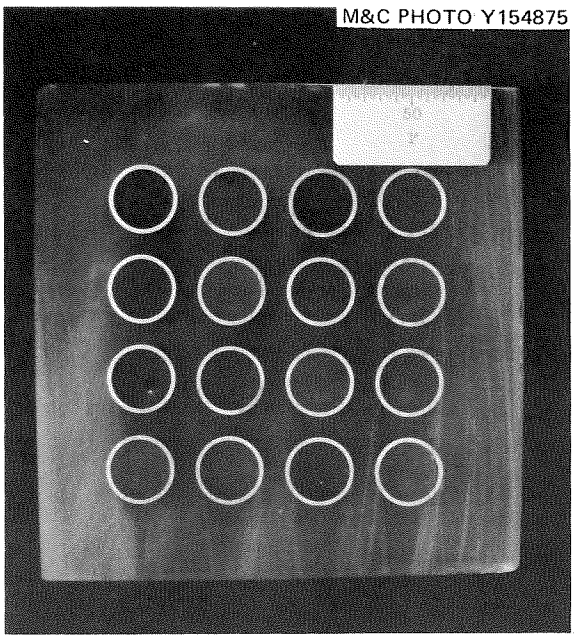

Fig. 40. Section of undeformed region of B-2 at —6.9-cm elevation.

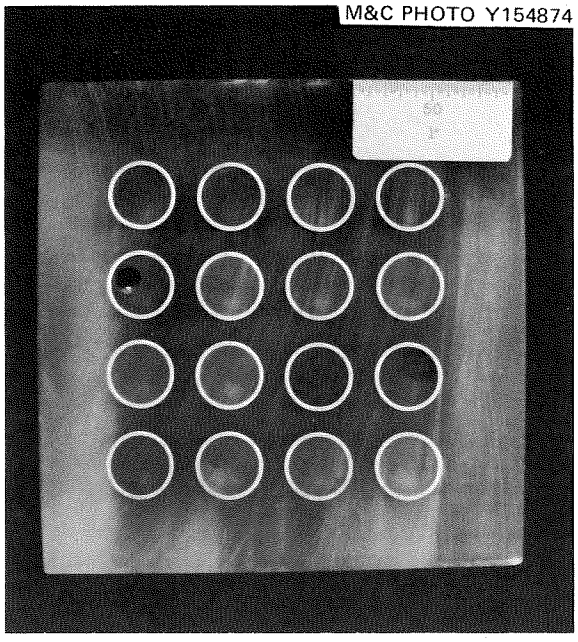

Fig. 41. Section of B-2 at 0.0-cm elevation — the bottom of the heated length.

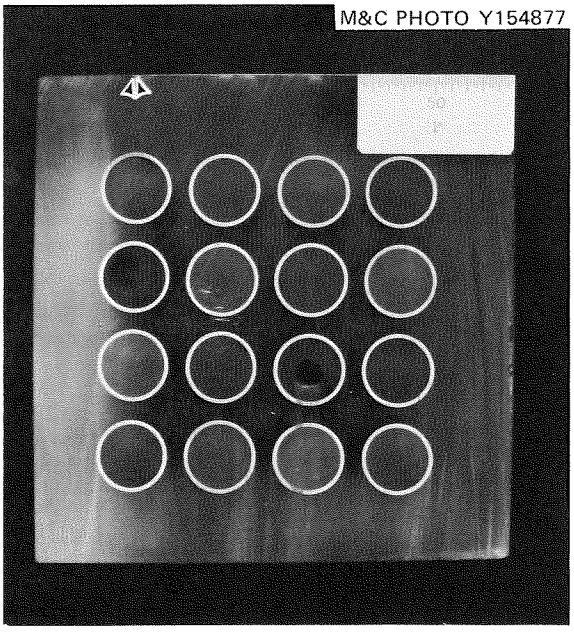

Fig. 42. Section of B-2 at 1.8-cm elevation.

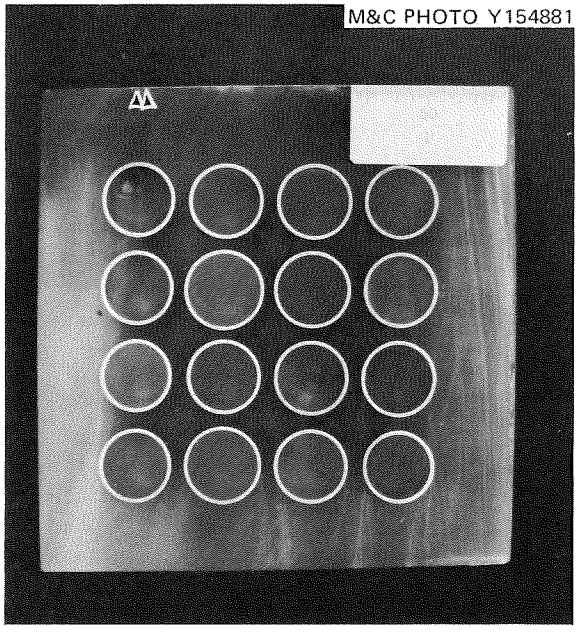

Fig. 43. Section of B-2 at 3.4-cm elevation.

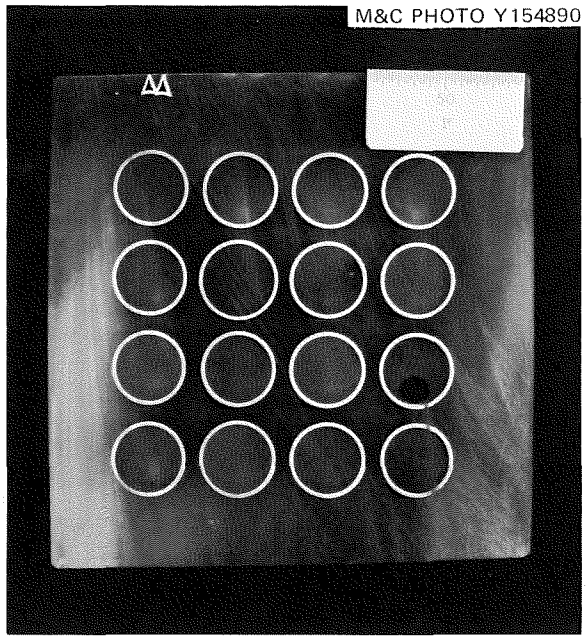

Fig. 44. Section of B-2 at 5.0-cm elevation.

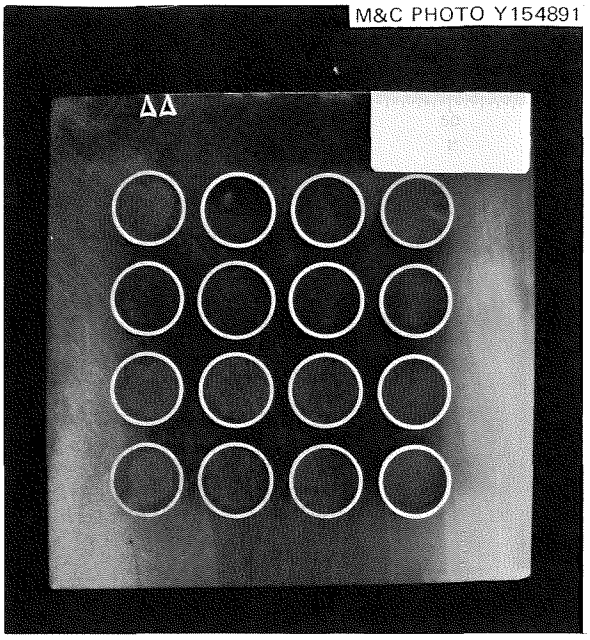

Fig. 45. Section of B-2 at 6.9-cm elevation.

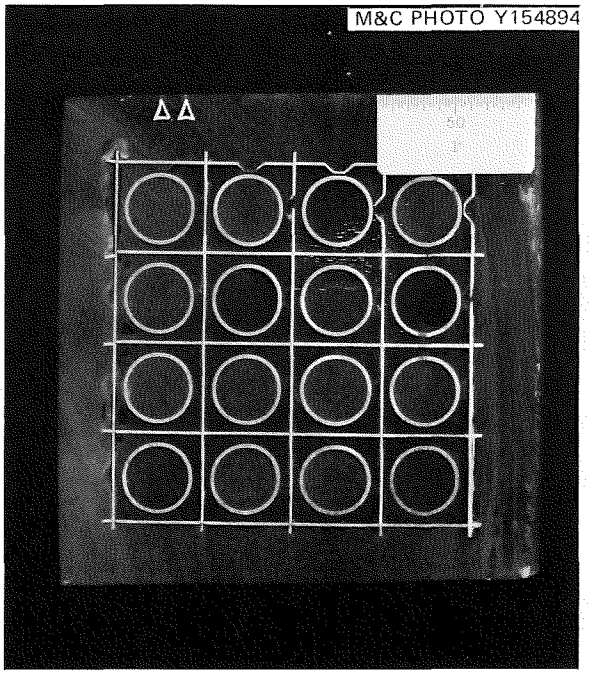

Fig. 46. Section through lower grid of B-2 at 8.8-cm elevation.

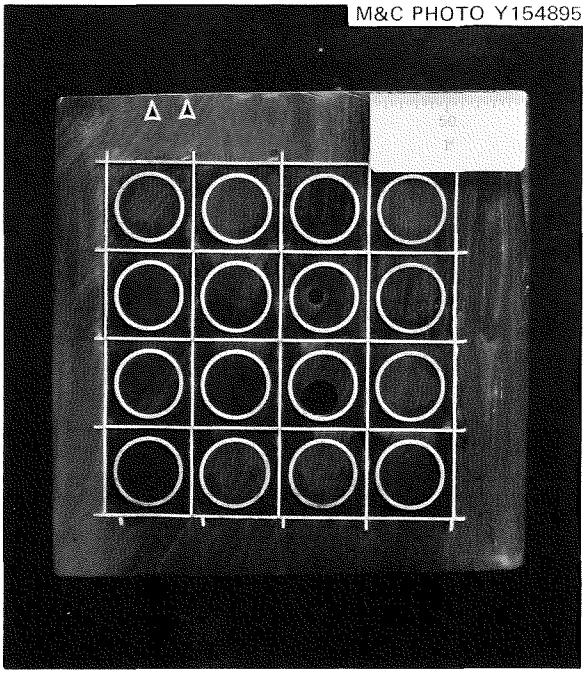

Fig. 47. Section through lower grid of B-2 at 11.5-cm elevation.

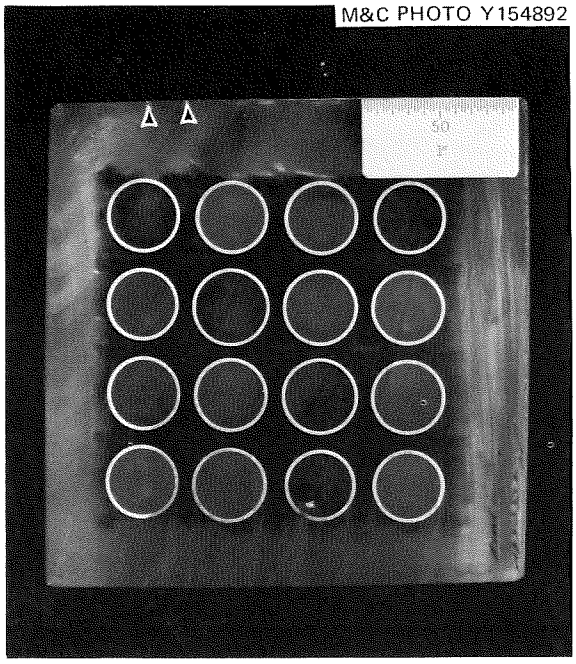

Fig. 48. Section of B-2 at 13.3-cm elevation.

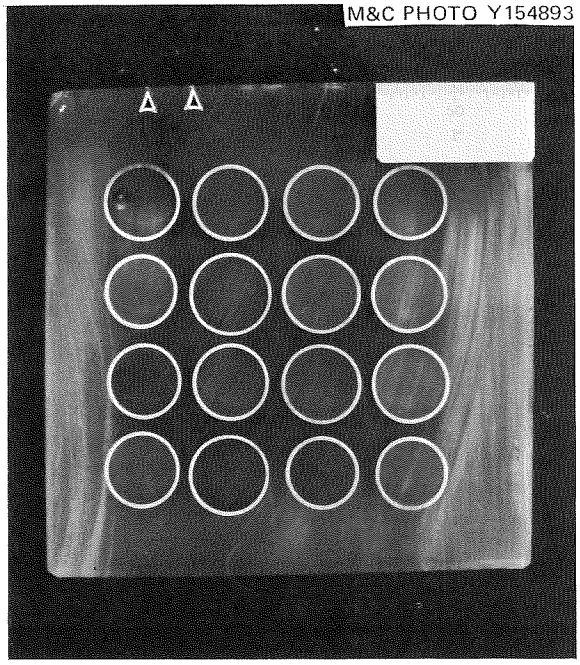

Fig. 49. Section of B-2 at 15.1-cm elevation.

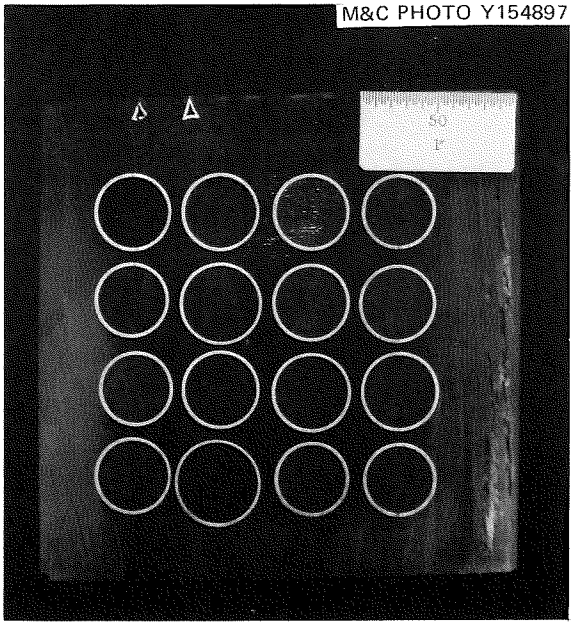

Fig. 50. Section of B-2 at 16.8 cm elevation.

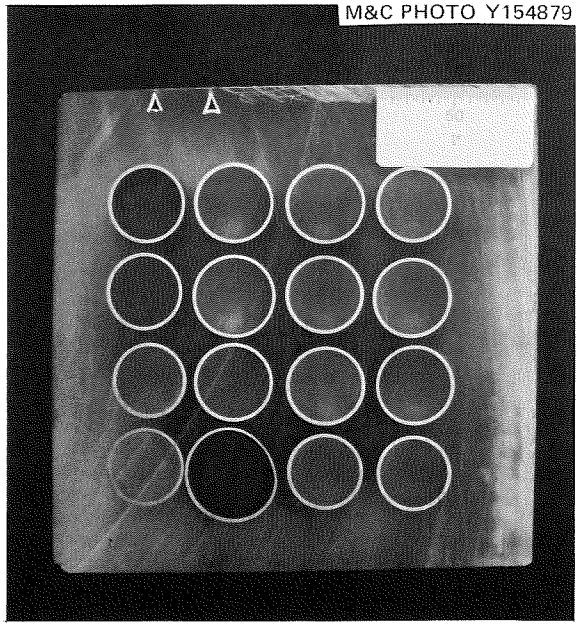

Fig. 51. Section of B-2 at 18.1-cm elevation.

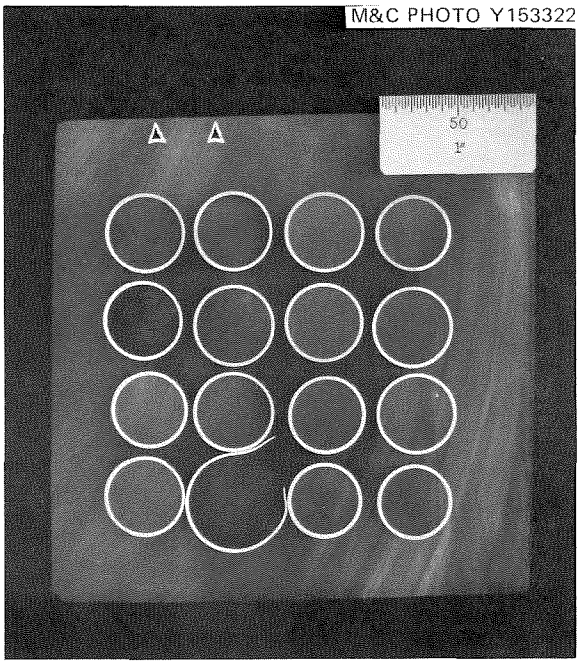

Fig. 52. Section of B-2 at 19.5-cm elevation.

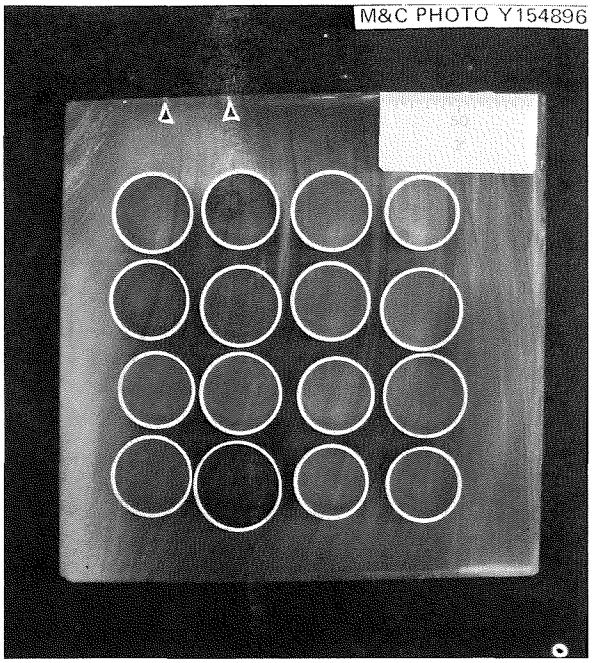

Fig. 53. Section of B-2 at 21.4-cm elevation.

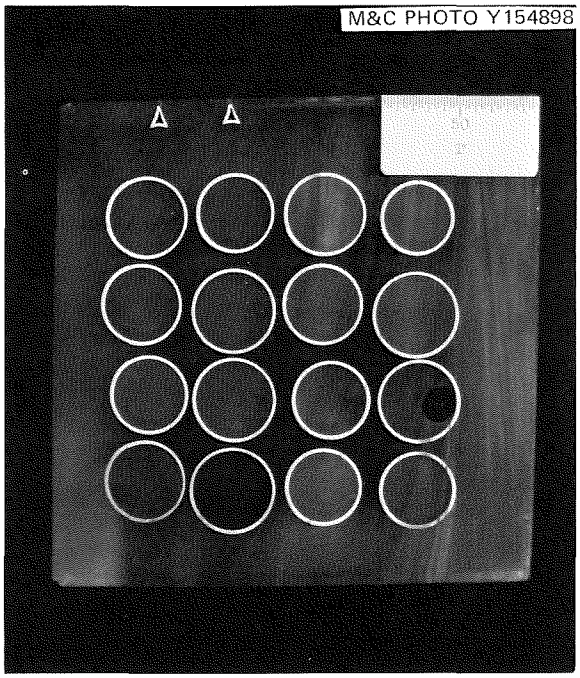

Fig. 54. Section of B-2 at 23.2-cm elevation.

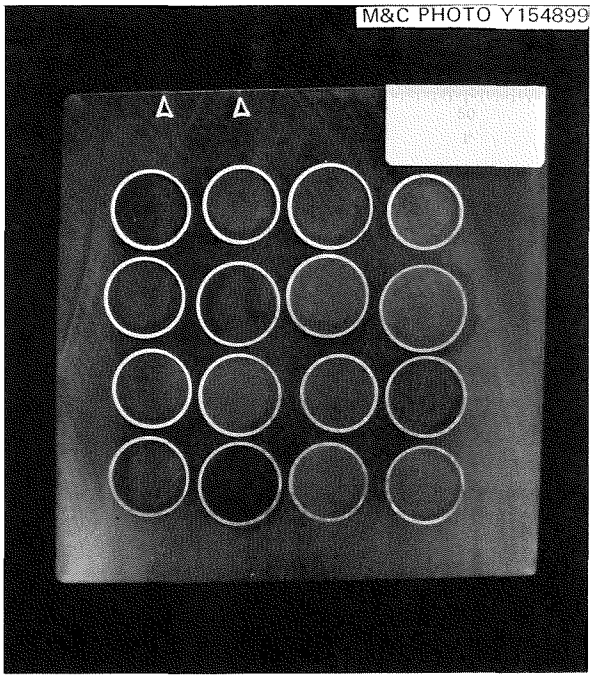

Fig. 55. Section of B-2 at 25.0-cm elevation.

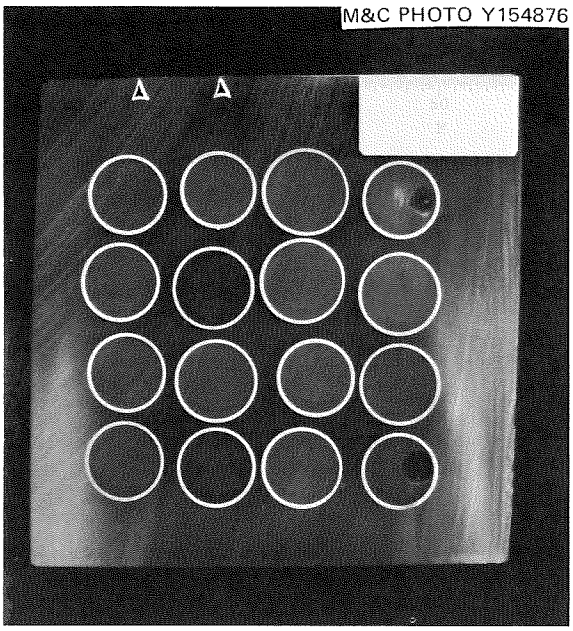

Fig. 56. Section of B-2 at 26.9-cm elevation.

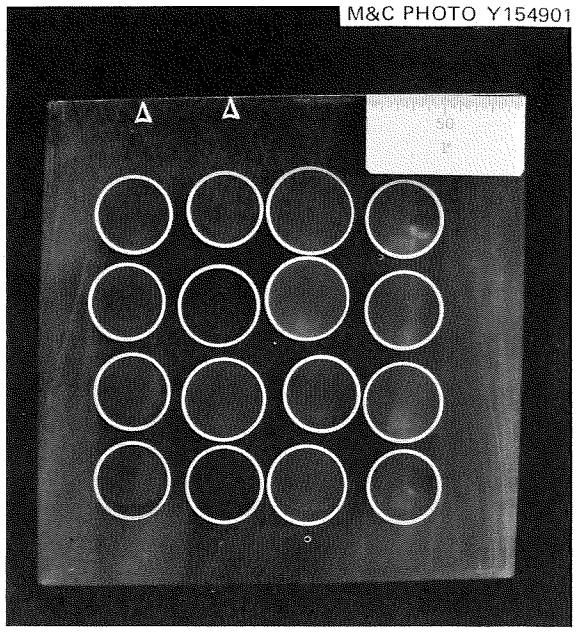

Fig. 57. Section of B-2 at 28.5-cm elevation.

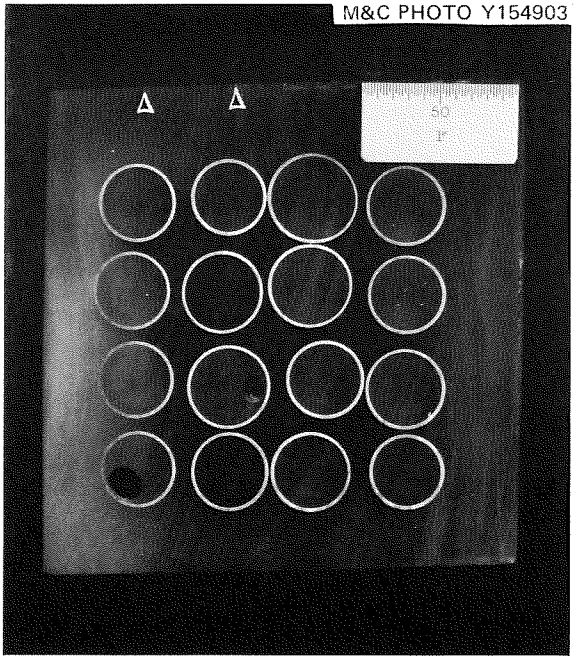

Fig. 58. Section of B-2 at 30.0-cm elevation.

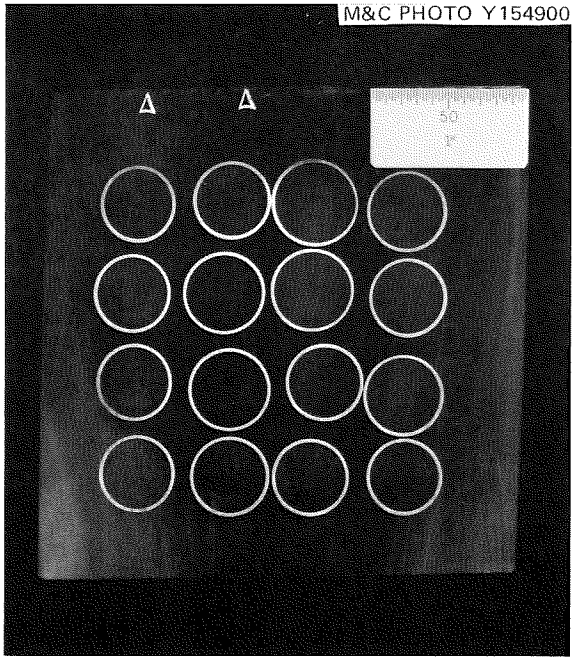

Fig. 59. Section of B-2 at 32.0-cm elevation.

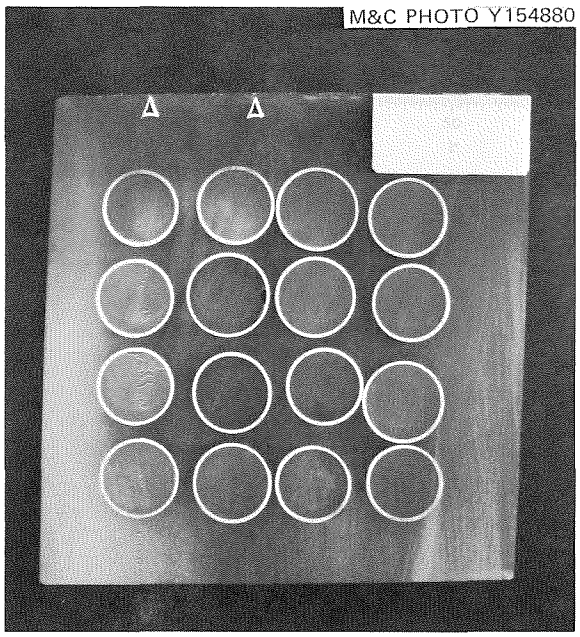

Fig. 60. Section of B-2 at 34.0-cm elevation.

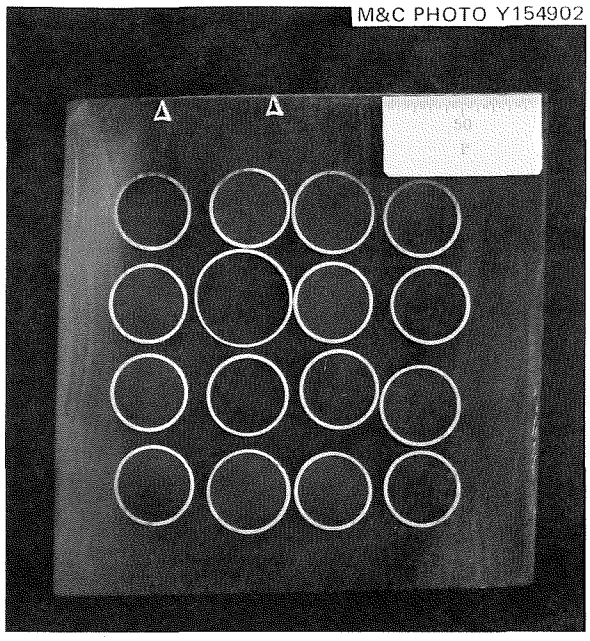

Fig. 61. Section of B-2 at 35.9-cm elevation.

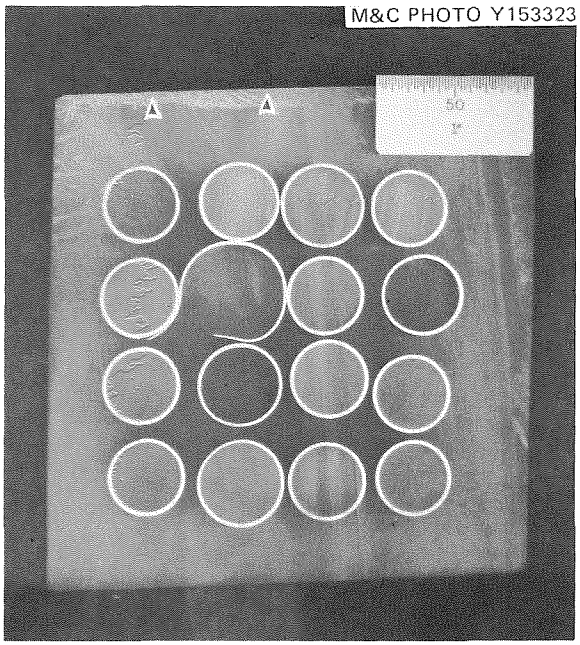

Fig. 62. Section of B-2 at 37.7-cm elevation.

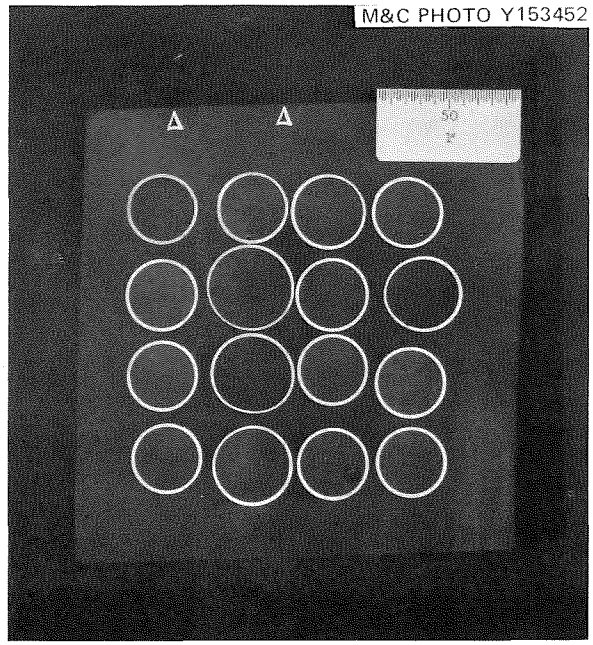

Fig. 63. Section of B-2 at 39.5-cm elevation.

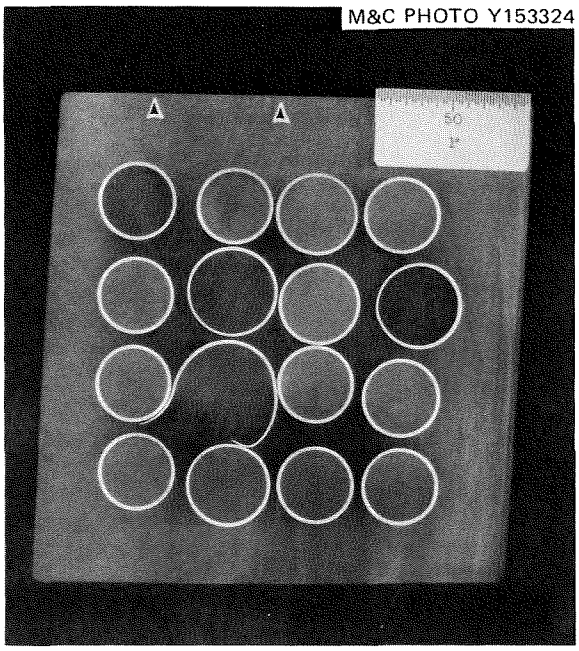

Fig. 64. Section of B-2 at 41.2-cm elevation.

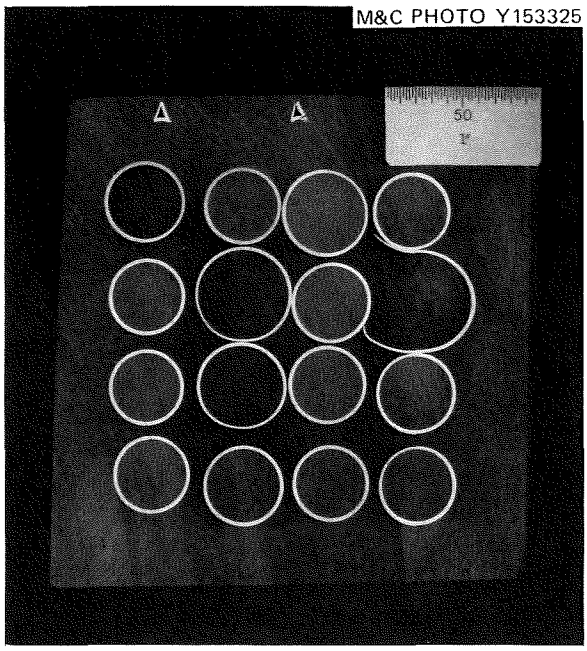

Fig. 65. Section of B-2 at 43.3-cm elevation.

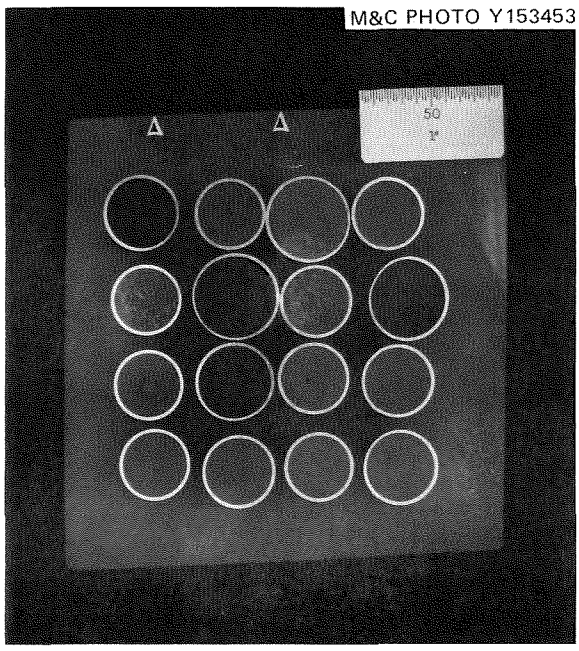

Fig. 66. Section of B-2 at 44.7-cm elevation.

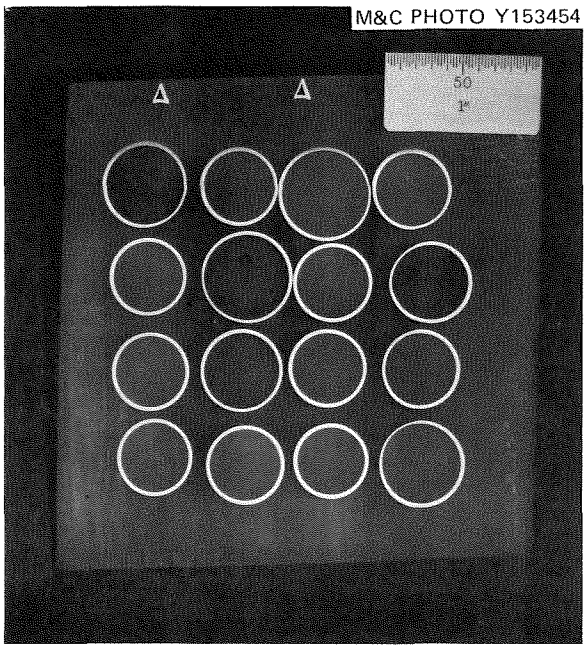

Fig. 67. Section of B-2 at 46.2-cm elevation.

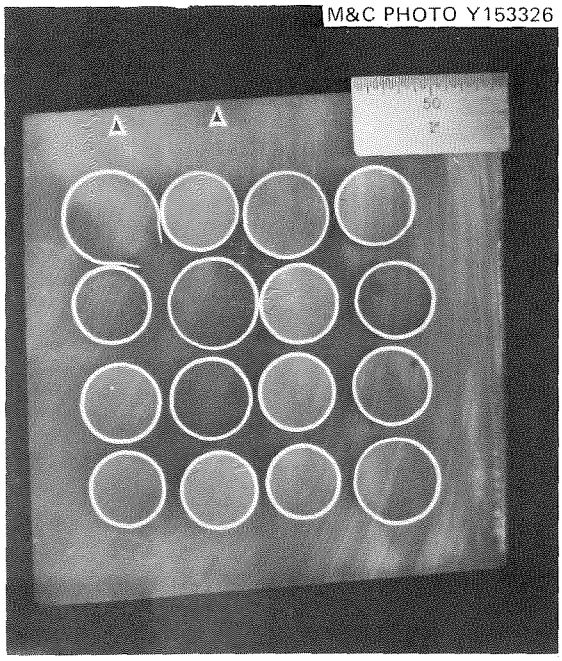

Fig. 68. Section of B-2 at 47.7-cm elevation.

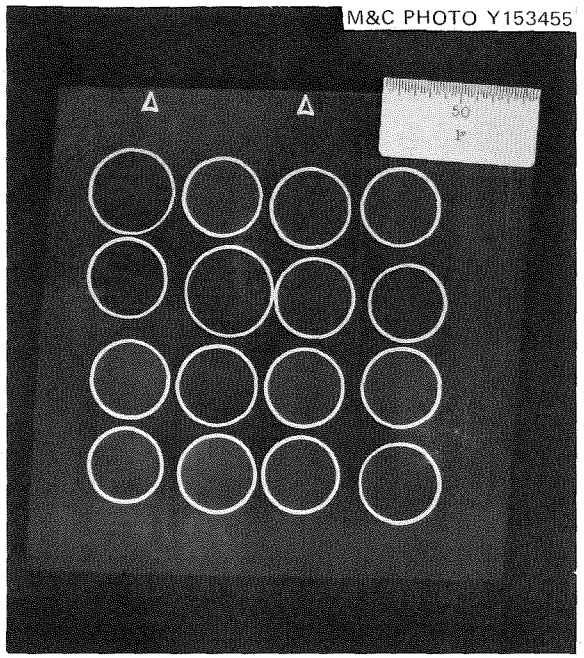

Fig. 69. Section of B-2 at 49.7-cm elevation.

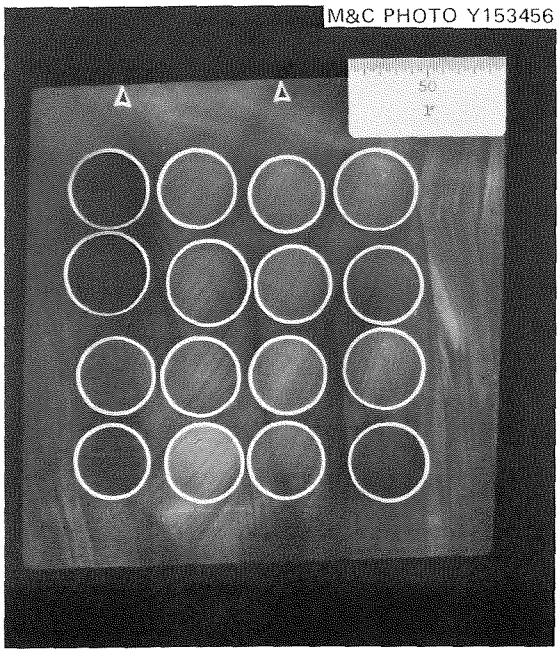

Fig. 70. Section of B-2 at 51.6-cm elevation.

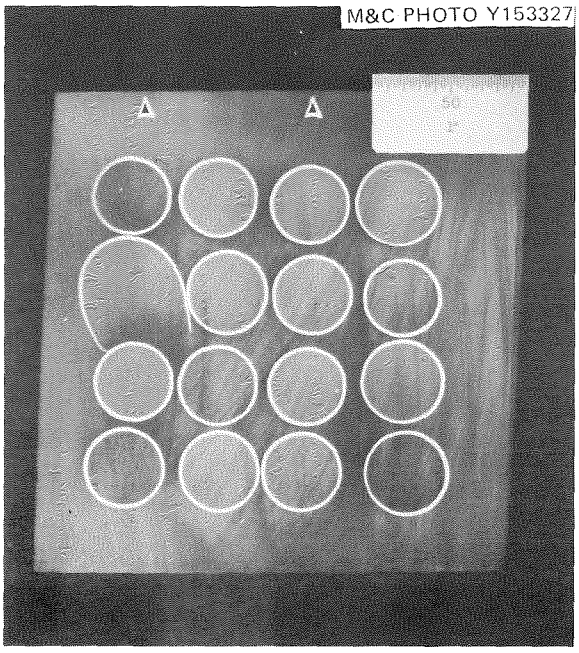

Fig. 71. Section of B-2 at 53.5-cm elevation.

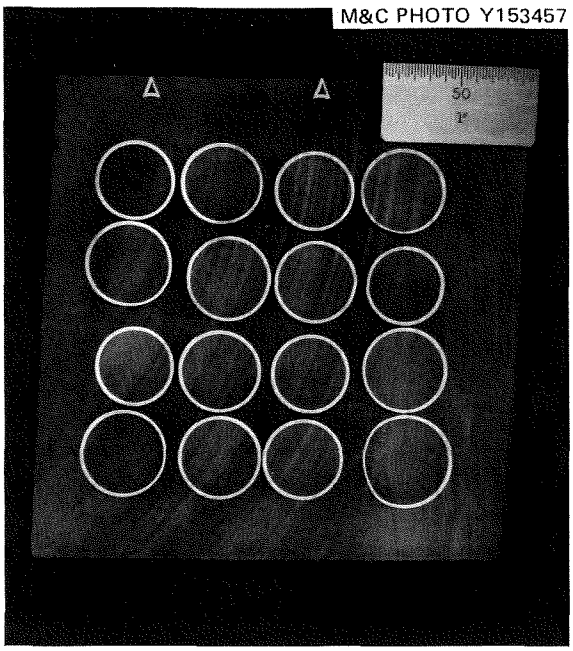

Fig. 72. Section of B-2 at 54.9-cm elevation.

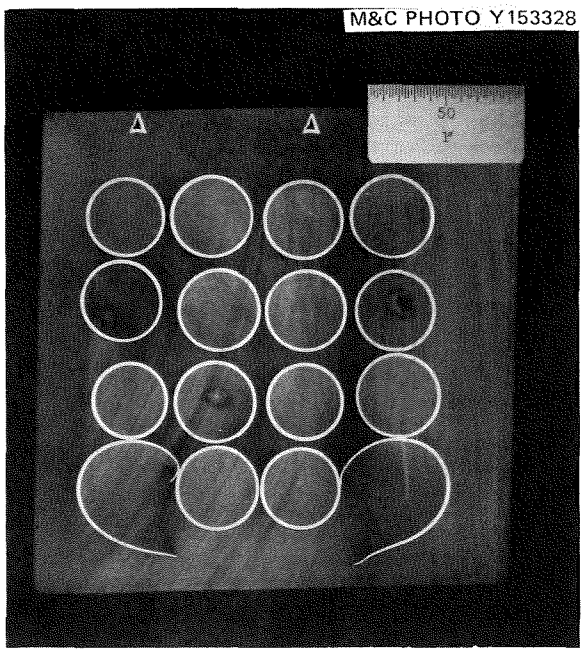

Fig. 73. Section of B-2 at 56.2-cm elevation.

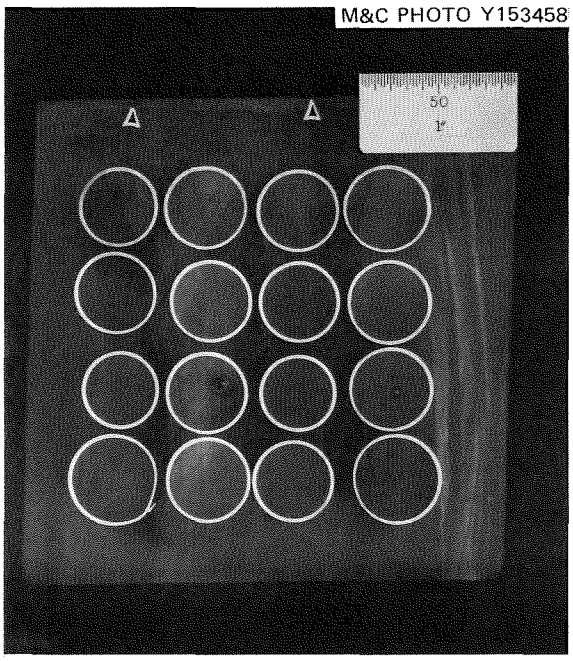

Fig. 74. Section of B-2 at 57.6-cm elevation.

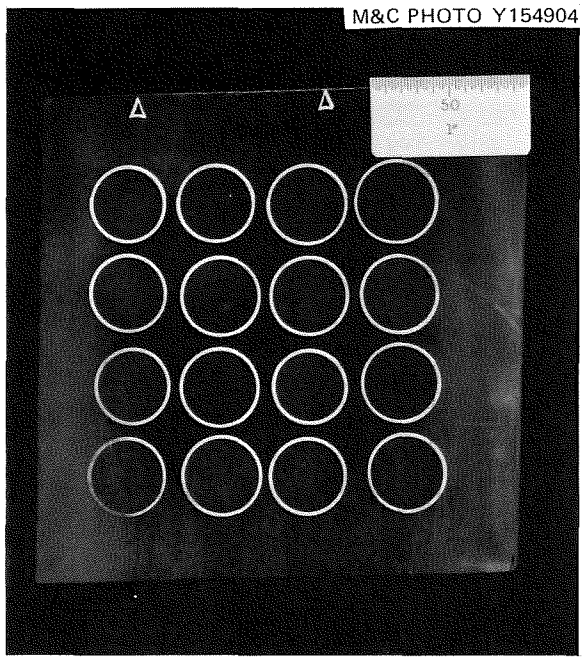

Fig. 75. Section of B-2 at 59.8-cm elevation.

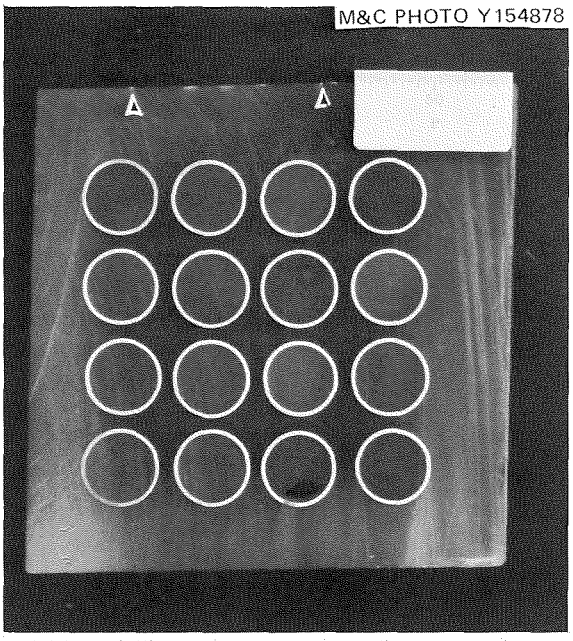

Fig. 76. Section of B-2 at 61.8-cm elevation.

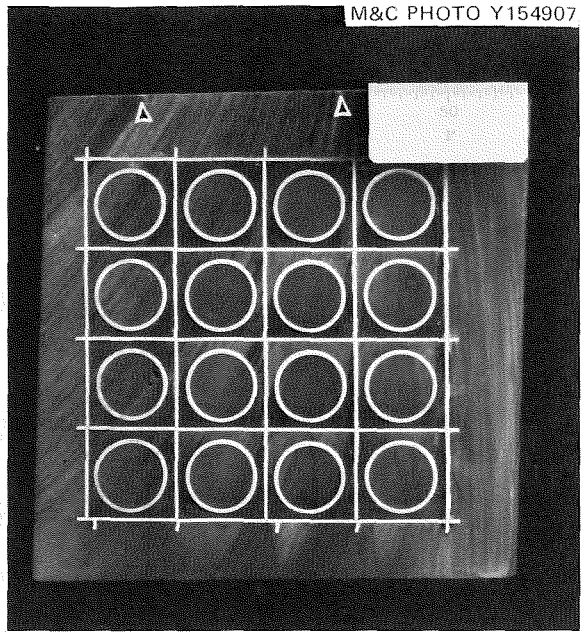

Fig. 77. Section through upper grid of B-2 at 63.8-cm elevation.

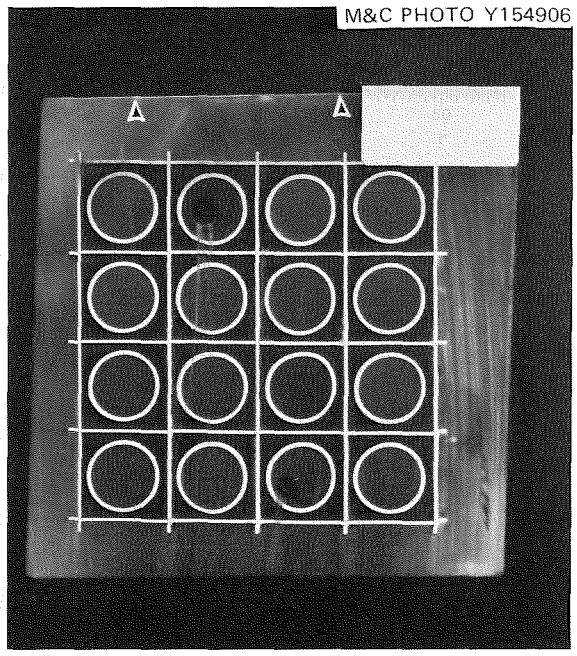

Fig. 78. Section through upper grid of B-2 at 66.5-cm elevation.

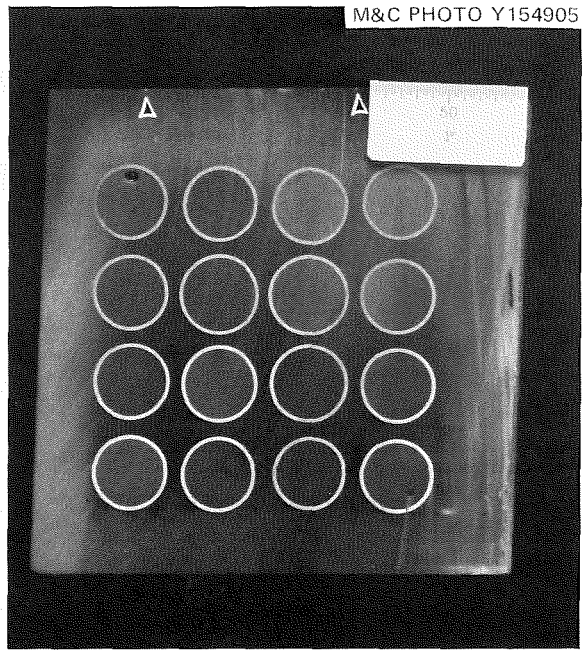

Fig. 79. Section of B-2 at 68.4-cm elevation.

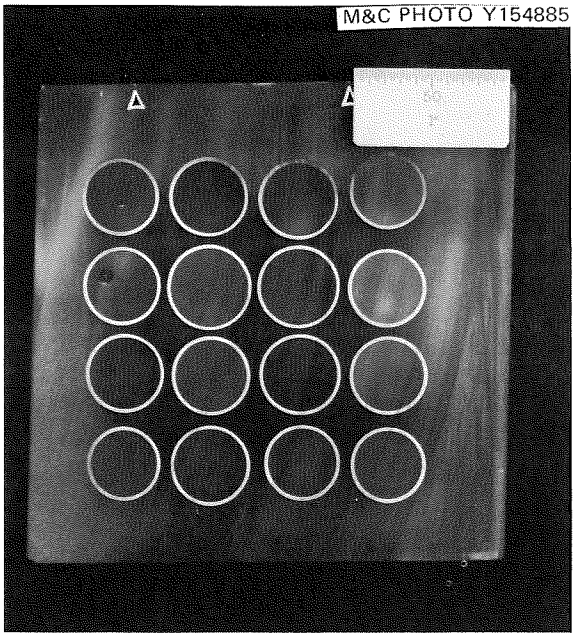

Fig. 80. Section of B-2 at 70.1-cm elevation.

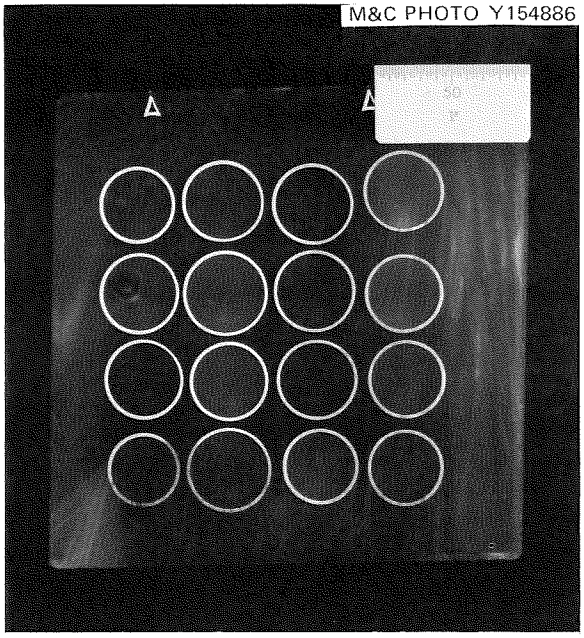

Fig. 81. Section of B-2 at 71.6-cm elevation.

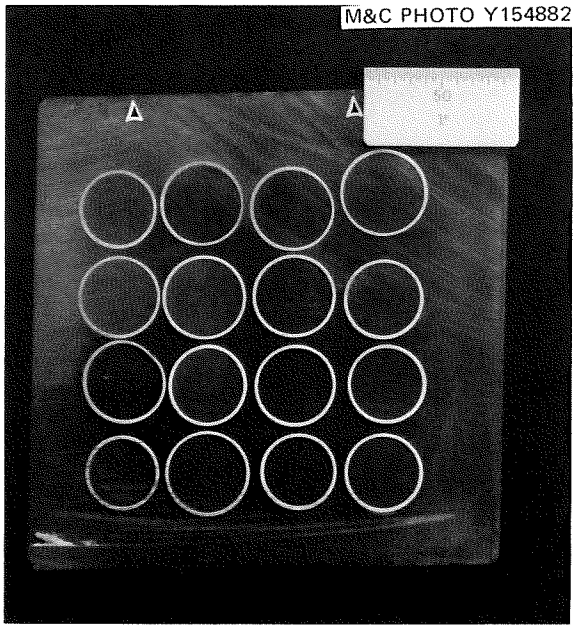

Fig. 82. Section of B-2 at 73.1-cm elevation.

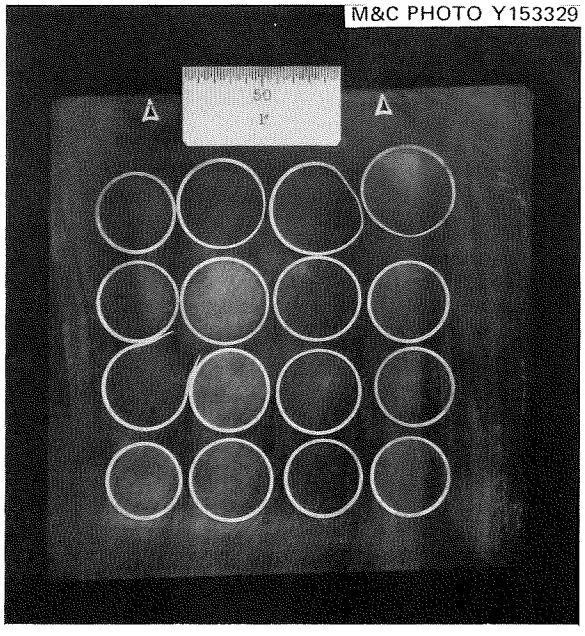

Fig. 83. Section of B-2 at 74.6-cm elevation.

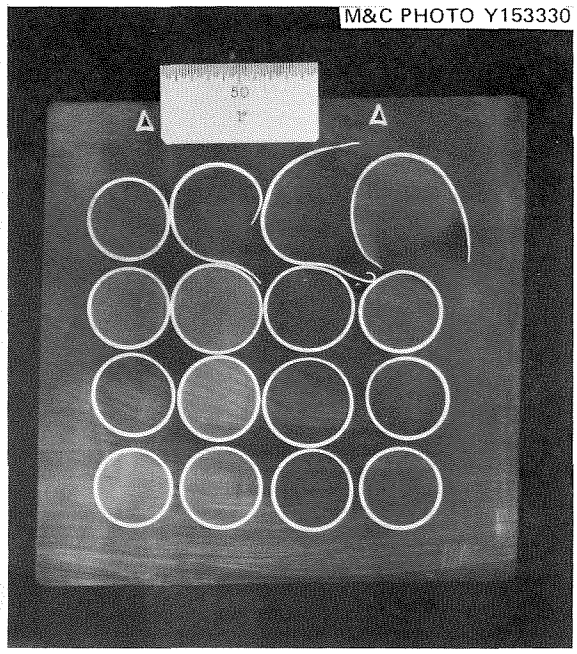

Fig. 84. Section of B-2 at 76.2-cm elevation.

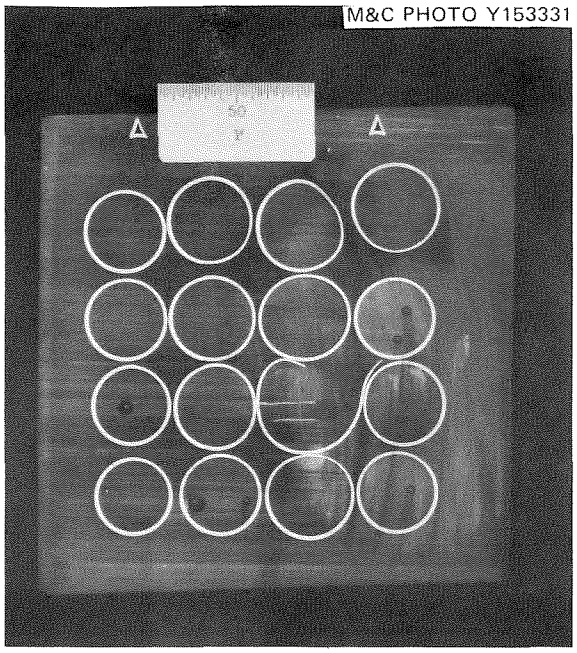

Fig. 85. Section of B-2 at 78.0-cm elevation.

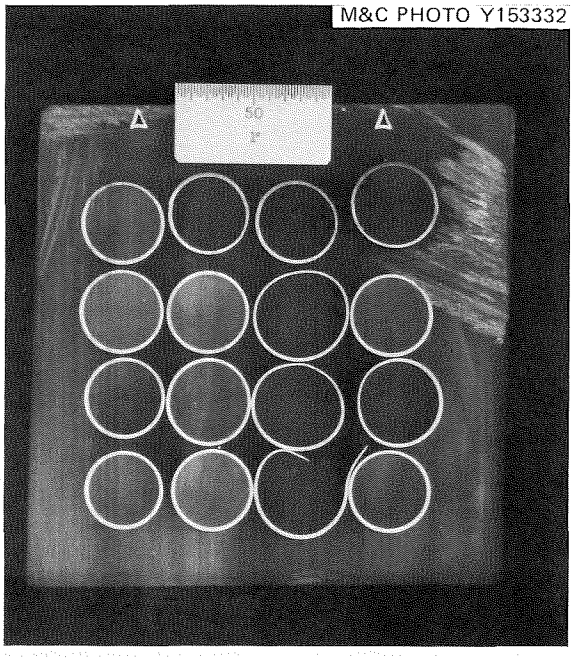

Fig. 86. Section of B-2 at 79.5-cm elevation.

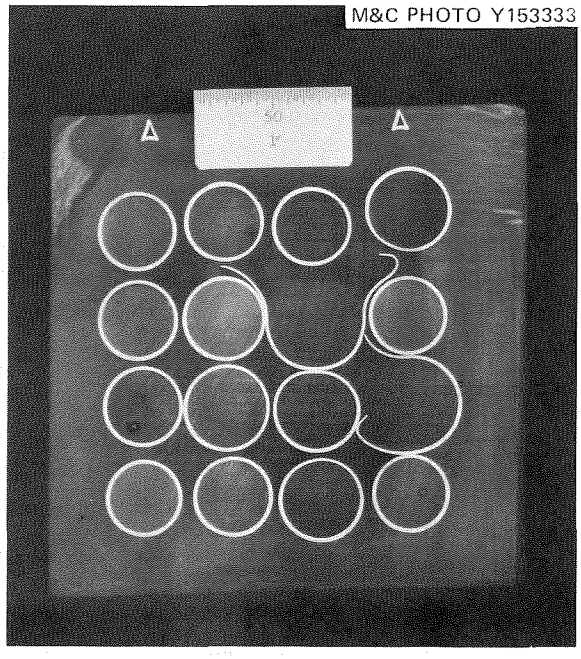

Fig. 87. Section of B-2 at 81.6-cm elevation.

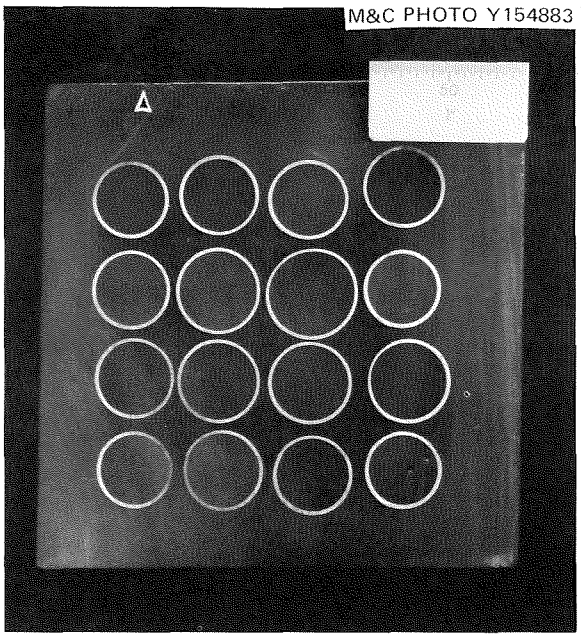

Fig. 88. Section of B-2 at 83.8-cm elevation.

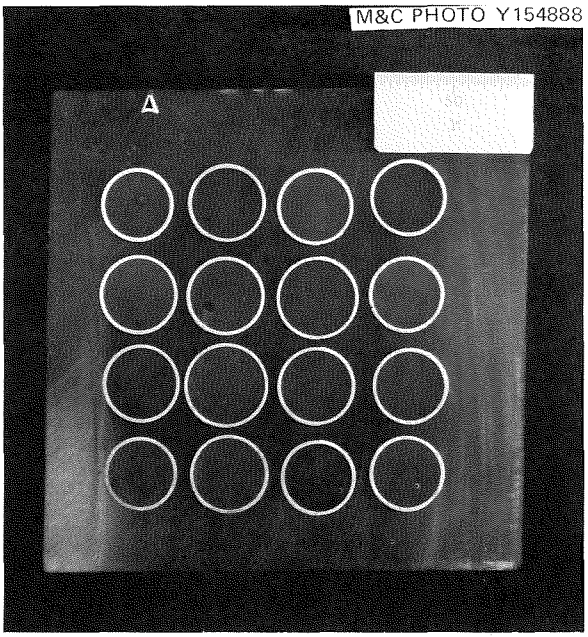

Fig. 89. Section of B-2 at 86.0-cm elevation.

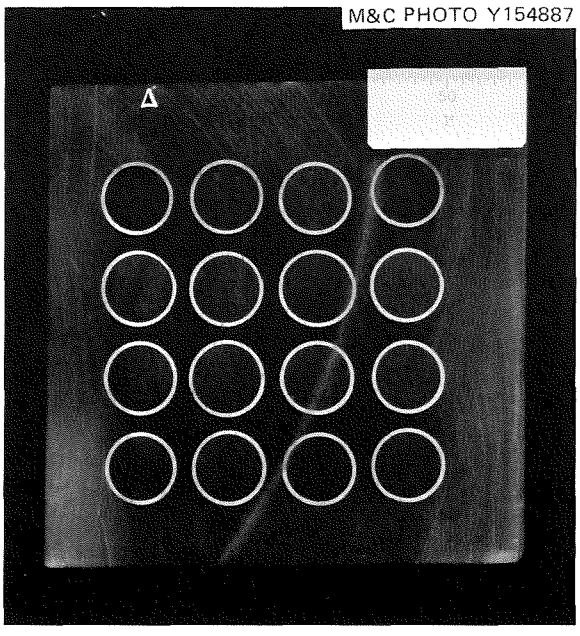

Fig. 90. Section of B-2 at 88.1-cm elevation.

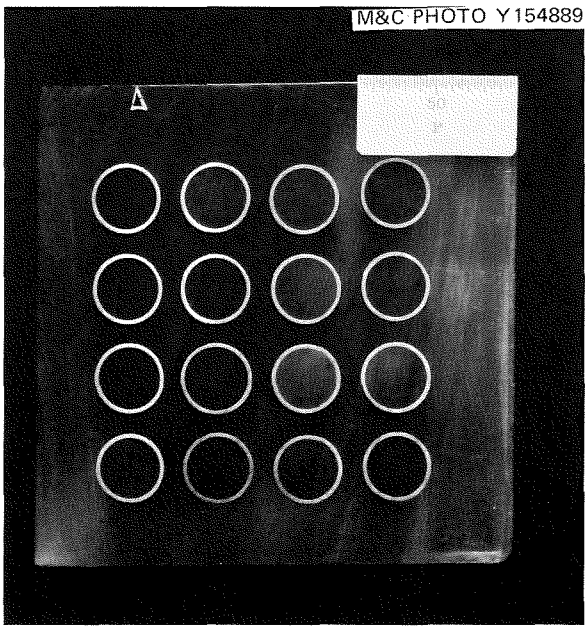

Fig. 91. Section of B-2 at 89.9-cm elevation.

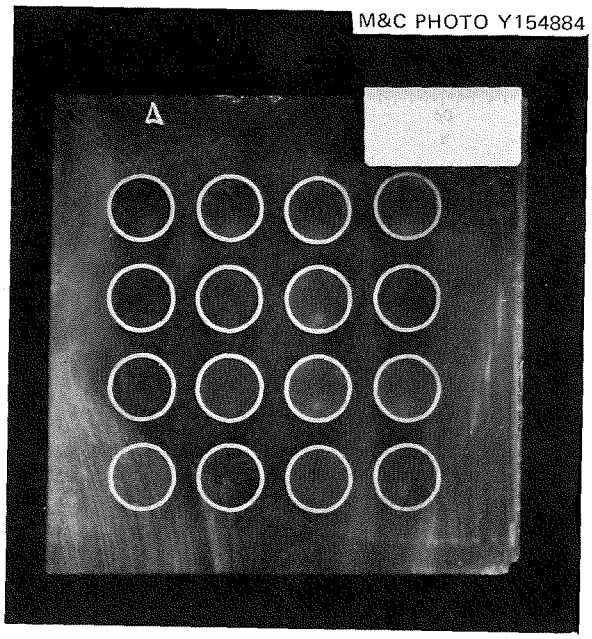

Fig. 92. Section of B-2 at 91.5-cm elevation.

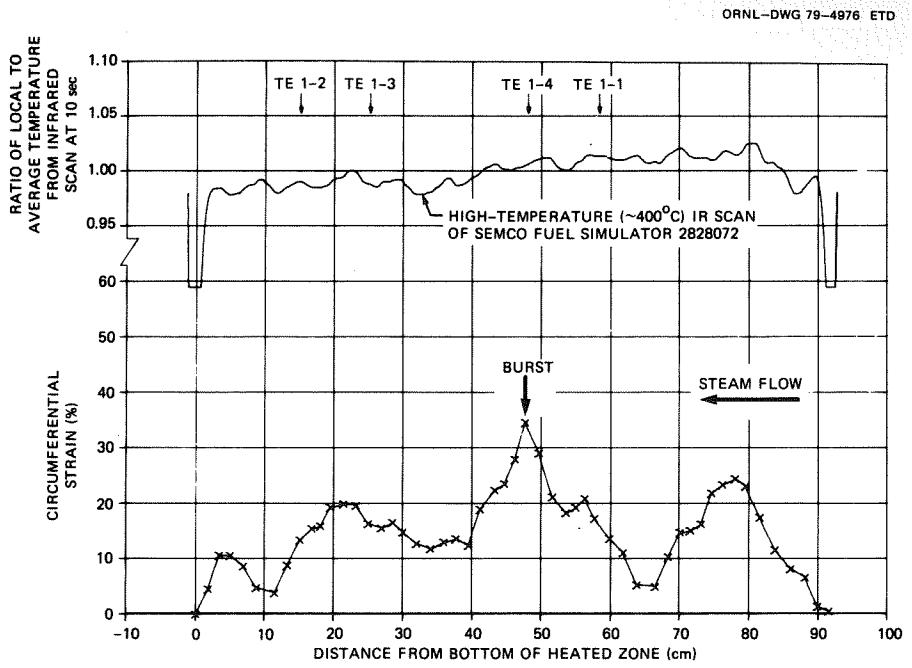

Fig. 93. Deformation profile of tube 1 in B-2 test.

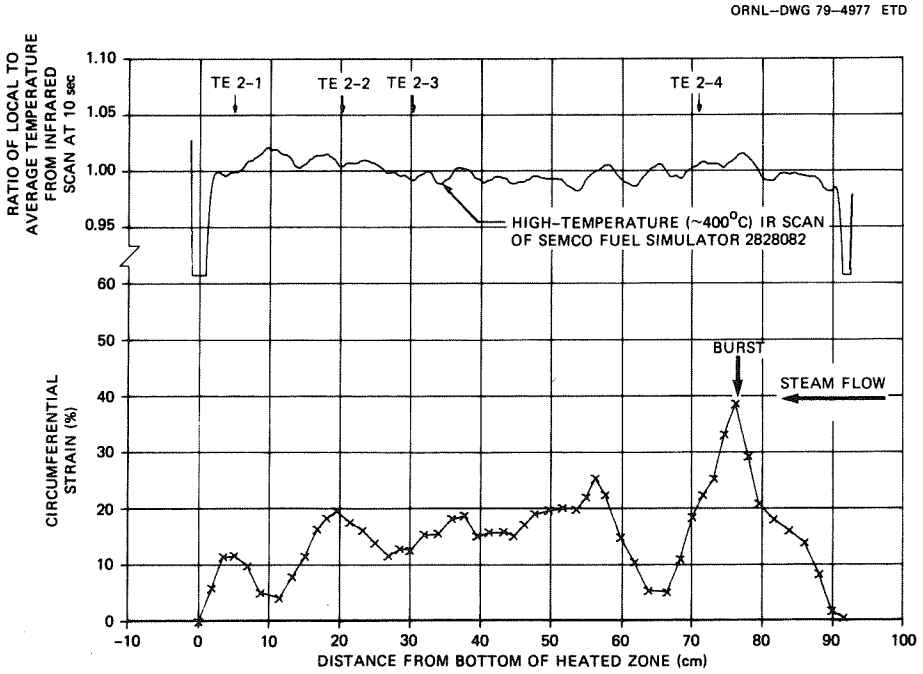

Fig. 94. Deformation profile of tube 2 in B-2 test.

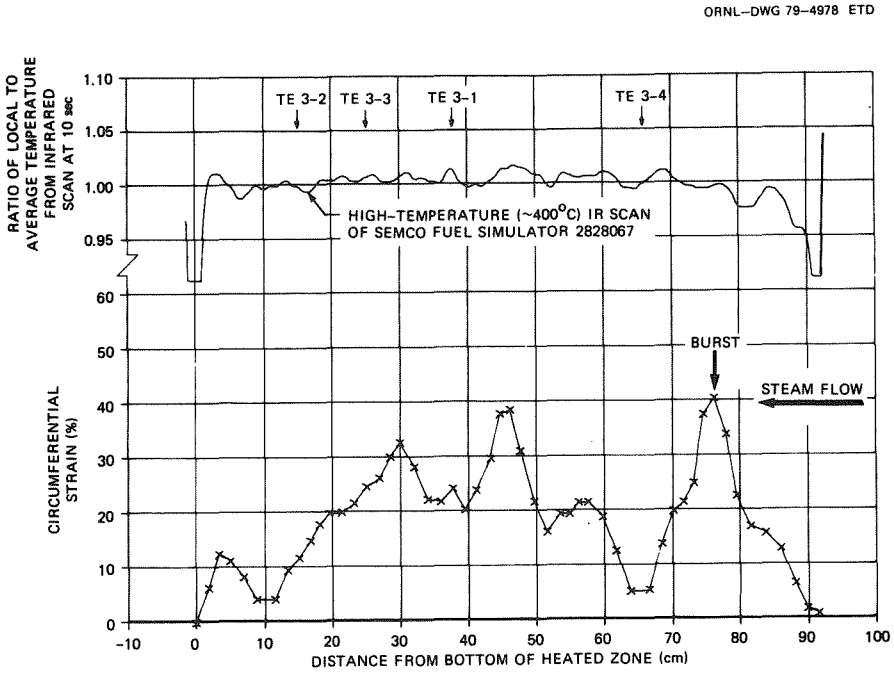

Fig. 95. Deformation profile of tube 3 in B-2 test.

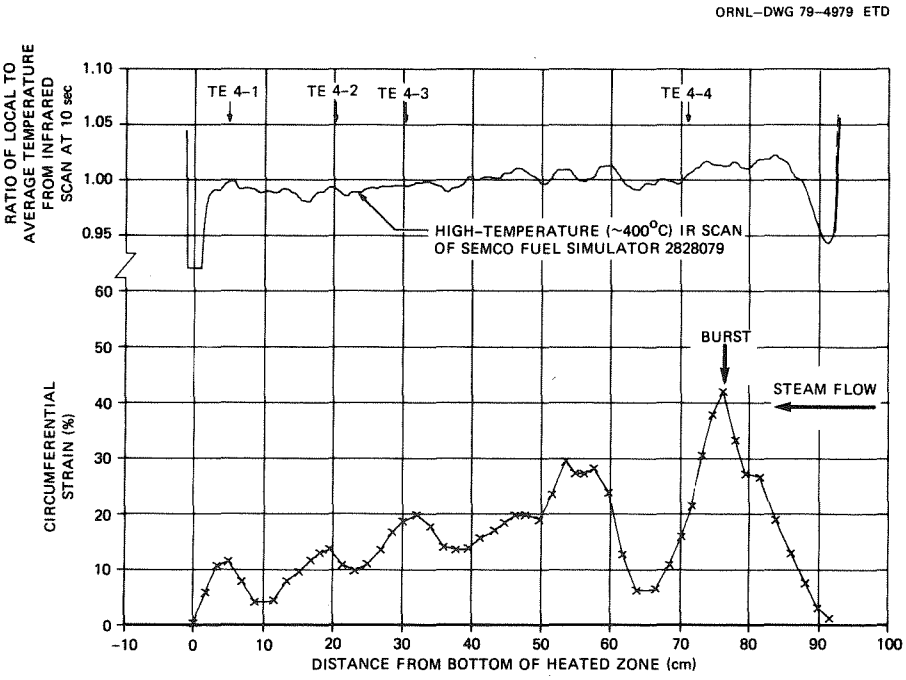

Fig. 96. Deformation profile of tube 4 in B-2 test.

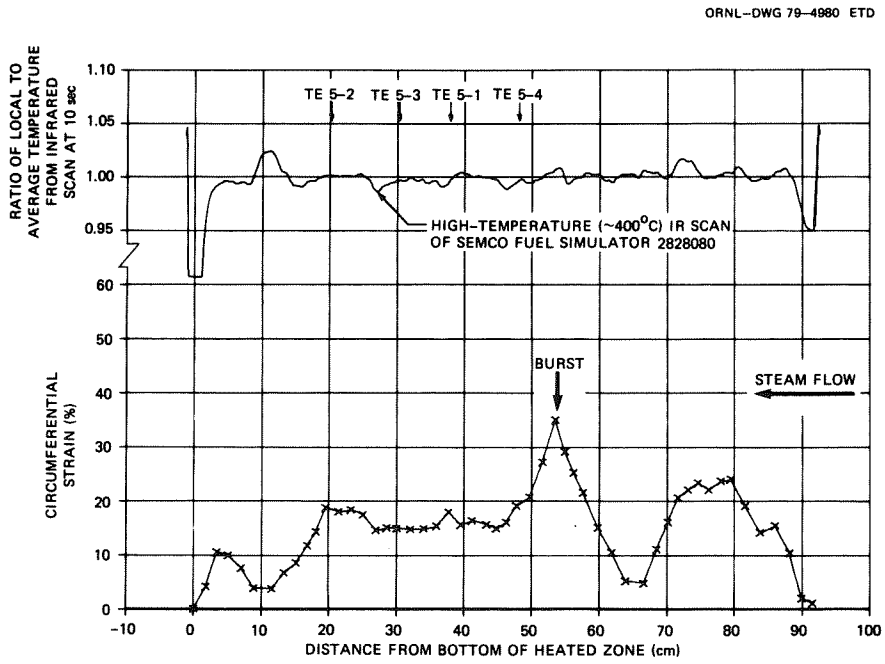

Fig. 97. Deformation profile of tube 5 in B-2 test.

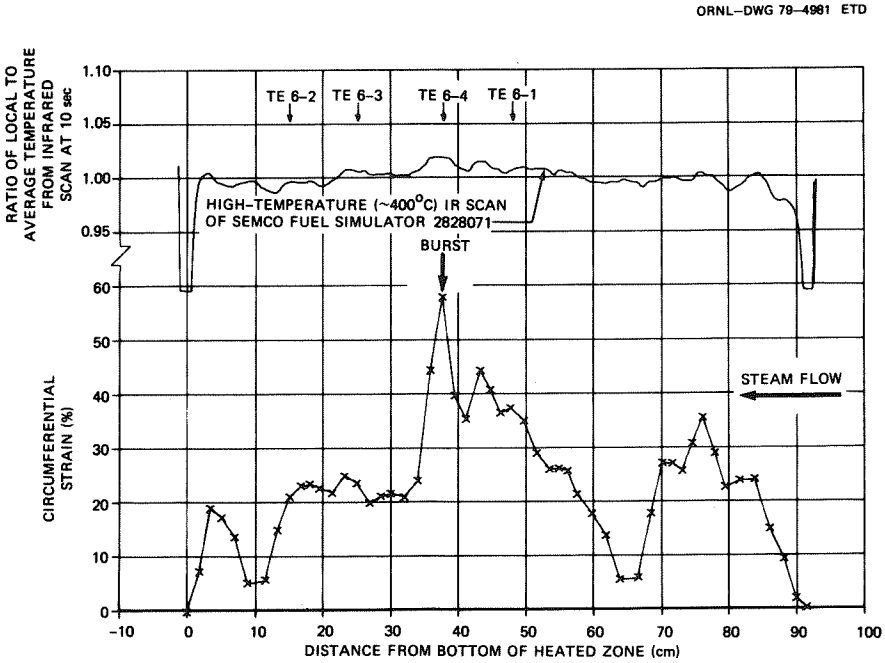

Fig. 98. Deformation profile of tube 6 in B-2 test.

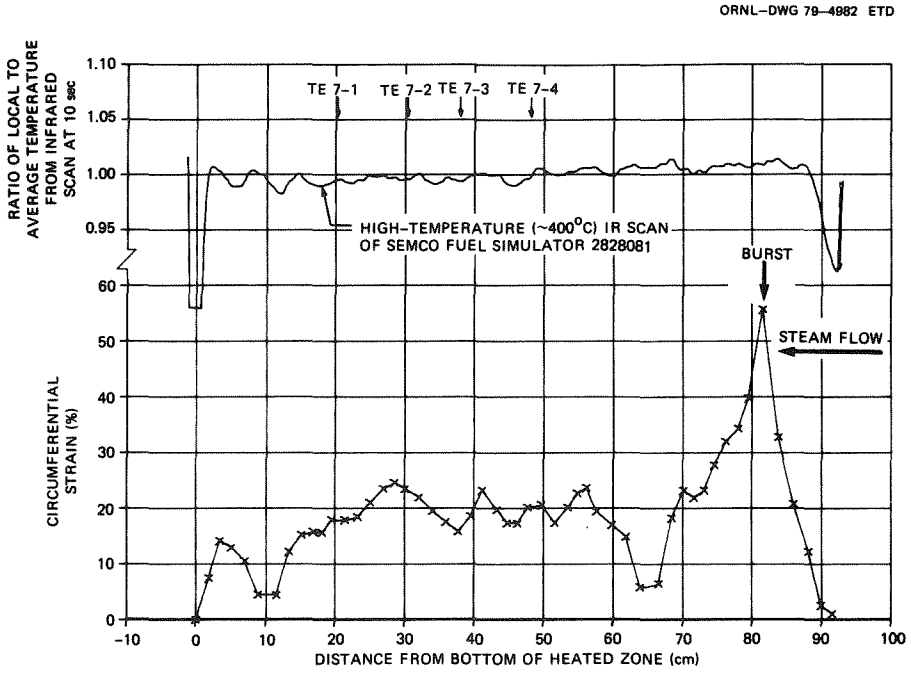

Fig. 99. Deformation profile of tube 7 in B-2 test.

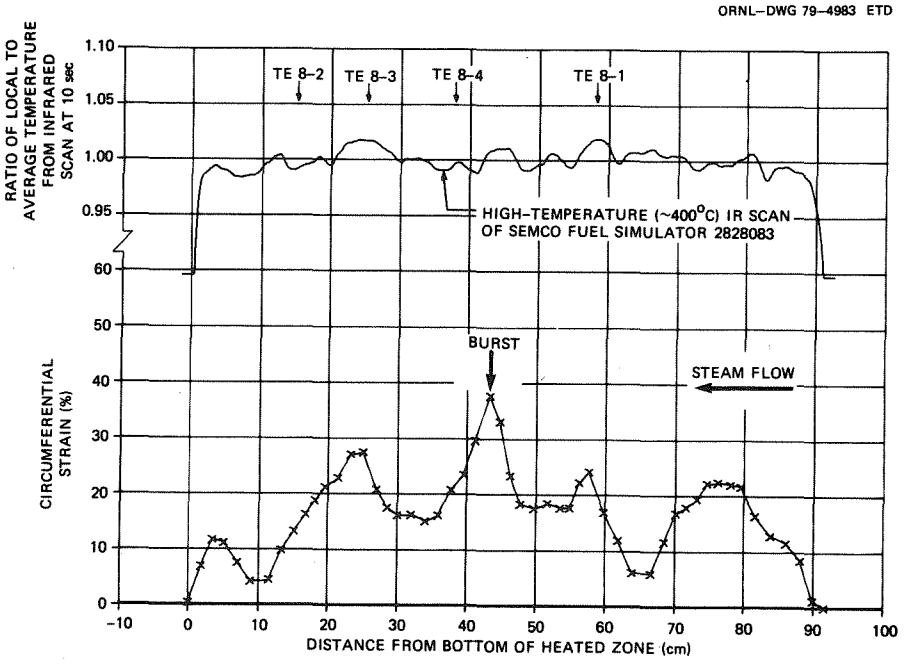

Fig. 100. Deformation profile of tube 8 in B-2 test.

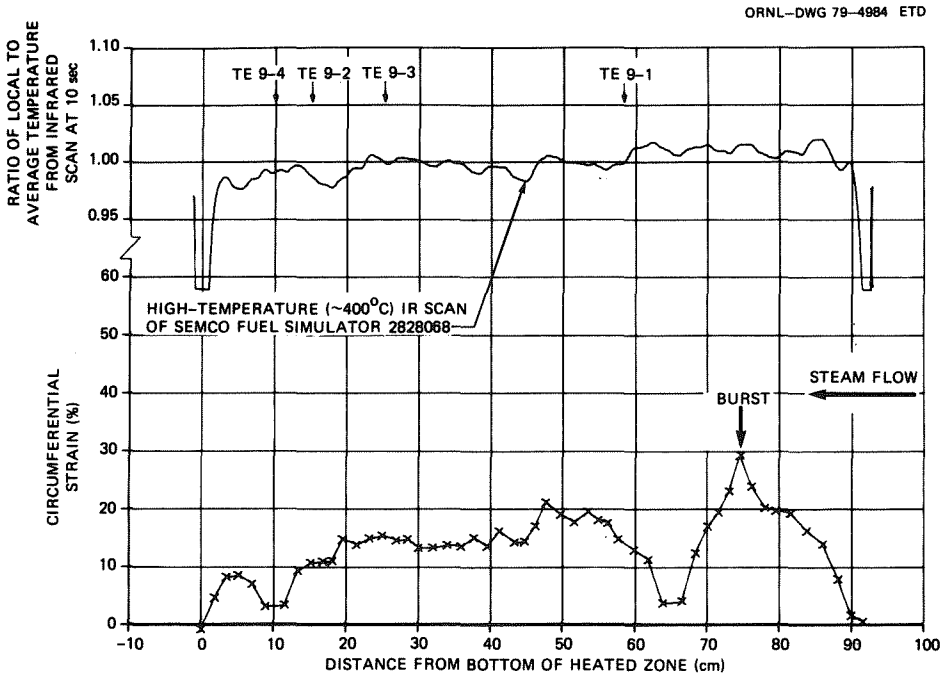

Fig. 101. Deformation profile of tube 9 in B-2 test.

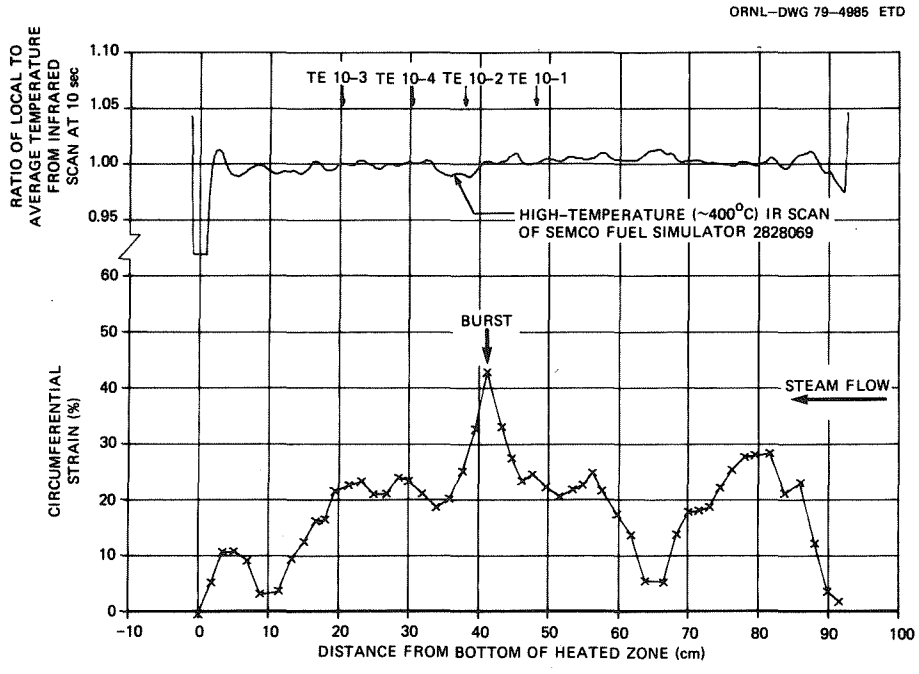

Fig. 102. Deformation profile of tube 10 in B-2 test.

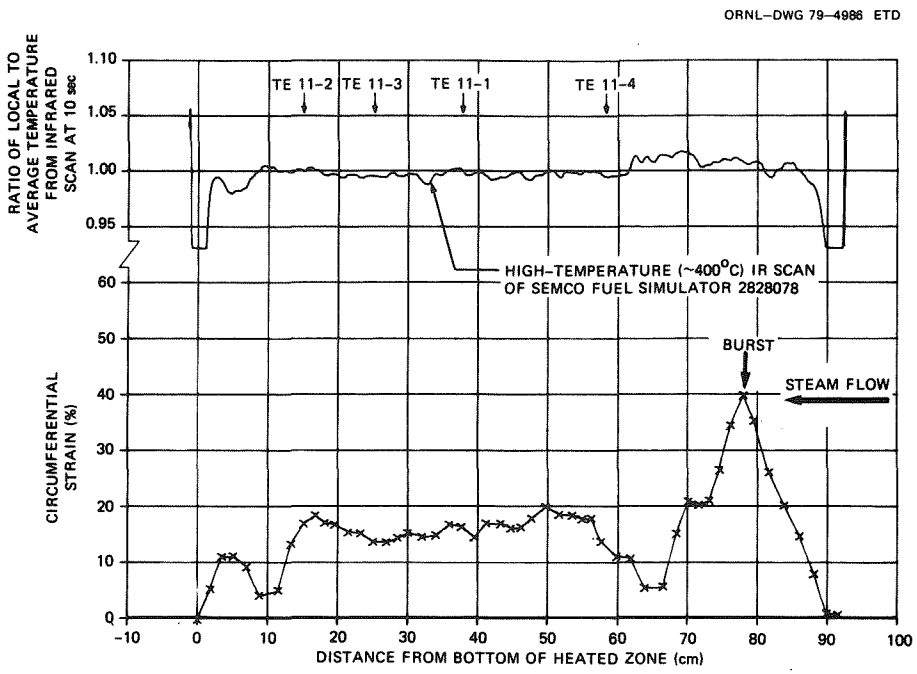

Fig. 103. Deformation profile of tube 11 in B-2 test.

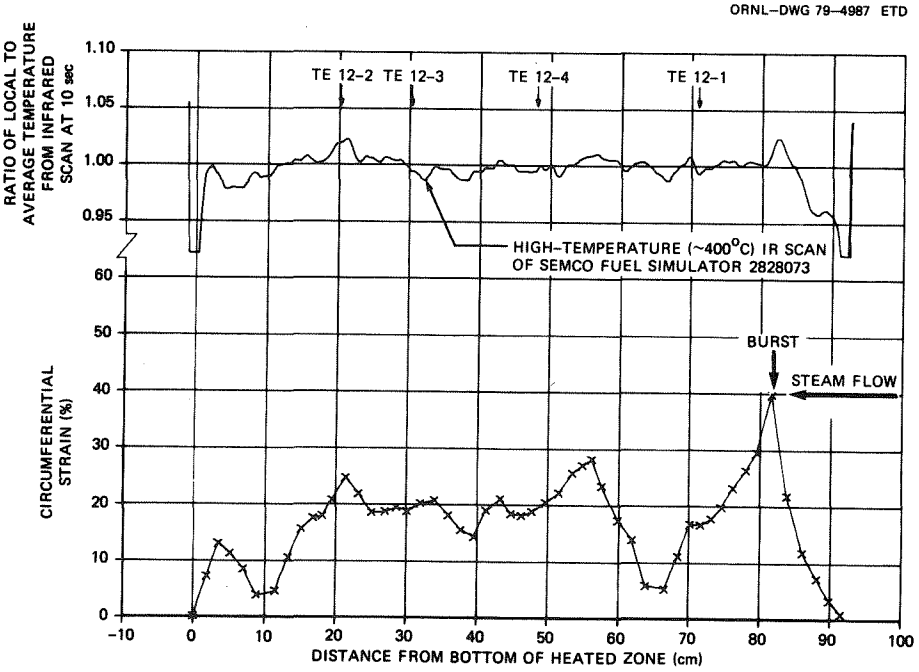

Fig. 104. Deformation profile of tube 12 in B-2 test.

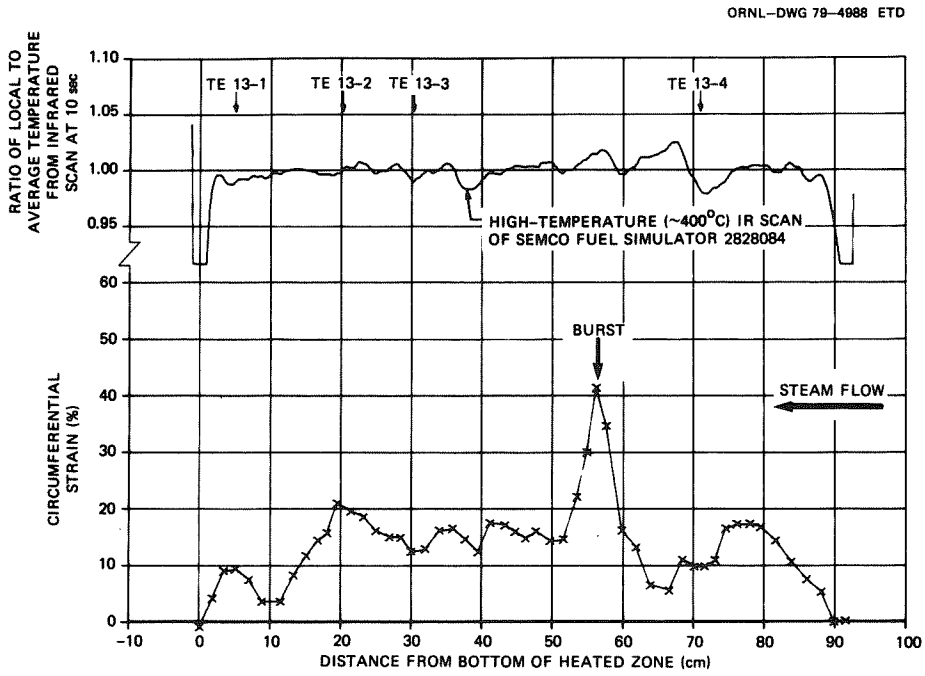

Fig. 105. Deformation profile of tube 13 in B-2 test.

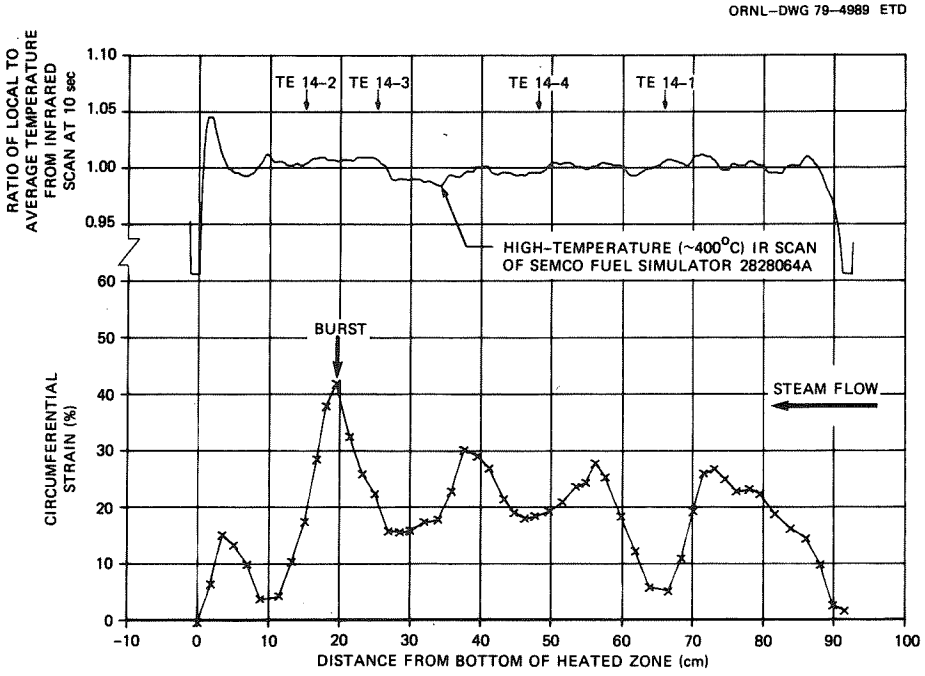

Fig. 106. Deformation profile of tube 14 in B-2 test.

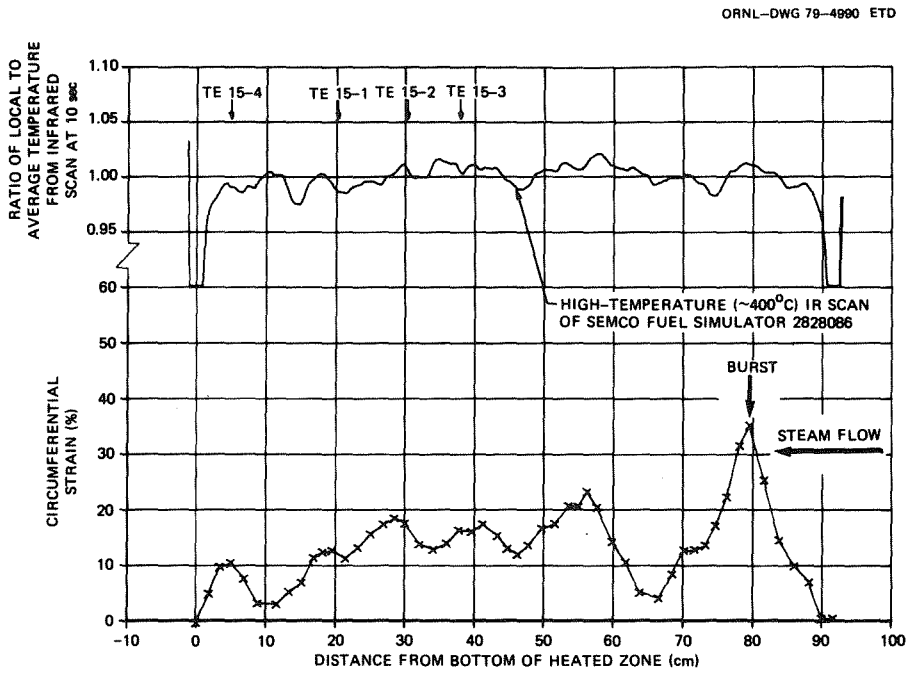

Fig. 107. Deformation profile of tube 15 in B-2 test.

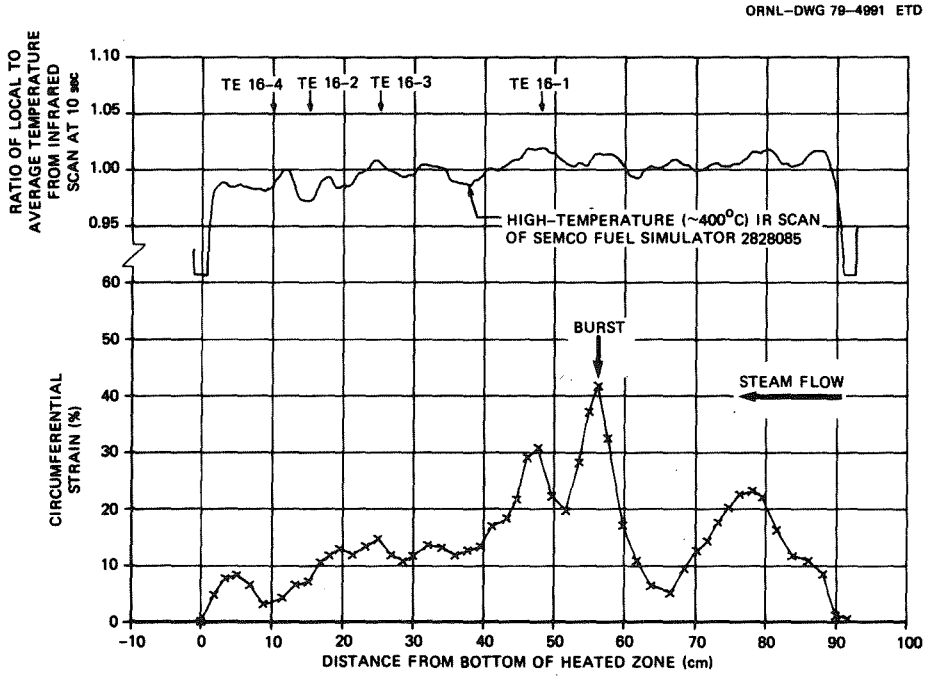

Fig. 108. Deformation profile of tube 16 in B-2 test.

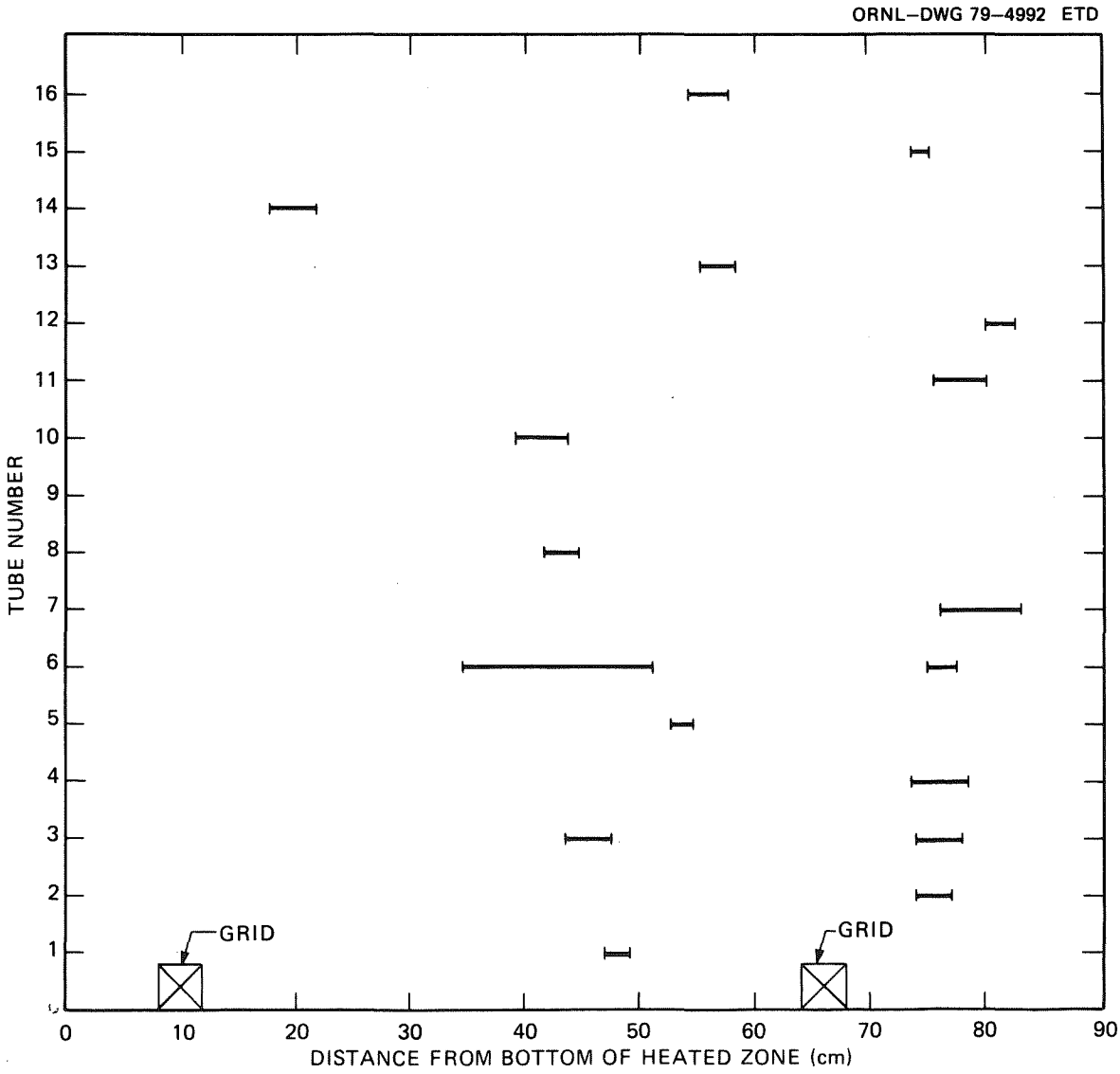

Fig. 109. Portions of tubes with greater than 32% strain in B-2 test.

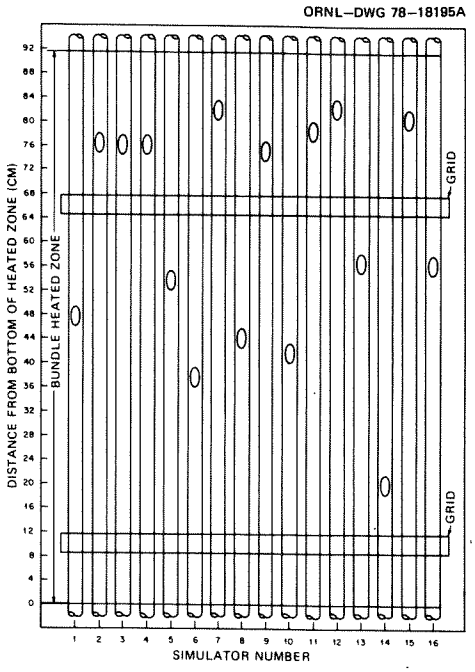

Fig. 110. Axial distribution of bursts in B-2 test.

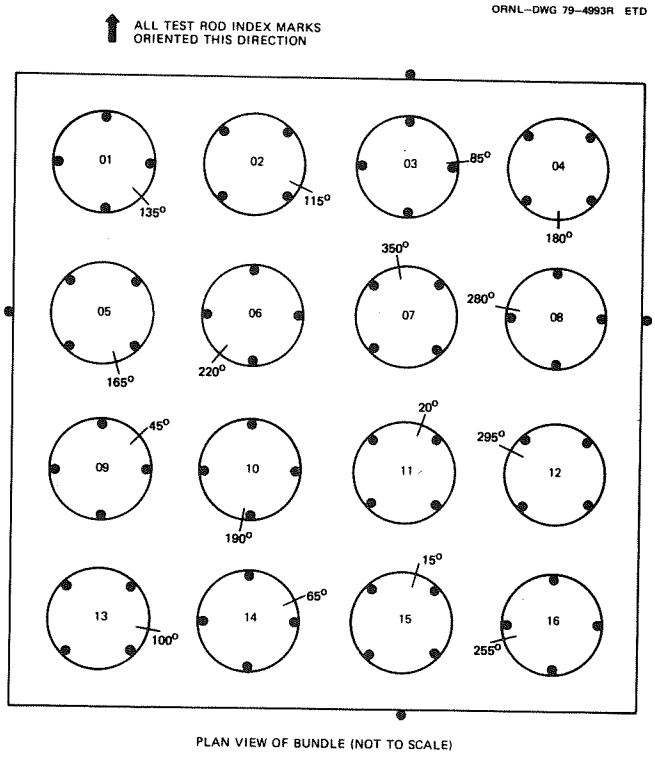

Fig. 111. Angular distribution of bursts in B-2 test.

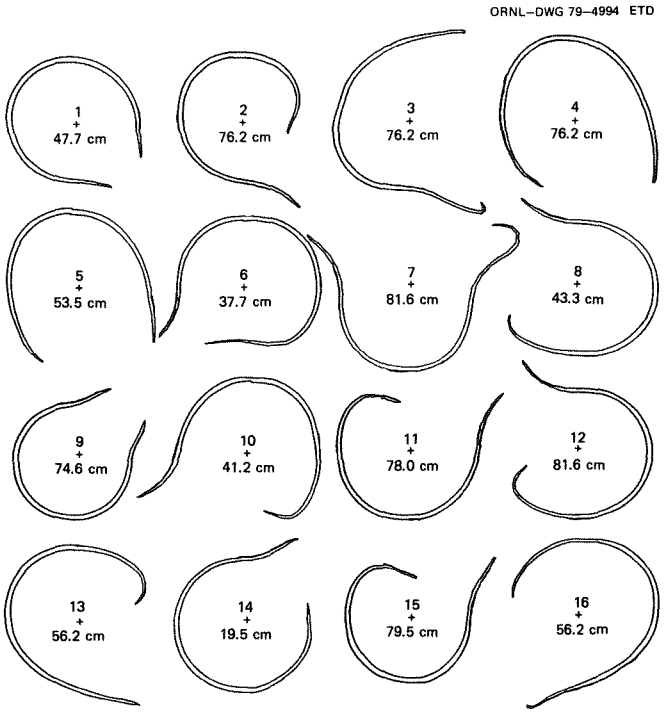

Fig. 112. Composite layout of burst orientations in B-2 test. Tube-to-tube pitch greatly exaggerated for clarity; axial locations of burst are noted.

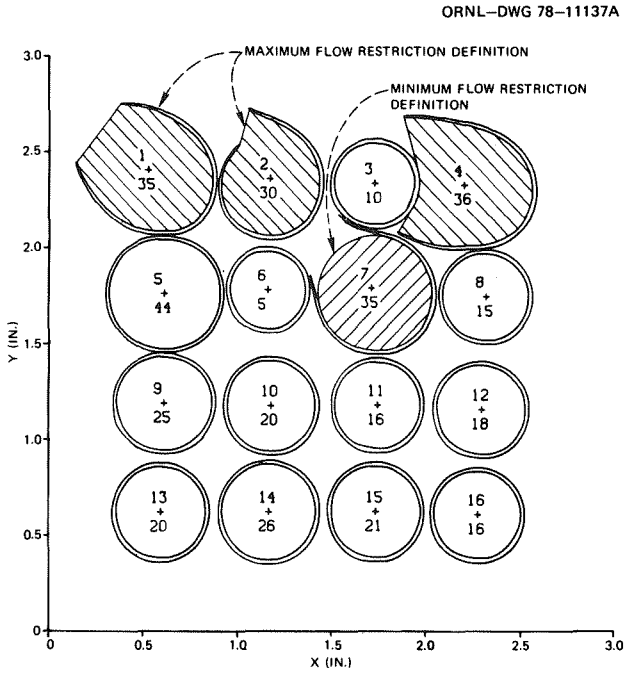

Fig. 113. An example of a computer simulation of a bundle cross section showing definitions of maximum and minimum flow restrictions for burst tubes.

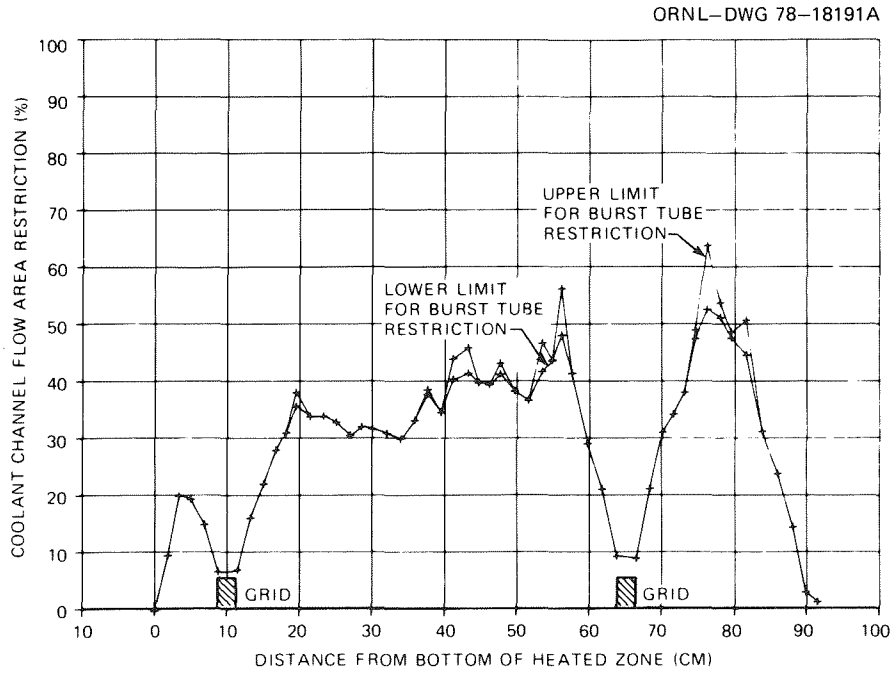

Fig. 114. Coolant channel flow area restriction in B-2 based on a rod-centered unit cell and estimated upper and lower limits of burst tube flow restriction.

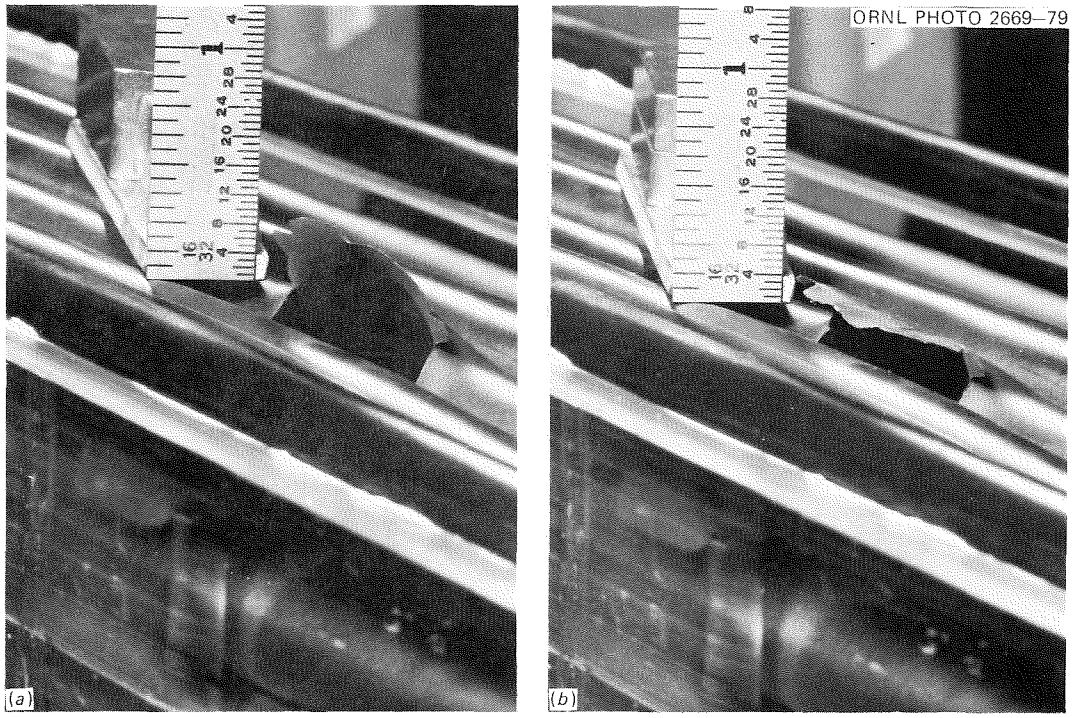

Fig. 115. Tube 3 burst flare-out before (a) and after (b) bending to avoid interference with wall of flow shroud 1.

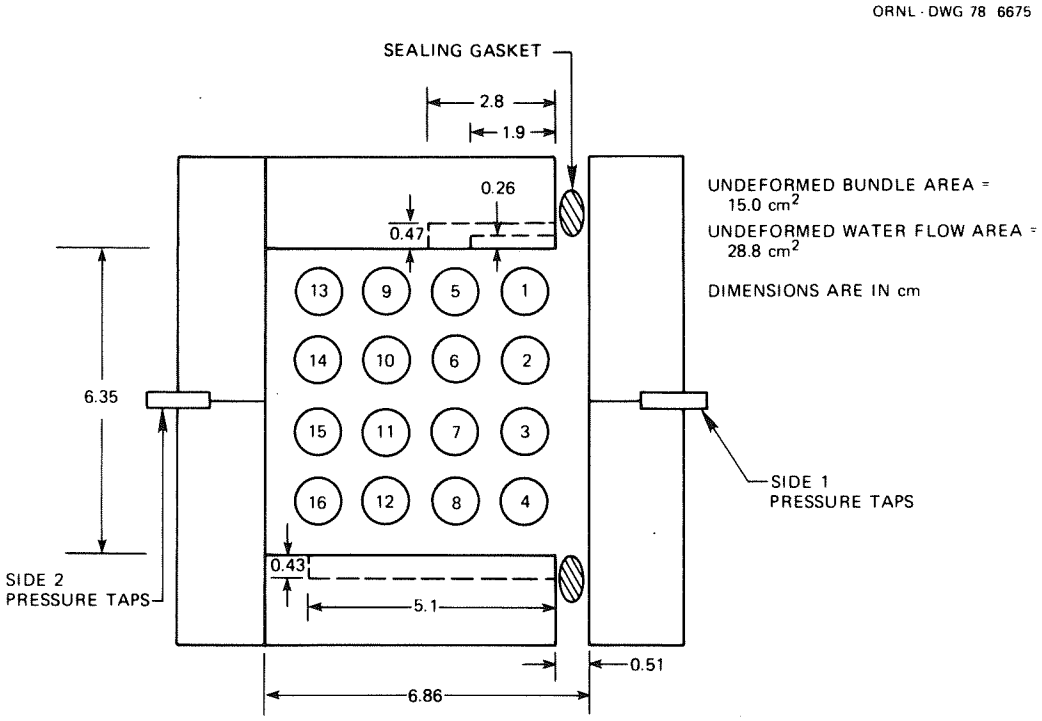

Fig. 116. Flow test configuration of B-2 in shroud 1.

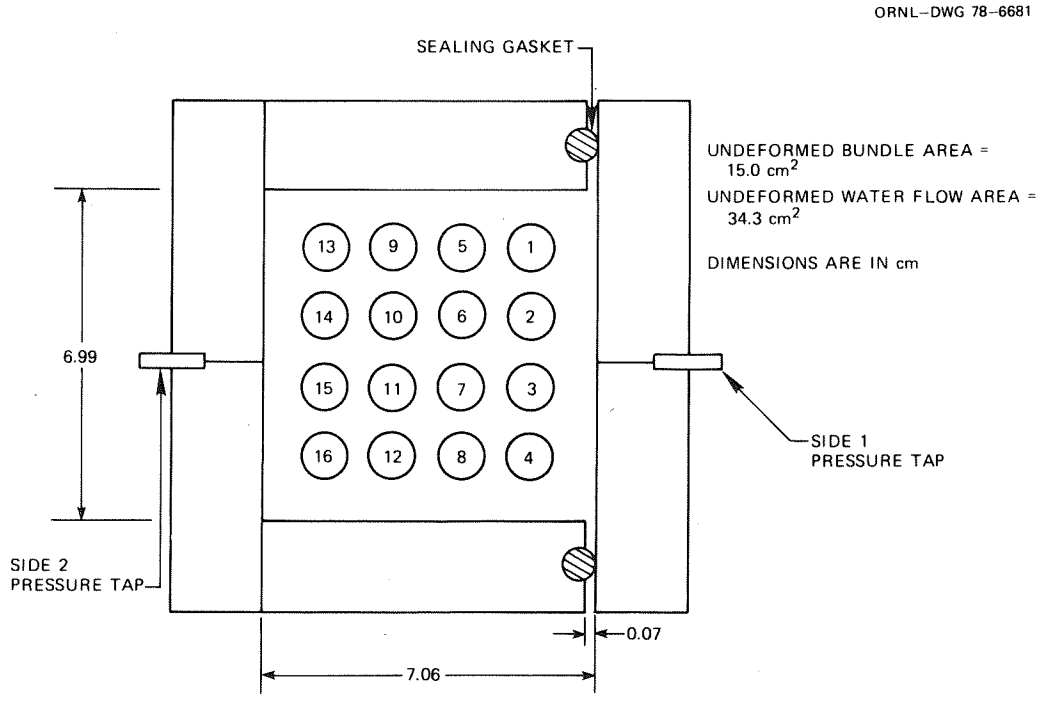

Fig. 117. Flow test configuration of B-2 in shroud 2.

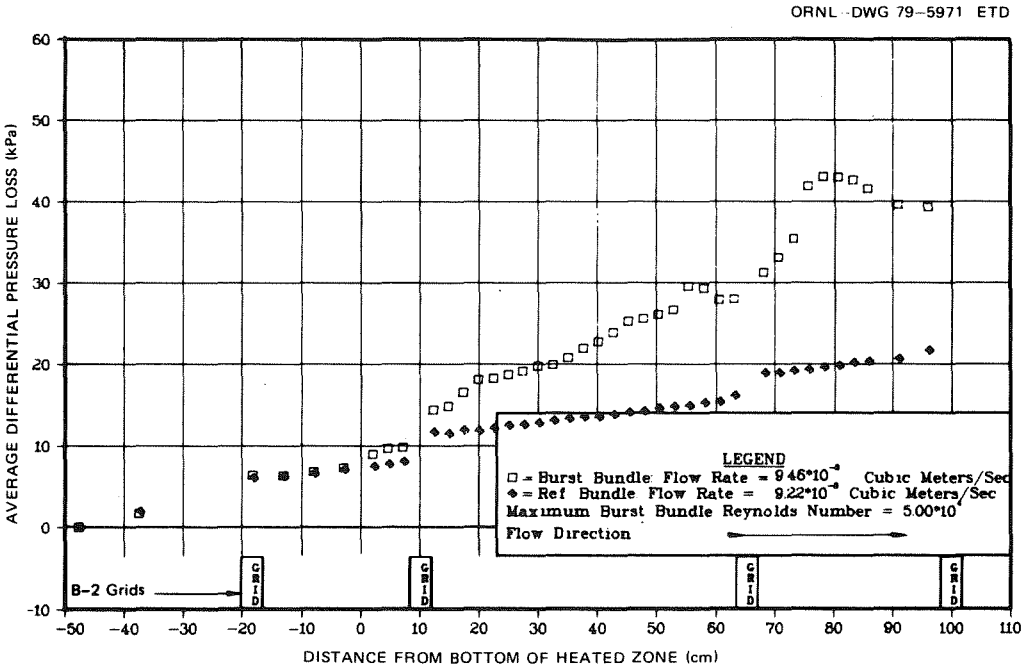

Fig. 118. B-2 and reference bundle axial pressure loss profiles at a nominal flow rate of 0.0093 m^3/sec in shroud 1.

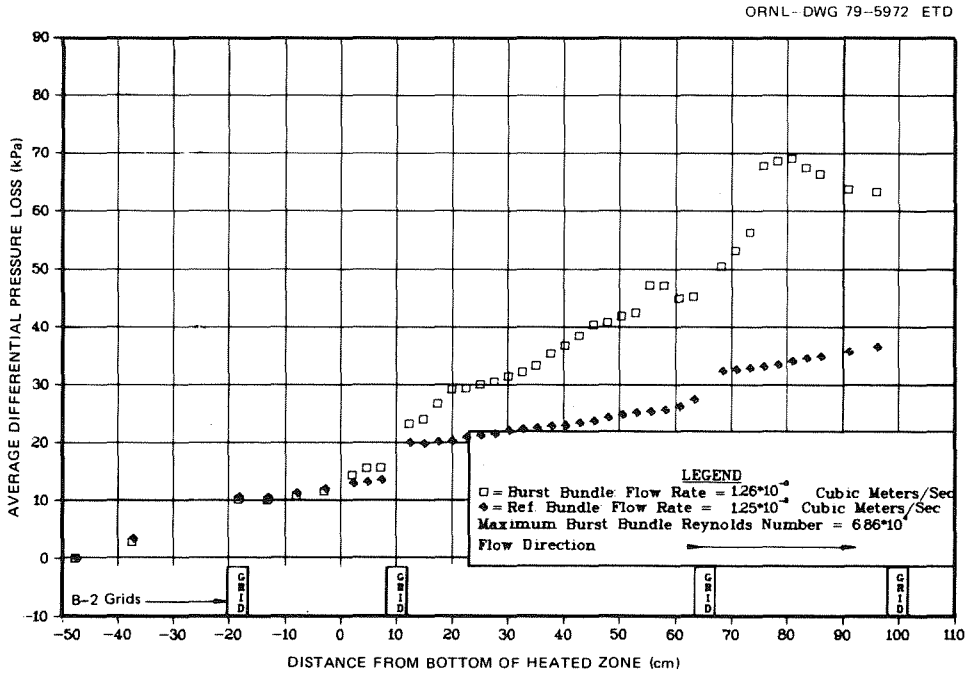

Fig. 119. B-2 and reference bundle axial pressure loss profiles at a nominal flow rate of 0.013 m^3/sec in shroud 1.

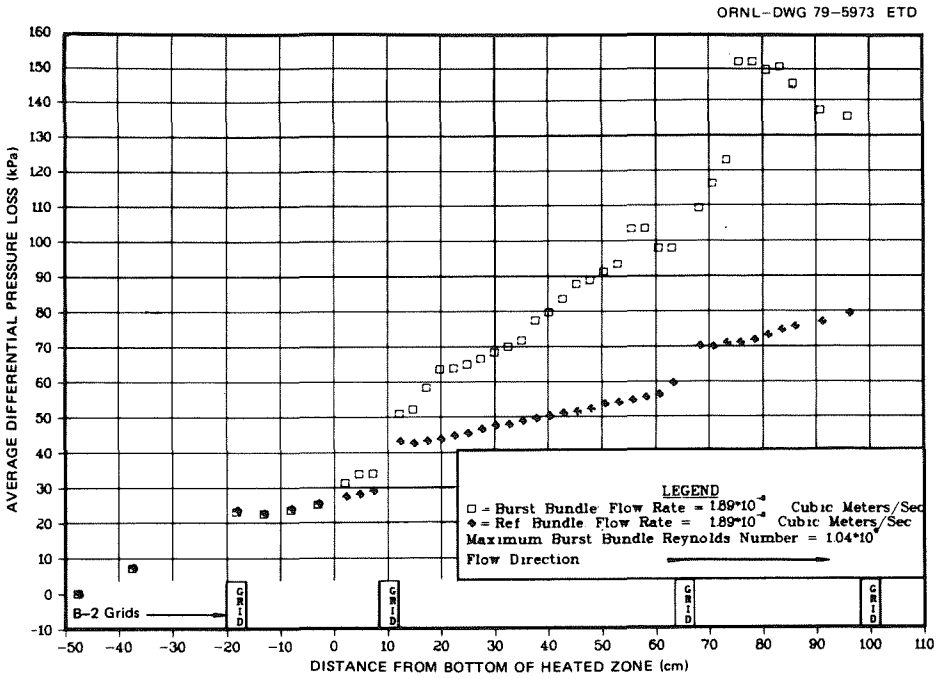

Fig. 120. B-2 and reference bundle axial pressure loss profiles at a nominal flow rate of 0.019 m^3/sec in shroud 1.

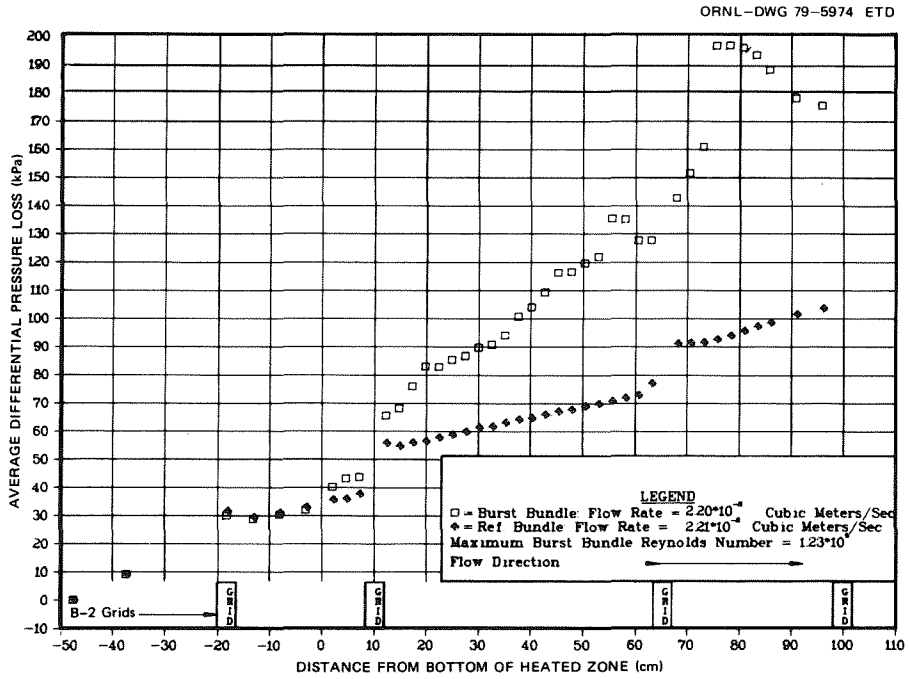

Fig. 121. B-2 and reference bundle axial pressure loss profiles at a nominal flow rate of 0.022 m^3/sec in shroud 1.

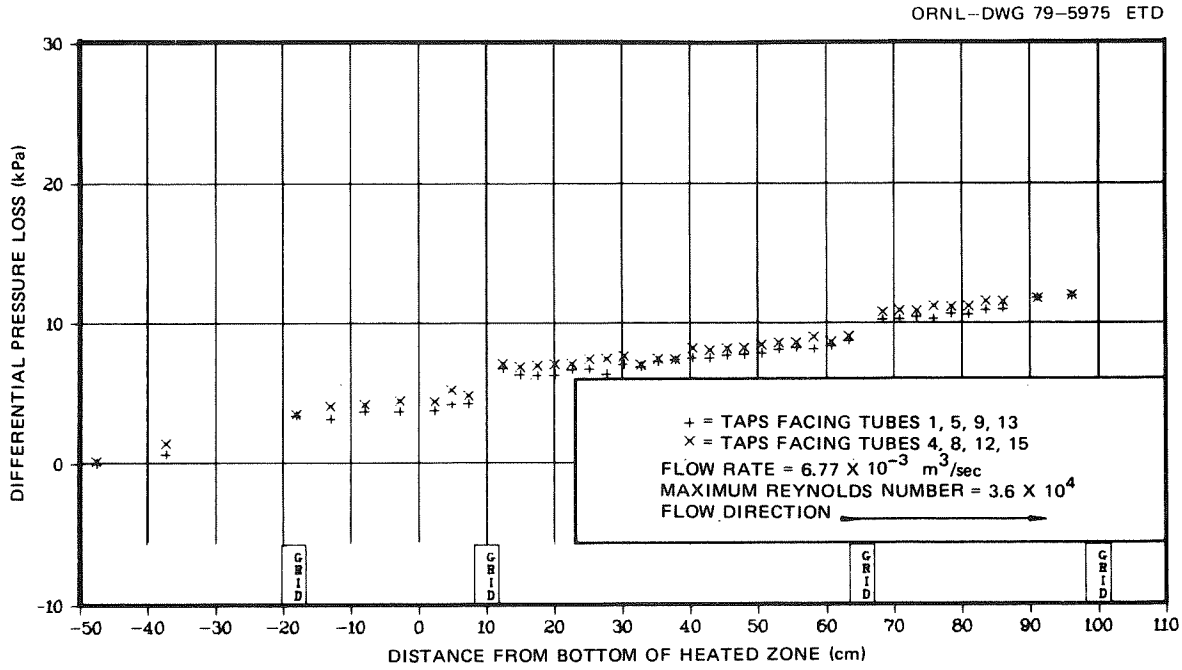

Fig. 122. Reference bundle axial pressure loss profile for a flow rate of 0.0068 m^3/sec in shroud 1.

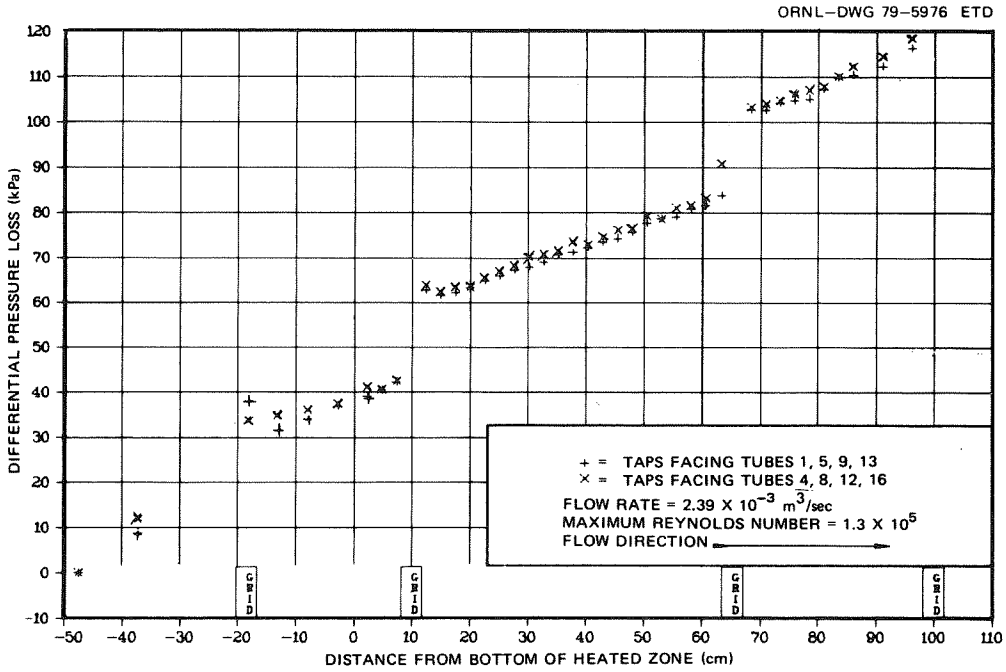

Fig. 123. Reference bundle axial pressure loss profile for a flow rate of 0.024 m^3/sec in shroud 1.

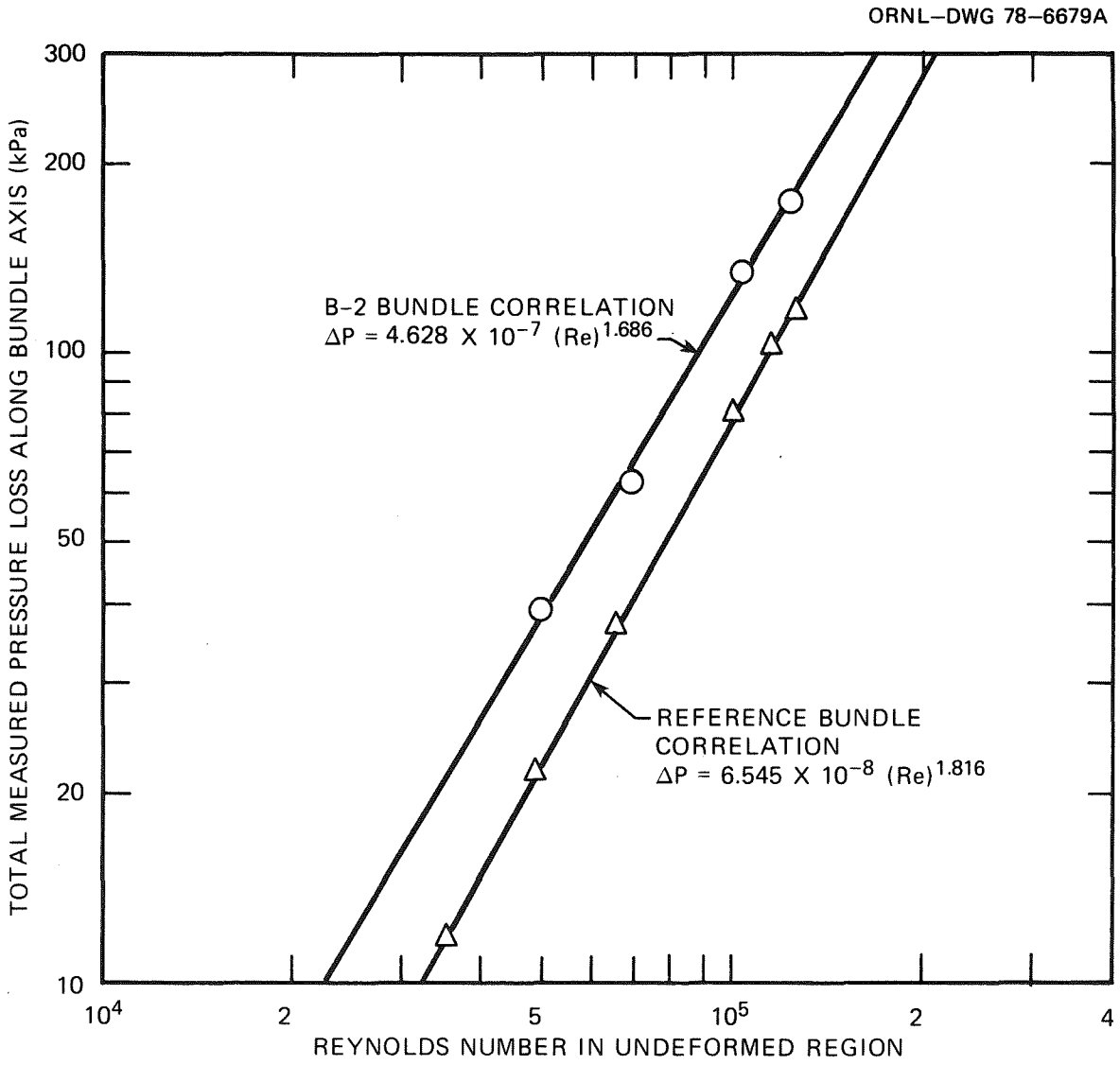

Fig. 124. Extrapolation of B-2 and reference bundle pressure losses to other Reynolds numbers in shroud 1.

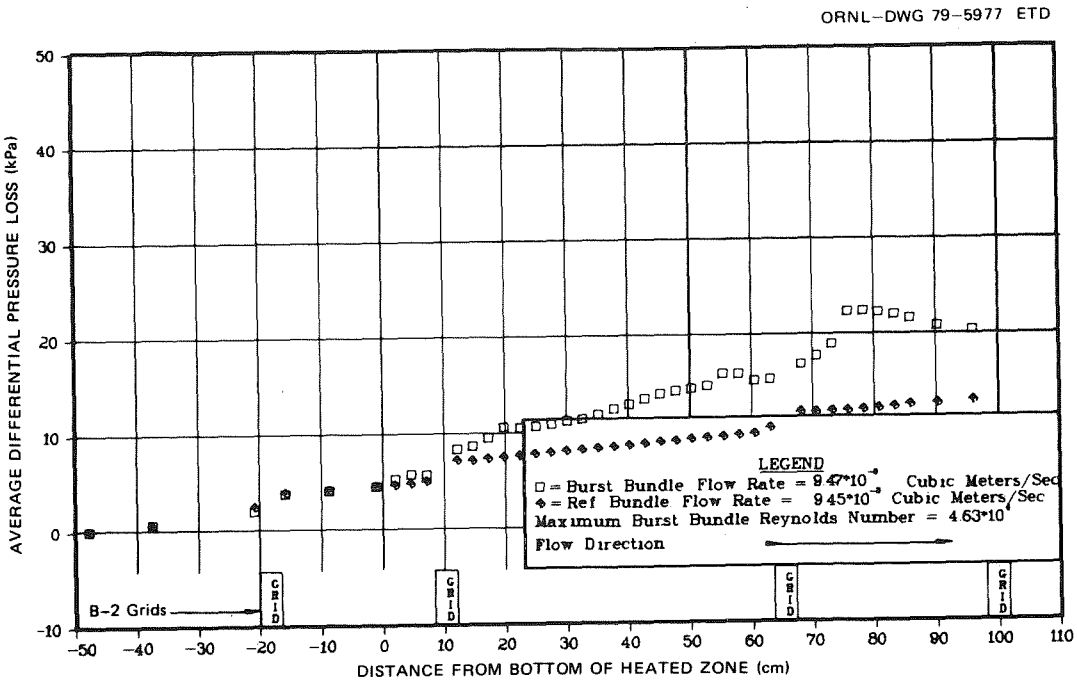

Fig. 125. B-2 and reference bundle axial pressure loss profiles at a nominal flow rate of 0.0095 m^3/sec in shroud 2.

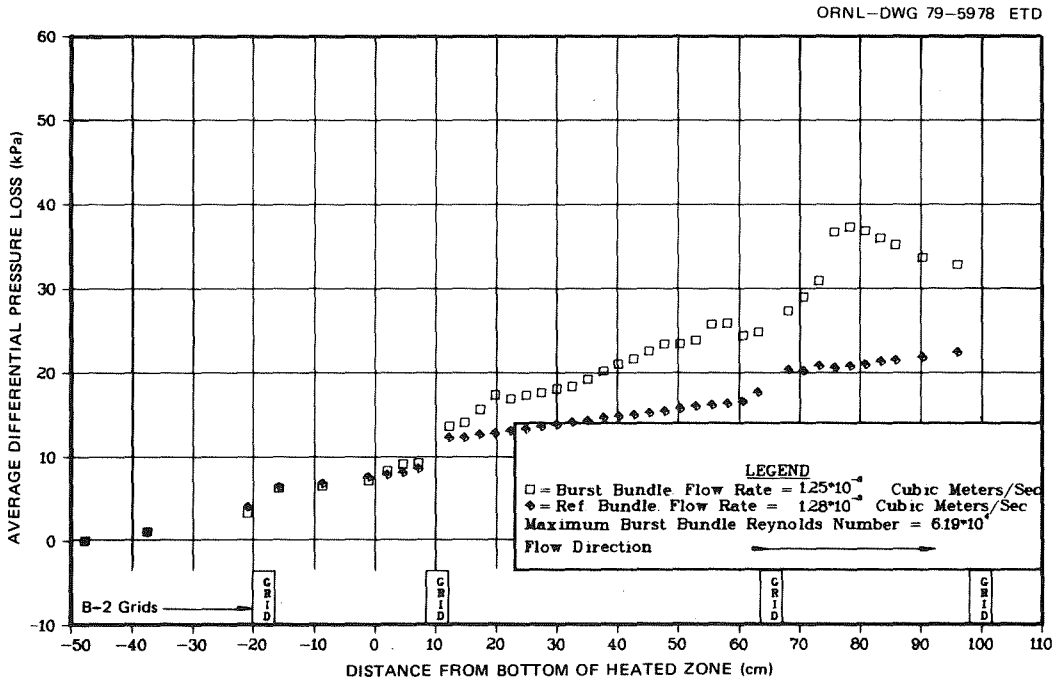

Fig. 126. B-2 and reference bundle axial pressure loss profiles at a nominal flow rate of 0.013 m^3/sec in shroud 2.

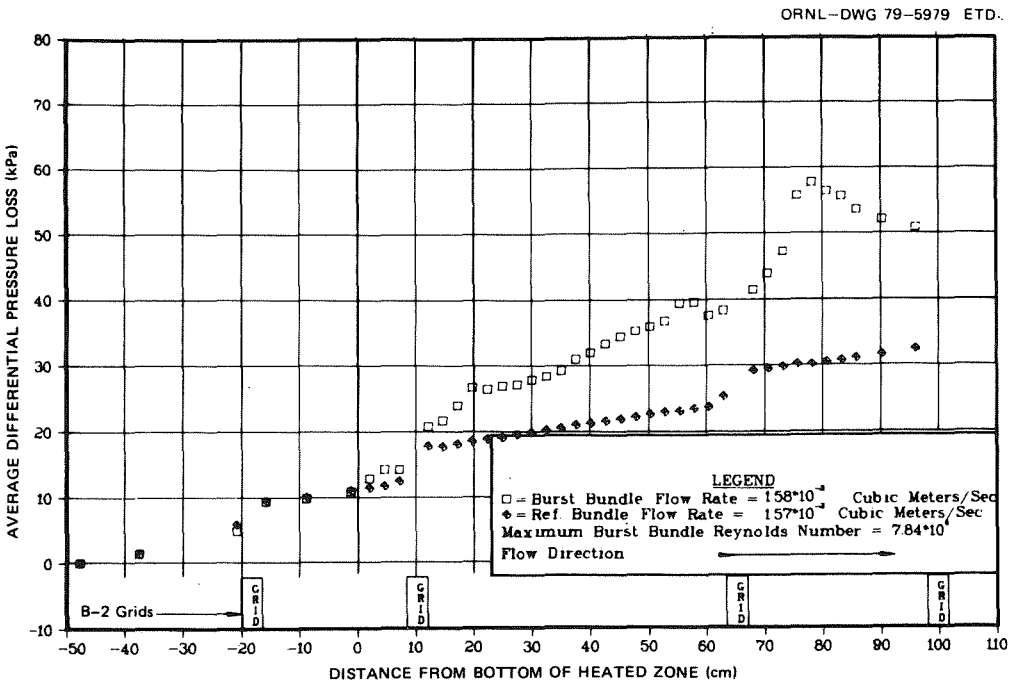

Fig. 127. B-2 and reference bundle axial pressure loss profiles at a nominal flow rate of 0.016 m^3/sec in shroud 2

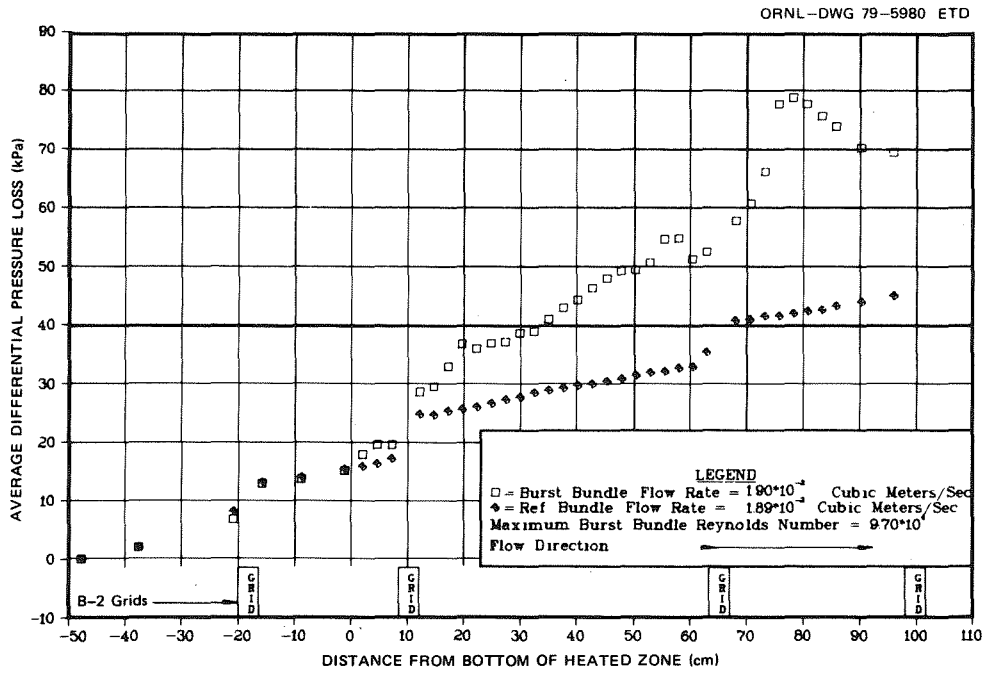

Fig. 128. B-2 and reference bundle axial pressure loss profiles at a nominal flow rate of 0.019 m^3/sec in shroud 2.

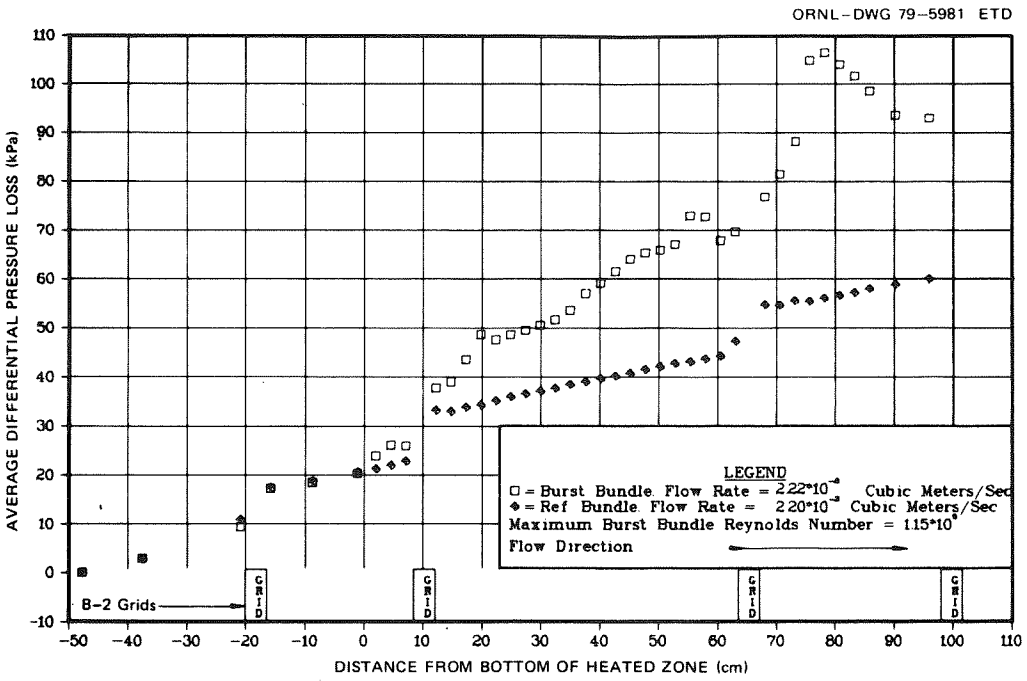

Fig. 129. B-2 and reference bundle axial pressure loss profiles at a nominal flow rate of 0.022 m^3/sec in shroud 2.

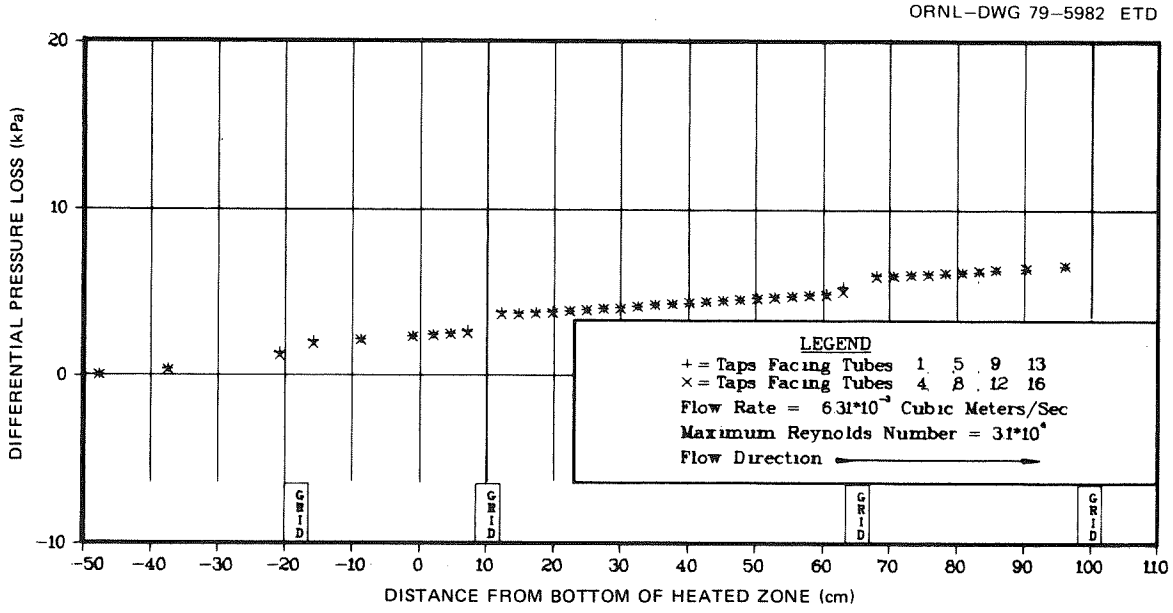

Fig. 130. Reference bundle axial pressure loss profile for a flow rate of 0.0063 m^3/sec in shroud 2.

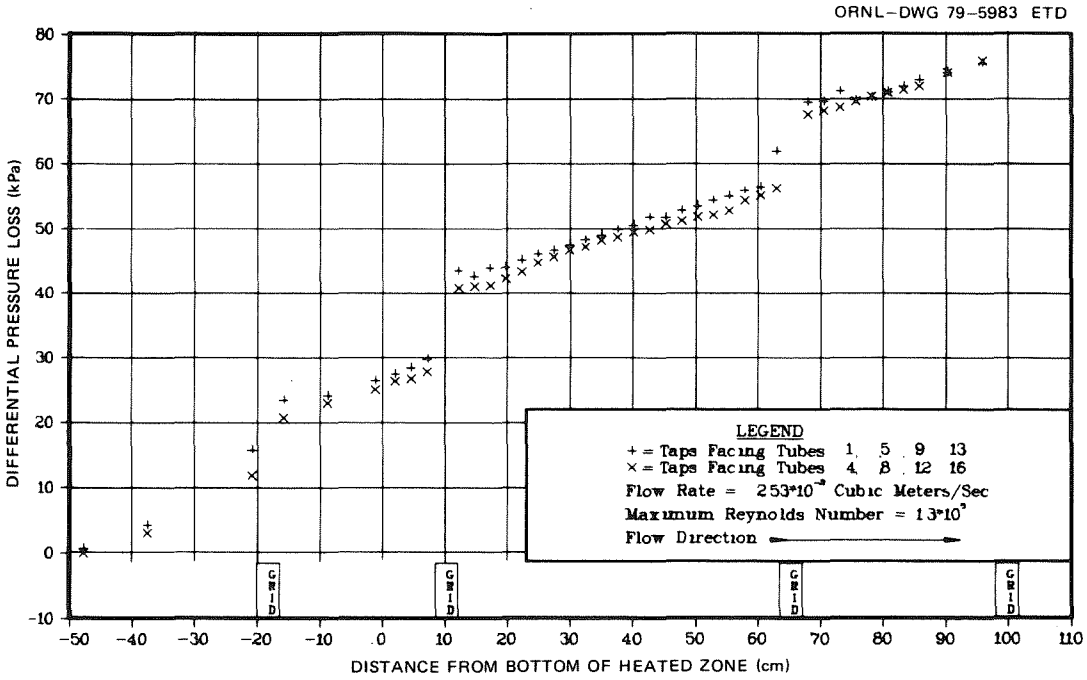

Fig. 131. Reference bundle axial pressure loss profile for a flow rate of 0.025 m^3/sec in shroud 2.

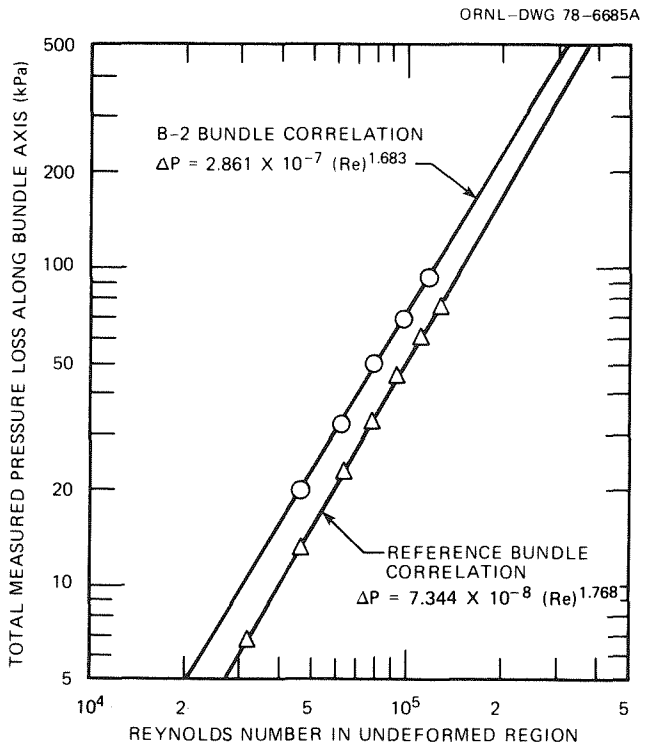

Fig. 132. Extrapolation of B-2 and reference bundle pressure losses to other Reynolds numbers in shroud 2.

ORNL/NUREG/TM-337
Special Distribution

Internal Distribution

1-10. R. H. Chapman
11. J. L. Crowley
12. D. O. Hobson
13. A. W. Longest
14. J. F. Mincey
15. F. R. Mynatt
16. J. L. Rich
17. Patent Office
18. Nuclear Safety Information Center
19-20. Central Research Library
21. Document Reference Section
22-24. Laboratory Records Department
25. Laboratory Records (RC)

External Distribution

26. R. A. Adamson, Mail Code V-03, General Electric Company, Vallecitos Atomic Laboratory, P.O. Box 846, Pleasanton, CA 94566
27. D. L. Burman, Westinghouse Nuclear Fuel Division, P.O. Box 355, Pittsburgh, PA 15230
28. C. E. Crouthamel, Exxon Nuclear, Inc., 2955 George Washington Way, Richland, WA 99352
29. D. L. Hagrman, EG&G Idaho, Inc., INEL, Idaho Falls, ID 83401
30. A. L. Lowe, Babcock and Wilcox Company, P.O. Box 1260, Lynchburg, VA 24505
31. P. A. Smerd, Combustion Engineering, Inc., 1000 Prospect Road, Windsor, CT 06093
32. M. Fischer, Projekt Nukleare Sicherheit, Kernforschungszentrum Karlsruhe, 75 Karlsruhe, Federal Republic of Germany
33. S. Kawasaki, Fuel Reliability Laboratory III, JAERI Tokai Research Establishment, Takai-mura, Naka-gun, Ibaraki-ken, Japan
34. D. O. Pickman, UKAEA Springfields Nuclear Power Development Laboratories, Springfields, Preston (Lancs) PP4 ORR, England
35. Chief, Fuel Behavior Branch, Office of Nuclear Regulatory Research, Nuclear Regulatory Commission, Washington, DC 20555
36. R. O. Meyer, Core Performance Branch, Office of Nuclear Reactor Regulation, Nuclear Regulatory Commission, Washington, DC 20555
37. M. L. Picklesimer, Fuel Behavior Branch, Office of Nuclear Regulatory Research, Nuclear Regulatory Commission, Washington, DC 20555
38. Director, Office of Assistant Manager, Energy Research and Development, DOE, ORO
39. Director, Reactor Division, DOE, ORO
40-41. NRC Public Document Room, Nuclear Regulatory Commission, Washington, DC 20555
42-43. Technical Information Center, DOE, Oak Ridge, TN 37830